A Study of Effects on *MMP14* Transcriptional Regulation and Angiogenesis by Hypoxia and Statins

A Thesis submitted by

Andrew Douglas Moore

In fulfilment of the requirements for the Degree of Doctor of Philosophy

September 2014

Supervisors

Professor Shu Ye

Professor Kairbaan Hodivala-Dilke

Statement of Originality

I, Andrew Douglas Moore, confirm that the research included within this thesis is my own work or that where it has been carried out in collaboration with, or supported by others, that this is duly acknowledged below and my contribution indicated. Previously published material is also acknowledged below.

I attest that I have exercised reasonable care to ensure that the work is original, and does not to the best of my knowledge break any UK law, infringe any third party's copyright or other Intellectual Property Right, or contain any confidential material.

I accept that the College has the right to use plagiarism detection software to check the electronic version of the thesis.

I confirm that this thesis has not been previously submitted for the award of a degree by this or any other university.

Signature: 

Date: *24/09/2014*

Details of collaboration:

The thesis contains immunostaining of both human atherosclerotic plaques and murine atherosclerotic plaques in the results section. I performed the murine atherosclerotic plaque immunostaining but the human atherosclerotic plaque immunostaining was performed by Dr Feng Zhang. The human atherosclerotic plaque immunostains are included in this thesis as they provide clinical relevance to the research story.

The electrophoretic mobility shift assay and luciferase assays were performed by Dr Conrad Hodgkinson before the start of my PhD. They are included in this thesis as they fulfil part of the overall research story.

Abstract

Atheromas contain hypoxic areas which upregulate HIF1α expression, promoting angiogenesis and unstable lesion formation. Simvastatin stabilises atheromas through preventing rupture and neovascularisation. Atheromas express matrix metalloproteinase 14 (MMP14) which degrades matrix proteins and promotes neovascularisation. *MMP14* is upregulated by hypoxia and contains Hypoxic-Inducible Factor (HIF) recognition sequences (5'-RCGTG-3'). My project sought to investigate if HIF1α interacts with the *MMP14* promoter to enhance MMP14 expression, and whether simvastatin attenuates this effect, inhibiting angiogenesis.

Immunostaining of atheromas identified MMP14 and HIF1α localisation. Protein-DNA binding assays were performed on human umbilical vein endothelial cells (HUVECs) and showed HIF1α bound to the *MMP14* promoter in hypoxia, which was significantly decreased by simvastatin. To assess gene regulation, a human *MMP14* promoter-firefly luciferase reporter construct was transfected into C166 endothelial cells alongside HIF-overexpression plasmids and mutations of the *MMP14* promoter region at HIF recognition sequences. Overexpression of HIF1α and HIF1β increased MMP14 activity which was abolished by introducing the mutations and diminished by simvastatin in a HIF-dependent manner. Immunoblots, flow cytometry, scratch assays and bromodeoxyuridine incorporation showed *HIF1α* knockdown and simvastatin significantly attenuated hypoxia upregulated MMP14 expression, migration and proliferation in a HIF1α-dependent manner.

Angiogenesis was assessed using *in vivo* sponge angiogenesis assays and *ex vivo* aortic ring assays cultured in hypoxia or normoxia, with or without 0.1μM simvastatin, and MMP14 inhibitor, utilising $HIF1\alpha^{fl/fl}Tie1Cre^{+}$ and wildtype littermates. Simvastatin perturbed angiogenesis through decreasing MMP14 expression in a HIF1α-dependent manner.

The results show hypoxia upregulates MMP14 through HIF1α interaction with the *MMP14* promoter. Simvastatin attenuates MMP14 upregulation which reduces HIF1α:*MMP14* promoter interaction. *HIF1α* knockdown and simvastatin treated HUVECs show less migration and proliferation, equivalent to that of MMP14 inhibition. Simvastatin inhibits neovascularisation in a HIF1α-dependent manner. These results suggest simvastatin may stabilise atheromas through inhibiting MMP14 driven angiogenesis which may have further implications in the treatment of atherosclerosis.

Acknowledgements

This work was supported by the British Heart Foundation [FS/11/28/28758].

I would like to thank my supervisors Professor Shu Ye and Professor Kairbaan Hodivala-Dilke for their support and advice throughout my PhD, as well as for giving me the opportunity to undertake this research. I also want to thank the British Heart Foundation for funding my PhD and arranging conferences that have contributed to my progression throughout my studies.

I would like to thank my team and friends at Charterhouse Square. In particular my thanks go to Sue Shaw-Hawkins for her invaluable advice for future career progression and personal support. Having seen me from my nervous interview to confident researcher, Sue has been a fantastic lab manager and friend. As well as this I would like to thank my Clinical Pharmacology research team, particularly Fu Liang Ng and Kate Witkowska. Fu has been there since the beginning teaching the cell culture protocols, western blots and devising the ChIP protocol with me. Kate joined the team halfway through my PhD but has been an asset to the group and to my research. Their enthusiasm and critical thinking have aided my research and provided light relief when things don't go as planned.

As well as my team in Clinical Pharmacology I would like to extend my gratitude to Biochemical Pharmacology in providing the HUVECs for my cell culture work and advice on techniques which were not routinely performed in my department. Sarah Headland has been a major help in explaining and teaching me techniques, as well as aiding in some of the more complex experiments, and introducing me to colleagues that could help where she was unable to. I would also like to thank Louise Reynolds, Delphine Lees, Tanguy Lechertier, and Bruce Williams

from my Tumour Biology group for their help in the murine work and discussion of my work in laboratory meetings.

I would like to extend my thanks to my friend Will Day for teaching me the principles of flow cytometry and always finding time to help with planning flow cytometry experiments. My thanks also go to James Gillet from the BSU for looking after my mice breeders and helping me to gain confidence in animal handling.

Last but not least I would like to thank my family for their support throughout the PhD. They have been there to pick me up during the tough times and celebrate the good times as well. My fiancée Lauren who has had to endure late stressful nights whilst I plan experiments, prepare talks, and work late into the evenings but has encouraged me all the way and listened keenly to my outward thinking. My brother Tom who I know would be cheering me on and provided ears for me when no one else was around.

All of your help has allowed me to progress and I can't thank you all enough.

Table of Contents

List of Figures

List of Tables

List of Abbreviations

4S	The Scandinavian Simvastatin Survival Study
ACAT	Acyl-coenzyme A:cholesterol-acyltransferase
AFCAPS/TEXCAPS	Air Force/Texas Coronary Atherosclerosis Prevention Study
AKP	Alkaline Phosphatase
ANOVA	Analysis Of Variance
AHA	American Heart Association
Apo-B100	Apolipoprotein-B100
BCA	Bicinchoninic Acid
BrdU	5-Bromo-2'-deoxyuridine
BSA	Bovine Serum Albumin
CFSE	Carboxyfluorescein succinimidyl ester dye
CHD	Coronary Heart Disease
ChIP	Chromatin Immunoprecipitation
CVD	Cardiovascular Disease
DAB	3,3'-diaminobenzidine
DAPI	4',6-diamidino-2-phenylindole
DNA	Deoxyribonucleic Acid
dNTPs	Deoxynucleotide Triphosphates
DTT	Dithiothreitol
ECL	Enhanced Chemiluminescence
ECM	Extracellular Matrix
EMSA	Electrophoretic Mobility Shift Assay
eNOS	Endothelial Nitric Oxide Synthase
esiRNA	Endoribonuclease-prepared siRNAs
FACS	Fluorescent Activated Cells Sorting
FBS	Foetal Bovine Serum
FCS	Foetal Calf Serum
FDA	Food And Drug Administration
FIH	Factor Inhibiting HIF
HATs	Histone acetyltransferases
HDACs	Histone deacetylase
HIF	Hypoxia-Inducible Factor
HMG-CoA	3-Hydroxy-3-Methylglutaryl Coenzyme A
HRE	Hypoxic Response Element
HRP	Horseradish Peroxidase
HSP	Heat Shock Protein
HUVEC	Human Umbilical Vein Endothelial Cells
ICAM-1	Intercellular Adhesion Molecule 1
IRE	Iron Responsive Element

IRP	Iron Regulatory Protein
LDL	Low Density Lipoprotein
MLEC	Mouse Lung Endothelial Cell
MMP	Matrix Metalloproteinase
MT-MMP	Membrane Type Matrix Metalloproteinase
MTT	3-(4,5-dimethylthiazol-2-yl)-2,5-diphenyltetrazolium bromide
PI	Propidium Iodide
PBS	Phosphate Buffered Saline
PHD	Prolylhydroxylases
PLGF	Placental Growth Factor
PVDF	Polyvinylidene difluoride
ROS	Reactive Oxygen Species
SDS	Sodium Dodecyl Sulphate
TBST	Tris-Buffered Saline and Tween 20
TGFα	Transforming Growth Factor-α
TGFβ	Transforming Growth Factor-β
TIMPS	Tissue Inhibitors of MMPs
TNFα	Tumour Necrosis Factor-α
VCAM-1	Vascular Cell Adhesion Molecule 1
VEGF	Vascular Endothelial Growth Factor
VHL	von Hippel-Lindau
vWF	von Willebrand Factor
WHO	World Health Organisation
WOSCOPS	The West of Scotland Coronary Prevention Study

1. Introduction

1.1 The Vascular System

The cardiovascular system is composed of the heart, vasculature, and the blood and is vital for transporting nutrients and oxygen to target tissues, removing metabolic waste products, and delivering immune responses to affected areas of the body [1]. The vasculature is a closed loop consisting of the arteries, veins and capillaries, which continually circulate blood throughout the body [1]. The different types of vessel are classified by their size and location within the vasculature [2].

The cardiovascular system is divided into the pulmonary and systemic circulation. The pulmonary circulation transports deoxygenated blood from the heart to the lungs via the pulmonary arteries, where the blood is oxygenated and returned back to the heart through the pulmonary veins. The systemic circulation carries oxygenated blood from the heart to the cells, tissues and organs of the body.

The aorta is the largest artery and originates from the left ventricle, from here it branches into a network of arteries, which once at their target tissue branch into the smallest arterioles [2]. Capillaries link the arterioles to venules which take the deoxygenated blood from the tissues and merge into small veins, delivering deoxygenated blood to the venous side of the circulation. The small veins merge into larger veins until ultimately they converge into the two largest veins, the venae cavae, where they empty into the right atrium of the heart [2].

Both the venous and the arterial blood vessels have the same basic structure, with an outer layer known as the *tunica externa*, a middle layer or *tunica media*, and an inner layer known as the *tunica intima*. However the size and organisation of these layers differs between these types of vessels (Fig. 1).

The *tunica externa*, also known as the *tunica adventitia,* is comprised almost entirely of fibro-elastic connective tissue which provides structural support to the vessel [3]. The predominant structural proteins are collagen and elastin fibres which allow for the strength and elasticity that the vessels require. Longitudinal smooth muscle cells are also commonly located in this layer. In the larger of the arteries and veins the *tunica adventitia* contains its own blood supply, the *vasa vasorum*, which provides nutrients to cells that would be too far from for the nutrients and gases to move via diffusion. The difference between veins and arteries arises from the relative thickness of the *tunica externa* in relation to the overall diameter of the vessel. In veins and venules this layer comprises the majority of the vessel wall, whereas in arteries and arterioles it represents approximately half of the overall thickness [2].

The *tunica media* is the muscular layer of the vessel and is comprised, in large, of smooth muscle cells which are arranged circularly around the lumen of the vessel, as well as elastin fibres which allow the vessels to stretch. The *tunica media* tends to be more highly organised and thicker in larger arteries as they play a vital role in the transport of large quantities of blood [3]. The external elastic laminar coats the thick layers of smooth muscle cells and provides structural support [3]. The medial layer within the venous circulation is a lot thinner and less organised than the arterial vessels, leading the veins to have thinner, less rigid walls which allow them to hold a larger proportion of circulating blood [2].

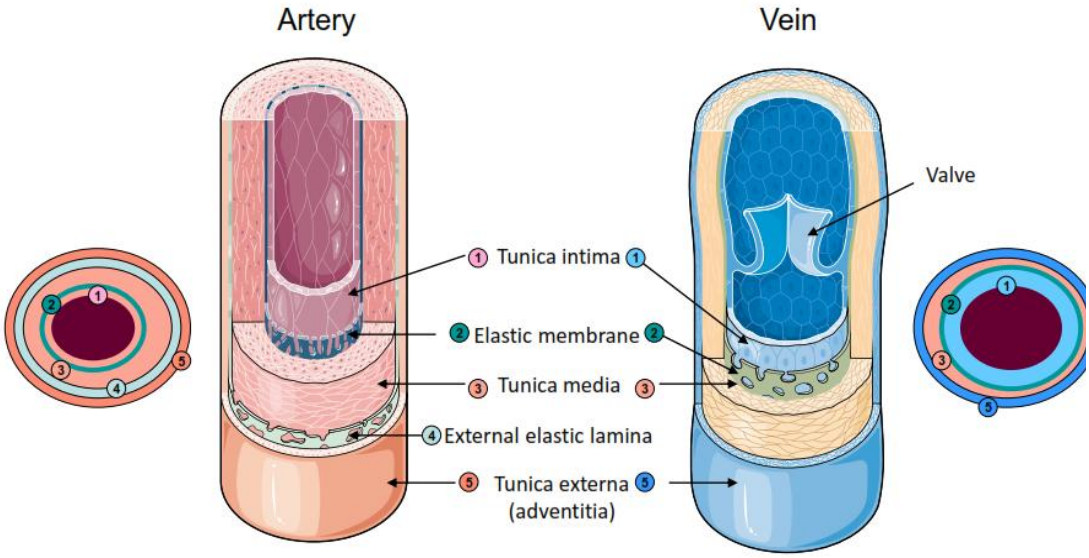

Fig. 1 – Schematic showing the basic structure of the arteries and veins. Adapted from Servier Medical Art [4]

Arteries contain a further band of elastic fibres which wraps the innermost layer, the *tunica intima*. The *tunica intima* is the thinnest layer of the vasculature and is characterised by its single endothelial cell layer which lines the lumen of the vessel and is mounted onto the basal lamina [3]. Beneath the basal lamina is a network of fibro-elastic connective tissue which allows support and flexibility of the endothelial cells [3]. The veins differ from the arteries as they contain valves, which protrude into the lumen of the vessel and prevent the backflow of blood (Fig. 1).

The vascular endothelium forms the innermost layer of the entire vasculature in both blood vessels and lymphatic vessels [2]. It plays an important role in many physiological functions, including controlling vasomotor tone, trafficking of blood cells, angiogenesis, formation of connective tissue, and in innate and adaptive immunity [5, 6].

1.2 Endothelial Cells

Endothelial cells are a highly metabolically active cell type that provide a semipermeable barrier between the blood and the vessel wall which is vital for the transport of nutrients and regulating the tissue fluid balance. They are especially important in allowing the transfer of macromolecules and fluid between the interstitial space as loss of function can lead to inflammation [7].

Endothelial cells are typically flat, with a thickness which varies from less than 0.1µm in capillaries and veins to 1µm in the aorta [5]. They are a heterogeneous cell population in that they differ in morphology and function depending on their location in the vascular system. This can be seen by comparing endothelial cells in the smallest arterioles and venules, where the endothelial cells are longer and narrower in the arterioles in comparison to the venules [2]. They are heterogenous in both a structural and a molecular sense with evidence showing that different proteins are expressed in different vascular beds [5,8]. An example of this can be seen in the expression profile of von Willebrand Factor (vWF) which has low expression in capillaries and high expression in the aorta [8].

The function between arterioles and venules also differ in that the arteriolar endothelial cells major role is controlling vascular tone, whereas endothelial cells from post-capillary venules are the primary site of leukocyte trafficking [2]. It has been shown that endothelial cells cultured from different locations throughout the vasculature have different permeabilities. The lowest permeability is attributed to the arterial endothelial cells, with the highest seen in the microvessels, followed by the venule endothelial cells [7]. There are several molecules known to

increase blood vessel permeability including thrombin, bradykinin, and oxidants. In addition to this there are molecules that stabilise endothelial cell junctions, therefore decreasing permeability. These molecules include angiopoietin-1 and sphingosine-1-phosphate.

As well as having a role as a permeable and physical barrier the endothelial cells also have roles in endocrine regulation with the ability to produce and release a host of growth factors including nitric oxide, endothelin and prostaglandins. The endothelial layer is able to sense changes in the bloods flow rate, blood pressure and concentration of humoral substances. This allows the quick release of vaso active substances that can respond to dynamic changes in the blood [9].

The vascular endothelium is supported by the extracellular matrix (ECM) which provides an essential scaffold for organising endothelial cells into blood vessels. The ECM is a dynamic structure which has multiple roles in cell support, adhesion and signalling and influences on cell migration, proliferation, differentiation, polarity and survival [10]. The ECM is comprised of many structural proteins including the collagens, laminins, fibronectins, nidogen, proteoglycans and elastins.

Endothelial cell adhesion to the ECM is required for proliferation, migration, morphogenesis, survival, and ultimately the stability of the vasculature [11]. A disruption to the normal physiological functioning of the endothelium can lead to the development of a number of pathological conditions including cancer and cardiovascular disease.

1.3 Cardiovascular Disease

Cardiovascular diseases (CVD) comprise the major disorders of the heart and the arterial circulation [12] and remain the leading cause of death worldwide, with over 17.3 million deaths in 2008 being attributed to CVD [13]. They are a major public health concern globally with impaired quality of life, loss of independence and high mortality rates [12]. In the UK the burden of CVD on the economy exceed £30 billion per annum, with NHS costs alone being higher than £14 billion, and predicted to rise further [14]. It is predicted by the World Health Organisation that by 2030, almost 23.3 million people will die from CVDs and they will remain the single leading cause of death globally [15].

There are several risk factors that are associated with the likelihood of developing CVD. The major risk factors for developing CVD include tobacco use, high blood pressure, raised blood glucose levels, physical inactivity, obesity and abnormal lipid levels [16]. Most of these risk factors can be incurred due to behavioural choices and can be remedied through altered lifestyle choices. However, other factors, such as ethnicity, gender and age are acquired or inherited, in turn influencing our response to environmental risk factors. Sex and age are major risk factors with CVD mortality. Incidence and prevalence rates are increasing steeply, roughly doubling each decade, with males likely to develop CVD ten years younger than females [14].

Cardiovascular diseases affect the heart and blood vessels and include hypertensive disorders, ischaemic heart disease, cerebrovascular disease and peripheral vascular disease [13]. Most CVDs are the result of reduced blood flow to the heart, brain or peripheral tissues caused by the formation of fatty plaques, or atheromas, which silently build up in different arteries during

adult life (Fig. 2). The atheromas begin as fatty streaks, composed of fat-loaded blood cells, which gradually progress, becoming larger and more complex, turning into intermediate lesions, which in turn, form a fibrous plaque. This multifactorial process is known as atherosclerosis and can be caused by impaired endothelial cell function, increase in LDL-cholesterol, inflammation of vasculature, and influx of leukocytes into the vessel wall [17]. The atheromas eventually cause obstructions and narrowing of the arteries and can trigger a local thrombosis, completely blocking the blood flow, resulting in a heart attack, stroke or ischaemic leg [14]. The thrombus can develop in two ways, either on the surface of the plaque, due to endothelial cell degradation, or within the plaque itself after plaque rupture [18].

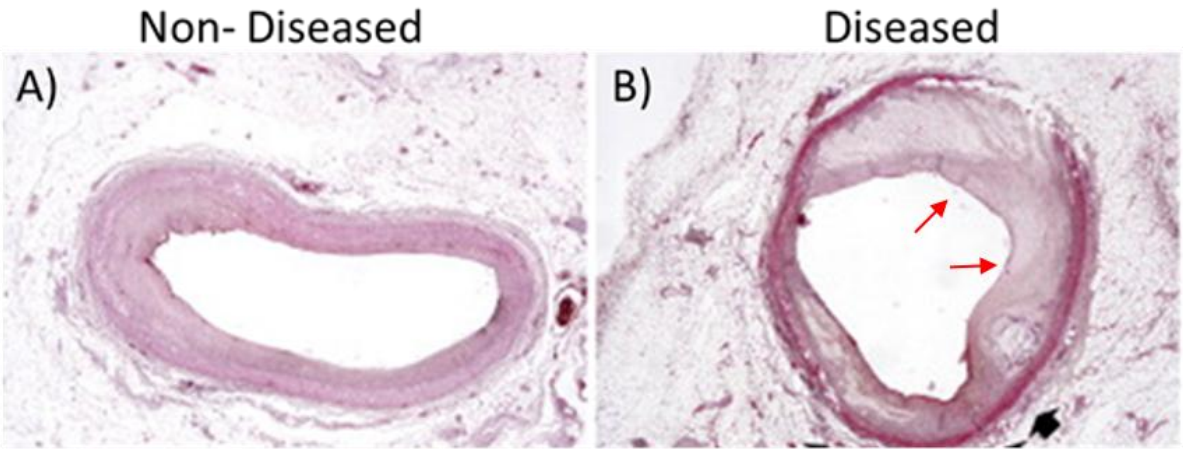

Fig. 2 – Photomicrographs of non-diseased (A) and atherosclerotic carotid arteries (B) The disease vasculature is characterised by the formation of the fatty plaque, indicated by the red arrows (Adapted from Agrogiannis et al., 2013) [19]

Atherosclerosis has a major impact on society and is responsible for a large proportion of CVDs. In 2008, out of the 17.3 million cardiovascular deaths, heart attacks were responsible for 7.3 million deaths and strokes were responsible for 6.2 million deaths [13]. As discussed above, there are several risk factors which lead to the progression of atherosclerosis including the use of

tobacco, an unhealthy diet, diabetes, physical inactivity, poverty, obesity, the male gender and genetic disposition [13]. Unhealthy behaviours can lead to metabolic and physiological changes including hypertension, obesity, diabetes and dyslipidaemia, which in turn, induce endothelial dysfunction through mechanisms including free radical oxidation and haemodynamic strain [20] causing damage to the blood vessels due to the progression of atherosclerosis [13].

1.4 Formation of the Plaque

During atherogenesis there is a defined series of morphological and biological changes within key players including inflammatory cells, low density lipoprotein (LDL), cholesterol, and smooth muscle cells [17]. These changes contribute to the formation of the plaque which gradually enlarges, with increased inflammation, and leads to blockage of the vessel (Fig. 3).

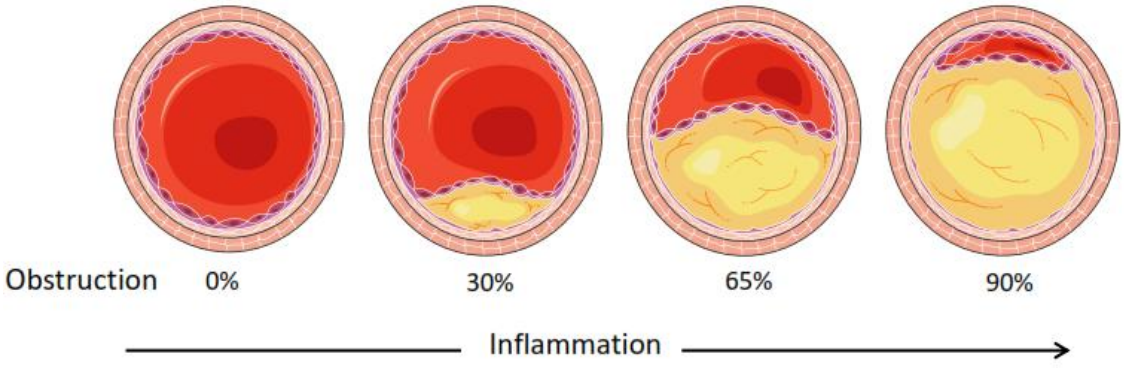

Fig. 3 – The progression of atherosclerosis. As inflammation increases the plaque thickens leading to almost complete obstruction of the vasculature. Adapted from Servier Medical Art [4]

The endothelium is a cell monolayer which allows the transport of nutrients between the blood and the tissues. A force that is acting on the endothelial cells is fluid shear stress, which affects the morphology of the cells. It has been seen that cells in the tubular regions of arteries, where the fluid shear stress is weaker, are ellipsoid in shape and aligned in the direction of the blood flow. When the blood flow is disturbed, for example at branch points in the artery, endothelial cells tend to be more polygonal in their shape without a particular orientation [17]. The endothelium in this area is weakened and becomes increasingly permeable to lymphocytes and monocytes. This happens, for example, when there is an increase in LDL cholesterol and other macromolecules, making the area vulnerable for lesion formation [13]. The extent of effect from differences in shear stress tension can be seen clearly in the regulation and expression of genes where it has been shown that in a porcine model 764 genes are differently expressed in low shear stress regions compared to high stress regions [21]. The differently expressed genes have key roles in apoptosis and senescence, and have been shown to contribute to the formation of atherosclerosis [22].

One of the factors contributing to the formation of atherosclerotic plaques are autoimmune responses involving cholesterol and heat shock proteins (HSP), particularly HSP60 [23]. HSP60 is upregulated in response to infection, and activates both the innate and adaptive immune systems. Under stressful conditions, endothelial cells translocate HSP60 to the cell surface. A co-expression of both adhesion molecules, such as intercellular adhesion molecule 1 (ICAM-1) and vascular cell adhesion molecule 1 (VCAM-1) [24], and HSP60 leads to a reaction for attachment and destruction of endothelial cells by the immune system against HSP60. Following this, intimal infiltration by mononuclear cells leads to the plaque formation [23].

Activated T cells, in particularly CD4, are the first cells to infiltrate into the arterial intima and this occurs early on in the formation of the lesion [23]. Following this, macrophages invade into the vessel wall which is a primary event toward the eventual formation of the atheroma [25]. The phagocytes engulf LDL via endocytosis and convert into foam cells with cytoplasmic, membrane bound lipid droplets [26]. The uptake of LDL particles by macrophages is mediated by a group of receptors that recognize a wide array of ligands [17]. Foam cell formation is mediated by acyl-coenzyme A:cholesterol-acyltransferase (ACAT) which esterifies cholesterol and allows more efficient transport into macrophages [27]. In addition to esterification the formation of foam cells requires the LDL to be highly oxidised by reactive oxygen species (ROS) which are produced by endothelial cells and macrophages as well as several enzymes. Oxidised LDL is less susceptible to degradation by the lysosome of macrophages and therefore a foam cell is formed [20]. Even when the LDL is minimally oxidised by oxidative waste a pro-inflammatory activity can be seen, which can go unnoticed by macrophages [17]. The minimally oxidised form of LDL stimulates the endothelial cells to produce pro-inflammatory adhesion molecules and growth factors which recruit circulating monocytes and lymphocytes to the vessel wall of the lesion [17]. This interaction has also been attributed to the intimal calcification of atherosclerotic plaques, which can further reduce the elasticity of the vasculature [28].

A number of adhesion molecules, including selectins, aid in the first process of migration though the endothelial surface by binding to the leukocytes and facilitating leukocyte rolling along the surface [17]. The macrophages, as well as the endothelial cells and smooth muscle cells, express CD40 which produces inflammatory cytokines, adhesion molecules and proteases upon binding with its ligand, CD40L. This interaction is important for the production of ECM and for the migration and proliferation of smooth muscle cells [17].

Once through the endothelial cell barrier, the inflammatory cells and LDL migrate into the sub-endothelial matrix [13]. The transport and retention of LDL are increased in the areas that are vulnerable for plaque development, which is greater when the levels of circulating LDL are increased [17]. Lipid accumulation in the plaque generates ROS which can lead to endothelial dysfunction and an increase in permeability, which in turn promotes more lipoprotein migration [20]. LDL can undergo modifications including oxidation, lipolysis, proteolysis and aggregation, which can all lead to increased local inflammation as well as to the formation of foam cells. The foam cells form through interactions between the LDL and macrophage receptors [17].

A necrotic core forms as the macrophages and foam cells begin to die, which contributes to further inflammation and stress of the plaque as well as proteolytic breakdown [29]. The necrotic core gradually increases in size due to increased infiltration of foam cells and lipids from broken down erythrocytes [25]. Smooth muscle cells from the media layer of the vessel wall, migrate to the necrotic core and secrete a collagen-rich matrix which covers the site with a fibrous cap [20]. Cells and lipids continue to gather in the atheromatous plaque which enlarges and protrudes into the vessel lumen. As the process continues the fibrous cap thins and the endothelial surface starts to split and crack making it liable to rupture [17]. When the plaque ruptures, a thrombus forms which if large enough can block the blood vessel. This leads to clinical events such as a heart attack or a stroke if this occurs in a coronary or cerebral artery, respectively [13]. The thrombus forms when lipid fragments and cell debris from the plaque are released into the vessel lumen, exposing them to thrombogenic agents on the endothelial surface.

1.5 American Heart Association Classification

The development of atherosclerotic plaques can be classified according to the American Heart Association (AHA) system [30]. This system aims to categorise the stages of the lesion by the components and histology of the vessel. Trying to classify plaques into a numerical system can be a challenge as plaques are heterogeneous with respect to the amounts of their different components [18]. Other systems have been developed which aim to characterise the plaques by their morphological features [31], but the AHA numerical classification is a widely accepted classification.

The first stage of the development of the atherosclerotic plaque is the type I lesion, or initial lesion, which is when the lipid deposits first become microscopically and chemically detectable but are not visible by the naked eye. Macrophages and foam cells are the key cellular components of these lesions which are most frequent in infants and children. The lesions have been seen in adults that have minimal atherosclerosis or in locations that are resistant to lesion formation. The initial changes in the vessel intima are minimal with small isolated groups of foam cells infiltrating the intimal space (Fig. 4) [32].

Type II lesions are when the lesion is first identifiable by yellow coloured streaks or spots on the intimal surface of the arteries. The lesion is not entirely defined by the fatty streak but also by its microscopic composition. They contain a greater amount of foam cells than the type I lesions which are arranged in layers rather than as isolated cells. As well as foam cells they also contain more macrophages and also smooth muscle cells containing lipids and T lymphocytes. Type II lesions are common in the aorta with 99% of children between the ages of 2 to 15 years having

these lesions [32]. They have been noted to appear in coronary arteries around puberty whereby approximately 65% of children between 12 to 14 years of age have either type I or II lesions [33].

Type III lesions are a stage that bridges the gap between type II lesions and atheromas, and are therefore often referred as intermediate lesions or preatheromas. There is identifiable adaptive intimal thickening and its histologically distinguishable features include extracellular pools of lipid droplets and particles which form among the layers of smooth muscle cells. The lipid pools lie below layers of macrophages and foam cells and push smooth muscle cell layers apart. Type III lesions can be distinguished from type II lesions by their increased free cholesterol, fatty acid and other lipid derivatives (Fig. 4) [32].

Type IV lesions, or atheromas, contain a lipid core which is a dense build-up of extracellular lipids which occupies a large area of the intima [34]. The type IV lesions are the first lesions that are classified as advanced lesions as they cause this disorganisation and thickening of the arterial wall. Although the vascular wall is thickened the lumen of the blood vessel is not always narrowed. The lipid core causes great intimal disorganisation with smooth muscle cells and intracellular matrix dispersing as well as being replaced by extracellular lipids. Calcification occurs in type IV lesions which can be seen to affect the smooth muscle cells as well as the lipid cores [34].

Between the lipid core and the endothelial surface the intima contains macrophages, foam cells and smooth muscle cells. Around the periphery of the lipid core macrophages, foam cells and lymphocytes are commonly more densely packed, which make it more liable to rupture. The

death of macrophages which invade the lipid pool is responsible for the conversion of intimal thickening to the start of the fibroatheroma (Fig. 4) [25].

The lesion can progress from a type IV lesion to a type V lesion with a marked increase in fibrous connective tissue formed. This lesion is known as a fibroatheroma due to the increased fibrous connective tissue infiltrating the atheroma and surrounding the lipid cores (Fig. 4) [34]. This further distorts the normal cellular and intercellular matrix structure of the intima. The lymphocytes, foam cells and macrophages are no longer limited to the intima in type V lesions and start to migrate into the media and adventitia. Smooth muscle cells in the media are also affected and being lesser in number and disarranged.

The clinical manifestations leading to morbidity and mortality from atherosclerosis are mainly due to type IV and type V lesions which have disruptions in the surface of the endothelium, or haemorrhage within the plaque. This leads to thrombogenic agents coming into contact with the plaque components, forming a thrombus and blocking the arteries [34]. When this occurs the lesion is classified as a type VI, or complicated lesion. The defining features of type VI lesions are one or more, of a surface defect, haematoma, or thrombosis. This means that the type VI lesion may not necessarily progress from a type V but may develop straight from a type IV lesion [30]. It is also noted that the lesions may themselves also block the vessel and produce a clinical event without developing into a type VI lesion (Fig. 4) [30]

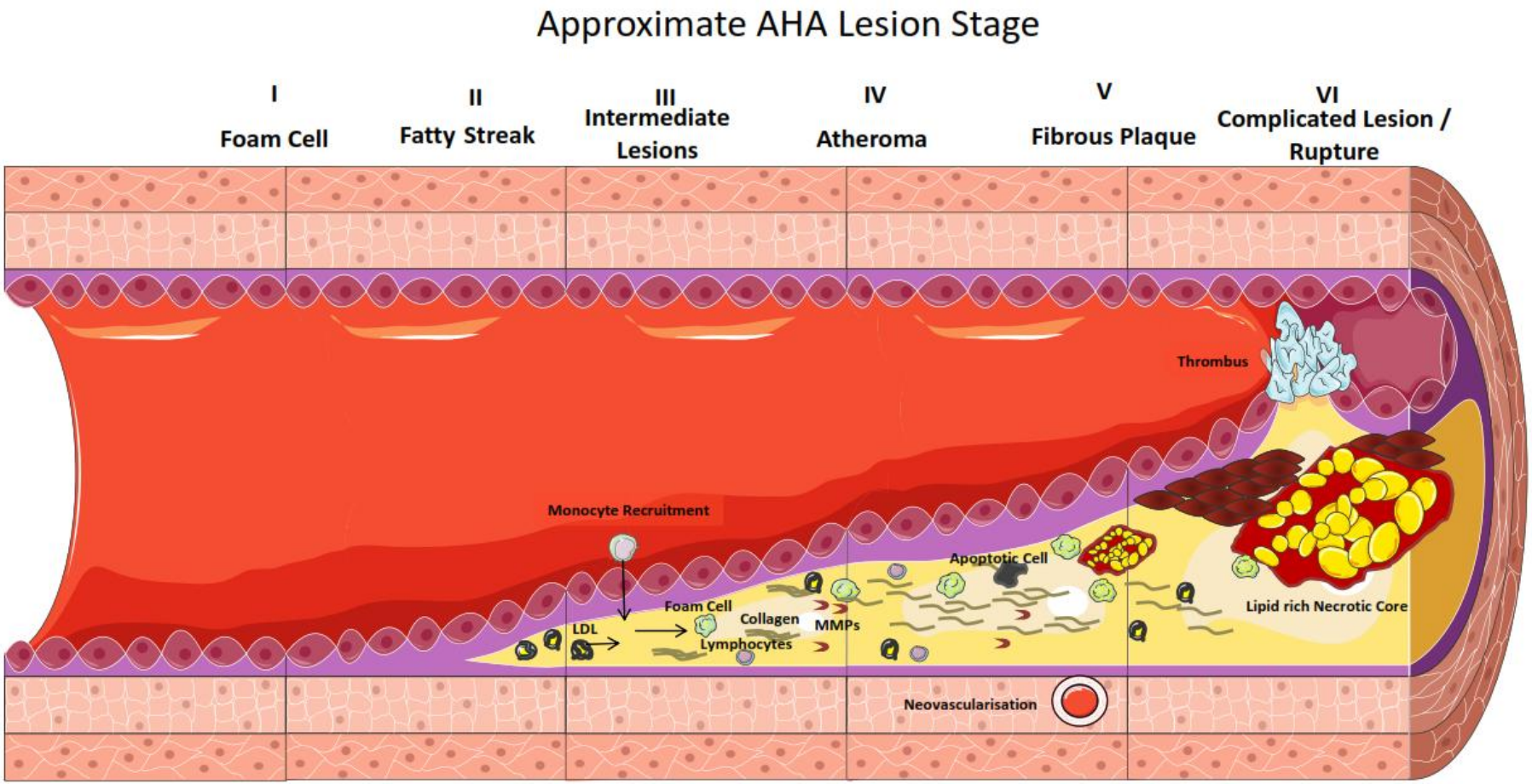

Fig. 4 - The progression of the atheroma showing approximate AHA lesion stage and the components of the atherosclerotic plaque.

Adapted from Servier Medical Art [4]

1.6 Hypoxia in the Plaque

Evidence has proved that hypoxia plays an important role in the pathogenesis of many major diseases, with increased roles seen in diseases such as, inflammatory diseases, heart disease, cancer and wound healing [35]. It has also been shown that hypoxia is involved in endothelial dysfunction, typically in severe hypoxia [36].

It has long been thought that hypoxia in the plaque has a key role in plaque progression. The luminal blood and the *vasa vasorum* of the adventitia provide the oxygen and nutrients for the intima and media of the artery wall [37]. As the plaque progresses and thickens the diffusion of oxygen is impaired. Hypoxia occurs in vessel walls where the maximal oxygen diffusion limit exceeds 200µm [38]. The intimal thickness alone of advanced atherosclerotic lesions have been found to be far greater than this limit which results in areas of the plaque becoming hypoxic [39]. In most lesions there is a hypoxia-negative rim of around 100 to 250µm which borders the lumen of the vessel [39].

It is not just the diffusion limit of oxygen which causes areas of the plaque to become hypoxic but the increased demand of oxygen from metabolically active inflammatory cells which accumulate in the core of the lesion [39]. It is therefore commonly the macrophage and foam cell rich regions that show the highest levels of hypoxia [40]. Although hypoxia is commonly present in macrophages and foam cells, not all of them are hypoxic. However some foam cells are hypoxic even though they lie within the oxygen diffusion capacity [39]. Interestingly, the formation of foam cells and increased inflammation are promoted by hypoxia [37].

Metabolism in the plaque can result in the generation of ROS through the inefficient use of oxygen by the mitochondria during oxidative phosphorylation [41]. These ROS cause cell dysfunction and death through oxidising cellular lipids, proteins and nucleic acids [42]. As well as causing cell dysfunction, an increase in ROS under hypoxic conditions is required for the activation of the master regulator of oxygen homeostasis HIF (Hypoxia-inducible Factor) [42].

1.7 Hypoxia-Inducible Factor

The HIF complex of proteins were discovered in 1991 when studies on the erythropoietin gene lead to the identification of a transcriptional regulator in hypoxic conditions [43,44]. Upon purification of the protein, it was discovered that HIF1 exists as a heterodimeric protein composed of two different subunits, a 120kDa HIF1α unit and a 91-94kDa HIF1β subunit [45]. These proteins belong to the basic-loop-helix per-aryl hydrocarbon Sim protein nuclear translocator family [46]. Interactions between the two basic-loop-helix domains leads to dimerization, which stabilises the protein and allows the units to bind to the hypoxia response element (HRE) (5'-RCGTG-3') DNA consensus sequence [46]. The HIF1β subunit is constitutively expressed and is not affected by hypoxia [47], but the HIF1α subunit is highly regulated by oxygen levels. HIF1α is continually synthesised but is rapidly degraded with a half-life of around 5 minutes in normoxic conditions [48]. If stabilised HIF1 is able to bind to other coactivators, p300 and CBP, to form the HIF response complex. The HIF response complex targets many biological processes and also upregulate the prolylhydroxylases (PHDs), acting as a negative feedback loop. This leads to the attenuation of HIF in prolonged hypoxic conditions and sets a new oxygen threshold for the activation of HIF [49].

In most adult tissues oxygen concentrations range from 3% to 5% and when any decrease is seen a graded response to the hypoxic conditions is observed [35]. These concentrations are substantially less than the ambient air, 21% oxygen, and or in a main artery, ~13% [36]. The expression of HIF1α is only upregulated at the protein level by hypoxia as there is no effect of hypoxic conditions on HIF1α mRNA [50].

There are other isoforms of HIF1α, HIF2α and HIF3α, which are able to compensate for each other in knock-down experimental conditions [51]. The isoforms also have self-regulatory roles through either inhibiting or promoting the other isoforms expression, which can be shown by HIF1α expression increasing and HIF2α decreasing when HIF3α is silenced [52].

HIF2α was discovered by searching for proteins that shared similar homology to HIF1α [53] and was shown to be upregulated in murine endothelial cells. Furthermore, it was seen to regulate VEGF, glycolytic enzymes and other proteins governed by the HRE sequence [53]. HIF2α differs to HIF1α in its expression pattern, showing a more tissue specific pattern rather than the ubiquitous expression of HIF1α. HIF2α is primarily expressed in endothelial cells, kidney and lung epithelial cells, bone marrow macrophages, as well as cells derived from neural crest tissue during development [54]. HIF2α expression is controlled by a similar oxygen gradient response involving FIH and the PHDs as HIF1α, although recent evidence has shown that an iron responsive element (IRE) is also present and controlled by an iron regulatory protein (IRP). Depending on the amount of cellular iron present, IRP can prevent HIF2α translation, which differs to the regulation seen in the other HIFs.

HIF3α was identified in 1998 through the cloning of a cDNA fragment that contained 61% homology to the hypoxic responsive domain of HIF1α [55]. HIF3α shows marked differences to the other HIFs in the lack of a transactivation domain [55] and therefore does not form the active HIF transcription factor with HIF1β [56]. Unlike the other HIFs, HIF3α has no known activation role and instead it is believed to be a negative regulator of HIF transcription [56].

Although the different HIF isoforms are closely related they all have their own distinct roles in controlling gene expression. It is widely accepted however that HIF1α is the most important isoform for hypoxic control of genes [52].

1.7.1 Hypoxia-Inducible Factor 1 Alpha

HIF1α is a downstream activated molecule of the phosphatidylinositol 3-kinase (PI-3-kinase) pathway and is also known to be activated via the mitogen activated protein kinases (MAPKs). HIF1α is activated through phosphorylation by the p42 and p44 MAPKs in response to hypoxia, which also enhance the transcriptional activity of HIF1 [57]. Additionally, HIF1α is also upregulated by the PI-3-kinase pathway via a post-transcriptional mechanism [58].

In normoxia there are two identified ways in which HIF1α is degraded using hydroxylation and ubiquitinylation [59]. The first is the hydroxylation of HIF1α at two proline residues (Pro-402 and Pro-564) in the oxygen-dependent degradation domain. This promotes the interaction with the von Hippel-Lindau ubiquitin ligase complex (VHL) which polyubiquitinylates HIF1α and targets it for degradation by the proteasome (Fig. 5) [59]. The second method involves β-hydroxylation of

an asparagine residue (Asn-803) which inhibits the interaction of HIF1α with its co-activators p300 and CBP (Fig. 5). This hydroxylation of HIF1α is catalysed by factor inhibiting HIF (FIH) at the asparagine residue and by PHDs at the proline residues. The PHDs are termed the prolylhydroxylase domains enzymes (PHD1, PHD2 and PHD3) [59]. Each of the PHDs acts to suppress HIF activity but PHD2 has been found to have more activity on HIF1α than the other PHDs [59]. It has been found that the PHD enzymes bind the VHL complex through an interaction with the tumour suppressor LIMD1 which enables HIF1α to be effectively degraded [60].

The prolyl hydroxylases are dependent on oxygen for their activation and therefore their action is reduced in hypoxic conditions [59]. This permits the dimerisation of HIF1α with HIF1β which bind to their co-activators to form an active HIF response complex. The active HIF response complex locates to the promoter region of the gene of interest and increases its transcription (Fig. 5).

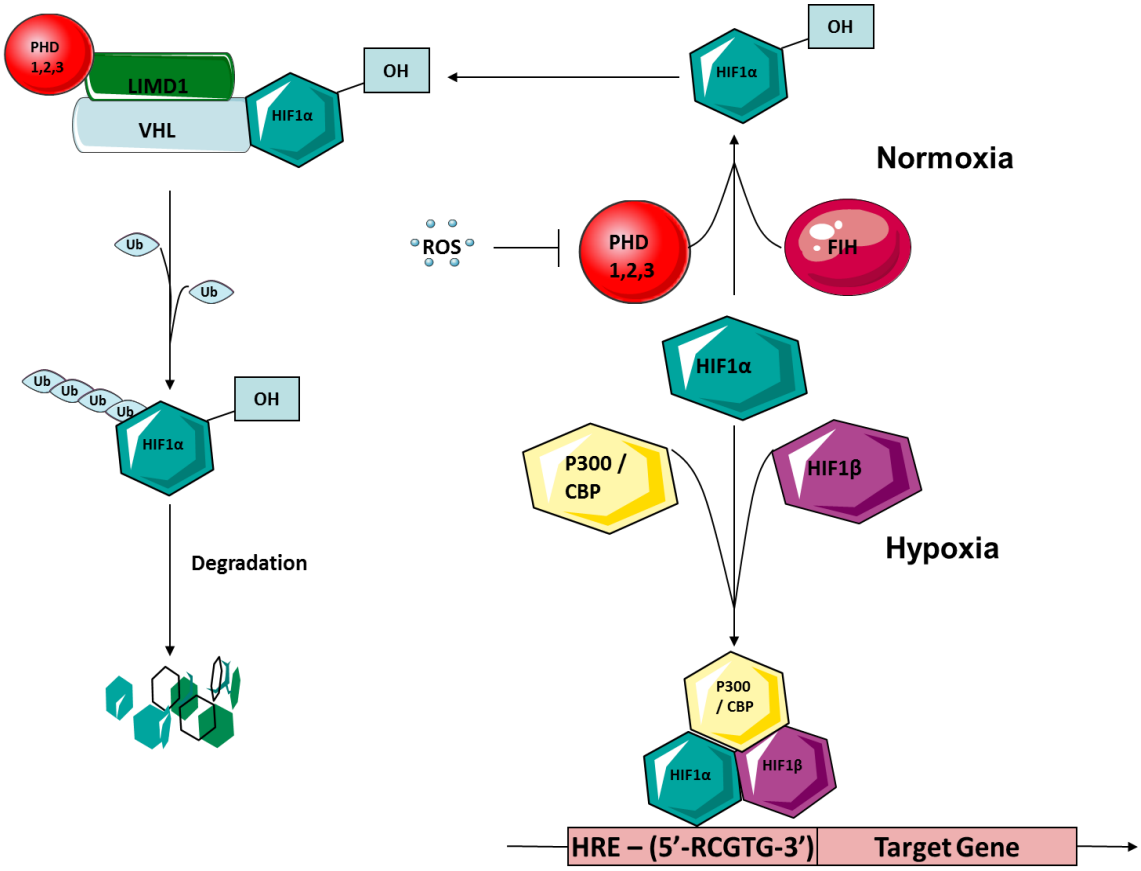

Fig. 5 – The regulatory pathway of HIF1α in hypoxia and normoxia. HIF1α is stablised and binds to the cofactors HIF1β, P300 and CBP in hypoxia to form the HIF response complex, but is targetted for degradation in normoxia by Prolyl Hydroxylases and FIH.

There are hundreds of genes that are upregulated by HIF1α, and they have vital roles in cell growth, apoptosis, cellular metabolism, and angiogenesis [61]. HIF1α generates a response to hypoxia both at the cellular level, in changing to anaerobic metabolism, and at the tissue level, through the promotion of angiogenesis. An imbalance of HIF1α can lead to disease and is known to have roles in the pathogenesis of cancer [62], pulmonary hypertension [63] as well as atherosclerosis [39]. Dysregulation of these genes is implicated in the progression of the plaque to a complicated lesion. Of interest, is the upregulation of angiogenic genes such as Vascular

Endothelial Growth Factor (VEGF), Tie2 and Placental Growth Factor (PLGF) which promote neovascularisation into the plaque to provide nutrition to areas of hypoxia [64]. Prolonged exposure of macrophages to hypoxic conditions has been shown to lead to an increased expression of genes involved in angiogenesis as well as transporter proteins [65]. The large population of macrophages in atheroma can therefore be affected by the hypoxic conditions and HIF1α.

Although hypoxia is known as the key upregulator of HIF1α there are other factors that can lead to its upregulation. Hormones such as insulin and heregulin have been shown to increase HIF1 activation and HIF1α accumulation through the PI-3-kinase and rapamycin signalling pathway [66]. In hypoxia, insulin increases HIF1α protein levels, binding to DNA, and increases HIF1α-mediated gene activation. It does this not by decreasing degradation or increasing transcription, but through increasing HIF1α translation [66]. Glucose has also been shown to have an important role in the activation and regulation of HIF1 with glucose being required for HIF1 activation in hypoxic conditions [67].

As well as being upregulated in hypoxia, HIF1 can also accumulate and activate during normoxia. This process is driven by cytokines, growth factors, hormones and ROS [68]. Cytokines such as interleukin-1β and tumour necrosis factor-α have been shown to enhance the binding of HIF1 to DNA, as well as increase HIF1 accumulation [68,69]. This has great importance with respect to inflammation as cytokines are upregulated during an inflammatory response, which in turn would increase intracellular levels of HIF1. These include immune responses which as well as promoting HIF1α expression also increase angiogenesis into the atheroma [70].

1.8 Neovascularisation in the Plaque

In normoxic conditions, blood vessels are nourished by oxygen diffusing from either the lumen of the vessel or from the adventitial *vasa vasorum*. When hypoxic areas occur in the plaque and the diffusion is insufficient to meet the metabolic demands of newly formed tissue, new blood vessels are formed in order to supply the areas that are outside the usual capacity for oxygen diffusion.

Neovascularisation is the process of generating new blood vessels from either pre-existing vasculature, via angiogenesis, or from endothelial precursor cells, termed vasculogenesis [1]. Angiogenesis is the predominant form of neovascularisation in atherosclerosis and is mediated by endothelial cells sprouting primarily from the *vasa vasorum* [71] leading to the formation of new capillaries [72]. This is stimulated when the intima thickens past the oxygen diffusion gradient, causing hypoxic areas to form, which upregulates HIF1α and in turn activates angiogenic response genes [35].

Non-diseased coronary arteries do not contain vasculature in their intima or media [73], however most human atherosclerotic plaques do contain neovasculature [74]. This indicates that the formation of the new microvessels is due to the progression of the plaque, rather than the neovascularisation being the cause of the atherosclerosis [72].

The process of angiogenesis begins with an increase in the permeability of the microvessels, through the upregulation of VEGF [75,76], and degradation of the matrix surrounding the vasculature. Endothelial cells then migrate and proliferate in the required direction governed by genes including angiogenin [77], tumour necrosis factor-α (TNFα) [78], and transforming growth factor-α (TGFα) [79]. This results in thin walled, permeable sprouts which are matured and maintained by cytokines including transforming growth factor-β (TGFβ) [80] and by the formation of the basement membrane. The new blood vessels are further enhanced by the recruitment of smooth muscle cells and pericytes [81].

Neovascularisation in the atherosclerotic plaque is present in three regions, the adventitia, the intima-media border, and in the intraplaque region. The microvessels invade from the adventitial layer, through the medial elastic lamina and then break though into the plaque [81]. As the plaque progresses the microvessel density increases, indicating that the new vessels play a role in the development of the plaque [82].

The endothelial integrity of the new microvessels is severely compromised with incomplete inter-endothelial contact and an inadequate recruitment of mural cells. Moreover, detachment of the endothelial cells from the basement membrane is common. This leads to an increase in blood-derived inflammatory cell infiltration into the plaque, promoting necrotic core expansion and overall plaque progression [82]. The leakage of the blood vessels is not the only reason for the increase in leukocytes. It has been seen that the neovasculature expresses the leukocyte adhesion molecules E-selectin, ICAM-1 and VCAM-1 more abundantly than the lumen of the arterial endothelium, thus enhancing leukocyte accumulation in the plaque [74].

Early stage plaques show the presence of neovascularisation with microvessels observed in stage II plaques associated with macrophages and immature mast cells. The microvessels become more common in intermediate plaques, with either sparsely or densely packed microvessel accumulation. Build-ups of lipoproteins are observed to surround these vessels, suggesting that the lipids are using the new vasculature to invade the plaque [83]. In the more advanced plaques, the vessels are more abundant with the more severe plaques tending to have a larger number of adventitial vessels [71] .

Neovascularisation in atheromas is an important target for therapy as analysis of plaques has shown that unstable lesions are associated with a higher degree of neovascularisation [82].

1.9 Plaque Instability

It was initially thought that the increased plaque size leading to the narrowing of the blood vessel lumen was the primary cause of clinical events such as myocardial infarction and strokes. It is now known that, although this stenosis can obstruct the vessel, the most common cause of a clinical event is plaque rupture, which occurs in 75% of fatal coronary events [84]. A ruptured plaque leads to the formation of a thrombus due to either endothelial degradation or intraplaque haemorrhage [18]. The thin fibrous cap contains slight openings and fissures in plaque ruptures which brings the circulating blood into direct contact with the thrombogenic components of the lipid core. This leads to the formation of the thrombus and potentially to clinical events [18].

Histological assessment has identified distinguishing characteristics which are associated with the vulnerability of the plaque to rupture, including size of the plaque [85], a large cholesterol and oxidised lipid-rich plaque core, a thin fibrous cap with weakened smooth muscle cell and collagen availability, inflammatory cell infiltration and increased neovascularisation [86].

The increased neovascularisation of the atheroma plays an important role in the progression from a stable asymptomatic state into a high-risk unstable lesion [25]. The new leaky vasculature provides new pathways for leukocytes, red blood cells, cholesterol and other molecules to enter the plaque. This leads to an increased necrotic core mass and inflammatory cell induced apoptosis [25].

Localised mechanical shear stress forces can also cause the plaque to rupture through affecting its structural integrity. Once the plaque ruptures, a thrombus forms around the exposed pro-thrombogenic core, which can eventually occlude the vessel [20]. Increased plaque disruption enhances the likelihood of an intraplaque thrombosis occurring [85]. The majority of plaque ruptures occur at the shoulder regions of the atheromas, where the lipid depositions, and inflammatory cells are commonly located [87–89]. This has been attributed to the mechanical stress of the plaque being shifted to this region where there is less structural integrity [87,88].

Matrix metalloproteinases (MMPs) are proteolytic enzymes that degrade the ECM and are highly expressed in macrophage-rich areas of the atherosclerotic plaque, particularly at the shoulder regions of the cap. The MMPs may therefore promote the weakening of the cap and further destabilise the plaque leading to rupture [90]. These will be discussed in detail in section 1.12.

Research has looked into the potential of preventing neovascularisation in atherosclerotic plaques through the use of angiogenesis inhibitors, and thereby increasing plaque stability. It has been found that by using endothelium-specific angiogenesis inhibitors, such as the type XVIII collagen fragment endostatin and TNP-470, there is a decrease in plaque size of 85% and 70%, respectively [91]. Angiostatin treatment has also been shown to markedly reduce neovasculaturisation invading the atheroma from the *vasa vasorum* of murine models [92]. Other drugs including simvastatin have also shown beneficial effects on reducing angiogenesis in atherosclerotic plaques[93].

1.10 Statins

Some of the most commonly prescribed drugs to prevent and treat cardiovascular disease are 3-hydroxy-3-methylglutaryl coenzyme A (HMG-CoA) reductase inhibitors (statins) which are the most important and most widely prescribed class of lipid and cholesterol lowering drugs [94,95].

HMG-CoA reductase catalyses the rate-limiting step in the biosynthesis of cholesterol, and thus inhibition leads to a decrease in cholesterol and in a reduction in atherogenic events [94]. The first statin drug, mevastatin, was discovered in the 1970s and was shown to inhibit hepatic cholesterol synthesis through inhibition of HMG-CoA reductase (Fig. 6) [96].

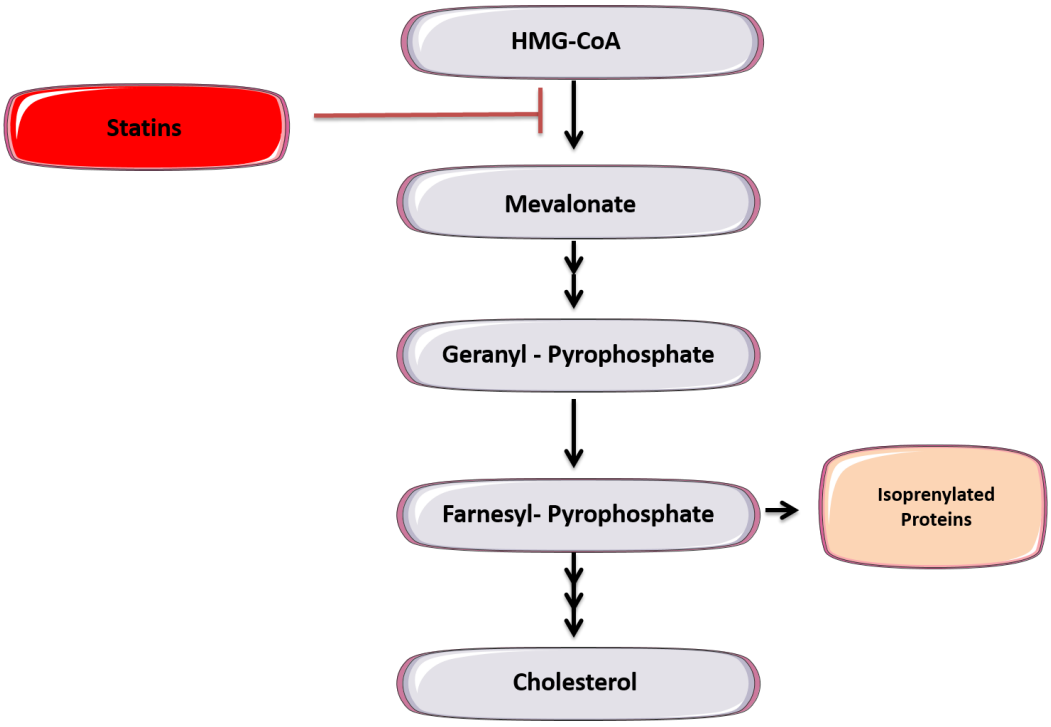

Fig. 6 – The mode of action of statins. This family of drugs competitively inhibit the conversion of 3-hydroxy-3-methylglutaryl coenzyme A to mevalonate with an end reduction in cholesterol.

The first statin that was approved for clinical use was lovastatin which was approved by the U.S. Food and Drug Administration (FDA) in 1987 [95]. Since then there have been several more statins identified, with seven of them being approved for clinical application to date. These statin drugs can be classified by their origin, either from a natural source or obtained through chemical synthesis [95]. Natural statins are commonly derived from fungal metabolites and include lovastatin, pravastatin and simvastatin [97]. The newer synthetic compounds are markedly different in their chemical structure from the natural statins but they retain the HMG-CoA-like structure which is responsible for the HMG-CoA reductase inhibition [98].

Statins function by competitively inhibiting HMG-CoA reductase which subsequently lowers cholesterol production [96]. Statins have a much higher affinity for the active site of HMG-CoA reductase than its substrate HMG-CoA and therefore are potent inhibitors [99]. As well as preferentially occupying the active site of HMG-CoA reductase, statins alter the conformation of the enzyme. This prevents HMG-CoA reductase from attaining a functional structure and further inhibits the pathway [100].

Following the reduction in hepatocyte intracellular cholesterol concentration, there is an increase in the expression of hepatic LDL receptors. The increase in LDL receptors leads to enhanced clearing of LDL and its precursors from the circulation [95].

Statins have also been shown to decrease VLDL synthesis through the inhibition of Apolipoprotein-B100 (Apo-B100) production. This is achieved by limited lipidation of Apo-B100, leading to increased degradation. Apo-B100 is involved in VLDL synthesis, alongside cholesterol esters, triglycerides and phospholipids, and thus a decrease in Apo-B100 leads to the inhibition of VLDL synthesis [101]. A reduction in VLDL synthesis also leads to a reduction in triglycerides, which can be seen in patients treated with atorvastatin, cerivastatin, and pitavastatin [102].

As well as having inhibitory effects on the formation of VLDL, LDL, triglycerides and cholesterol, statins have also shown upregulatory effects on HDL and apolipoprotein A-I [103]. Interestingly statins are shown to increase apolipoprotein A-I through activation of its promoter and suppressing the Rho signalling pathway, through inhibiting the production of isoprenoid intermediates [102]. Apolipoprotein A-I is the main component of HDL and therefore its upregulation leads to a higher concentration of HDL. The upregulation of HDL leads to another

key mechanism which is aided by statins. Reverse cholesterol transport whereby cholesterol is actively taken up by the liver via a multistep process from the plasma requires HDL and lecithin:cholesterol acyltransferase. These esterify the cholesterol so that it can be taken up by the liver and excreted into bile [104].

Endothelial function is known to be improved by lowering cholesterol levels, as hypercholesterolemia reduces the production and increases the degradation of endothelial derived nitric oxide [105]. Through lowering cholesterol levels statins cause an increase in nitric oxide levels which are important for proper endothelial function [106].

In addition to having lipid and cholesterol lowering effects statins can also improve cardiovascular events through actions independent of cholesterol lowering. These actions are known as pleiotropic effects of statins and have provided new insights and potential treatments for a variety of diseases, including Alzheimer's, rheumatoid arthritis and cancer [95].

The pleiotropic effects are commonly mediated by statins inhibition of mevalonate synthesis, which blocks the synthesis of isoprenoid intermediates, such as farnesyl pyrophosphate (Fig. 6) [107], and leading to accumulation of inactive GTP-binding proteins in the cytoplasm. These small GTP-binding proteins include Rho, Rac, Ras, Rap and Ral which are important substrates for the post-translational modification by prenylation [94] and have a vital role in cellular signalling events including controlling proliferation, migration, and apoptosis. As well as inhibition of mevalonate synthesis, statins have been found to alter other signalling pathways including the activation of Akt through phosphorylation. The exact mechanism of this has not been elucidated however it is known to be mediated by the PI-3-kinase pathway [108,109]. The activation of AKT has been

linked to an increase in endothelial nitric oxide synthase (eNOS) production, which can be attributed to a more healthy endothelium [109].

Simvastatin and lovastatin have been shown to increase the transcriptional activation of eNOS gene in human endothelial cells *in vitro* [110] . This occurs through an increased polyadenylation of the eNOS mRNA transcript, leading to post-transcriptional stabilisation of the mRNA[111]. The increased polyadenylation is due to the inhibition of the Rho signalling pathway affecting the actin cytoskeleton [111]. Statins have also been shown to activate the PI-3-kinase/Akt pathway, which also leads to an increase in eNOS expression. Statins also have post-translational upregulatory mechanisms for eNOS upregulation, commonly mediated through phosphorylation of serine and threonine residues [112].

In addition to inhibiting the isoprenylation of the GTP-binding proteins, statins are also known to exert their pleiotropic effects through affecting the lipid rafts. Statins may disrupt or deplete lipid rafts, affecting further signal transduction [113].

As well as increasing nitric oxide levels, statins are also able to reduce inflammatory cell infiltration into atherosclerotic lesions through inhibiting adhesion molecules such as ICAM-1 [114], VCAM-1 and E-selectin [115] which is an important step in preventing the progression of the plaque.

The prevention of inflammatory cells from binding and infiltrating into the plaque is not the only mechanism of lowering inflammation. Statins can also alter the expression of chemokines, such

as interleukin-8 and monocyte chemoattractant protein-1 which control leukocyte migration to the plaque [116].

Statins' pleiotropic effects are not limited to affecting endothelial function as they also decrease vascular smooth muscle cell and macrophage proliferation [117,118], reduce the activity of platelets [119], stabilise atherosclerotic plaques [120], and act as an antioxidant [121]. Through inhibiting signalling through the Rho pathway, statins have been shown to have beneficial effects in inhibiting cardiac hypertrophy [122]. Furthermore, their wide-ranging effects do not only impact cardiovascular health, but are able to also reduce MHC class II molecules via inhibiting their transcription [123]. Recent evidence suggests that statins are able to increase the degradation of proteins, including HIF1α, through increasing their ubiquitination [124]. This has implications for treatment of diseases such as atherosclerosis and cancer where HIF1α plays a role in their pathophysiology.

The pleiotropic effects can be biphasic, whereby different concentrations of statins result in different effects. This is the case for atorvastatin, as cell migration and angiogenesis was increased with concentrations lower than 0.1μmol, but inhibited at higher concentrations [125]. These complex pharmacokinetics of statins make them a subject of intense research and are, for the most part, still not well understood.

The biphasic effects could be due to a switch mechanism whereby at low dose concentrations activation of genes occurs, but at higher doses an inhibition of the isoprenoid intermediates and other factors leads to a decrease in activity. This can be related to the process of angiogenesis whereby at low statin concentrations eNOS can be activated leading to increased angiogenesis,

but at high statin concentrations reduction of isoprenoid intermediates and other angiogenic proteins leads to inhibition of angiogenesis [126].

The effects of statins have been assessed in clinical trials which have revealed some interesting effects in reducing the risk of coronary heart disease (CHD) events. The West of Scotland Coronary Prevention Study (WOSCOPS) and the Air Force/Texas Coronary Atherosclerosis Prevention Study (AFCAPS/TEXCAPS) evaluated the effects of statins in groups that had no previous evidence of CVD. These studies showed that statins reduce the risk of major CHD events in patients with high and normal LDL-cholesterol levels [95]. The Scandinavian Simvastatin Survival Study (4S) shows a 42% reduction in total mortality amongst patients with coronary artery disease that were taking 20 or 40mg/day simvastatin as well as a 34% reduction in coronary events [127].

1.11 Simvastatin

Simvastatin was first produced by Merck using the name ZOCOR® and was approved by the U.S. FDA in 1998 [128]. In 2006, after the term of the patent expired simvastatin was added to the World Health Organisations (WHO) list of essential medicines [129] and since then it has become one of the most commonly prescribed statin drugs with 67% of statin prescriptions in the UK being for simvastatin in 2007 [130].

Simvastatin is a semi-synthetic compound as it is of fungal origin, but contains a chemical modification of the lovastatin side chain [98] whereby the 2-methylbutanoyl side chain is replaced

by a 2,2-dimethylbutanoyl side group (Fig. 7) [131]. It is a hydrophobic statin and is able to pass through cell membranes non-specifically through a simple diffusion mechanism[132].

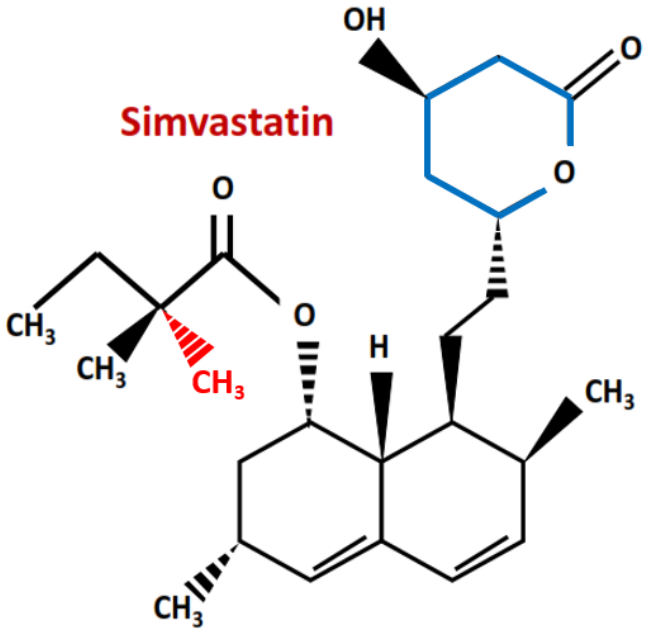

Fig. 7 – The chemical structure of simvastatin. The modified 2,2-dimethylbutanoyl side group shown in red and lactone ring in blue.

The average daily dose of simvastatin to treat cardiovascular diseases is 20-40mg with a maximal dose of 80mg [133]. Simvastatin is administered as an oral dose in a pro-drug form, whereby the lactone ring undergoes reversible hydrolysis to form the active simvastatin acid (Fig. 7) [134]. As with most drugs once administered, simvastatin is concentrated in the liver whereby it is metabolised by the cytochrome P450 3A4 pathway. The majority of simvastatin is retained in the liver and the circulating concentration is low, with only 5% of active simvastatin detected in the circulation [100]. This is common for all of the statins but simvastatin and lovastatin have the lowest detectable concentration in the circulation [100].

Simvastatin is known to greatly reduce cholesterol and to improve cardiovascular functioning [127]. It also has beneficial effects seen for other diseases whereby it has shown to prevent the growth of breast cancer [135], affect apoptosis in cancer cells [136] and reduce inflammatory arthritis [137]. It is therefore a statin that has been widely used in research. Although simvastatin has been shown to have beneficial effects in treating cardiovascular disease, it also has significant side effects with myalgia, jaundice and hypersensitivity being some of the listed complications of using the drug [133]. Furthermore, simvastatin has been shown to have teratogenic effects when taken during the first trimester of pregnancy, with adverse effects seen in the migration, proliferation and apoptosis of trophoblastic cells [138].

Simvastatin has been shown to affect angiogenesis whereby it can both promote angiogenesis in ischaemic myocardium, but also inhibit angiogenesis in the aortic arch [139]. This in part has been attributed to a decrease in HIF1α levels of samples treated with simvastatin [139]. Further studies on simvastatin's effect on HIF1α have speculated that alongside other statins it is able to inhibit the binding of HIF1α to the HRE of platelet-derived growth factor B and endothelin-1 [140].
It is known that patients that take simvastatin are less liable to plaque rupture, which are plaques that are characteristically defined by having a thin fibrotic collagen cap. It has been shown that a mechanism for this is simvastatin's ability to increase the expression of prolyl-4-hydroxylase-1-α which is involved in collagen synthesis [141]. Simvastatin has also been found to affect the expression of matrix metalloproteinases (MMPs) [142], which are key components of the plaque causing tissue degradation and potential instability. Key MMPs which have been identified as having their expression levels decreased by simvastatin are MMP3 [143], MMP9 [144,145] and MMP14 [146]. This shows that simvastatin may have a role in increasing plaque stability through inhibiting the production of MMPs.

1.12 Matrix Metalloproteinases

The matrix metalloproteinases (MMPs) are a family of at least 23 secreted or cell surface zinc-dependent enzymes that are capable of degrading ECM proteins, clotting factors, cell adhesion molecules, lipoproteins and growth factors [147] and seem to influence almost every aspect of mammalian biology [148]. Also known as matrixins, the MMPs have 24 identified genes in man, but there is a duplicated MMP23 gene. Some MMPs are excluded from the nomenclature list as they were shown to be identical to other identified MMPs [149].

Most MMPs generally have low activity levels in normal steady-state tissues [149], with their expression primarily regulated at the transcriptional level by a variety of growth factors, chemical inducers, physical stress, inflammatory cytokines, hormones, cell-to-cell, and cell-to-matrix interactions [149,150]. MMPs are mainly secreted or membrane bound proteins, commonly activated extracellularly, but there is evidence that some MMPs are activated intracellularly where they can interact with other intracellular proteins [151].

The majority of MMPs are not constitutively expressed and instead are induced according to their physiological or pathophysiological roles. Transcriptional regulation is an important regulatory step in controlling MMP expression. The regulation can occur via histone acetylation and deacetylation [152], DNA methylation [153], as well as by transcription factors binding to specific *cis*-regulatory elements within the promoter region of the genes [154].

The binding of transcription factors to relevant *cis* elements is a main regulatory step of transcriptional control of MMPs. MMPs contain several *cis*-regulatory elements in their

promoter regions which allow regulation by activators such as, Sp-1, AP-1, PEA3, β-catenin, and NF-kB [154]. The MMPs can be split into three groups according to the *cis*-elements contained in the gene promoter region. Most of the MMPs contain both a TATA box and an AP-1 binding site and are classified into the first group. The second group includes *MMP8*, *MMP11*, and *MMP21*, which contain a TATA box but do not have the AP-1 binding site [154]. The final group does not contain a TATA box and includes *MMP2*, *MMP14* and *MMP28*. This group is mainly regulated by the SP-1 family of transcription factors as well as containing other *cis*-elements such as HRE's and AP-2 sites [154].

Histone acetylation is another method of gene regulation used to control MMP expression. This process involves the reversible unravelling of DNA binding to histone proteins. This allows the transcription factors to access the DNA regulatory elements more easily. The acetylation process is controlled by the histone acetyltransferases (HATs) whilst deacetylation is controlled by the histone deacetylase (HDACs). Histone deacetylation is an inhibitory step which binds the DNA back to the histones, preventing the genes from being activated [152]. It has been shown that the use of HDAC inhibitors can either repress or activate the expression of different MMPs at both the mRNA and protein level [155].

Some MMPs undergo DNA methylation in order to control their gene expression. DNA methylation occurs at CpG islands within the promoter regions of genes and is governed by DNA methyltransferases. The methylation occurs at cytosine residues and further prevents the binding of DNA transcription factors to gene regulatory elements. *MMP9* has been shown to be affected by DNA methylation in lymphoma cells with increased DNA methylation being inversely correlated with the gene's expression in these cells [153]. As well as *MMP9* it has also been seen

that MMP3 is controlled by methyltransferases with the knockout of methyltransferases increasing *MMP3* expression in colon cancer cells[156].

In addition to the transcriptional regulation of MMPs, there is also a wealth of factors that regulate them at the post-transcriptional level. These include activation and inhibition by other proteins, such as α2-macroglobulin and tissue inhibitors of MMPs (TIMP), and miRNA, such as microRNA-146b which has been shown to downregulate MMP16 in glioma [157]. The activity of MMPs is also dependent on temporal and tissue specific cleavage of MMP zymogens [158]. Most MMPs are synthesized as zymogens with the capability of being activated by other MMPs. Some MMPs, particularly the membrane type MMPs, have a furin activation domain [149]. This area is targeted by a furin molecule which cleaves the MMP and removes the pro-peptide. There are also other less specific inhibitors of MMPs including the more general protease inhibitor α2-macroglobulin, the membrane bound glycoprotein RECK [159], as well as thrombospondin [160]. Other synthetic inhibitors of MMPs, such as tetracycline, prevent the zinc cofactor from binding and are non-selective inhibitors of MMPs [161].

As well as being regulated by activation, MMPs are also influenced by TIMPs which inhibit activated MMPs and are their key regulators and inhibitors at the protein level [147]. So far, there have been four TIMPs identified and shown to affect MMPs with different affinities. Like MMPs, TIMPs are regulated at the level of transcription by growth factors, cytokine and chemokines and also respond to stimuli at the transcription level [155].

The four TIMPs are in general broad-spectrum inhibitors of MMP activity but there are some notable differences in specificity between them. It has been seen that TIMP1 has more of a

restricted inhibition range than the other TIMPs with a low affinity for the MT-MMPs and MMP19 [162]. As well as this there are some differences in the affinities of other TIMPs with MMPs, such as TIMP2 and TIMP3 which are weaker inhibitors than TIMP1 for MMP7 [163].

The mechanism of TIMP inhibition of MMPs has been discovered by the use of crystallography where it has been seen that the TIMPs overall structure is “wedge-like” which is able to interact with active site of the MMPs by forming a non-covalent 1:1 stoichiometric complex [149]. The inhibition is reversible but is resistant to heat denaturation and proteolytic degradation [164]. TIMPS are therefore key regulators of the MMPs but they have also been shown to have important roles in MMP activation, such as TIMP2 which is an important cofactor in the activation of MMP2 by MMP14 [155].

The roles of TIMPs alongside MMPs are well characterised but they are also known to have biological activities that are independent of MMPs. TIMPs are able to modulate cell proliferation, cell migration, apoptosis and invasion whilst also exerting anti-angiogenesis abilities. These activities may be partly due to MMP inhibition but many of them have been shown to be independent of MMP inhibition, such as interacting directly with cell specific receptors in order to induce cellular responses [162].

More specifically it has been shown that TIMP1 promotes cell growth in keratinocytes and fibroblasts [165,166]. It has also been found that TIMP1 and TIMP2 increase the expression of Ras-GTP utilising different signalling pathways. TIMP1 activates the MAPK pathway and TIMP2 can signal via the PI3K pathway [167].

It is well established that TIMPs are able to attenuate angiogenesis through the inhibition of pro-angiogenic MMPs, such as MMP9 and MMP14. However, TIMP2 and TIMP3 have been found to exert anti-angiogenic activity independent of their MMP inhibitory activities, thus enhancing their importance for diseases such as cancer and atherosclerosis [168].

The importance of TIMPs in cardiovascular disease has been shown through analysis of patients plasma following acute myocardial infarction whereby elevated TIMP1, TIMP2 and TIMP4 levels were noted [164]. Studies on mice have shown that both TIMP1 and TIMP3 deficiency lead to cardiovascular disease progression. Mice that lack TIMP1 expression have smaller atheromas but have increased aneurysm formation [169]. As well as this it has been shown that TIMP3 deficiency in mice leads to disrupted matrix homeostasis with spontaneous left ventricular dilation, cardiomyocyte hypertrophy and contractile dysfunction [170]. The balance between MMPs and TIMPs is critical for the ECM remodelling and cellular functioning and therefore it is vital that these processes are tightly controlled [149].

The identification of MMP structure has been achieved through the use of X-ray crystallography [149]. The MMPs have a common domain structure with a signal peptide, a propeptide of about 80 amino acids, a catalytic metalloproteinase domain of about 170 amino acids, a hinge region of variable lengths and, a C-terminal haemopexin domain of around 200 amino acids (Fig. 8) [149,155]. The catalytic metalloproteinase domain contains a zinc binding motif, HEXXHXXGXXH, which activates the MMP upon the co-factor's binding. Preceding this site is a conserved methionine residue, which forms a "Met-turn". This supports the active site structure around the zinc ion [171]. The propeptide domain contains a cysteine switch motif, PRCGXPD, which inhibits the binding of the catalytic zinc ion to the zinc binding motif through an unpaired cysteine residue.

This keeps the MMPs inactive by preventing a water molecule from binding to the zinc ion which is essential for catalysis [149]. Activation of the MMP occurs when the cysteine-zinc linkage is disrupted through cleavage of the propeptide by proteolytic cleavage [148].

The propeptide contains a proteolytic cleavage site which is used to activate the pro-MMP into an active MMP. Serine proteases, opportunistic bacterial proteinases and other MMPs are able to enzymatically cleave the propeptide to form the active enzyme [149,172]. Partial cleavage of the propeptide is common and often requires completion by the MMP intermediate itself, or by other active MMPs. This process has been termed "stepwise activation" due to the incomplete nature of the first cleavage [149]. Once the propeptide domain has been removed a conformational change occurs which exposes the catalytic domain to the ECM substrate [172]. This catalytic domain is conserved with a high degree of homology between the MMPs and therefore does not play a role in substrate specificity [172]. There is a substrate specific pocket, known as the S1' pocket, which varies in depth and is located to the right of the zinc atom. This pocket is hydrophobic in nature and is one of the determining factors of substrate specificity in MMPs [149].

In all of the MMP family members except MMP7, MMP23 and MMP26, a hinge region links the catalytic domain to the c-terminus haemopexin-like domain (Fig. 8) [155]. The haemopexin domain structure has been identified as comprising of a four-blade-β-propeller [173]. This domain has a key role in substrate specificity, binding to ECM proteins on the basis of the sequence at the C-terminus [155]. It is also the region which is inactivated by the binding of TIMPs which locate to and competitively block the active site of the MMP [149].

The membrane type MMPs (MT-MMPs) contain a few distinct features which differ from the rest of the MMPS including the presence of a transmembrane spanning domain, or a glycosylphosphatidylinositol anchor, with a potential furin cleavage site located within the propeptide domain (Fig. 8). The furin cleavage site is a potential mechanism to activate the MT-MMP prior to its secretion [155].

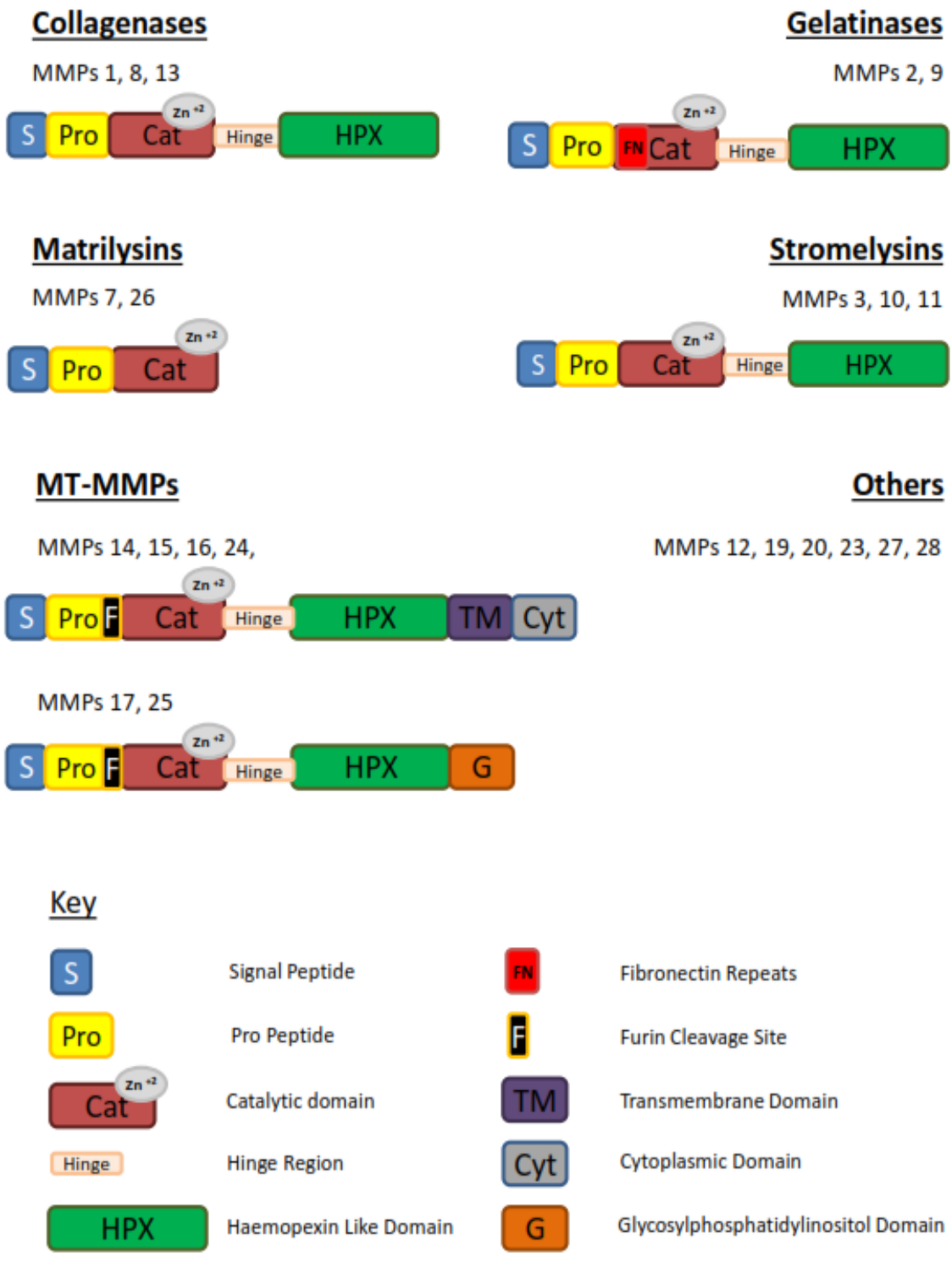

Fig. 8 – The structure of the MMPs categorised by their functional classification.

MMPs are traditionally subdivided into different groups, the collagenases, gelatinases, stromelysins, matrilysins and membrane-type, determined by substrate specificity, structure and cellular location [155]. The collagenases cleave interstitial collagens I, II, and III three quarters of the way to the N-terminus providing two distinct fragments[151]. In addition, the collagenases are able to cleave some other ECM molecules and soluble proteins. The stromelysins have a similar structural arrangement to the collagenases but they are unable to cleave the interstitial collagens. As well as cleaving some ECM components the stromelysins also cleave and activate a number of pro-MMPs[151]. The gelatinases include MMP2 and MMP9 and are able to digest gelatins as well as other ECM molecules including type IV, V and XI collagens and laminin [149]. They contain a distinct fibronectin repeat in their catalytic domain. The matrilysins are easily identified as they lack the C-terminal haemopexin domain. Alongside the cleavage of ECM components the matrilysins are able to cleave cell surface molecules including E-cadherin, Fas-ligand and pro-tumour necrosis factor a [149]. The MT-MMPs are anchored to the membrane either through a transmembrane domain or a glycosylphosphatidylinositol anchor (Fig. 8). They are capable of activating other MMPs, such as MMP2, as well as cleaving the ECM components[151].

The MMPs were originally thought to be primarily involved in cleaving ECM substrates and in maintaining ECM homeostasis but it is now recognised that they have much more complex functions [155]. These include regulating cell growth, regulation of apoptosis, affecting cell proliferation, migration, invasion and metastasis, cleaving adhesion molecules, enhancing angiogenesis and vascular permeability and modulating inflammation and immunity [174]. Some of these functions are due to MMPs role in ECM homeostasis which alters other interactions. The breakdown of ECM molecules and cell surface molecules alters cell-matrix and cell-cell

interactions. The breakdown of the ECM releases bound growth factors allowing receptors to be activated [149]. More recently however, there has been evidence that as well as extracellular targeting, MMPs may also have an intracellular role, with some MMPs also containing a nuclear localisation signal [175]. As well as this, a number of non-ECM molecules are also substrates for MMPs, including other MMPs, which can lead to further signalling cascades. Many of these substrates are important for MMPs' mediating functions such as cell migration, differentiation, angiogenesis and inflammation [149].

Similarly, due to their function in the aforementioned processes, MMPs have been associated with disease progression. Research into the role of MMPs in cancer has been ongoing with the identification that MMPs are important in many processes involved in the progression of cancer including cell metastasis [176], invasion [177], and angiogenesis [178]. MMPs were therefore identified as a potential target for therapy due to their ability to prevent progression of cancer. MMP therapeutics however were unsuccessful in clinical trials as some MMPs have contradictory effects at different stages of cancer progression [179] with some MMPs leading to tumour progression, and others exerting anti-tumour functions [180]. MMPs also act in a signalling cascade either by activating or inhibiting other MMPs, therefore targeting MMP activity and expression may lead to an imbalance of other MMPs.

In addition to cancer, MMPs have been identified to be contributors to other disease processes including diseases of the central nervous system [181], asthma and chronic obstructive pulmonary disorder [182], and inflammatory conditions such as arthritis [183], and cardiovascular disease [147,149]. It has become clear that MMPs play an important role in the progression of atherosclerosis with all of the classes of MMPs as well as TIMPs being expressed in areas of atheromas [90].

Observational studies have shown both the mRNA and enzymatic forms of the MMPs to be present in the atheromas, with a potential role in plaque disruption suggested [18].

The collagenases play a predominant role in the atherosclerotic plaque with all three of the collagenases showing expression. MMP1 has been shown to be expressed in the fibrous cap and shoulder regions of the atherosclerotic regions [90,184]. MMP13 expression is localised to endothelial and smooth muscle cells within the lesion itself [185]. MMP8 has also been shown to be expressed in atheromas, predominantly at the fibrous cap where there is a rich abundance of collagen I and III [186]. This may suggest that the collagenases are associated with plaque vulnerability through degradation of the fibrous plaque. The collagenases, however, are not just associated with lesion instability. Research shows that MMP8 has an active role in atherosclerosis progression. This has been seen in *MMP8* null mice, having a reduced amount of atheromas containing a denser proportion of collagen when *MMP8* is knocked out[187]. MMP8 has also been attributed to increasing angiogenesis and therefore may provide a potential mechanism for neovessels to form in the atherosclerotic plaque [188].

The gelatinases are amongst the most researched of the MMPs in relation to atherosclerosis and are known to be highly expressed in the fatty streaks and shoulders of the plaque [90,189]. The identification of the gelatinases in the fatty streaks suggests that they may be involved in the formation of the atheroma [189].

The stromelysins, represented in the atherosclerotic plaque by MMP3, have been shown to be present in smooth muscle cells and macrophages within the atheroma. MMP3 is therefore suggested to be involved in the growth of the plaque as well as their destabilisation [190].

MMP7 expression has been demonstrated in atherosclerotic lesions, particularly associating with macrophages, and is suggested that it may cleave proteoglycans and destabilise the cap [191]. Studies of *MMP7* knockout mice showed little effect on atheroma development and stability, but there was an increase of smooth muscle cells within lesions as well as an increased rate of apoptosis [192]. This suggests that MMP7 has an important role in vascular smooth muscle cell recruitment and necrotic core development.

An interesting finding was that plaques that have a thinner cap tend to have higher levels of *MMP1*, *MMP3*, *MMP7* and *MMP12* mRNA. As well as this plaques that have ruptured have a much higher level of MMP12 [193]. It is also interesting that hypoxia has been shown to upregulate several MMPs, including MMP7 and MMP14 [194,195].

MMP14 can be detected in both normal and atherosclerotic arteries, with a particularly high expression seen in macrophages, foam cells and in vascular smooth muscle cells of atherosclerotic lesions [196,197]. The high expression in of this protein these cells may cause plaque disruption when activated by pro-inflammatory mediators [196,197].

MMP14 is of increasing interest in relation to atherosclerosis as it has been found to be able to promote angiogenesis [198,199], activate other MMPs within the atherosclerotic plaque [200–202] and lead to plaque instability. These findings show that MMP14 is an important molecule in the pathogenesis of atherosclerosis.

1.13 Matrix Metalloproteinase 14

MMP14 was first identified in 1994 by Sato *et al* and was the first known member of the membrane type metalloproteinases, also known as MT1-MMP. It was shown to activate MMP2 and have a potential role in tumour invasiveness [200]. MMP14 was found to be a protein of 582 amino acids in length and to encode a protein of 63-66kDa [200]. Further studies of the human genome has led to MMP14s gene being mapped to chromosome 14q11-q12 [203–205], which is similar to that of the mouse genome [206].

Many studies on the transcriptional control of MMP14 have been investigated in the context of cancer. These studies have shown that MMP14 is transcriptionally controlled by Krüppel-like factor 8 [207]. It is also shown that the MMP14 promoter is under Sp1 transcriptional regulation and also contains HRE sites which are activated by HIF2α [208]. In endothelial cells it has been shown that MMP14 is regulated by Egr1 and Sp1, which bind to a GC-rich sequence at position -288 to -275 from the start of transcription [209,210].

MMP14 is expressed on the surface of many cell types including macrophages, endothelial cells, smooth muscle cells, cardiac myocytes and epithelial cells [211]. Like the other MT-MMPs, MMP14 contains a furin cleavage site, characterised by the conserved Arg-Arg-Lys-Arg-Arg sequence between the pro-peptide and catalytic domains [212] (Fig. 8). MMP14 is activated by furin which cleaves the pro-peptide and the catalytic domains between an Arg^{111} and Tyr^{112} resulting in the pro-peptide and the activated MMP14 protein [212]. It has been shown that the activation of MMP14 by furin occurs intracellularly after its release from the golgi apparatus [213]. Another regulator of MMP14 is cell-ECM interactions whereby it has been shown that stretched cardiac

fibroblasts have an increase in MMP14 expression at both the mRNA and protein levels [214]. Activated MMP14 can homodimerise on the cell surface through the haemopexin domain [215]. It is found that this homodimerisation and activation is between the β-Blades IV and I [216].

TIMPs are known to inhibit MMPs and have been seen to do so with different affinities. TIMP1 is the only TIMP so far identified to be a poor inhibitor of all the MT-MMPs [217,218]. As well as playing a role in the inhibition of MMP14, TIMP2 is able to complex with MMP14 to activate pro-MMP2. MMP14 is functionally associated with MMP2 in that MMP14 is able to activate the pro-MMP2 zymogen to form the fully functional MMP2, which is important for cell invasion and growth [200].

MMP14 acts as a cell surface receptor for TIMP2, which forms a complex that binds to pro-MMP2 [219]. TIMP2 binds to the catalytic site of MMP14 using its inhibitory N-terminal domain [220]. The pro-MMP2 molecule then binds to the C-terminal domain of TIMP2 via the haemopexin domain. In order to be activated another MMP14 molecule needs to be in close proximity to this complex and be free of a TIMP2 molecule, which is facilitated by the ability of MMP14 to homodimerise through the haemopexin domain [215].

The MMP14-TIMP2-pro-MMP2 complex is only able to process the pro-MMP2 into an intermediate protein. In order to become fully activated the pro-MMP2 molecule has to undergo self-autolytic cleavage [221]. In order for the activation of MMP2 to be effective there has to be a fine balance in the concentration of TIMP2. Excessive levels of TIMP2 results in an inhibitory effect as the activator complex cannot be formed [221,222].

As well as activating MMP2 there are other MMPs that MMP14 is able to activate, such as MMP8 and MMP13, either on its own, or in a cascade involving MMP2 [201,202]. MMP14 also has a broad ECM substrate specificity with important roles in degrading components including type I, II, and III collagens as well as fibronectin, gelatin, proteoglycan, vitronectin, laminin-1, and fibrin [223,224].

MMP14 knockout mice have been developed to characterise more clearly the function of MMP14. It has been shown that the *MMP14* knockout mice display skeletal abnormalities and defective vasculature which can be detected 3-5 days after birth [199,225]. The skeletal abnormalities include dwarfism, arthritis, craniofacial dysmorphism, osteopaenia, and fibrosis of soft tissues. This has been attributed to the lack of collagenolytic activity which is necessary for the modelling of skeletal and connective tissues [225]. The knockout mice commonly die approximately 3 weeks after birth when their body weight is 30-40% of their wild-type litter mates[199]. MMP14 is expressed in the osteoclasts [226], highlighting its importance in the bone development [227]. MMP14 is also highly expressed in developing vascular tissues, kidney cells and muscle tissue in the developing mouse embryo [206].

MMP14 is located on the surface of cell membranes which means that it is able to directly clear ECM components in the path of the cell. However, its role in cell migration is not just limited to remodelling the ECM, but also by releasing growth factors in the ECM [228], processing cell adhesion molecules [229] and activating other MMPs. It has been found that MMP14 is important in the lung development, where it is a downstream signalling molecule of EGFR [230]. The epithelial branch formation within the lungs is also incomplete when *MMP14* is knocked out which has been attributed to a lack of ECM cleavage for the formation of the branches [230].

MMP14 was first identified as being involved in tumour cell invasion [200] but it is now clear that MMP14 has roles in many diseases as diverse as asthma [231], obesity [232] and arthritis [233]. As well as this, MMP14 has been found to be an inducer of angiogenesis [234].

The defective vasculature seen in *MMP14* knockout mice showed that MMP14 has a vital role in vasculogenesis and indicated a role in angiogenesis [199]. One of the ways in which MMP14 can promote angiogenesis is through increasing the expression of VEGF [234]. VEGF is not the only factor that MMP14 exerts an effect on to increase angiogenesis. Semaphorin 4D is a ligand that when processed can bind to plexin-B1 and promote tubulogenesis. MMP14 is able to process inactive semaphorin 4D into its soluble form, and promote angiogenesis [235]. MMP14 is also able to cleave ECM components allowing a path for invasion of new tubules [198].

MMP14 expression has been detected in the atherosclerotic plaque with high expression seen in smooth muscle cells, macrophages and endothelial cells [196,236]. This expression is markedly increased in hypoxic conditions, which has been shown in hepatoma cells [195], and in choroid retinal endothelial cells of monkeys [237]. It has also been shown that HIF1α increases MMP14 expression in cancer cells, whereby siRNA targeting HIF1α caused a marked decrease in MMP14 expression [238,239].

As discussed previously, atheromas develop hypoxic areas as their size and necrosis increases, leading to an increase in MMP14 levels. The *MMP14* gene contains two putative HRE's in the promoter region showing that hypoxia is a likely regulator of its expression [208]. An increase in MMP14 expression leads to an increase in VEGF expression [234,237] and, subsequently, neovascularisation of the plaque. As well as leading to increased neovascularisation, enhanced

MMP14 expression can destabilise the atheromas through the ECM cleaving properties of MMP14. Vulnerable plaques show a marked increase in MMP14 expression compared to stable plaques which shows the importance of MMP14 in the pathogenesis of atherosclerosis [240].

1.14 Summary

With atherosclerosis being a major contributor to worldwide morbidity and mortality, and predicted to increase further still, there is an ever growing need to understand the molecular mechanism governing the development of atheromas. Simvastatin is commonly prescribed to patients with cardiovascular disease and is known to stabilise atheromas through preventing rupture and neovascularisation by decreasing HIF1α and levels of certain MMPs [139,142]. With MMP14 expression being located in atherosclerotic plaques, and having increased expression through hypoxic activity, a role for simvastatin could be to reduce MMP14 activity either directly, or through inhibition of HIF1α. MMP14 expression is known to be reduced by simvastatin treatment [146] but a link with hypoxia and HIF1α has not been established. Elucidating these links may provide valuable insights into improved drug targeting strategies.

My project involves identifying a potential regulation of MMP14 expression by HIF1α in vascular endothelial cells. In particular, the effects of simvastatin on angiogenesis via HIF1α and MMP14 activity using *in vitro, ex vivo* and *in vivo* models will be explored. This will provide new insights into MMP14 gene regulation in angiogenesis and atherosclerosis and further knowledge into the beneficial effects of simvastatin treatment, whilst offering new opportunities for drug development.

1.15 Hypothesis

HIF1α binds to the MMP14 promoter in hypoxic conditions upregulating MMP14 activity, which is attenuated by simvastatin. HIF1α depletion and simvastatin will attenuate angiogenesis through inhibiting MMP14 in a HIF1α-dependent manner.

1.16 Project aims

1. To characterise HIF and MMP14 co-localisation in blood vessels in atheromas
2. To study the role of the HIF-response elements in the MMP14 gene promoter region
3. To assess the effect of HIF on MMP14 expression in endothelial cells
4. To study the effects of statins on hypoxia-induced MMP14 expression and angiogenesis

2. Materials and Methods

For the formulation list of the buffers used in the method section please see Appendix I.

2.1 Ethical Clearance

All experiments involving human tissue were carried out under the relevant ethical clearance number 08/H0704/140, approved by the East London & The City REC Alpha.

2.2 Cell Culture

To maintain sterility all cell work was conducted in a laminar flow hood which was disinfected regularly with 70% ethanol and sterilised using an ultraviolet light. The work on human cells was approved by the responsible ethics committee.

2.2.1 HUVEC Supplements

A cocktail of supplements proven to aid the growth of HUVECs when added to the culture media [241] were used. The HUVEC supplements were made by dissolving heparin sodium salt, thymidine, endothelial cell growth supplement and β-endothelial human cell growth factor (Sigma Aldrich, UK) in Medium 199 (Sigma Aldrich, UK) to a 100X stock solution in a 1ml aliquot. Thymidine and heparin sodium salt were dissolved in double distilled water to stock solutions with concentrations of 50mg/ml and 10,000 units per ml, respectively. A thymidine and heparin

sodium salt solution was prepared by sterile filtering 500µl of thymidine and 10ml of heparin sodium salt stock solutions through a 0.22µM membrane, producing final concentrations of 25mg per ml of thymidine and 10,000 units per ml of heparin sodium salt. Three 15mg vials of endothelial cell growth supplement and one vial 25mg β-endothelial human cell growth factor were dissolved in the thymidine and heparin solution to final concentrations of 4.5mg per ml and 2.5mg per ml respectively. Medium 199 was added to make the final volume of the 500X HUVEC supplement stock to 20ml, before aliquoting into 1ml aliquots and storing at -80°C until use.

2.2.2 HUVEC Cell Culture

Human umbilical vein endothelial cells (HUVEC) were used for the cell based experimental procedures. The cells were isolated by the Department of Biochemical Pharmacology at the William Harvey Research Institute, from umbilical cords donated by patients from the maternity ward at the Royal London Hospital, and commonly supplied at passage one. The cells were grown on 0.04% gelatin coated flasks in M199 Media (Sigma Aldrich, UK) supplemented with one aliquot of 500X HUVEC supplements, 100units per ml of penicillin, 0.1mg/ml streptomycin solution, 2mM of glutamine and 15% foetal bovine serum (FBS). The cells were incubated at 37°C with 5% CO_2 for optimal growth conditions. The cells were washed in sterile autoclaved phosphate buffered saline (PBS) [242] (Appendix I), and media was changed every two to three days. The cells were identified as endothelial by their characteristic cobblestone morphology.

2.2.3 Passaging of HUVECs

When the HUVECs were 80% confluent the cells were passaged in a 1:4 or 1:6 ratio as described below. The HUVECs were washed with sterile PBS before the addition of 0.25% trypsin-EDTA solution (Sigma Aldrich, UK) to cover the monolayer of cells. The cells were incubated for 1 to 2 minutes, or until the cells rounded and lifted from the bottom of the flask, before the addition of serum containing HUVEC media to inactivate the trypsin. If the cells required plating at a specific density the cells were counted using a haemocytometer (Hawksley, UK) and seeded onto new flasks, coated with 0.04% gelatin. All experiments were performed on HUVECs that were below passage 6.

2.2.4 Cryopreservation of HUVECs

HUVECs were washed with sterile PBS before 0.25% trypsin-EDTA solution (Sigma Aldrich, UK) was added to cover the monolayer of cells. The cells were incubated for 1 to 2 minutes at room temperature, or until the cells rounded and lifted from the bottom of the flask. HUVEC media was then added to the cells to inactivate the trypsin. The cell suspension was aliquoted into a 15ml centrifuge tube and spun at 1,250rpm to form a pellet. The supernatant was removed and the cell pellet was resuspended in freezing media containing 10% dimethyl sulphoxide (Sigma Aldrich, UK), 70% FBS and 20% HUVEC media, which has shown to be effective at preserving cells for frozen storage [243]. The solution was dispensed into 1.8ml cryovials (Thermo Scientific, UK) and placed in a cryopreservation container (Thermo Scientific, UK) filled with isopropanol for gradual freezing, 1°C per minute, and storing at -80°C. After two hours the cells were

removed from the freezing container and placed in -80°C for mid-range storage or in liquid nitrogen, -196°C, for long term storage.

2.2.5 Resuscitation of Cryopreserved HUVECs

HUVECs that had been frozen at -80°C or stored in liquid nitrogen were thawed rapidly in a 37°C water bath for 1 minute. The cell suspension was transferred into a 15ml centrifuge tube and resuspended slowly in serum free M199 media (Sigma Aldrich, UK) to prevent rapid changes in the DMSO gradient. The cells were centrifuged at 1,250rpm for 5 minutes to form a cell pellet. The cell pellet was resuspended in complete HUVEC media before transferring to the relevant cell culture flasks, pre coated in 0.04% gelatin.

2.2.6 Preparation of Simvastatin Solution

The preparation of simvastatin followed documented methods to ensure effective activation and storage [244,245]. Simvastatin (5mg) (Sigma Aldrich, UK) was dissolved in 100µl of 100% ethanol and 150µl of 0.1N NaOH, which hydrolysed, opened and activated the lactone ring through incubating at 50°C for 2 hours. Subsequently, the pH was corrected to 7.0 by the addition of 1N HCl in a drop by drop manner. The solution was topped up by the addition of double distilled water to a final concentration of 5mM, then aliquoted into 500µl samples and stored at -80°C. A 5µM working stock solution of simvastatin was made by diluting 50µl of the 5mM simvastatin solution in 49.95ml of HUVEC media. The working solution was then used in subsequent experiments to achieve a concentration of 0.1µM of simvastatin. The working solution was

stored at 4°C and discarded after 1 month's use. A vehicle control equivalent was produced at the same time, in the same manner, but without the addition of simvastatin. Simvastatin, or the control, was added 24 hours before experiments commenced, if not stated otherwise. Simvastatin was used at a concentration of 0.1µM, unless otherwise stated, following a concentration panel analysis of HUVEC cultures.

2.2.7 Hypoxic Conditions

In order to obtain hypoxic conditions a hypoxic chamber (Stem Cell Technologies, UK) was used. This apparatus provides an enclosed environment which can be filled with gas to a required concentration. Published protocols were followed to ensure the accurate use of the hypoxic chamber [246].

A petri dish filled with double distilled water was placed at the bottom of the hypoxic chamber to maintain a humidified environment. The cells were then placed on the shelf above the water bath and the hypoxic chamber was tightly sealed using the O-ring. The two valves were opened; one valve was connected to a flow meter (Stem Cell Technologies) and the other to an oxygen meter (Greisinger, Germany). The gas in the hypoxic chamber was replaced by flushing the chamber with nitrogen gas (BOC, UK) until the oxygen meter read <1% oxygen. A hypoxic gas containing 1% oxygen, 5% carbon dioxide, and nitrogen as a balance (BOC, UK) was used to obtain standard hypoxic conditions [247]. The flow meter was connected to the hypoxic gas canister and filled with the gas until 1% O_2 conditions was achieved. To prevent pressure increase inlet and outlet valves were used to allow the air to flow into and out of the chamber whilst the hypoxic conditions were achieved. Once the correct conditions were maintained the

valves were closed and the chamber was placed in a 37°C incubator for various time points, as specified. Normoxic cultures were maintained at 21% oxygen.

2.3 *In Vitro* Assays

2.3.1 Protein Extraction

The cells were washed twice with ice cold PBS which was then totally drained from the cell culture flask. The cells were lysed directly by the addition of RIPA buffer [248] containing 1X protease inhibitors [249] (100µl per T25 flask) (Appendix I). HIF1α has a half-life of less than 5 minutes in normoxia [250], so it was vital that all work in normoxia was performed quickly, until the cells were lysed in RIPA buffer containing protease inhibitors. Cell scrapers were then used to lift all of the cells and lysate into a corner of the flask before pipetting the lysate into a 500µl tube and incubating on ice. The lysate was mixed using a vortex mixer every 5 minutes for half an hour before centrifuging at 1,250rpm for 10 minutes at 4^{o}C. The supernatant was transferred to a new 500µl tube and frozen at -80°C until quantification.

2.3.2 Protein Quantification

The bicinchoninic acid (BCA) protein assay reagent method (Thermo Scientific, UK) was used to quantify and standardise the protein lysates in a 1:2 dilution. The BCA method has proven effective at quantifying protein levels as a stable purple colour is produced upon the complex of BCA with copper ions (Cu^{+}) produced when cupric sulphate is reduced by peptide bonds of

proteins [251]. The amount of Cu^{+} produced is proportional to the amount of protein present in the solution. The colour increases proportionally with higher protein concentrations and preferentially absorbs light at a wavelength of 562nm [251], allowing quantification of protein using a plate reader. The technique has been adapted and there are now protocols that allow for the determination of proteins that are in samples containing high reducing agents such as β-mercaptoethanol [252].

A bovine serum albumin (BSA) standard was prepared in RIPA buffer with a range of concentrations between 0µg/ml to 2µg/ml. The BSA standard had 10µl of each concentration loaded into a 96 well plate in duplicate, and 5µl of the samples were dispensed into neighbouring wells in duplicate. The samples were diluted by the addition of 5µl of RIPA buffer. The BCA working reagent was prepared and 200µl was added to each of the standards and samples before incubating at 37°C for 30 minutes under normal CO_2 conditions. The plate was allowed to cool to room temperature before analysing the protein concentrations using a plate reader (Dynex, MRX Revelation) at 562nm wavelength. The quantified proteins were assessed and concentrations were calculated from a calibration curve before using RIPA buffer to standardise the proteins to 1.25µg/µl. A 5X sodium dodecyl sulphate (SDS) loading dye (Appendix I) was added to the samples which were then frozen at -20°C until needed.

2.3.3 siRNA Nucleofection

The use of short interfering RNA (siRNA) to knockdown mRNA and reduce the expression of proteins was first developed after the discovery of RNA interference (RNAi) in *Caenorhabditis elegans* [253]. RNAi is mediated by siRNA which is generated from longer double stranded RNA by an RNase protein, Dicer. The resultant siRNA is around 22 nucleotides in length and is targeted to mRNA by the RNA-induced silencing complex (RISC) following RNA helicase activity to form a single stranded active siRNA. The siRNA binds to a complementary mRNA sequence, targeting it for cleavage [253]. Transfection allows the delivery of foreign nucleic acid into cells and utilises liposomal, calcium phosphate, viral or electroporation delivery [254]. In general, it has been easier to transfect immortalised cell lines compared with primary cells. The use of siRNA alongside transfection-based methods has allowed for the knockdown of specific proteins of interest in the laboratory. The use of the nucleofection technique allows for the introduction of nucleic acid via an electrical impulse, and has proved effective at transfecting primary cell lines [254].

HUVECs were transfected using a Nucleofector II device (Lonza, UK) with either a HIF1α targeted siRNA or a control scrambled siRNA (Santa Cruz, USA). HUVECs were trypsinised and resuspended in HUVEC media and counted using a haemocytometer (Hawksley, UK). A maximal capacity of 1.5 million cells can be nucleofected at one time and therefore the correct quantity was aliquoted in a 50ml Falcon tube before centrifuging to form a pellet. All media was removed before resuspending the pellet in HEPES buffered saline (HBS) [255] and 400nM of the relevant siRNA. The cells were transferred to electroporation cuvettes (VWR, UK) and nucleofected using program U-001 as recommended by the manufacturer. Following nucleofection treatment the cells were resuspended in complete HUVEC media before seeding

onto the relevant culture flasks, pre-coated with 0.04% gelatin, with media replaced 24 hours later.

2.3.4 Immunoblotting

Western blot electrophoresis is a well-established semi-quantitative method for detection of protein types within cells and tissues. The immunoblotting protocol followed standard procedures and is described below.

The SDS-PAGE acrylamide gels were prepared using the Mini-PROTEAN tetra cell casting module (Bio-Rad, UK) which was loaded with the specific concentration of acrylamide gel required. The concentration of acrylamide gel that was used for the western blots was 10%. The separating gel was prepared first and loaded into the casting module, the addition of 1ml of butanol to the gel before it had set made sure that the gels were level. Once the gels had set the butanol was removed and the gels were washed with distilled water, before drying using filter paper. The stacking gel was then added to the casting module to set above the running gel, the loading comb was added to the top of the gel and allowed to set. The formula for the 10% gel is shown below.

Table 1 - The formulation of the 10% running gel and 6% stacking gel used during SDS-PAGE immunoblotting

Running Gel		Stacking Gel	
Reagent	Volume	Reagent	Volume
Double Distilled Water	3.2 ml	Double Distilled Water	2.13 ml
30% Acrylamide (Fisher Scientific)	2.67 ml	30% Acrylamide (Fisher Scientific)	0.8 ml
1.5M Tris-HCl pH 8.8	2 ml	0.5M Tris-HCl pH 6.8	1 ml
10% SDS	80 µl	10% SDS	40 µl
10% APS	80 µl	10% APS	40 µl
TEMED	5.33 µl	TEMED	2.67 µl

The protein samples were denatured at 60°C for 4 minutes in SDS loading buffer (Appendix I), vortex-mixed and centrifuged, before loading into the wells. After setting up the Tetra-lock Mini-protean (Bio-Rad, UK) electrophoresis apparatus and 10% acrylamide gel, 25µg of each protein sample was loaded per well and 5µl of a colour plus pre-stained protein ladder (New England Biolabs, UK) was loaded into one well to act as a marker.

The distance migrated through the gel was strictly dependent upon the molecular weight of the protein. The gel was run at 100V for 15 minutes in running buffer [242] (Appendix I) to allow the samples to migrate through the stacking gel. The voltage was then increased to 120V and run for a further 1 ½ hours. After the samples had migrated the required distance through the acrylamide gel it was placed into the transfer apparatus, as described below. The proteins were transferred onto polyvinylidene difluoride (PVDF) membranes (GE Healthcare, UK), pre-soaked in 100% methanol for 10 minutes, using the Mini Trans-Blot Module (Bio-Rad, UK). Blotting pads and filter papers were pre-soaked in transfer buffer for 10 minutes and assembled as

described in (Fig. 9). The gel was removed from the running cassette and laid on top of the filter paper and blotting pad. The PVDF membrane was placed on top of the gel. Filter paper and blotting pads were then placed on top and any trapped air was removed using a roller (Fig. 9). The proteins were electro-transferred in transfer buffer [242] (Appendix I) for 2 ½ hours at 60V.

Fig. 9 – Protein transfer assembly. The diagram shows the layers necessary for the transfer of separated proteins onto a membrane, in preparation for immunoblotting.

Ponceau S staining solution (0.1% ponceau S in 5% acetic acid) (Sigma Aldrich, UK) was used to detect efficient transfer of proteins. The PVDF membrane was rinsed in the ponceau S staining solution for 10 minutes. The membrane was rinsed in distilled water to remove background staining. Any detectable proteins can be seen by a red stain in the location of the proteins. The ponceau S stain reversibly to the proteins and can therefore be completely removed by several washes with distilled water.

After the proteins had been transferred the PVDF membranes were cut at 80kDa. The membranes were then blocked in 5% non-fat skimmed milk (Marvel, UK) in Tris-Buffered Saline and Tween 20 (TBST) (Appendix I) for 1 hour on a plate rocker. Following blocking the membranes were rolled into a 15ml falcon tube containing the relevant antibody. The top section of the membrane, over 80KDa, was incubated with mouse-anti-HIF1α (1:750; BD Biosciences, UK) and the bottom section with the house keeping protein mouse-anti-β-actin (1:1000, Abcam, UK) made in 4.5ml of 5% non-fat skimmed milk in TBST. The membranes were then incubated overnight in the corresponding antibody overnight at 4°C on a slow rolling mixer.

The following day the membranes were washed three times with TBST for 10 minutes on a plate rocker. The membranes were then incubated for 1 hour at room temperature in the horseradish peroxidase (HRP) conjugated secondary antibody anti-mouse IgG-HRP (1:3000; New England Biolabs, UK) made in 5% non-fat skimmed milk in TBST. After the secondary antibody incubation the membranes were washed three times with TBST for 10 minutes per wash to minimise non-specific signal.

The membranes were briefly dried before the addition of enhanced chemiluminescence (ECL) reagent (Appendix I) [256], which reacts with the HRP-conjugate emitting luminescence and can be detected using X-Ray film. The ECL was prepared by mixing equal volumes of ECL solution 1 and ECL solution 2 and keeping in the dark (Appendix I). ECL reagent was added to cover the membrane and allowed to incubate for 5 minutes before excess reagent was removed. They were then transferred to a film cassette to protect them from light and taken to a dark room. The membranes were exposed to CL-Xposure film (Thermo Scientific, UK) for 1-10 minutes, to

obtain the optimal signal which depends on the primary and secondary antibody affinity and the HRP conjugate reacting with the ECL to form the luminescence reaction. The film was then developed using a western blot film developing machine (Konica Minolta SRX-101A).

Following the detection of the β-actin housekeeping protein the bottom section of the membranes were incubated in the western stripping buffer [242] for 30 minutes at 50°C. The membranes were then washed three times in TBST for 10 minutes each wash at room temperature before re-blocking of the membrane using 5% non-fat skimmed milk in TBST for 1 hour. The membranes were re-rolled into 15ml centrifuge tubes containing rabbit-anti-MMP14 (1:1000; Abcam, UK) made in 4.5ml of 5% non-fat skimmed milk in TBST. The membranes were then incubated overnight at 4°C on a slow rolling mixer.

The following day the membrane was washed three times with TBST for 10 minutes on a plate rocker. The membrane was then incubated for 1 hour at room temperature in the horseradish peroxidase conjugated secondary antibody anti-rabbit IgG-HRP (1:3000; New England Biolabs, UK) made in 5% non-fat skimmed milk in TBST. After the secondary antibody incubation the membrane was washed three times with TBST for 10 minutes per wash. The membrane was briefly dried before being submerged in the ECL reagent for 5 minutes. The excess reagent was removed and the membrane transferred to a cassette to protect it from light and taken to a dark room where the membrane was exposed to CL-Xposure film (Thermo Scientific, UK) for 2 minutes. The film was then developed using a western blot film developing machine (Konica Minolta SRX-101A). Data was collected by measuring the densitometry of the western blot bands and standardising these readings to a background control using FIJI software [257].

2.3.5 Flow Cytometry of HUVECs

Flow cytometry is a technique that was developed in the late 1960s [258], and allows the analysis of size, granulation, internal complexity as well as cell markers making use of fluorescent dyes or antibody conjugates[259]. A laser is targeted at the cell which scatters the light to be detected by relevant probes. The technique has been refined and improved drastically with a number of lasers and probes now available allowing for the detection of up to 20 parameters [260]. An addition benefit of using flow cytometry is that it allows for sorting of cells depending on their antigenic markers. This allows for selection of specific populations of cells which can then be analysed or cultured independently from other cell types.

For flow cytometry analysis HUVECs, either transfected or untransfected, were seeded into 6 well plates at a density of approximately 300,000 cells per well. Once the HUVECs were 80% confluent, 24 hours after seeding, wells were incubated in the presence of 0.1µM simvastatin or a vehicle control for 24 hours. The following day media was replaced. The cell cultures were incubated in either hypoxic (1% O_2) or normoxic conditions for 12-16 hours. The cells were washed and detached from the gelatin coated flask using accutase solution (Sigma Aldrich, UK) and transferred to a 1.5ml centrifuge tube. The cells were centrifuged for 5 minutes at 4,500rpm at room temperature to form a pellet, before resuspending in 1% BSA diluted in PBS and kept on ice.

The cells were transferred to corresponding wells of a 96 well plate, ensuring that there was a mixed population of cells in two wells to act as controls, one for an unstained control, and one for a secondary only control. The plate was centrifuged at 2000rpm for 1 minute to form a

pellet and supernatant was discarded. The cell pellets were resuspended in IC fixation buffer (eBioscience) and incubated for 10 minutes at room temperature. Following incubation with fixation buffer 100µl of permeabilisation buffer (eBioscience) was added before centrifuging at 2000rpm for 1 minute. Cell pellets were washed two times in permeabilisation buffer and cells were recovered from suspension by centrifugation at 2000rpm for 1 minute.

After the last wash, MMP14 primary antibody (1:100; Abcam, UK) diluted in the permeabilisation buffer was added to the cells and incubated on ice for 30 minutes. The cells were then centrifuged for 1 minute at 2000rpm before washing 3 times with permeabilisation buffer. Following the last wash the secondary antibody, either goat-anti rabbit IgG-Alexa-488 (1:400; Invitrogen, UK) or donkey-anti rabbit IgG-Alexa-594 (1:1000; Abcam, UK) diluted in permeabilisation buffer, was added to the cell pellets and incubated on ice in the dark for 30 minutes. The samples were washed three times in permeabilisation buffer before resuspending in 1% BSA in PBS. The samples were transferred to corresponding fluorescent activated cells sorting (FACS) tubes and kept in the dark at 4°C until analysis using a FACSCalibur or Fortessa flow cytometry machine (BD Biosciences, UK).

The cells were gated to exclude any dead cells or debris, as well as to exclude any doublet cells that were collected (Fig. 10). The unstained control cells were used to determine the positively stained population and these cells were selected for.

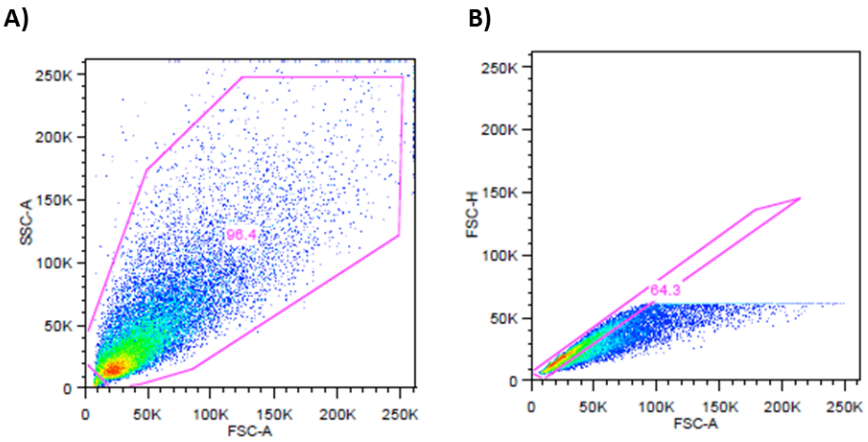

Fig. 10 – The gating logic used to analyse flow cytometry samples. A) Gating to exclude dead cells and debris determined through the analysis of the forward and side scatter plots. B) Gating to exclude doublet cells determined by the analysis of the forward scatter.

2.3.6 Immunohistochemistry

Immunohistochemical staining is a popular method for both research and diagnostic laboratories. The technique relies on the use of specific antibodies for detection of antigens, followed by either enzymatic or fluorescence visualisation [261]. The use of immunostaining has allowed for the characterisation of cell surface structures, morphology and traceability of cells which is commonly used in the detection of cancer metastasis in histopathology laboratories [261,262]. There are two methods for preparing tissues for staining once obtained. These are either paraffin embedding or cryosectioning [261].

2.3.7 Paraffin embedded sections

Carotid atherosclerotic plaque specimens were collected from the Vascular Surgery Department of Royal London Hospital. The atherosclerotic plaques were embedded in paraffin wax and were sliced to 5µm sections using a microtome before mounting on glass microscope slides. The sections were allowed to dry overnight before heating to 65°C to confirm attachment to the slide.

The sections were deparaffinised and hydrated by washing twice with xylene, followed by 100% ethanol, 70% ethanol and distilled water for 5 minutes per wash. The sections were immersed into preheated antigen retrieval solution (10mM citrate pH 6.0) [263] in a water bath at 95°C for 30 minutes. This breaks the crosslinks of the antigens and allows more efficient binding of the antibody. The sections were then allowed to cool at room temperature for 20 minutes before rinsing twice in PBS for 5 minutes.

To prevent non-specific binding, the sections were blocked using 10% FBS diluted in PBS (blocking solution) for 30 minutes. The MMP14 primary antibody (1:150; Abcam, UK) diluted in 10% FBS in PBS was added to the sections and incubated for 2 hours in a humidified chamber. Following this the sections were rinsed twice in PBS for 5 minutes before the addition of the goat-anti rabbit IgG-HRP secondary antibody (1:300; Santa Cruz, USA) and incubation for 1 hour in the humidified chamber. The sections were then washed in PBS twice for 5 minutes before the addition of the peroxidase substrate (DAB-Dako-K346). The sections were incubated with the 3,3'-diaminobenzidine (DAB) solution for 3 minutes at room temperature before washing with PBS twice for 5 minutes. The HIF1α antibody (1:50; BD Biosciences, UK) and VE-Cadherin

antibody (1:100; Abcam, UK) were diluted in 10% FBS in PBS, added to the sections, and incubated at 4°C overnight in the humidified chamber.

The following day the sections were removed and washed twice with PBS for 5 minutes. The goat-anti mouse-alkaline phosphatase antibody (1:50; Abcam, UK) was prepared in 10% FBS in PBS and incubated on the sections for 2 hours at room temperature in the humidified chamber. The sections were washed twice with PBS for 5 minutes before incubating the sections for 6 minutes with Fast Red solution. To stop the reaction the sections were rinsed with distilled water. A drop of haematoxylin was added to the sections and incubated for 2 minutes before rinsing with water for 10 minutes and drying the slides at 65°C. The sections were mounted with mounting medium and stored at room temperature before examination with the Axioplan microscope (Zeiss, UK).

2.3.8 Frozen Sections

The *APOE* knockout mouse model is an important animal model for atherosclerosis as they are known to form atherosclerotic lesions with similar morphology to humans [264]. *APOE* knockout mice were fed a high fat diet to induce the formation of atherosclerosis.

Atheroma tissue was collected, frozen and sectioned from *APOE* knockout mice in collaboration with Dr Qingzhong Xiao from the Clinical Pharmacology department at the William Harvey Research Institute. These were then fixed in cold acetone for 15 minutes. The sections were washed for 5 minutes three times in PBS. Following the washes, the sections were heated to 75°C for 20 minutes, which inactivates the endogenous alkaline phosphatase (AKP)/HRP activity.

The sections were allowed to cool to room temperature before incubating with avidin blocking solution (Insight Biotechnology, UK) for 15 minutes, followed by Biotin blocking solution (Insight Biotechnology, UK) for 15 minutes. The sections were washed for 5 minutes in PBS before incubating with 3% H_2O_2 made in methanol solution (v/v) for 15 minutes to inactivate the peroxidases. The sections were then blocked with 5% FBS for 30 minutes before incubating with rat anti-endomucin (1:200; Santa Cruz, USA), rat-IgG control, rabbit-HIF1α (1:75; Novus Biologicals, UK) or rabbit-IgG control in 5% FBS overnight in 4°C.

The following day the sections were washed three times for 5 minutes before incubating with the secondary antibody, goat-anti-rat-biotin (1:200; VectorLabs, UK) or goat-anti-rabbit-HRP (1:200; Cell Signalling, UK), for 60 or 120 minutes at room temperature. Sections that were biotinylated were washed twice in PBS for 5 minutes and incubated with ABC Vectastain (Vectorlabs, UK) for 30 minutes. PBS washes were repeated as before, and the sections were developed using DAB (Vectastain) until colour development was seen with the naked eye, usually 1-3 minutes. The sections were washed twice with PBS for 5 minutes to stop the reaction before incubating overnight with the second primary antibody at 4°C, rabbit-MMP14 (1:75; Abcam, UK), rabbit-HIF1α (1:75; Novus Biologicals, UK), rat-F4/80 (1:50; Abcam, UK), rat-endomucin (1:200; Santa Cruz, USA) or the relevant rat or rabbit controls.

Following the second primary antibody incubations the sections were washed three times with PBS for 5 minutes before incubating with the secondary antibody, anti-rabbit-AP or anti-rat-AP (both 1:100; Sigma Aldrich, UK). The sections were washed twice for 5 minutes with PBS before incubating with Fast Red (Sigma Aldrich, UK) and developing for 5-15 minutes until colour development was detected. The colour development was stopped by washing twice with PBS

for 5 minutes before cleaning the sections and allowing to dry. Sections were counterstained with haematoxylin (Sigma Aldrich, UK) for 2 minutes before washing twice with PBS for 5 minutes and drying for 10 minutes at 60°C. The sections were then mounted with mounting media (Sigma Aldrich, UK) and analysed with the Axioplan microscope (Zeiss, UK).

2.3.9 Chromatin Immunoprecipitation Assay

The Chromatin Immunoprecipitation (ChIP) assay is a technique that allows for the study of protein interactions with specific DNA sequences [265]. The first ChIP assay was developed in 1984 by Gilmour and Lis [266]. The early technique involved using UV light to cross link the DNA to the protein irreversibly. In 1997 the ChIP assay was adapted so that it could be used for mammalian cells. The detection of DNA was also improved by using PCR analysis rather than Southern Blots [267]. The ChIP assay can use a crosslinking method, such as formaldehyde treatment or UV radiation, to link the proteins to DNA. Following this the chromatin is sheared with a sonicator to reduce it reduce it to shorter fragments, between 100bp to 1000bp, that can be assessed. It is also possible to use nucleic acid digestion for proteins that bind to DNA with high affinity [265]. The ChIP assay followed a modified protocol provided by Merck Millipore, UK. The details are outlined below.

HUVECs were cultured in 10mls of HUVEC media in 8xT75 flasks, with each condition requiring two separate T75 flasks. The four conditions used were hypoxic, normoxic, hypoxic with 0.1µM simvastatin and normoxic with 0.1µM simvastatin. Simvastatin was added to the cells that required treatment for 24 hours prior to the ChIP experiment. Cells that required hypoxic incubation were placed in the hypoxic incubator for 6 hours at 37°C. Following treatment the

proteins were cross-linked to DNA by the addition of 16% formaldehyde (Thermo Scientific, UK), to a final concentration of 1%, and incubated at room temperature for 10 minutes (Merck Millipore, UK). The cells were washed twice with ice cold PBS to remove any excess solution. The cells were then scraped in 1ml of PBS containing 1x protease inhibitors before aliquoting evenly into two 1.5ml microcentrifuge tubes per condition. A cell pellet was obtained by centrifuging the collected samples at 2,500rpm for 4 minutes at 4°C, which was subsequently resuspended in 200µl of ChIP lysis buffer (Appendix I) [268] containing protease inhibitors and kept on ice for 10 minutes. To shear the chromatin to 200bp-1000bp fragments, a probe sonicator was used. Optimised conditions showed that the most effective shearing occurred at 30% frequency, with a microtip limit of 3, for 35 seconds. To prevent the samples from overheating the samples were kept on ice and only sonicated in bursts for a maximum duration of 10 seconds.

Following sonication, the samples were centrifuged at 13,000g for 10 minutes at 4°C and the supernatant was collected and transferred to a new 1.5ml microcentrifuge tube. The samples were then diluted to 1ml with the addition of ChIP dilution buffer (Appendix I) [268], 20µl of each sample was taken as an input control and stored at -20°C. The sonicated lysates had 40µl protein G-agarose beads (Merck Millipore, UK) added and were rotated for 90 minutes at 4°C to reduce non-specific binding. The samples were centrifuged at 4000g for 1 minute to pellet the protein-G-agarose beads and the supernatant was collected and transferred to a new 1.5ml microcentrifuge tube. Five µl of the HIF1α immunoprecipitating antibody (Thermo Scientific, UK) were added to the supernatant before incubating at 4°C overnight on a roller.

The next day 60µl of protein G agarose/salmon sperm DNA (50% slurry) (Merck Millipore, UK) was added to the samples and incubated for 3 hours at 4°C on a roller, to pellet-down the antibody/DNA complex. The protein-G-agarose beads were pelleted by centrifuging the samples for 1 minute at 4000g. The supernatant was removed and the protein-G-agarose/antibody/DNA complexes were washed for 5 minutes by the addition of 1ml of each of four buffers, and centrifugation at 4000g to reform the pellet. The buffers were added in the following order; low salt buffer, high salt buffer, LiCl buffer and finally TE buffer (Appendix I) [268]. The DNA/protein complex was eluted from the antibody by the addition of 100µl of ChIP elution buffer (Appendix I) (Merck Millipore, UK) to the pelleted protein-G-agarose/antibody/DNA complexes. The samples were mixed and placed on a rotating platform for 15 minutes at room temperature before centrifuging at 4,000g and collection of the supernatant. This elution step was repeated so that the final elution gave a total of 200µl. To the eluted samples 0.4M NaCl was added before heating overnight at 65°C to reverse the protein-DNA crosslinks. The input DNA was also included at this step, with the addition of 4M NaCl.

The next day the DNA was extracted from the samples by the addition of 32µl of ChIP digestion buffer (Merck Millipore, UK) (Appendix I) and incubation for 1 hour at 45°C. The DNA was then recovered by using Wizard® SV Gel and PCR Clean-Up System (Promega, Southampton, UK), according to the manufacturers recommendations. Briefly 200µl of membrane dilution buffer was added to the samples which were then transferred to a DNA binding column, inside the collection tube. The samples were allowed to incubate for 1 minute at room temperature before centrifuging at 13,000g for 1 minute. The flow through was discarded and the filter was washed with 400µl of membrane wash solution, containing ethanol. The samples were centrifuged at 13,000g for a further minute before discarding the flow through and washing the

filter again with 400µl of membrane wash solution. The sample was centrifuged at 13,000g for 1 minute with the flow through discarded. The filter was allowed to air dry for 10 minutes before transferring to a new collection tube and adding 30µl of nuclease free water to the filter. The sample was centrifuged for 2 minutes at 13,000g, the flow through was collected and the DNA concentration was analysed using a Nanodrop spectrophotometer (ND-1000).

2.3.10 PCR of ChIP DNA

The polymerase chain reaction (PCR) was used to evaluate the effectiveness of the ChIP assay. PCR is a widely used technique in biological research which amplifies a specific region of DNA using selected primers. In order to amplify the DNA, a heat stable polymerase, isolated from the *Thermus aquaticus* bacterium, is required (Taq Polymerase). The reason for a heat stable polymerase is due to the temperature required to denature the DNA. The denaturing step unravels the DNA allowing access for the primers to the target DNA. Denaturation commonly occurs around 95°C. Following denaturation, the primers anneal to the DNA with optimal annealing occurring around 60°C but this is dependent on the composition of the nucleotides in the primers. The final stage of PCR is the extension which is where the amplification of DNA occurs, which is optimal for *Taq* polymerase at 72°C.

The PCR reaction for the ChIP assay amplified the *MMP14* promoter around the potential HIF-Binding site. The primers used were forward 5'-CAGCCTGCACCACAAAAAG-3' and reverse 5'-CTTCTCCCACAGCCTCTCCT-3' with an expected amplicon size of 160bp. The PCR consisted of 0.4µM of the forward and reverse primers, 200µM dNTPs (Bioline), 1.25 units of Taq polymerase (Sigma Aldrich, UK), 1x PCR Buffer, 2mM $MgCl_2$, and 20ng of the sample DNA

topped up to 25µl with nuclease-free water for each PCR reaction. The samples were vortexed and briefly centrifuged before loading onto the PCR thermal cycler (MJ Research) and loading the relevant program (Table 2).

Table 2 – Details of the ChIP assay PCR program optimised for amplification of the MMP14 gene promoter region

PCR Stage		Temperature	Time
Hot Start		95°C	5 minutes
Repeat Cycle 35 times	Denature	95°C	60 sec
	Anneal	57°C	60 sec
	Extend	72°C	30 sec
Extension		72°C	10 minutes
Hold		4°C	~

The PCR products were run on a 2% agarose gel, made in TBE (Sigma Aldrich, UK) with the addition of 0.0001% Gel Red (Biotium) to detect the DNA amplicons. Gel Red binds to the DNA through intercalation and electrostatic interaction and can be detected by emitting fluorescence under UV light (Biotium). Images were taken of the electrophoresis gels using a UV light viewer and UV reader software. Data was collected by measuring the densitometry of the PCR amplicon bands and standardising these readings to a background control using FIJI software [257].

2.3.11 Tube Formation Assay

The *in vitro* tube formation assay allows the analysis of promoters and inhibitors of angiogenesis using endothelial cells seeded onto a matrigel matrix. Cells attach to the matrigel, migrate towards each other and form tube like structures in response to a stimulus [269]. The technique allows for an analysis of multiple angiogenic parameters than other *in vitro* angiogenesis methods, that commonly only allow for the analysis of a single parameter [269].

The tube formation protocol followed a standard procedure developed in our laboratory using growth factor reduced Matrigel (BD Biosciences, UK) [188].

Matrigel (BD Biosciences, UK), 96 well plates and pipette tips were cooled to 4°C overnight, the day before the tube formation assay. The following day the 96 well plates were kept on ice in the culture hood and 30µl of Matrigel was used to coat the bottom of the tissue-culture wells, using the cooled pipette tips to prevent early Matrigel polymerisation. The plates were incubated in the 37°C incubator for 30 minutes to allow the Matrigel to polymerise. The cells that were to be used for the tube formation assay were washed and detached from their culture flasks using trypsin, before resuspending in complete HUVEC media and transferring to a 1.5ml centrifuge tube.

The cells were centrifuged at 1,250rpm for 5 minutes to form a cell pellet before resuspending in tube formation media (M199, 10ng/ml insulin, 1 % BSA, HUVEC supplements, 100units per ml of penicillin, 0.1mg/ml streptomycin solution, 2mM of glutamine), either with or without simvastatin supplementation. The cells were resuspended thoroughly to avoid clumping and

30µl aliquots were taken from each cell donor to be counted. The cells were counted using a haemocytometer (Hawksley, UK) and calculations were made to ensure that 15,000 cells (diluted to 100 cells/µl) were added to the relevant wells of a 96 well plate. The experiments were conducted with a hypoxic plate and a normoxic plate in parallel, with half of each plate being for simvastatin treated cells. The plates were incubated for 8 hours at 37°C in a humidified cell culture incubator.

The plates were then imaged using a brightfield microscope (Nikon) at 4x magnification to assess the tube formation. After the images had been taken the media was removed from the 96 well plates and 200µl of glutaraldehyde was added to fix the cells. The plates were stored at 4°C overnight.

The following day the glutaraldehyde was removed from the wells and 100µl of ice-cold acetone (-20^{o}C) was added to the cells for 10 minutes. The acetone was removed and 10% FBS made in TBS was added and incubated with the cells for 30 minutes. The solution was removed and 50µl of the primary antibody, anti-MMP14 (1:100; Abcam, UK), made in 10% FBS in TBS was added to the wells and incubated for 1 hour. Following the primary antibody incubation the cells were washed three times with 10% FBS in TBS before adding 50µl of the secondary antibody, Goat-anti-rabbit-FITC (1:200; Abcam, UK), for 1 hour. The cells were washed a further 3 times in 10% FBS in TBS before the addition of 4', 6-diamidino-2-phenylindole (DAPI) (Invitrogen, UK) and incubated for 30 minutes on ice in the dark.

The 96 well plates were analysed using a fluorescent microscope (AMG Evos Fl Microscope) and digital images were recorded. The images were analysed using the FIJI software with an

angiogenesis analysis software plugin [257,270]. The angiogenesis analysis software allows for effective measurement of several parameters including total branching length, number of junctions and number of nodes.

2.3.12 MMP14 Neutralisation

In order to assess MMP14 inhibition in several experiments an MMP14 antibody (Merck Millipore, UK) or a Rabbit IgG-control (Santa Cruz, USA) was added to cell cultures at previously published concentrations (2.12µg/ml) [271]. The MMP14 antibody is targeted to the catalytic domain of MMP14 and has shown to be effective in neutralising MMP14 activity [271]. The antibody was targeted at a conserved sequence in the catalytic domain of MMP14 between humans and mice and therefore was suitable for use in both human and murine studies.

2.3.13 *In vitro* Scratch Migration Assay

The *in vitro* scratch migration assay is a well-established method for analysing cell migration through the direct observation of cell migration in a cell monolayer culture across a cleared scratch [272,273]. Although the technique is simple it provides several advantages to other methods for analysing cell migration as it takes into account the cell-cell and cell-ECM interactions, which are often disrupted in other methods [272].

HUVECs were transfected with either HIF1α or scramble siRNA and seeded onto 12 well plates coated with 0.04% gelatin at a density of approximately 200,000 cells per well. The cells were cultured until they had achieved 80% confluency, in the presence or absence of 0.1µM

simvastatin. Subsequently, the cell monolayer was scratched using a p200 tip to introduce a wound. The cells were washed twice with PBS before replacing with HUVEC media with or without 0.1µM simvastatin and with an MMP14 neutralising antibody (2.12µg/ml) (Merck Millipore, UK) or a rabbit-IgG control (Santa Cruz, USA). The addition of the MMP14 neutralising antibody allowed for the analysis of MMP14 inhibition on cell migration.

The HUVECs were imaged at the 0 hour time point before placing in hypoxia. The HUVECS were then imaged after 6 hours and migration was assessed using FIJI analysis software [257]. The migration was analysed by measuring the wound width at the 0 hour time point and the 6 hour time point. This measurement was then used to determine cell migration. In order to limit bias the images were coded and measured in a blinded fashion, with several measurements taken for each image to obtain an average.

2.3.14 Bromodeoxyuridine Proliferation Assay

5-Bromo-2'-deoxyuridine (BrdU) is a thymidine analogue that can be used as a substitute and traced to measure proliferation. The BrdU is incorporated into the DNA during the S-phase of cell division and therefore successive divisions and proliferations can be traced through detection of the incorporated BrdU, commonly using immunohistochemistry [274].

The BrdU colorimetric cell proliferation ELISA kit (Roche) was used to assess the proliferation according to manufacturer's recommendations. HUVECs transfected with either HIF1α siRNA or scramble siRNA were seeded onto a 96 well plate coated with 0.04% gelatin. Simvastatin or a vehicle control was added 24 hours post transfection. BrdU was added to the cell cultures

before incubating in hypoxia for 12-16 hours with either 2.12µg/ml rabbit-IgG control or 2.12µg/ml MMP14 neutralising antibody. A blank control was used whereby BrdU was added to wells that did not contain any cells. A background antibody control was also prepared at this stage through incubating some cells without BrdU. Following the hypoxic incubation the HUVECs were fixed with the supplied fixing and denaturing solution for 30 minutes. Following fixation the cells were incubated with the anti-BrdU-peroxidase antibody for 90 minutes. The cells were washed three times with PBS before adding the substrate solution. Once the substrate solution was added the colorimetric readings were read using a plate reader at 370nm wavelength, with reference wavelength at 490nm. The readings were analysed and the blank control values were subtracted from each experimental well reading.

2.3.15 Apoptosis Assay

Flow cytometry can be used to study cellular apoptosis because of its ability to differentiate cell size using forward light scatter. This can determine if the cell has shrunk and therefore apoptotic, or enlarged and therefore necrotic [275]. Commonly however, more quantitative results are desired and therefore apoptotic marking antibodies and dyes, such as annexin V and propidium iodide (PI) can be used [276]. This method of apoptosis detection allows for the distinction of cells that are viable, necrotic or apoptotic [276], due to changes in the plasma membrane permeability and integrity [275]. Necrotic cells cannot exclude PI which intercalates with nuclear DNA in the nucleus emitting a red fluorescent signal. Apoptotic cells with an intact membrane are impermeable to PI and therefore no signal will be emitted [275]. Annexin V binds to the phosphatidylserine, which is usually intracellular but translocates during early apoptosis to

be expressed on the exterior cell membrane [275]. Utilising an annexin V-fluorochrome conjugated antibody alongside PI therefore allows for the detection and distinction of viable and non-viable cells as well as to differentiate between different stages of the apoptotic process.

The apoptosis assay followed the annexin V staining protocol provided by eBioscience. HUVECs were transfected with either a HIF1α siRNA or scramble control siRNA and cultured on 0.04% gelatin for 48 hours. The media was then replaced with conditioned media containing either 0.1µM simvastatin or vehicle, or 2.12µg/ml MMP14 inhibitory antibody or rabbit IgG control and grown for a further 24 hours, before placing in either hypoxic or normoxic incubation for 4 hours. A control culture containing 10µM MG132 was used as a reference for apoptosis, as it is a known inducer of apoptosis [277]. The cells were then removed from the culture dishes using accutase before pelleting, resuspending in 1% BSA in PBS solution and transferring to corresponding wells of a 96 well plate. The plate was centrifuged at 2000rpm for 1 minute to form a pellet, which was washed twice with 1% BSA in PBS. The cells were then washed once more with 1x binding buffer (eBioscience) before resuspending in 1x Binding buffer with 5µl of annexin V conjugated antibody (eBioscience). The cells were incubated at room temperature for 15 minutes in the dark before washing a further time with 1x Binding buffer. The cells were resuspended in 200µl 1x Binding buffer and 5µl of PI was added. The cells were taken to the flow cytometry facility and analysed using the LSRFortessa machine (BD Biosciences, UK).

2.3.16 Electrophoretic Mobility Shift Assay (EMSA)

The electrophoretic mobility shift assay (EMSA) is a technique used to discover protein and nucleic acid interactions. Initially, the technique was described by Eisinger in 1971 [278] with further modifications of the methodology by Garner and Revzin in 1981 [279]. The technique involves mixing nucleic acid sequences with proteins before separating the proteins using a polyacrylamide or agarose gel under electrophoresis. If the proteins and nucleic acids interact, a complex is formed which will run slower through the gel. The nucleic acids are tagged with an enzyme or a radioisotype for easy detection of protein nucleic acid complexes [280].

The EMSA was carried out by Dr Conrad Hodgkinson. The protocol involved the use of biotin-labelled, double-stranded oligonucleotide probes which were incubated with HIF1α and HIF1β proteins, synthesised using the TnT Quick Coupled Transcription/Translation System (Promega, Southampton, UK). The primer probe sequences that were used are displayed below (Table 3) and were annealed with their reverse complement sequences respectively.

Table 3 – Primer probe sequences used in the EMSA

Primer Probe Target	Primer Sequence (5' - 3')
MMP14 proximal HRE wildtype	AAACAAC**CACG**TCCCCAACCA
MMP14 proximal HRE mutant	AAACAAC**CTTT**TCCCCAACCA
MMP14 distal HRE wildtype	ATGGTGGC**ACGTG**TTTGTAGT
MMP14 distal HRE mutant	ATGGTGGC**TCGTT**TTTGTAGT

The probe and protein mixture were incubated in EMSA binding buffer (Appendix I) for 30 minutes on ice, before subjecting to non-denaturing polyacrylamide gel electrophoresis at 4°C. Free probes and probe-protein complex were detected using a LightShift Chemiluminescent EMSA kit (Pierce Biotechnology).

2.3.17 Luciferase Assay

Luciferase reporter assays are used as indicators of gene expression changes. The technique involves the cloning of a DNA sequence of interest into a plasmid vector. The cloned DNA sequence should be upstream of the luciferase reporter gene which will act as an indicator of the transcriptional efficiency of the DNA sequence of interest. Luciferase is commonly used as it provides a bioluminescent signal that can be quantified using a luminometer[281].

The luciferase assays were carried out by Dr Conrad Hodgkinson. Cultured mouse yolk sac endothelial cells (C166) were transfected with an *MMP14* gene promoter-firefly luciferase reporter gene construct, together with plasmids to overexpress HIF1β or HIF1α+HIF1β, and a plasmid containing the *Renilla luciferase* gene to serve as a reference for transfection efficiency. The transfected cells were exposed to hypoxia (1% oxygen) or maintained under normoxia for 18 hours. *MMP14* promoter activity was measured by dual-luciferase assays. Mutations were introduced in the *MMP14* promoter sequence at the HRE positions and subjected to HIF1α overexpression. Analysis was performed by dual luciferase assays. The transfected cells were cultured in the presence or absence of simvastatin (2μM), and exposed to hypoxia (1% oxygen) or maintained under normoxia for 18 hours. *MMP14* promoter activity was measured by dual-luciferase assays using the Glomax 20/20 system (Promega, Southampton, UK).

2.4 Murine Work

2.4.1 Breed Plan

A breed plan to produce HIF1α endothelial-specific knockout mice was created (Table 4) and utilised HIF1α$^{fl/fl}$ mice from The Jackson Laboratory (B6.129-I^{tm3Rsjo}/J) and Tie1 Cre^{+} mice which would target the knockout specifically for endothelial cells. The generation of these mice utilises Cre-Lox technology. Cre-Lox technology involves the use of the *cyclization recombinase* (*cre*) gene of the bacteriophage P1 and is a site specific DNA recombinase. *Cre* specifically recognises a DNA sequence known as the *locus of X-over of P1* (*LoxP)* site and excises the DNA between two of these sites. The use of the *cre* gene and the *loxP* site, incorporated into the mouse genome surrounding a gene of interest, allows for the excision of specific genes. When the *cre* gene is under the influence of a tissue specific promoter, such as that of Tie1, then the excision of the DNA flanked by the *LoxP* sites will only occur in tissues expressing this gene [282].

In order to produce HIF1α$^{fl/fl}$ Cre^{+} and HIF1α$^{fl/fl}$ Cre^{-} mice, 3 male HIF1α$^{fl/fl}$ mice from The Jackson Laboratory were purchased (B6.129-I^{tm3Rsjo}/J) and crossed with female Tie1 Cre^{+} females, kindly supplied by Professor Hodivala-Dilke. This breeding pair produced four potential outcomes which could be used for the next stage cross. The second cross involved the use of either male or female HIF1α$^{fl/wt}$; Tie1 Cre^{+} mice crossed with HIF1α $^{fl/wt}$; Tie1 Cre^{-} mice. This second stage cross had 12 possible outcomes, of which 4 genotypes could be used for the final breeding cross.

The final cross involved the use of either male or female HIF1α$^{fl/fl}$ Cre^{+} mice crossed with HIF1α$^{fl/fl}$ Cre^{-} mice of opposite gender. This final cross would produce both the knockout model and the control which were used in subsequent *in vivo* and *ex vivo* experiments.

Table 4 – Outline of the breed plan used to create HIF1α endothelial cell specific knockout mice

1st Breed Pair		
Male HIF1α$^{fl/fl}$	X	Female Tie1 Cre^{+}
2nd Breed Pair		
Male or Female HIF1α$^{fl/wt}$; Tie1 Cre^{+}	X	Female or Male HIF1α $^{fl/wt}$; Tie1 Cre^{-}
3rd Breed Pair		
Male or Female HIF1α$^{fl/fl}$; Tie1Cre^{+}	X	Female or Male HIF1α$^{fl/fl}$; Tie1Cre^{-}

2.4.2 DNA Extraction from Mouse Tissue

Ear snips are commonly used as a DNA source from laboratory rodents as this method also allows for future identification of the mice. In order to obtain DNA from the ear tissue an extraction process is performed, which involves lysing of the cell, salt precipitation of proteins and finally ethanol precipitation of DNA [283].

An ear snip was collected from 18-20 day old mice pups in a manner which would enable identification between the pups after they were genotyped. The DNA extraction followed a standard isopropanol / ethanol extraction protocol whereby the tissue was lysed in 700µl of DNA lysis buffer (Appendix I) [284] and 20µl of 20mg/ml Proteinase K before incubating in a water bath at 55°C overnight with several vortexes for the first three hours to disperse the tissue. The

following day the samples were removed from the water bath, vortex mixed, and 275µl of 5M NaCl was added. The samples were vortexed and then mixed on a rocker for 5 minutes at room temperature before centrifuging at 13,000rpm for 7 minutes. Following the centrifugation, the supernatant was transferred to a new 1.5ml microcentrifuge tube and 500µl of isopropanol was added. The sample was mixed on a rocker for 2 minutes before centrifuging at 13,000rpm for 5 minutes. The supernatant was discarded and the DNA pellet was washed with 500µl of 70% ethanol and centrifuged at 13,000rpm for 2 minutes. As much of the supernatant as possible was removed without disturbing the DNA pellet and the sample was left to air dry. Once the sample had been air dried, 70µl of nuclease free water was added to the sample which was subsequently vortexed and burst centrifuged before measuring the DNA concentration using a Nanodrop spectrophotometer (ND-1000). The DNA concentrations were standardised to 5ng/µl before use for PCR analysis.

2.4.3 Genotyping Mice

The DNA collected from the mice had to be genotyped for expression of Cre Recombinase, specific to Tie1, and the floxed HIF1α gene. The Cre Recombinase gene would either be present or absent, whereas the floxed HIF1α gene could either be floxed-floxed, floxed-wildtype, or wildtype-wildtype. The PCR consisted of 0.4µM of the forward and reverse primers, 200µM dNTPs (Bioline), 1.25 units of Taq (Sigma Aldrich, UK), 1x PCR Buffer, and 20ng of the sample DNA. To the Cre Recombinase primers 2.5mM $MgCl_2$ was added, and to the HIF1α primers 2mM $MgCl_2$, was added before topping up to 25µl with nuclease free water for each PCR reaction. The samples were vortexed and briefly centrifuged before loading onto the PCR thermal cycler (MJ Research) and loading the relevant program (Tables 5 and 6).

The HIF1α genotype could be assessed through the position of the bands in relation to a marker. The floxed genotype has an extra 50 base pair sequence of DNA and therefore has a slower electrophoretic mobility compared to the wildtype on an agarose gel during electrophoresis (Fig. 11) (The Jackson Laboratory).

Table 5 – Primer sequences and PCR conditions used to genotype mice for Cre Recombinase expression

Primer Name		Primer Sequence	
Cre Recombinase [285]		GCCTGCATTACCGGTCGATGCAACGA	
		GTGGCAGATGGCGCGGCAACACCATT	
PCR Stage		Temperature	Time
Hot Start		93°C	5 minutes
Repeat Cycle 35 times	Denature	93°C	30 Sec
	Anneal	67°C	30 Sec
	Extend	72°C	45 Sec
Extension		72°C	10 minutes
Hold		4°C	~

Table 6 – Primer sequences and PCR conditions used to genotype mice for HIF1α floxed expression

Primer Name		Primer Sequence	
HIF1α Genotype (The Jackson Laboratory)		CGTGTGAGAAAACTTCTGGATG AAAAGTATTGTGTTGGGGCAGT	
PCR Stage		Temperature	Time
Hot Start		94°C	5 minutes
Repeat Cycle 35 times	Denature	94°C	30 Sec
	Anneal	57°C	30 Sec
	Extend	72°C	45 Sec
Extension		72°C	10 minutes
Hold		4°C	~

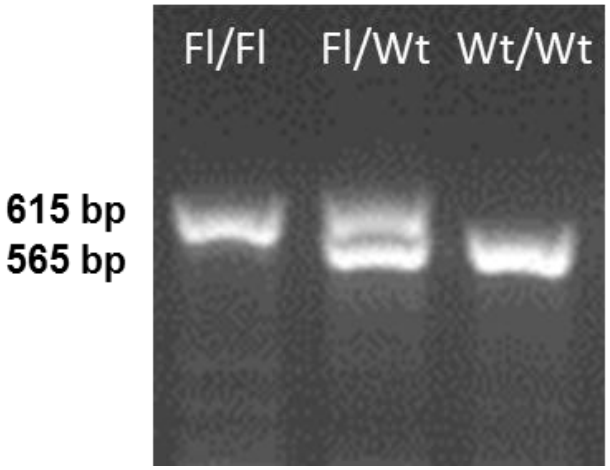

Fig. 11 – A representation of the different HIF1α genotypes after gel electrophoresis

2.4.4 Isolation of Primary Endothelial Cells from Mice Lungs

The isolation of primary endothelial cells from mouse lung tissue was carried out using well established methods described by Reynolds and Hodivala-Dilke[286].

HIF1α$^{fl/fl}$; Tie1Cre^{+} and HIF1α$^{fl/fl}$; Tie1Cre^{-} mice were sacrificed four to six weeks after birth. The mice were split according to genotype with four mice per endothelial cell preparation used to isolate the mouse lung endothelial cells (MLEC). The dissection was performed in sterile conditions using a class II culture hood to avoid contamination. Two sets of dissection equipment were used, one for the outside of the mouse and the other for inside the body cavity.

Prior to dissection the mice were cleaned with 70% ethanol to surface disinfect the mice and limit the possibility of contamination. Each mouse was dissected by first making an incision in the abdomen and cutting the peritoneal muscle wall to open the body cavity. The ribcage was cut and opened to expose the lungs. The lungs were removed by using forceps to lift the lungs and using sharp scissors to cut away the heart and connecting tissues. The lungs were placed in a petri dish containing 12ml of HamF12 solution. The lungs were cleaned from excess tissues, such as the trachea, and blood clots before rinsing in 70% ethanol and transferring to complete MLEC medium (Appendix I) [286]. Excess liquid was drained before mincing the lungs with scissors to form a paste. The minced lung was transferred to a 50ml tube containing preheated 0.1% collagenase made in PBS and incubated for 1 hour and 15 minutes at 37°C with occasional agitation.

Following collagenase treatment 10ml of MLEC medium was added before the tissue was further fragmented by mechanically disrupting the tissue through a 30ml syringe and a 19G needle several times. This was repeated using a 21½G needle to further break bigger clumps. The solution was filtered through a 70µm strainer before centrifuging at 1,200rpm for 3 minutes. The pellet was resuspended in 10ml of MLEC medium before dispensing in a T75 coated with 0.1% Gelatin, 10µg/ml fibronectin and 30µg/ml PureCol (Advanced Biometrix).

The following day the monocytes from the preparation were removed using magnetic sorting. The media was aspirated and washed three times with PBS before adding 6ml MLEC media and incubating at 4°C for 20 minutes. The media was aspirated and cells were washed with PBS before adding 3ml of rat-anti-FcyRII/III antibody at 1:1000 dilution, made in PBS, and placing at 4°C for 30 minutes. The flask was washed once with PBS before 3mls of MLEC supplemented with 10µl of anti-rat IgG-Dynabeads (Life Technologies) were added to the flask and incubated at 4°C with occasional agitation. The media was aspirated and cells were rinsed twice with PBS before detaching the cells from the flask using trypsin. Once the cells were detached they were resuspended in MLEC media before dispensing into a 15ml centrifuge tube and placing in a magnetic rack. The solution was left for 5 minutes for the magnetic beads to settle before the solution was removed and dispensed into a T75 coated with 0.1% gelatin, 10µg/ml fibronectin and 30µg/ml PureCol (Advanced Biomatrix) and incubated at 37°C with 5% CO_2 for 72 hours.

Following monocyte removal, endothelial cells were positively selected using a similar method. Endothelial cells were identified by their clustering together and cobblestone appearance. The media was aspirated and washed with PBS before adding 6ml MLEC Media and incubating at 4°C for 20 minutes. The media was aspirated and cells were washed with PBS before adding 3ml

of rat anti-CD102 antibody at 1:1000 dilution, made in PBS, and placing at 4°C for 30 minutes. The flask was washed once with PBS before 3mls of MLEC supplemented with 10µl of anti-rat IgG-Dynabeads (Life Technologies) were added to the flask and incubated at 4°C with occasional agitation. The media was aspirated and cells were rinsed twice with PBS before detaching the cells from the flask using trypsin. Once the cells were detached they were resuspended in MLEC media before dispensing into a 15ml centrifuge tube and placing in a magnetic rack. The solution was left for 5 minutes for the magnetic beads to settle before the solution was discarded. The beads were rinsed with MLEC media before dispensing in a T75 coated with 0.1% gelatin, 10µg/ml fibronectin and 30µg/ml PureCol (Advanced Biomatrix).

The cells were maintained by replacing the media every other day and passaging once the cells had reached 70-80% confluency.

2.4.5 Flow Cytometry of MLECs

MLEC cells were seeded onto four T25s per genotype. Once the MLEC cells were 80% confluent two of the T25s were incubated in the presence of 0.1µM simvastatin for 24 hours. The following day the media, with or without 0.1µM simvastatin, was replaced in all four of the culture flasks. The cell cultures were incubated in either hypoxic (1% O_2) or normoxic conditions for 12-16 hours. The cells were washed and detached from the T25 using accutase solution (Sigma Aldrich, UK) and transferred to a 1.5ml centrifuge tube. The cells were centrifuged for 5 minutes at 4,500rpm to form a pellet, before resuspending in 200µl of 1% BSA made in PBS and kept on ice.

A 96 well plate had 150µl of cells transferred to a well corresponding to each condition. The remaining cell solution was combined and aliquoted into 2 wells of the 96 well plate to act as controls, one for an unstained control, and one for a secondary only control. The plate was centrifuged at 2000rpm for 1 minute to form a pellet and supernatant was discarded. The cell pellets were resuspended in IC fixation buffer (eBioscience) and incubated for 10 minutes at room temperature. Following incubation with fixation buffer, permeabilisation buffer (eBioscience) was added before centrifuging at 2000rpm for 1 minute. The cell pellets were washed another two times in permeabilisation buffer with a centrifuge at 2000rpm between each wash.

After the last wash the rabbit-anti-MMP14 primary antibody and mouse anti-VE-CAD primary antibody (1:100 and 1:75; both Abcam, UK) made in the permeabilisation buffer were added to the cells and incubated on ice for 30 minutes. The cells were then centrifuged for 1 minute at 2000rpm before washing 3 times with permeabilisation buffer. Following the last wash the secondary antibodies, donkey-anti rabbit IgG-Alexa-594 and goat-anti mouse IgG-Alexa-488 (Both 1:2000; Abcam, UK), made in permeabilisation buffer were added to the cell pellets and incubated on ice in the dark for 30 minutes. The samples were washed three times in permeabilisation buffer before resuspending in 200µl of 1% BSA in PBS. The samples were transferred to corresponding fluorescent activated cells sorting (FACS) tubes and kept in the dark at 4°C until analysis using a Fortessa flow cytometry machine (BD Biosciences, UK).

The cells were gated to exclude any dead cells or debris, as well as to exclude any doublet cells that were collected. The unstained control cells were used to determine the positively stained population and these cells were selected for. To ensure that only endothelial cells were

analysed a final gate was added to analyse only cells that were positively stained for VE-Cadherin.

2.4.6 Aortic Ring Assay

In 1990 the *ex vivo* rat aortic ring assay was developed which aimed to bridge the gap between *in vivo* and *in vitro* assays for the study of angiogenesis [287]. The *in vitro* assays do not mimic the true *in vivo* environment and their information is usually seen as preliminary data which needs to be confirmed using more costly and demanding *in vivo* assays [288]. The use of *ex vivo* assays is more realistic than *in vitro* assays but less expensive and demanding than *in vivo* assays. This technique has been advanced and other animal models, such as mice, have been utilized for use in aortic ring assays.

The aortic ring assay was performed according to the protocol which has been optimised and established in my supervisor's laboratory and published by Baker et al. [289]

HIF1$\alpha^{fl/fl}$; Tie1Cre^{+} and HIF1$\alpha^{fl/fl}$; Tie1Cre^{-} mice that were 4 weeks old were culled by a clean break in the neck, to avoid stretching of the aorta and formation of a thrombus which can affect sprouting [289]. The mice were split according to genotype and kept separate throughout the assay. The dissection was performed in a sterile environment to avoid bacterial contamination with two pairs of dissection instruments used, one for outside the mouse and one for within the body cavity. Prior to dissection the mice were disinfected with 70% ethanol to further limit potential contamination.

The mice were dissected by first making an incision in the lower abdomen, slicing up to the shoulders, and pealing back the skin to allow access to the body cavity. An incision was made in the peritoneal wall, the ribcage was cut and opened to allow access to the lungs, heart and aorta. The lungs were removed to allow easy access to the aorta. The aorta was located and using a fine pair of forceps was lifted and separated from the connective tissue. The aorta was sliced at the base and top and transferred to a petri dish containing Opti-MEM media (Life Technologies) supplemented with penicillin and streptomycin.

The aorta was cleaned from adventitial tissue, fat and sprouting blood vessels using a dissection microscope before thin 1mm sections were cut using a scalpel. The sections of the aorta were separated before transferring into a clean dish of Opti-MEM and incubated overnight at 37°C in 5% CO_2.

Aortic rings were embedded on a collagen matrix within a 96 well plate. Separating rings for hypoxia or normoxia and with or without simvastatin treatment. Briefly collagen was diluted in DMEM media, to 1mg/ml, and neutralising the pH to a slightly basic pH, as indicated by the phenol red turning pink, with sodium hydroxide. The 96 well plate was tilted slightly before adding 50µl of the collagen solution to the wells. The collagen solution was added a few wells at a time to limit the chance of polymerisation before an aortic ring was added. Once the collagen was added to the well, an aortic ring was quickly added to the well and left to set by incubation at 37°C for 1 hour.

Opti-MEM solution containing 2.5% FBS and 30ng/ml VEGF was added to the aortic rings either with 0.1µM simvastatin or the PBS controlled equivalent. The aortic rings we then incubated for

three days at 37°C in either hypoxic (1% O_2) or normoxic conditions. The media was subsequently replaced every two days before ceasing the experiment on the sixth day after embedding. On the sixth day the amount of new vessels sprouting from the aorta were counted and quantified.

Aortas that were scheduled for immunofluorescence staining had their culture media removed and were washed with PBS. Following this 4% formalin was added to the aortas and left to incubate at room temperature for 30 minutes. The aortas were then washed three times for 15 minutes with permeabilisation buffer (PBS + 0.25% Triton-X100). The permeabilisation buffer was removed and the aortas were incubated with DAKO-Protein block (DAKO, UK) for 30 minutes at 37°C. During the incubation the antibody solution was prepared. FITC-probe tagged MMP14 antibody (BIOSS Antibodies, USA) was used at a concentration of 1:150. The BS1-Lectin-TRITC stain (Sigma Aldrich, UK) was used at a concentration of 1:1000. The antibodies were diluted in PBLEC buffer at their desired concentration and added to the aortas following the incubation with DAKO-Protein Block and incubated in the dark overnight at 4°C.

The following day the aortas were washed three times for 15 minute washes with PBS + 0.1% Triton-X100 before a 15 minute wash with distilled water. The aortas were mounted on a microscope slide with ProLong® Gold Antifade reagent with DAPI (Invitrogen, UK) and left to set in the dark overnight at room temperature.

Images of the aortas were taken using the Axioplan microscope (Zeiss, UK) using the same exposures for each condition. FIJI software [257] was used for analysis of the images. The fluorescence analysis consisted of outlining a blood vessel sprout in the green colour channel

(MMP14). The outlined sprout was then analysed using the mean grey value, which corresponds to the degree of fluorescence per pixel.

2.4.7 Sponge Angiogenesis Assay

There are several *in vivo* assays that measure angiogenesis including the corneal pocket assay and the chick chorioallantoic membrane assay, but often these methods lack an effective quantification method [290]. The rat sponge assay technique was developed in 1987 and aimed to provide an angiogenic model that was easily quantifiable [290]. This assay allows for the measure of blood flow, using radioactive clearance measurements, as well as new blood vessel infiltration by histological methods [291]. The sponge assay has been adapted to be used in mice [292] and also substituted in the use of Matrigel instead of sponge, so that parameters such as haemoglobin concentration can be measured [293].

The sponge angiogenesis assay followed the published protocol developed in Professor Hodivala-Dilke's laboratory [292]. HIF1$\alpha^{fl/fl}$; Tie1Cre^{+} and HIF1$\alpha^{fl/fl}$; Tie1Cre^{-} mice that were 4 to 6 weeks old were selected for this assay. The mice were subcutaneously injected with either 10mg/kg of simvastatin (Abcam, UK), dissolved in PBS and prepared as described previously, (Merck Millipore, UK) or a PBS control for 28 days.

On the 13th day of injections the mice were shaved along their flanks under isoflurane anaesthetic. The following day a sterile polyether sponge (approximately 1 x 0.5 x 0.8cm^3) (Caligen Foam, UK) was inserted subcutaneously into the flanks of the mice. The mice were firstly anaesthetised using isoflurane before injecting Carprieve 5.0% w/v in their scruff.

Following this a small incision was made on the lower back and a cavity was produced using forceps before inserting a trocar containing the sponge into the cavity. The sponge was implanted and the wound was then closed using a wound clip. The sponges were injected every other day with 100µl of 10ng/ml VEGF or 100µl of PBS as a negative control, producing a total of 8 distinct experimental groups (Table 7).

Table 7 – Experimental group design for the sponge angiogenesis assay

Genotype	Injection Site	
	Subcutaneous	Sponge
HIF1α WT	PBS	PBS
	PBS	VEGF
	Simvastatin	PBS
	Simvastatin	VEGF
HIF1α KO	PBS	PBS
	PBS	VEGF
	Simvastatin	PBS
	Simvastatin	VEGF

After 14 days post implantation the mice were sacrificed and sponges removed and fixed in 4% formalin overnight at 4°C. The next day, the sponges were sliced longitudinally and transferred to 70% ethanol before paraffin embedding by the Barts Cancer Institute Pathology department.

Blood vessel infiltration was assessed by immunohistochemistry, as previously described (Section 2.2.7.), using 6µm sections which were stained for rat anti-endomucin (1:200; Santa Cruz, USA). The sections were also stained for MMP14 (1:75; Abcam, UK) in order to detect differences between the differently treated groups. The difference with the previously described immunohistochemistry staining technique involved the use of 1% NGS buffer in PBS for blocking antigens and preparing the endomucin and MMP14 antibody. The rat anti-

endomucin antibody also required an anti-rat IgG-biotin and Vectastain (Vector Labs) tertiary antibody system to enhance the signal. The number of endomucin positive vessels was assessed and counted using the Axioplan microscope (Zeiss, UK) at multiple 20x optical fields.

2.5 Statistical Analysis

All statistical analyses were carried out using GraphPad Prism 5.00 (CA, USA) and IBM SPSS Statistics 22 (NY, USA) software. The data is presented as mean + standard error of the mean, unless otherwise stated. Statistical significance was determined using parametric statistical tests such as one-way analysis of variance (ANOVA), and t-tests as well as non-parametric statistical tests such as Kruskall-Wallis ANOVA. P-values less than 0.05 were considered statistically significant.

2.6 Experimental Design

Experiments were conducted on separate cell references for each experimental group. Therefore no same cell reference was used more than once for each experiment. In order to limit experimental bias, assays were analysed in a blinded fashion where appropriate.

3. Optimisation and Preliminary Results

3.1 Optimisation Results

3.1.1 Optimisation of Immunoblots

Immunoblotting is a key technique for protein expression analysis that had to be optimised to ensure the correct antibodies and concentrations were used for future experiments. As well as this, the harvesting of the protein itself needed to be optimised to ensure that there was minimal HIF1α degradation which occurs rapidly when samples are exposed to normoxic conditions.

It was important that the correct housekeeping antibody was selected which is not affected by hypoxic conditions. After a literature search it was found that common housekeeping genes, such as GAPDH [294], are affected by hypoxia. In order to ensure the control normalisation was effective β-Actin was selected as the housekeeping gene as it is not affected by hypoxic conditions [295].

Protein extraction began with enzymatic cell detachment and pellet formation. This pellet was then disrupted and lysed in RIPA buffer to extract the protein from the lysate. This technique was successful for detecting MMP14 (Fig. 12A) levels on western blots but was not as successful at detecting HIF1α levels (Fig. 12B). It was therefore decided that a new technique for protein extraction was required with direct addition of RIPA buffer added to the cell culture flasks being the accepted method. This technique provided good detection of MMP14 (Fig. 12C) and gave

better results for detection of HIF1α (Fig. 12D) and the housekeeping protein β-Actin (Fig. 12E). This is likely due to less opportunity for HIF1α degradation as well as direct lysis of the cells providing a greater amount of cells for protein extraction.

The first antibody that was used to detect HIF1α expression (Abcam, UK) contained a strong signal at a non-specific band at 60-65kDa (Fig. 12B). Upon contacting the manufacturer of the antibody it was confirmed that the non-specific band was unknown. The non-specific band was of high intensity making it difficult to assess HIF1α levels. Therefore, it was decided that a new antibody should be used (BD Biosciences, UK) which did not detect any non-specific bands (Fig. 12D).

As the research progressed an antibody that would be able to detect HIF1α in mice was required. To test the new antibody MLEC cultures were grown in hypoxia before lysing the cells in RIPA buffer to extract the protein. The new antibody was raised in a rabbit host (Pierce) and produced a specific band for HIF1α at the expected size of 110kDa (Fig. 12F).

HIF2α was also assayed in order to see if a different expression was seen in subsequent *HIF1α* knockdown experiments. This antibody (Abcam, UK) showed weaker expression compared to the other antibodies (Fig. 12G). This may be due to the need to strip the membrane of the HIF1α antibody expression before re-probing with anti-HIF2α. The HIF2α antibody also showed two non-specific bands at approximately 80kDa (Fig. 12G).

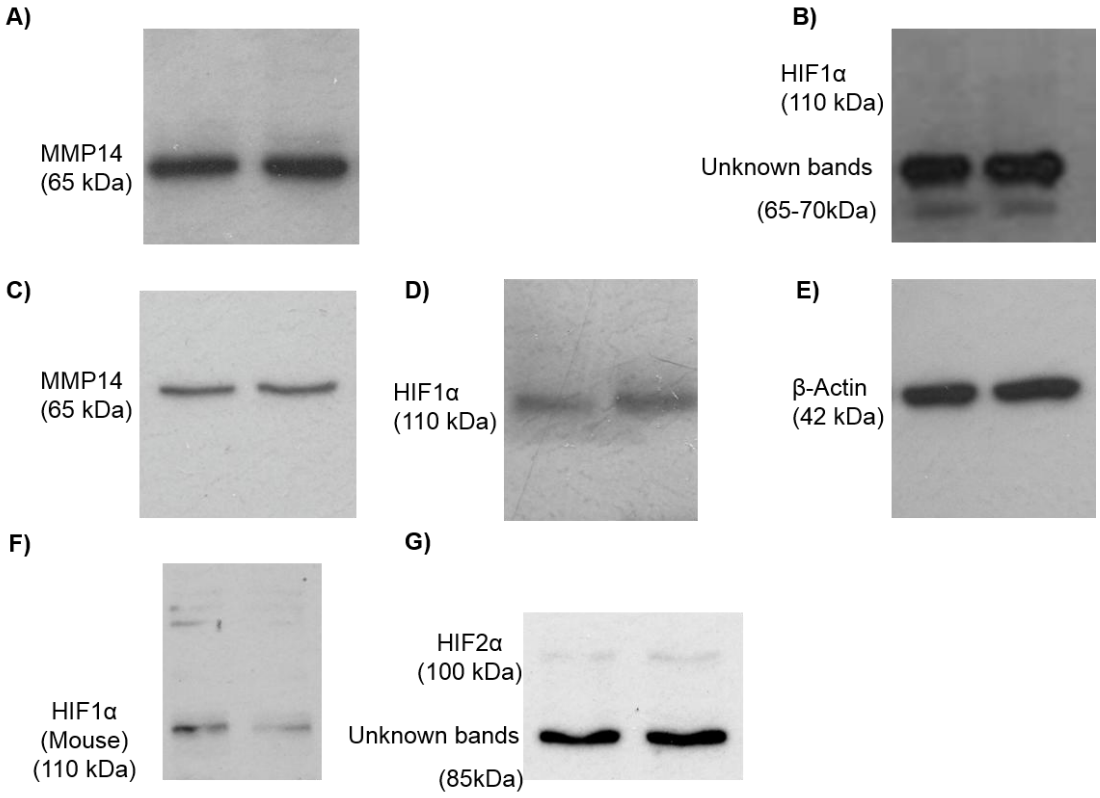

Fig. 12 – Immunoblot optimisation results. A) MMP14 expression following protein extraction from a cell pellet. B) Immunoblot result after using Abcam antibody for HIF1α showing non-specific bands. C) MMP14 expression after protein extraction using direct RIPA buffer. D) HIF1α expression after protein extraction of HUVECs using direct RIPA method as detected by BD Biosciences antibody. E) β-actin expression used as a housekeeping gene. F) HIF1α expression in MLECs detected by Pierce antibody after direct RIPA protein extraction. G) HIF2α expression in MLECs detected by Abcam antibody following direct RIPA protein extraction and PVDF membrane stripping after previous antibody detection.

3.1.2 Optimisation of Simvastatin Concentration

It was important to ensure that the concentration of simvastatin used was within a range that was not harmful to the HUVECs whilst still exerting an effect which was possible to detect. To make sure that the correct concentration of simvastatin was used a search of literature was conducted to assess the ranges commonly used. Following this endeavour, HUVECs were cultured in 6 well plates and differing concentrations of simvastatin were added to each of the wells. The cells were cultured in normoxic conditions over 48 hours and the HUVEC morphology was assessed (Fig. 13).

The simvastatin concentration panel shows that as the concentration of simvastatin increases there is more cell death. It is also clear that increasing simvastatin concentrations leads to morphological changes in the HUVECs which obtain a more spindle like appearance (Fig. 13). The simvastatin concentration panel made it clear that the optimal concentration of simvastatin to use in subsequent experiments was 0.1µM.

Using 0.1µM simvastatin as the selected concentration is more pharmacologically relevant as it is a relatively low dose of simvastatin [125] and more similar to concentrations in the blood stream, where concentrations are less than 0.02µM [134].

The luciferase assays however were conducted at 2µM as decided by Dr Conrad Hodgkinson.

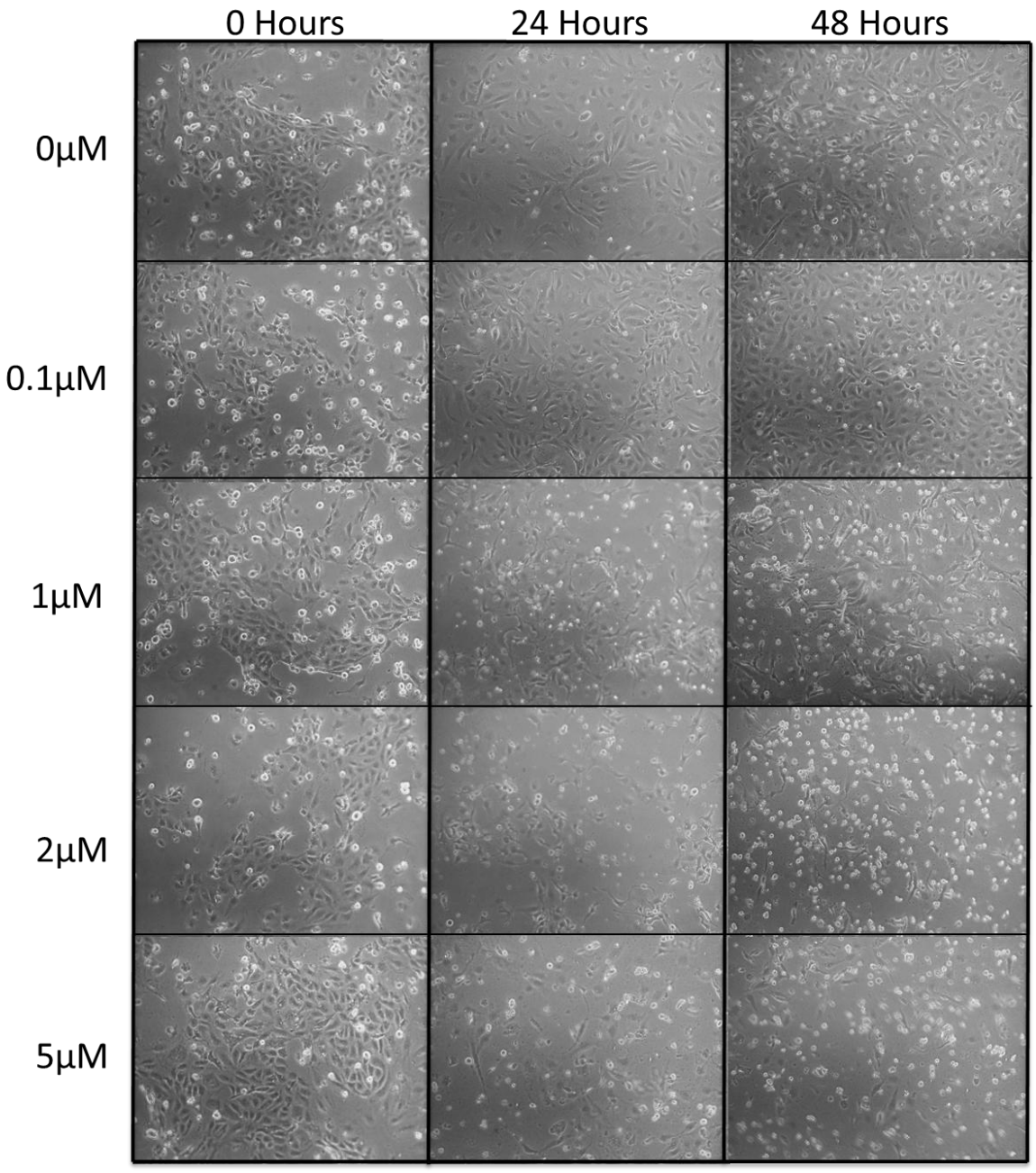

Fig. 13 – The effects of increasing simvastatin concentrations on HUVECs morphology over 48 hours.

3.1.3 Ethanol Vehicle Test

Simvastatin was dissolved in ethanol and therefore it was important to make sure that ethanol was not having an effect on protein expression. As the final concentration of ethanol added to the cell media was less than 1:50,000, an effect is unlikely. An immunoblot was conducted on whole-cell lysates of HUVECs cultured without any additive, with simvastatin, or with a matching ethanol vehicle control. The results showed that the use of ethanol had no clear effect on the expression of proteins of interest (Fig. 14).

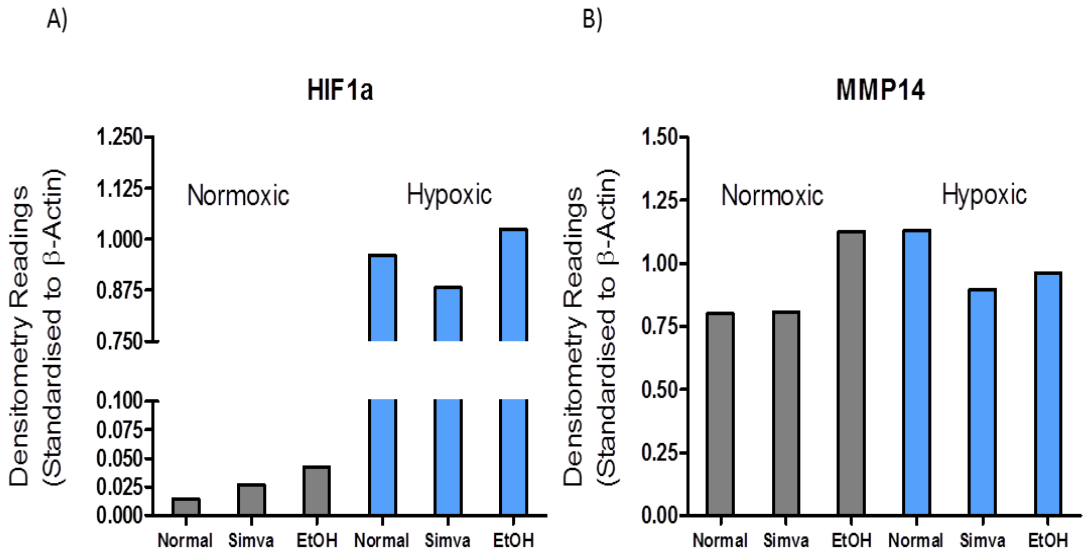

Fig. 14 – Ethanol vehicle test. Immunoblots were performed on cells grown without an additive, with 0.1µM simvastatin, or with an equal amount of ethanol. It was shown that there was not a large difference in protein expression. The trend that is shown by the addition of ethanol shows the reverse to that of simvastatin treatment. The results shown are standardised to the β-actin as a loading control.

3.1.4 Hypoxia Time Course

Once the correct antibodies had been chosen and conditions for the immunoblots were optimised, it was vital that HIF1α expression was measured at their highest level, as well as MMP14. A hypoxic time course was therefore set up whereby protein was extracted and assessed at intervals to ensure that the optimal time was chosen for subsequent studies.

The cells were cultured in hypoxia, with or without 0.1μM simvastatin over a range of time points. The chosen time points were 0 hours, 2 hours, 4 hours, 8 hours, 16 hours and 24 hours. It was seen that both HIF1α and MMP14 levels were highest expressed at 4 hours in both simvastatin and untreated media, with HIF1α protein levels increasing sharply at 4 hours before falling sharply to expression levels that matched those of the normoxic condition levels at 8 hours for untreated media (Fig. 15A). The simvastatin treated media also had peak HIF1α expression at 4 hours but maintained expression through until the 8 hour time point (Fig. 15B).

The MMP14 levels were fairly constant throughout the time course however, there was a peak seen at 4 hours with a slight decline in expression after the 4 hour time point in untreated cells (Fig. 15C). Simvastatin treatment did not appear to effect MMP14 protein expression over the time course (Fig. 15D).

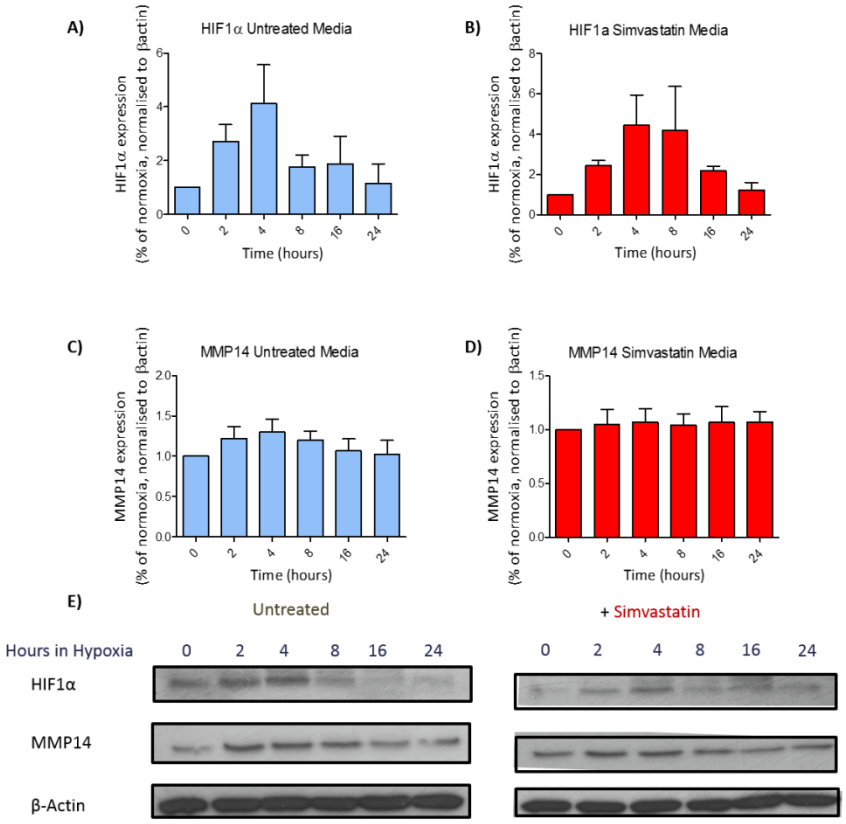

Fig. 15 – Immunoblot results of HUVECs undergoing a hypoxic time course in untreated or 0.1µM simvastatin treated media. The time course densitometry analysis results of A) HIF1α immunoblot in untreated media, B) HIF1α immunoblot in simvastatin media, C) MMP14 expression in untreated media, and D) MMP14 in simvastatin media. E) A set of representative immunoblots. All results shown are standardised as the % of normoxia expression normalised to the β-actin loading control. Bar charts are representative of mean + SEM from 4 separate experiments.

3.1.5 ChIP Optimisation

The chromatin immunoprecipitation assay needed to be optimised as laboratory-made reagents were used alongside a protocol designed for a kit. As well as this, ChIP assays need to be optimised for cell type and equipment used to ensure optimal shearing of the chromatin. The first optimisation step included the test of two sonication time points which would shear the chromatin to different sizes and provide an indication of the optimal time to shear chromatin between 200-800 base pairs. Optimal shearing occurred at 40 seconds at 30% duty cycle for HUVECs (Fig. 16A).

The following step was to minimise the presence of non-specific DNA, preventing it from interacting with the immunoprecipitation step. Different amounts of Protein-G agarose beads were used to clear non-specific DNA. The effectiveness of DNA clearance was assessed by a PCR reaction using the DNA obtained from this clearing step. It was seen that decreasing volumes of Protein-G agarose increased the yield of target DNA (168bp) whilst there was no considerable change in non-specific DNA. It was therefore decided that the optimal conditions involved the use of 40µl of Protein-G agarose to clear non-specific DNA (Fig. 16B).

Once the optimisation of clearing non-specific DNA was complete the actual immunoprecipitation step needed to be optimized to ensure that the Protein-G-agarose-antibody-antigen complex had enough incubation time to complex together. The immunoprecipitation incubation was suggested to only take 1 hour in order to precipitate out the required ab-antigen complex and so initially this time point was used. The immunoprecipitation efficacy was determined using end point PCR at three separate stages, before clearing, after clearing and a waste fraction that would usually be discarded. It was seen

that the most specific fraction was the waste fraction and showed that normally the target DNA would be discarded (Fig. 16C). It was decided that the immunoprecipitation incubation time should therefore be increased and was therefore tested at 2 hour and 3 hour time points. The results show that by increasing the incubation time to three hours there was better specificity with minimal DNA loss in the waste fraction (Fig. 16D).

Differing protocols suggested using either high NaCl concentrations, or low NaCl concentrations for the elution of DNA. Addition of both the higher (8M) and lower (0.4M) concentration were analysed alongside each other. It was found that the higher concentration of NaCl drastically reduced the amount of DNA eluted as seen by the decreased intensity of the specific band at 16µbp (Fig. 16E). Therefore, it was decided that the lower concentration of NaCl should be used.

Finally it was confirmed that the optimal conditions for subsequent experiments would include sonication for 40 seconds at 30% frequency, pre-clearing of the non-specific DNA using 40µl of protein-G-agarose, and to immunoprecipitate for 3 hours. In order to elute the DNA the lower concentration of 0.4M NaCl was used.

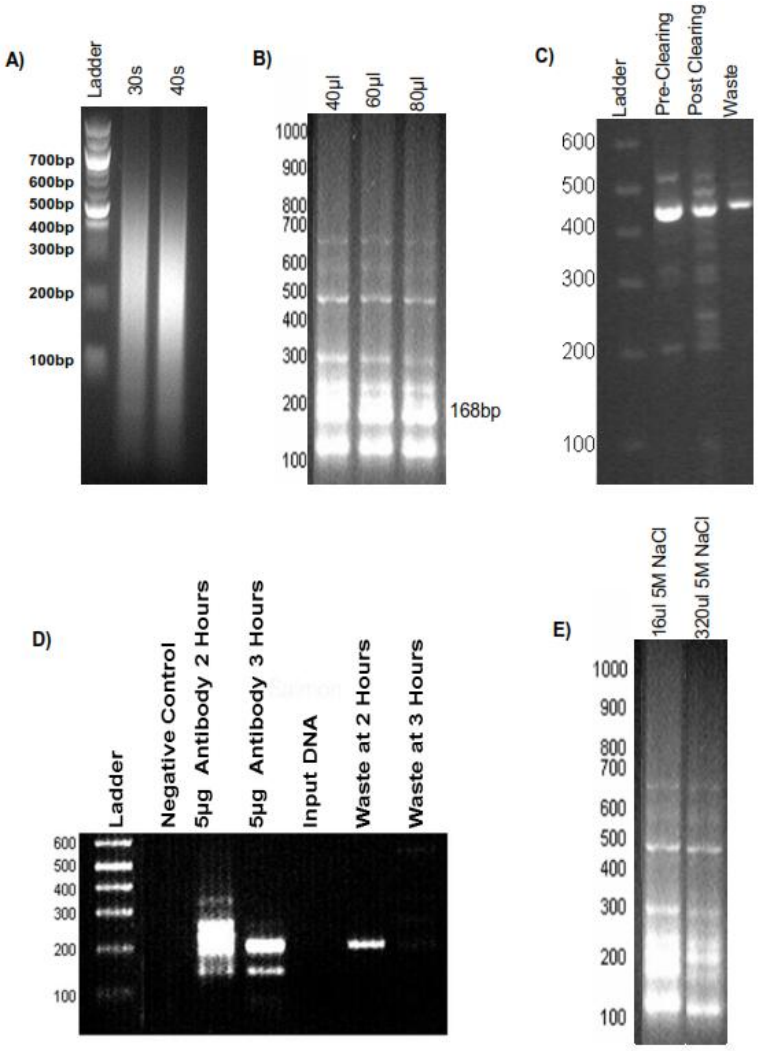

Fig. 16 – The stages of HUVEC ChIP optimisation. A) A gel electrophoresis image of the shearing of chromatin by a probe sonicator showing that the optimal conditions of shearing occur at 40 seconds. B) Pre-clearing of non-specific DNA with increasing volumes of protein-G-agarose beads from left to right of the electrophoresis image. C) Testing the efficacy of the immunoprecipitation incubation showing the pre-clearing DNA, post-clearing DNA and waste DNA PCR reactions. D) Optimisation gel electrophoresis image of immunoprecipitation. E) DNA elution optimisation using low NaCl concentrations and high concentrations of NaCl respectively.

3.1.6 siRNA Optimisation

HUVECs, like most primary cell lines, are known to be difficult to transfect [296] and therefore a number of different techniques were tested in order to optimise the knockdown of HIF1α in HUVECs. The first method involved the use of endoribonuclease-prepared siRNAs (esiRNA) which are formed by cleaving longer double strands of RNA with an endonuclease. This produces siRNA which are similar to those generated by Dicer *in vivo.* Validated knockdown of HIF1α was not achieved by using this technique however and so it was decided to move to more traditional siRNA.

HUVECs were transfected with the relevant siRNA or a nuclease free water control. The cells were allowed to proliferate for 72 hours to allow the siRNA to inhibit mRNA translation into protein and any remaining protein to degrade. The HUVECs were then placed in hypoxia or normoxia for 4 hours before collecting the protein lysate. The effect of transfection was assessed by using immunoblotting. Unfortunately using this method the results are not clear as there is no specific pattern of *HIF1α* knockdown and subsequent effect on MMP14 expression activity seen (Fig. 17).

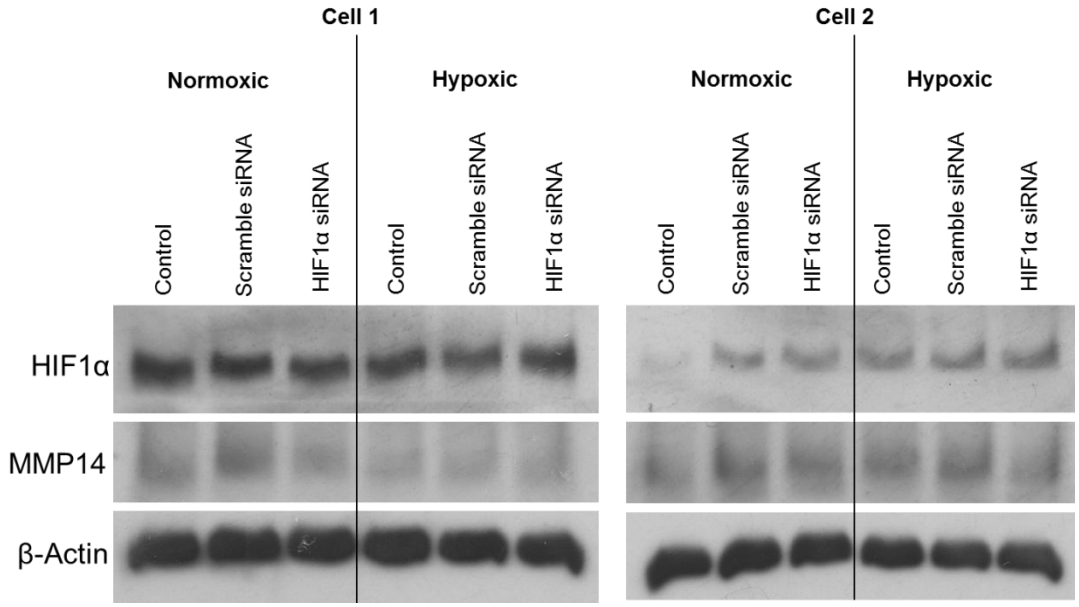

Fig. 17 – Immunoblots of the optimisation of *HIF1α* siRNA transfection. No clear pattern of *HIF1α* knockdown between the two different cell types and conditions can be seen.

Following the failure of detecting knock-down of *HIF1α* using a lipid based transfection method it was decided to try to introduce the siRNA into the HUVECs using electroporation. Electroporation involves the use of high voltage to permeabilise the cell membrane of the target cell, which allows siRNA in the surrounding buffer to enter the cell. Every cell type requires different electroporation conditions and therefore it is important to optimise [297].

The electroporator used was the Nucleofector II device (Lonza, UK) which recommends HUVECs should be electroporated using either of two pre-set programmes (A-034 or U-001) [298]. The commercial kit recommends using their own buffer, however the relevant literature [255] and comments from the scientific community, indicated that HEPES buffered saline (HBS) could be used as an alternative. A panel was set up using the two different recommended programmes, either HBS or PBS, and a green fluorescent protein (GFP) plasmid reporter to show transfection

efficiency. Potential cell death and transfection efficiency were assessed using fluorescence microscopy (Fig. 18A). Flow cytometry of these cells was then used to test for actual transfection efficiency, measuring for GFP as a marker of plasmid uptake (Fig. 18B and C).

It was seen that the optimal condition was programme U-001 with the electroporation being performed in HBS (Fig. 18). This showed a transfection efficiency of over 60% whilst also showing less cell death (Fig. 18). The PBS buffer and also programme A-034 were less effective than the HBS buffer and programme U-001 and therefore these conditions were not pursued. It was therefore decided that this programme would be the most appropriate to use. Although a plasmid rather than siRNA was used for the transfection optimisation, in theory the transfection efficiency should be similar as the electroporation would permeabilise the membrane allowing uptake of either plasmid or siRNA.

A)

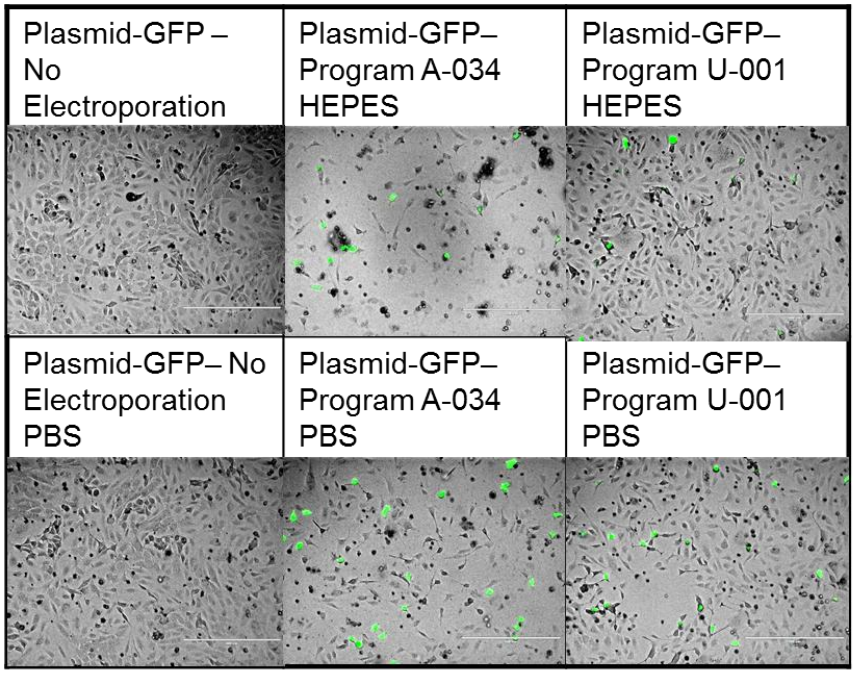

B)

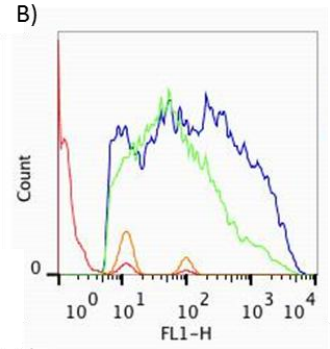

Colour	Sample Condition	Plasmid	Freq. of Parent	Freq. of Total
Green	HEPES Prog. U-001	GFP	67.8	62.6
Blue	HEPES Prog. A-034	GFP	49.3	45.6
Orange	HEPES – No Electroporation	GFP	0.017	0.016
Red	HEPES – NO Electroporation	None	92.6	92.6

C)

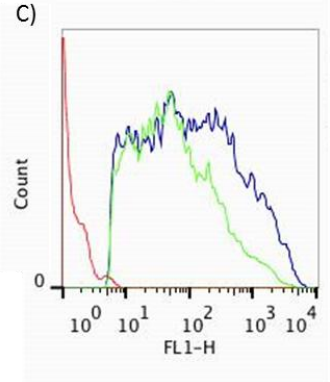

Colour	Sample Condition	Plasmid	Freq. of Parent	Freq. of Total
Green	PBS Prog. U-001	GFP	63.8	59.5
Blue	PBS Prog. A-034	GFP	46.0	43.2
Orange	PBS – No Electroporation	GFP	0	0
Red	PBS – NO Electroporation	None	93.5	93.5

Fig. 18 – The optimisation of siRNA nucleofection into HUVECs. A) Immunofluorescence microscopy of HUVECs transfected with GFP undergoing different nucleofection and reagent conditions. B) Flow cytometry analysis of HUVECs, using GFP as a marker of plasmid uptake, nucleofected in HEPES buffered saline buffer with differing nucleofection programs. C) Flow cytometry analysis of HUVECs GFP uptake into cells nucleofected in PBS nucleofection buffer with differing nucleofection programs.

3.1.7 Tube Formation Assay Optimisation

A simple time course, for *in vitro* tube formation assays, was set up in order to make sure that the optimal time for tube formation is used in subsequent experiments. This was partly due to the requirement of hypoxic treatment and the inability to visualise the tube formation process under these conditions. Therefore, a time course was set up using normoxic conditions to observe the opportune time to analyse my results. It was seen that tube formation occurred at 6 hours, but the tubes were more sparse and not completely formed (Fig. 19). At the 8 hour time point, however, complete, well defined, stable tubes could be observed (Fig. 19). The 8 hour time point was therefore selected for subsequent tube formation experiments.

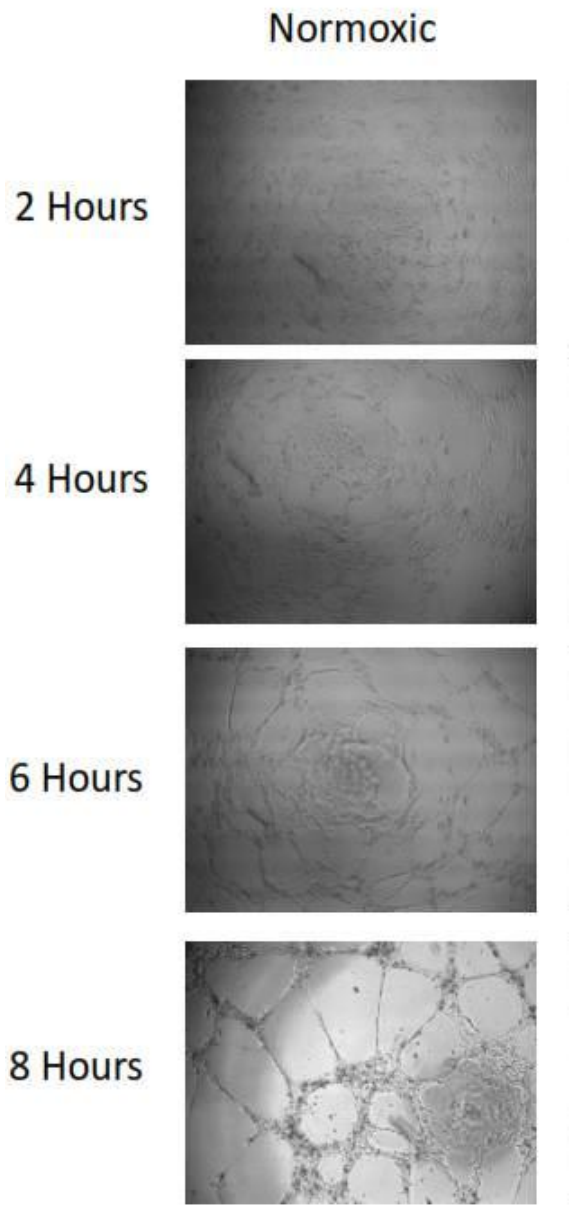

Fig. 19 – Tube formation assay time course of HUVECs seeded on reduced growth factor Matrigel. HUVECs were seeded on reduced growth factor Matrigel and observed every 2 hours for a total of 8 hours. It can be seen that tube formation begins at 4 hours in the normoxic condition. Well defined tubes are seen at 8 hours.

3.1.8 Aortic Ring Assays

In order to effectively evaluate the effects of experimental treatments using the aortic ring assay it was important to optimise the assay for the optimal sprouting duration. As with tube formation assays, aortic rings require hypoxic incubation, making it unviable to remove the cultures from hypoxia for daily analysis, as this will affect the hypoxic response. Due to high variation of sprouting observed in mice of different backgrounds, age and gender it is important before starting the final experiments that a time-course is set up to ensure that the sprouts are evaluated on the correct day and the effects of hypoxia are accounted for, whilst controlling for other variables.

The time-course indicated that the optimal day for assessing sprouting was observed on day 6 (Fig. 20). This is because the majority of the conditions have the highest amount of sprouting at this time point, only the hypoxic vehicle condition had a decrease in sprout numbers (Fig. 20). Therefore the 6 day time point was chosen for sprout evaluation.

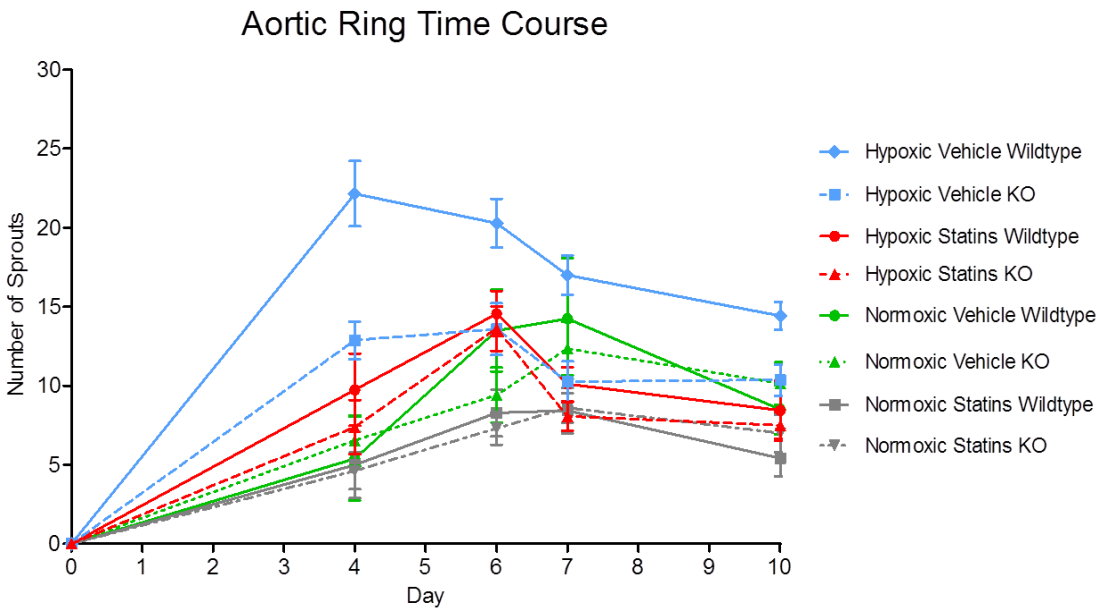

Fig. 20 – Aortic Ring assay time course on *Tie1 Cre*$^{+}$ *HIF1α*$^{fl/fl}$ and wildtype mice. The chart shows the number of sprouts produced by the different conditions over a period of 10 days, representative of mean + SEM from at least 6 aortic rings per group from 10 mice in total.

3.1.9 Aortic Ring Staining Optimisation

In order to see the effects of simvastatin, hypoxia, MMP14 neutralisation and endothelial *HIF1α* KO on MMP14 expression in the new blood vessels it was important to optimise staining for MMP14.

The staining of aortic rings is a simple process as all of the staining reactions can occur within the wells that the aortic rings are cultured in. However, the removal of aortic rings from the wells can be difficult and can often cause vessels to tear so it was important to practice beforehand.

Once the aortic rings had been cultured and sprouts counted they were fixed using 4% formalin and permeabilised with permeabilisation buffer. The aortic rings were blocked with DAKO-Protein block (DAKO, UK) before incubating with the MMP14 primary antibody (Abcam, UK) diluted in PBLEC Buffer (Appendix I). Three different concentrations of the primary antibody were used (1:100, 1:150, 1:200) in order to find the best staining conditions to provide a strong signal with low background noise.

Following the overnight antibody incubation the aortas were washed thrice for 15 minute periods with PBS + 0.1% Triton X-100. The secondary antibody anti-rabbit-IgG-FITC (1:750; Abcam, UK) and BS1-Lectin-TRITC stain (1:1000; Sigma Aldrich, UK) diluted in PBLEC buffer, were added to the aortic rings and incubated for three hours. The aortic rings were washed again with PBS + 0.1% Triton X-100 for three 15 minute washes before rinsing in distilled water.

Once the staining was completed, the aortic rings needed to be mounted onto a microscope slide. This involved scraping around the edge of the well with a needle and picking up the collagen surrounding the aortic ring carefully using forceps. It was important at this stage to limit instrument contact with aortic rings to minimise any breakage of the vessels. Once on a microscope slide a drop of ProLONG Gold Anti-Fade with DAPI (Life Technologies) was added and a coverslip placed on the slide. The slides were allowed to dry for 24 hours before imaging.

Neovessel formation from the aortic ring was observed at high magnification using the Axioplan microscope (Zeiss, UK). It was seen that there was high background noise for MMP14, even at the 1:200 dilution (Fig. 21C). Unfortunately, at the 1:200 dilution the staining of the vessels was quite weak and therefore diluting the antibody further was not an option (Fig. 21C). The high background could be due to the collagen trapping either the anti MMP14 antibody or the anti-rabbit-IgG-FITC antibody. However, staining with BS1-Lectin and DAPI was effective. As such, these conditions were adopted for future experiments (Fig. 21A and E).

It was decided that to reduce background noise a conjugated primary anti MMP14-FITC antibody (BIOSS Antibodies, UK) would be used at a concentration of 1:150. This would be more specific, require less washes, and remove the need for secondary antibodies and its non-specific matches. Upon viewing the newly stained aortic rings with the conjugated antibody it was seen that there was less background noise and good staining of MMP14 in the neovessels (Fig. 21D).

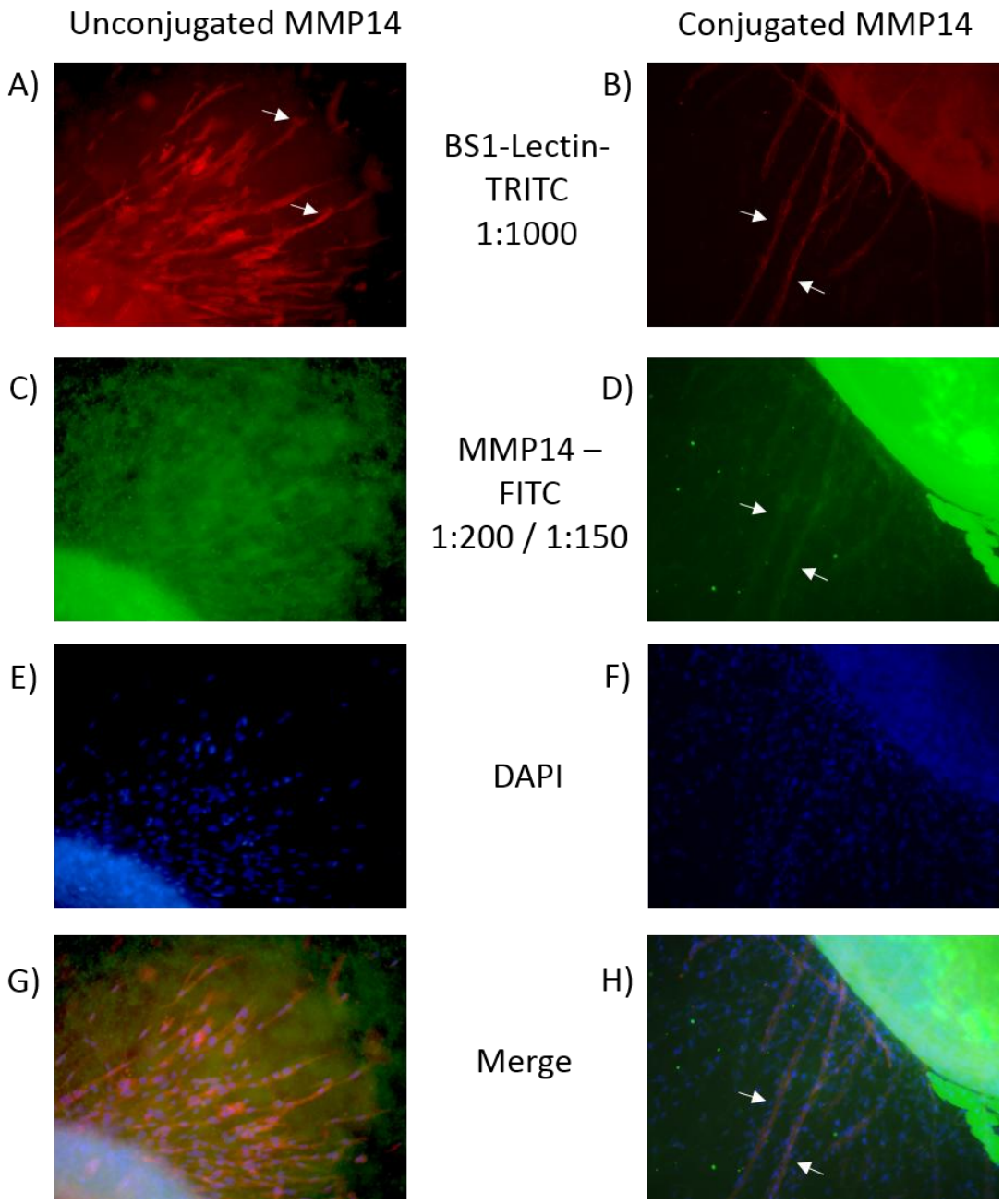

Fig. 21 – Optimisation MMP14 staining of aortic rings from *Tie1 Cre*$^{+}$ *HIF1α*$^{fl/fl}$ and wildtype mice. The left side of the image shows the unconjugated MMP14 antibody, with a separate FITC secondary antibody, producing high background. The right side of the image shows the conjugated MMP14-FITC antibody with less background staining. Arrows indicate clear defined sprouts.

3.1.10 Confirmation of HIF1α Endothelial Cell-Specific Knockout Mice

It was important to ensure that the *Tie1 Cre+ HIF1α*$^{fl/fl}$ that were generated were actually endothelial cell-specific knockouts for *HIF1α*. For this, sponge sections were used from the *in vivo* angiogenesis experiment. The sponge sections were stained according to the previously mentioned protocol using a rabbit anti-HIF1α antibody (1:75; Novus Biologicals, UK).

Upon analysis of the sections it was seen that vessels from the *Tie1 Cre+ HIF1α*$^{fl/fl}$ mice did not have a strong brown border, indicative of HIF1α, in compared to the wildtype littermates (Fig. 22A and B). This therefore showed that the *Tie1 Cre+ HIF1α*$^{fl/fl}$ mice were successfully bred and had no HIF1α expression in endothelial cells.

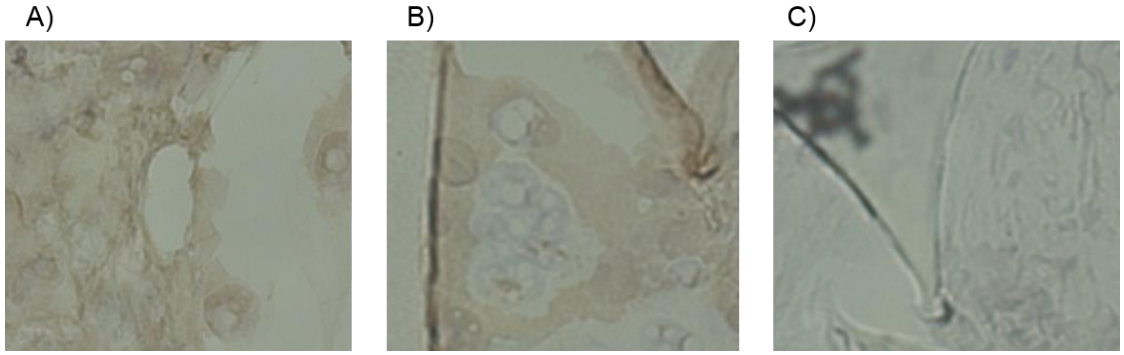

Fig. 22 – IHC staining of sponge with neovascularisation for confirmation of endothelial cell *HIF1α* knockout. A) HIF1α wildtype mice neovessel staining showing a thick brown border around the blood vessel. B) HIF1α endothelial cell specific knockout mice neovessel staining showing a weak border around the vessel. C) Isotype control stain showing no HIF1α staining.

3.2 Preliminary Results

3.2.1 Flow Cytometry for Apoptosis Assay

In order to define the cell viability of cells undergoing the different oxygen and drug treatments it was decided that flow cytometry would be used. This incorporated the detection of PI and annexin V.

Upon testing the cell viability it was seen that there was not much difference between the different cell conditions (Fig. 23). This could be due to weaker staining which meant a majority of the cells were classed as live as they were not identified via annexin V or PI. Another factor could be due to the siRNA transfection adversely affecting the cells or possibly due to there not being a difference in the viability of the cells.

This may also be due to apoptosis potentially not being a confounding variable in angiogenesis being affected by simvastatin's inhibition of HIF1α regulation of MMP14. As there was not a clear difference seen apoptosis assays were not used any further.

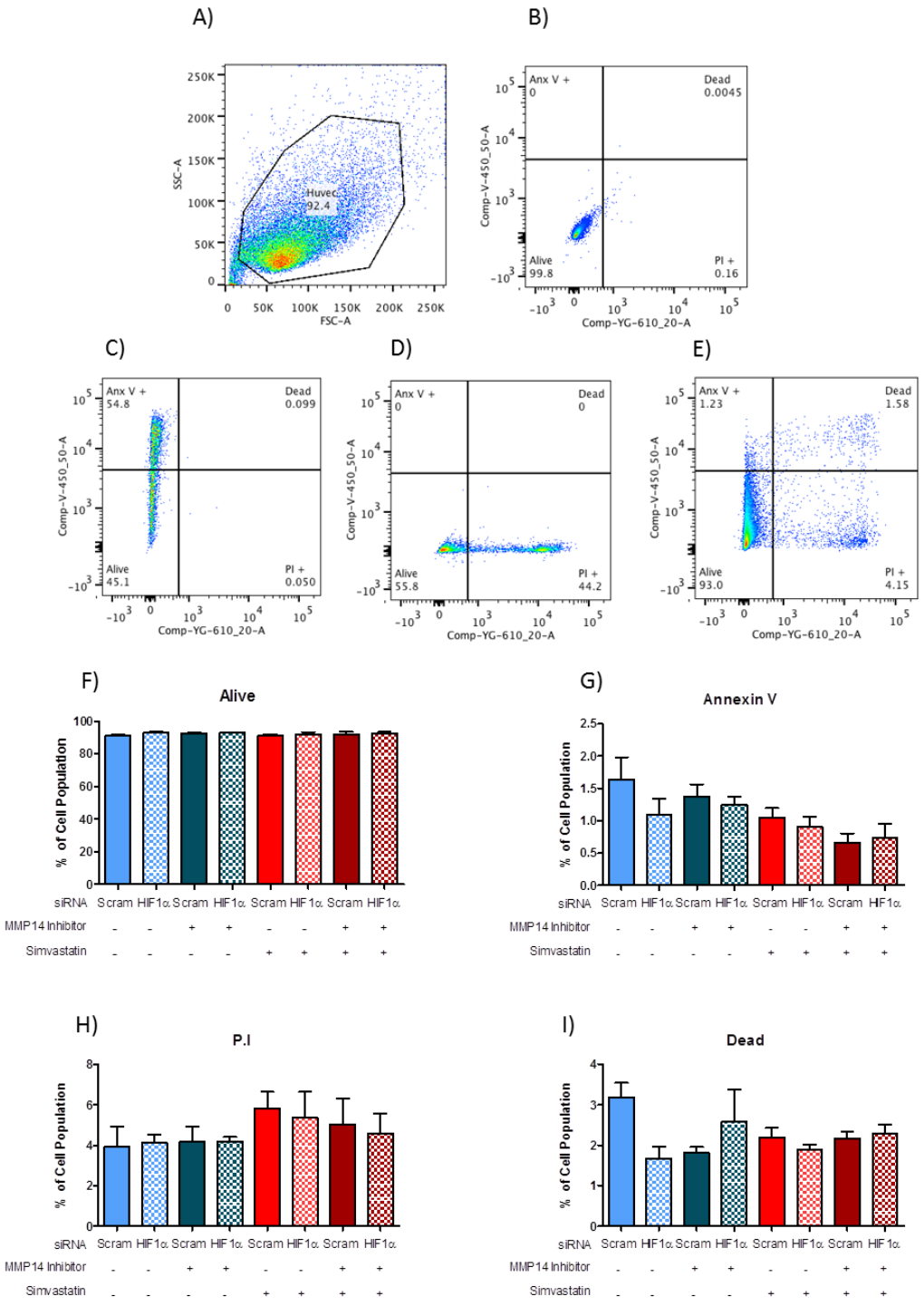

Fig. 23 – Apoptosis analysis using flow cytometry. A) The gating for the population of HUVECS. B) The analysis of unstained cells. C) The analysis of annexin V stained cells. D) The analysis of PI stained cells. E) An example of a flow cytometry readout of an analysed cell population. The proportion of cells that are F) classed as alive and viable, G) Annexin V positive and therefore apoptotic, H) PI positive and therefore necrotic, and I) Dead and unviable with no trend seen. Bar charts are representative of mean + SEM from 3 separate experiments.

3.2.2 Tube Formation Assays

Tube formation assays were used to observe effects of simvastatin and hypoxia on angiogenesis *in vitro*.

HUVECs were cultured on reduced growth factor Matrigel in hypoxic or normoxic conditions and in the presence or absence of 0.1µM simvastatin. The effect on tube formation can be analysed more quantitatively by looking at the total branching length, number of new nodes, and number of new junctions. It was seen that simvastatin reduced *in vitro* tube formation in both normoxic and hypoxic conditions with a significant decrease in total branching length (Fig. 24). There was slightly increased tube formation seen in hypoxic conditions compared to normoxic conditions (Fig. 24) which is potentially due to the upregulation of HIF1α which would activate angiogenesis promoting genes [64]. Addition of simvastatin significantly reduced new junctions and nodes formed in hypoxic conditions, but this effect was not observed in normoxic conditions (Fig. 24).

Following the incubation allowing for tube formation, the structures were stained for MMP14 expression. DAPI stain was used to identify the nuclei. Based on rough nuclei counts, simvastatin cultures appeared to have less nuclear stains which suggested that there may be more cell death in cultures that were exposed to simvastatin (Fig. 24E). This was also seen in cells that were exposed to hypoxia (Fig. 24E).

As the differences that were seen consisted of only a small change between the conditions it was decided that different angiogenesis methods should be used to further the work. This was

also partly due to the reasoning that angiogenesis is a multifactorial process that occurs by incorporating a number of different cells and stroma to form neovessels. The tube formation assay could be seen as being more a cell rearrangement or migration assay. Therefore more stringent *ex vivo* and *in vivo* assays took preference.

Further to this the project required testing of the effects of *HIF1α* knockdown or knockout on tube formation and angiogenesis. HUVECs nucleofected with their specific siRNA were not viable after 8 hours of the tube formation assay. Therefore a different method was required to assess *HIF1α* knockdown or knockout on angiogenesis. It was decided that the aortic ring assay would be a proficient technique to do this.

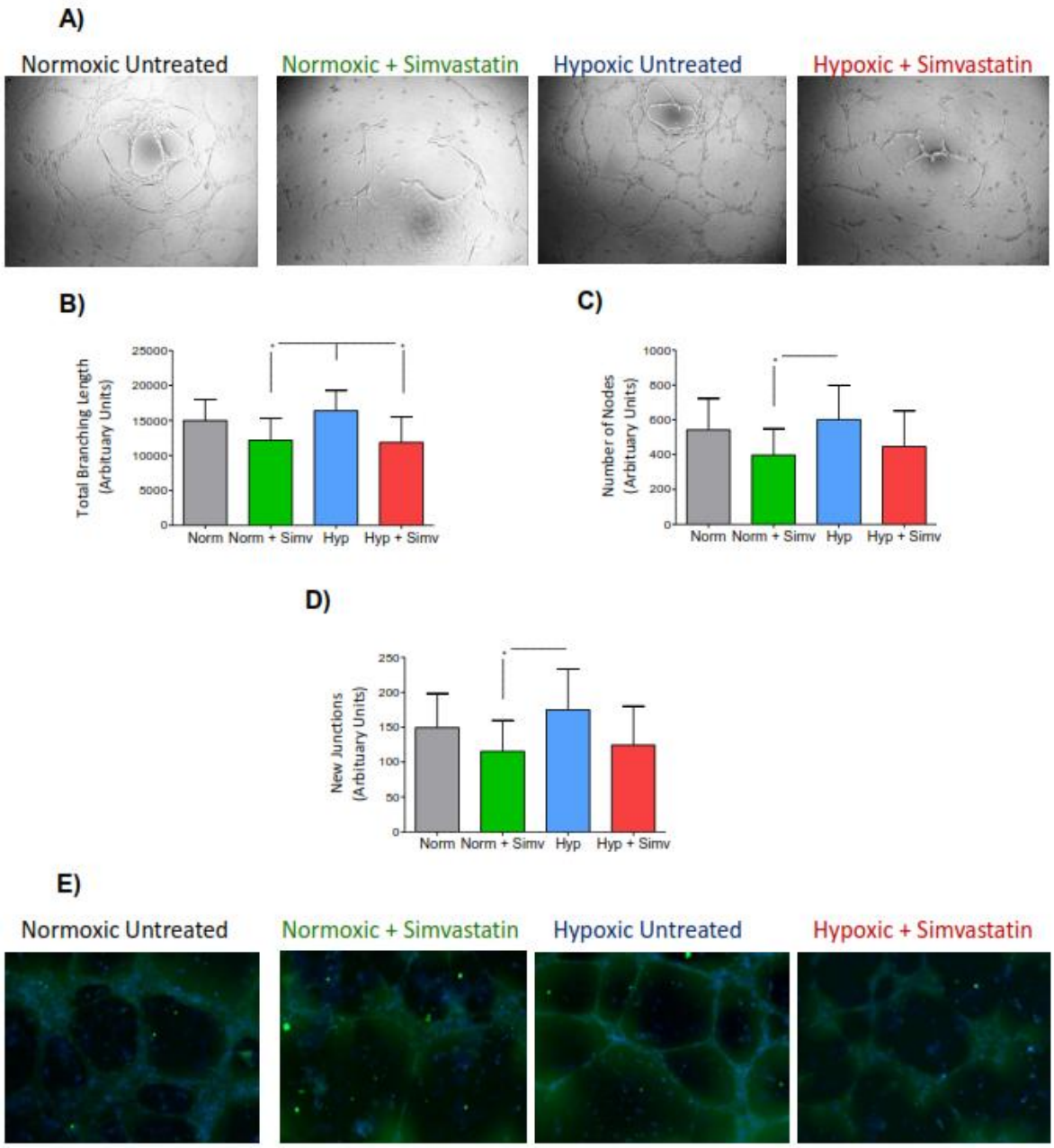

Fig. 24 – Tube formation results of HUVECs cultured on reduced growth factor 142Matrigel in hypoxic or normoxic conditions, in the presence of 0.1µM simvastatin or vehicle. A) Representative images of the four conditions from showing normoxic, normoxic and simvastatin, hypoxic, and hypoxic and simvastatin from left to right. B) The total branching length of the tubes. C) The new number of nodes formed by the HUVECS seeded in Matrigel. D) The new junctions formed by HUVECs in Matrigel in the different conditions. E) A panel of representative MMP14 (Green) and DAPI (Blue) stains performed on the formed tubes from the different conditions. Bar charts are representative of mean + SEM from 5 separate experiments. Statistical analysis was conducted using One Way ANOVA with Neuman-Keuls post testing. * = P<0.05

4. Results

4.1 HIF1α Regulation of MMP14 and its Effect on Endothelial Function

MMP14 had been identified to have HRE in the promoter region and regulated by HIF2α [208] but there was also evidence showing depleted HIF1α levels lead to diminished MMP14 levels [238]. My project sought to identify a regulation of MMP14 by HIF1α and then observe effects of this relationship on endothelial function.

4.1.1 HIF1α and MMP14 are Located in Atherosclerotic Plaques with Protein Colocalisation Observed Within Endothelial Cells and Macrophages

To observe HIF1α and MMP14 expression in atherosclerotic plaques, immunohistochemical analysis of atheroma tissue was conducted by Dr Feng Zhang. The atheromas were sourced from various hospitals around the country and were obtained following endarterectomy. It was seen that in adjacent sections of human atheromas both HIF1α and MMP14 were expressed in the neovessels of the atheromas, with apparent co-localisation of HIF1α and MMP14 (Fig. 25). This identified that MMP14 and HIF1α are expressed in the same location and therefore a potential interaction of HIF1α with MMP14 could occur.

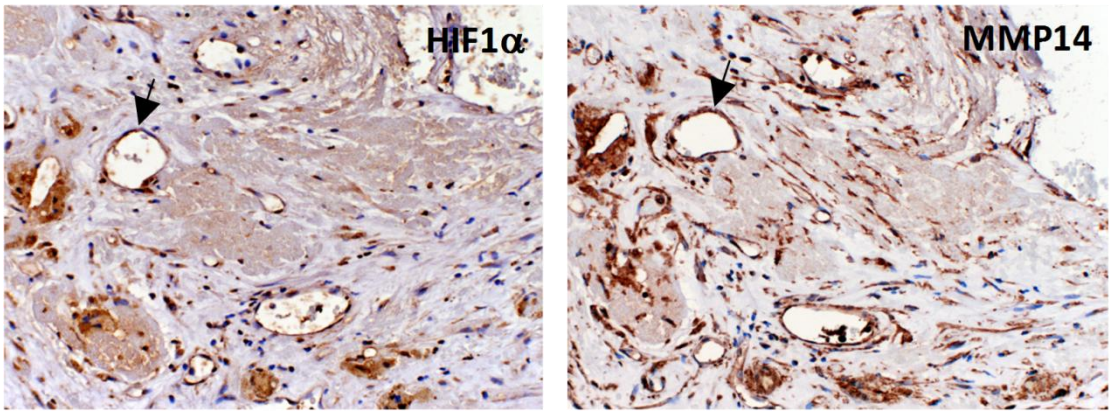

Fig. 25 – HIF1α and MMP14 showed colocalisation in the neovessels of atheromas. Immunohistochemical staining with black arrows indicating the staining of neovessels for HIF1α (left panel) and MMP14 (right panel) at 20x magnification. (Courtesy of Dr Feng Zhang).

As well as staining human atherosclerotic tissue mouse atheroma tissue was stained for HIF1α, MMP14 and the macrophage marker F4/80. *APOE* knockout mice were fed a high fat diet in order to produce atherosclerotic lesions. Following this the tissue was harvested and cryosectioned.

The mouse atheroma tissue was stained for an endothelial cell marker (endomucin) alongside HIF1α or MMP14 and for a macrophage marker (F4/80) alongside HIF1α. It was seen that both HIF1α and MMP14 colocalised with the endothelial cell marker in mouse atheromas (Fig. 26A and B). Furthermore, HIF1α colocalisation was observed with macrophage marker in the same tissue (Fig. 26C).

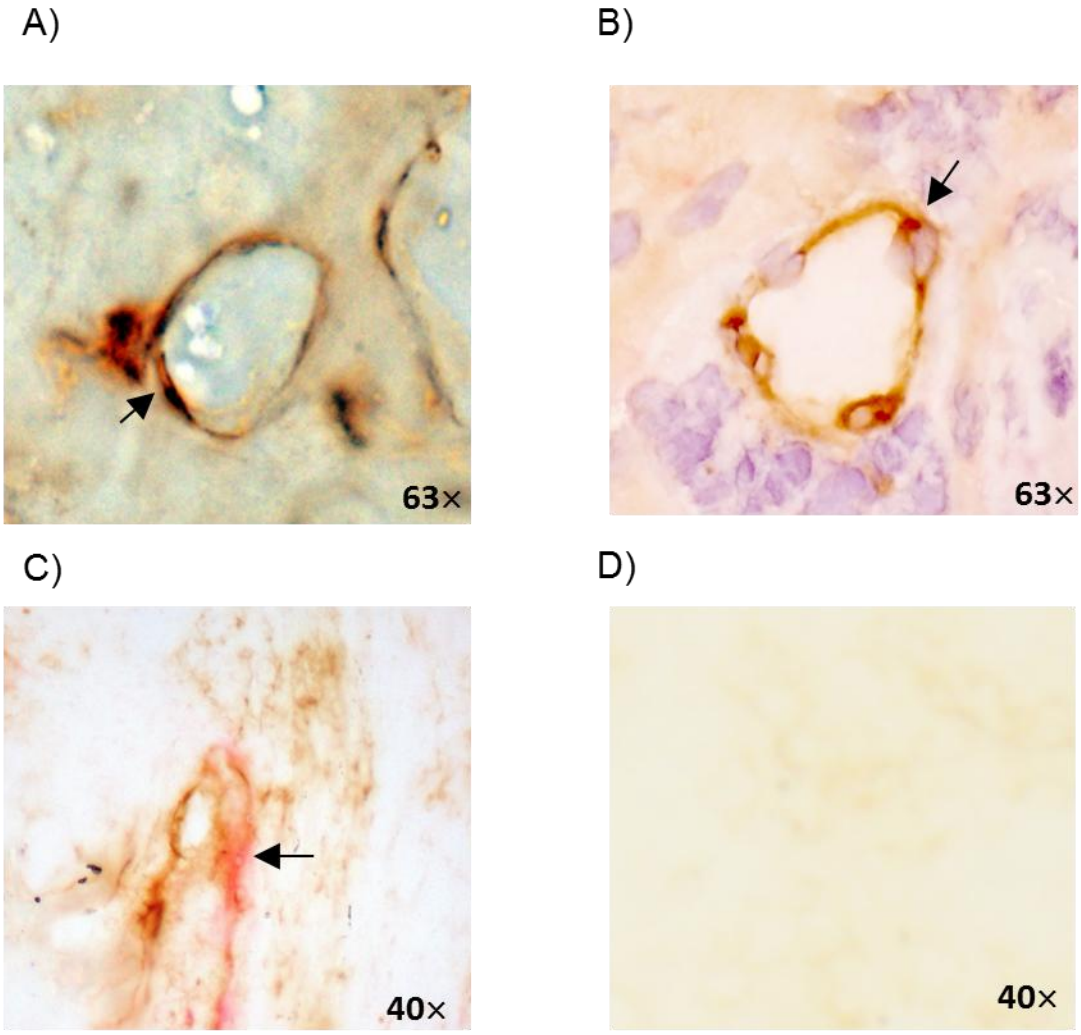

Fig. 26 – HIF1α and MMP14 colocalise with endothelial cells, and macrophages, in *APOE* knockout mouse atheromas. A) HIF1α (brown) colocalises with endomucin (red) in mouse atheroma tissue. B) MMP14 (red) colocalises with endomucin (brown) in mouse atheroma tissue. C) HIF1α (brown) colocalises with F4/80 (red) in mouse atherosclerotic tissue. D) Isotype control utilising species isotypes for the primary antibodies.

4.1.2 HIF1α Binds to the *MMP14* Promoter in Hypoxia but this is Attenuated by Simvastatin Treatment

To investigate the regulation of MMP14 by HIF1α a search of the *MMP14* promoter for HREs was conducted. It was found that *MMP14* contains two putative HREs in the gene promoter region at positions -125 to -129 and from -3568 to -3572, respectively, relative to the start of transcription. Additionally, another HRE after the start of transcription at position +144 to +148 is noted [208]. This suggested that MMP14 expression may be transcriptionally regulated by HIF1α.

EMSAs were conducted by Dr Conrad Hodgkinson utilising synthetic HIF1α and HIF1β cultured alongside biotin-labelled double stranded oligonucleotides. Short nucleotide sequences containing an enzyme tag corresponding to HRE sites in the proximal (-125 to -129) and distal (-3568 to -3572) promoter regions of *MMP14* were incubated with the protein extract from C166 endothelial cells.

It was seen that when the biotin-labelled double stranded oligonucleotides were incubated with HIF1α and HIF1β together there was a shift in mobility and a distinct band was seen, showing that a protein complex had formed and bound to the relevant nucleotide tag. This was seen in both the distal and proximal HRE sites (Fig. 27B lanes 5) thus providing evidence that HIF1α binds to the *MMP14* promoter.

When either HIF1α or HIF1β were absent there was no binding of the nucleotide probe to the proteins (Fig. 27B lanes 1-4). This showed that the fully functional HIF response complex needed to form in order for interaction with the HRE of *MMP14*.

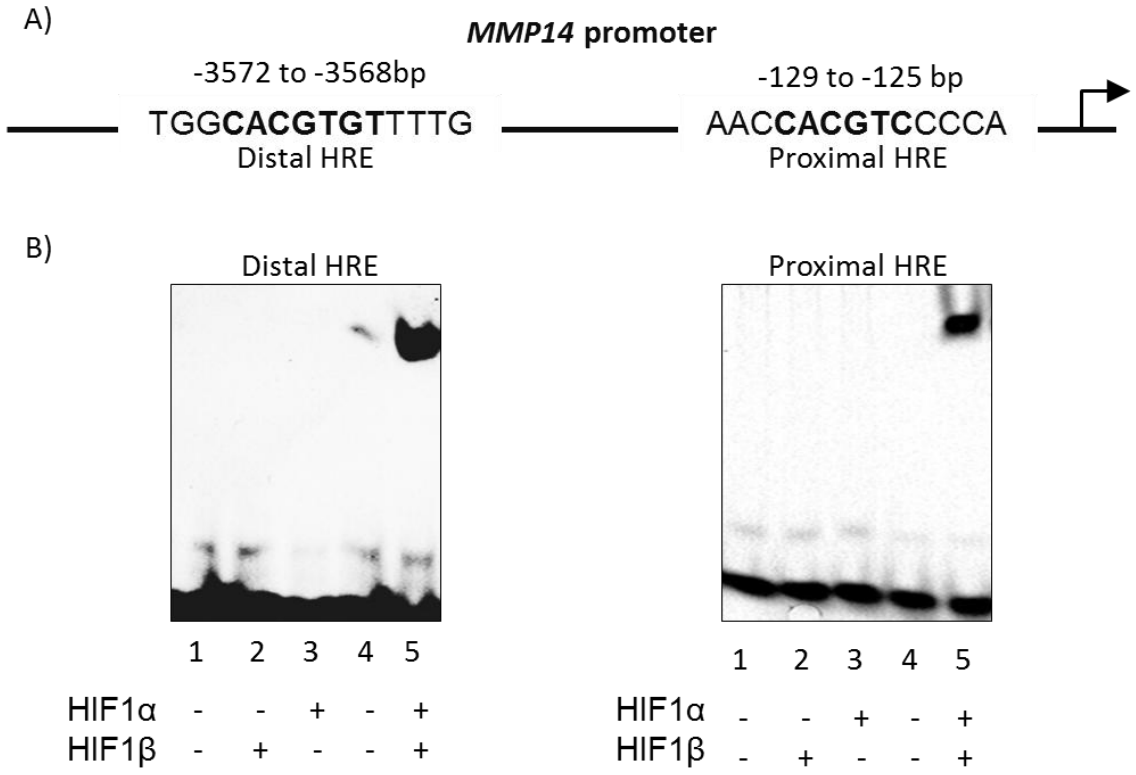

Fig. 27 – HIF binds to the *MMP14* promoter at both the distal and proximal HRE. Electromagnetic shift assay of MMP14 HRE sites in the presence or absence of synthetic HIF1α and HIF1β. A) A diagram indicating the positions of the distal and proximal HRE in the MMP14 promoter. B) A clear band is seen in both the distal (left side) and proximal (right side) HRE sites when both HIF1α and HIF1β are present (lane 5), however when either HIF1α or HIF1β are absent there is no band seen (lanes 1-4). The results are representative of 3 independent experiments. (Courtesy of Dr Conrad Hodgkinson).

To confirm the interaction of HIF1α with the *MMP14* promoter ChIP assays were also conducted. Chromatin immunoprecipitation assays were performed on cultured HUVECs either in hypoxia (1% O_2) or normoxia, with 0.1μM simvastatin or vehicle control to assess HIF1α interaction with the *MMP14* promoter and the effect of simvastatin on this. The chromatin was immunoprecipitated using a HIF1α antibody before PCR analysis using primers corresponding to the *MMP14* promoter proximal HRE site.

The ChIP assays showed that HIF1α binds to the *MMP14* gene promoter but that this was significantly attenuated by simvastatin treatment (Fig. 28). There was still some interaction of the HIF response complex with the *MMP14* promoter in hypoxic conditions treated with simvastatin, however this was markedly decreased (Fig. 28). There was no HIF1α and *MMP14* interaction in cells that were cultured in normoxic conditions (Fig. 28).

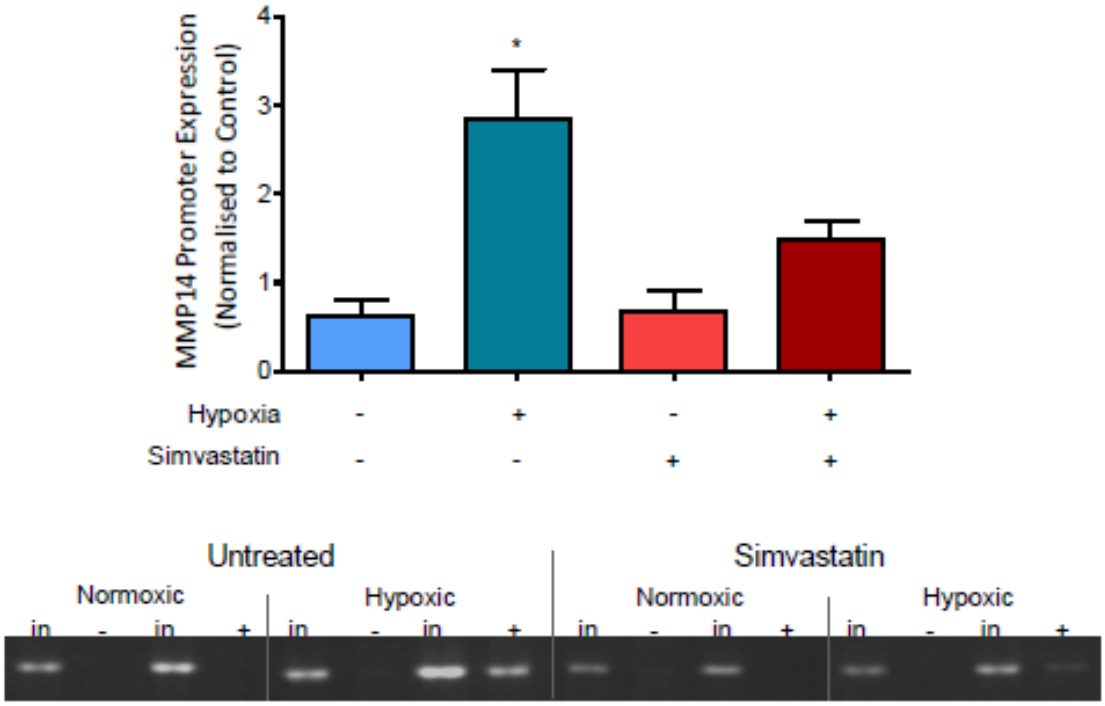

Fig. 28 – HIF1α binding to the *MMP14* promoter in HUVECs occurs in hypoxic conditions and is attenuated by simvastatin treatment. The graph shows results of HUVEC chromatin immunoprecipitation assay. HUVECs were cultured in normoxia or hypoxia, with or without 0.1μM simvastatin and immunoprecipitated for HIF1α before analysing for the MMP14 promoter. A) Bar chart representing observed results whereby hypoxia increased the localisation of HIF1α to the *MMP14* promoter while the addition of simvastatin reduced this affect. B) Representative gel image of the ChIP assay. Bar chart is representative of mean + SEM from 3 independent experiments. Statistical significance was analysed by One Way ANOVA with Neuman-Keuls post test. * = $P<0.05$.

4.1.3 Simvastatin Attenuates HIF1α Upregulated *MMP14* Promoter Activity

The EMSA and ChIP assays had shown that HIF1α binds to the *MMP14* promoter. In order to analyse the effect that this had on the activity of the promoter, luciferase reporter assays were carried out. The luciferase reporter assays were conducted by Dr Conrad Hodgkinson. C166 endothelial cells were transfected with a human *MMP14* gene promoter-firefly luciferase reporter gene construct, together with plasmids to overexpress HIF1α and HIF1β, HIF1β on its own, or an empty vector. Following successful transfection the cells were analysed using luciferase reporter assays.

The luciferase assays showed that *MMP14* promoter activity was increased when endothelial cells were overexpressing HIF1α and HIF1β in hypoxic conditions. This showed that HIF1α can upregulate *MMP14* when the stable HIF1 complex was formed (Fig. 29A). Additionally only a small effect was seen when HIF1β was present on its own, showing a need for HIF1α in the formation of the stable HIF response complex. As well as this we have shown an attenuation of *MMP14* promoter activity when mutations were introduced into the HRE, primarily at the proximal site, in both normoxic and hypoxic conditions (Fig. 29B). This showed that the upregulation of *MMP14* activity was due to the HRE. The distal HRE mutation showed a smaller attenuating effect than that of the proximal HRE mutation, whereby mutating the distal HRE alone showed only a minimal change in *MMP14* promoter activity (Fig. 29B), showing that the proximal HRE is the primary HRE for *MMP14* activity promotion. A cumulative diminishing effect was observed when both of the HRE were mutated in normoxia, although this was not seen in hypoxia (Fig. 29B).

MMP14 promoter activity was significantly increased in hypoxic conditions but the addition of simvastatin attenuated this effect (Fig. 29C). Mutations of the HRE in the *MMP14* promoter showed no change in response to hypoxia or simvastatin treatment (Fig. 29C).

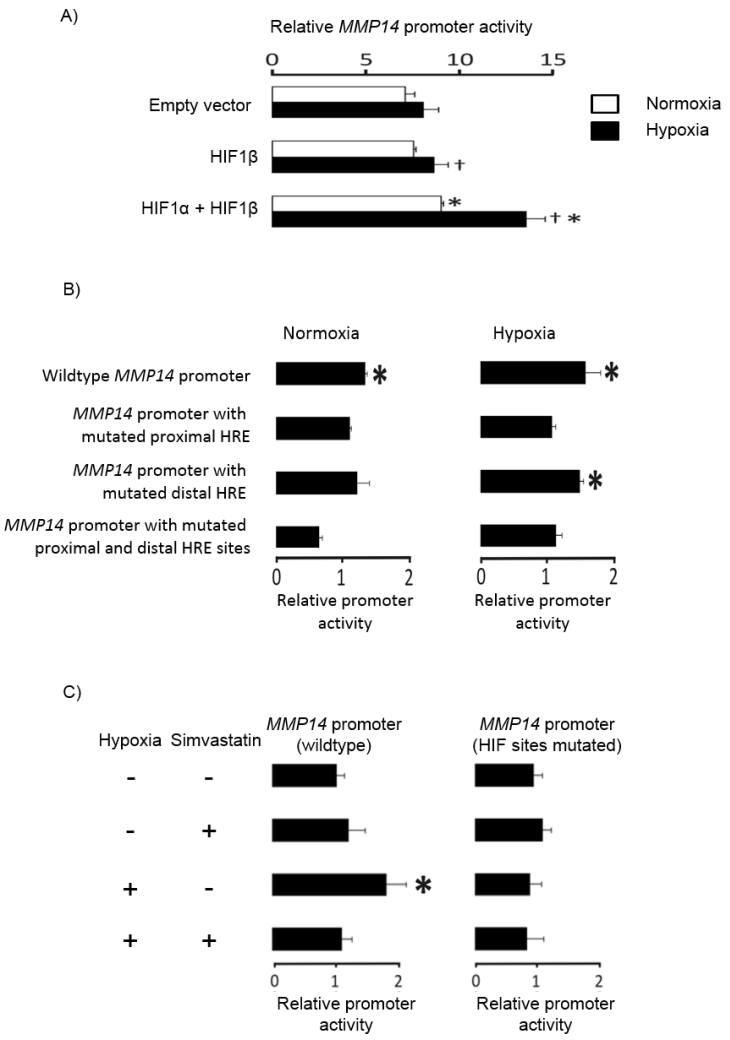

Fig. 29 – *MMP14* gene promoter activity is increased by HIF in hypoxic conditions and attenuated by simvastatin. Luciferase reporter assays of *MMP14* gene promoter activity. Cultured endothelial cells (C166) were transfected with an *MMP14* gene promoter-firefly luciferase reporter gene construct, together with experimental plasmids and a plasmid containing the *Renilla luciferase* gene. Transfected cells were exposed to hypoxia (1% O_2) or normoxia for 18 hours. *MMP14* promoter activity was measured by dual-luciferase assays. A) Relative *MMP14* promoter activity after transfection with plasmids to overexpress HIF1β, or HIF1α + HIF1β. Transfection with HIF1α + HIF1β increased *MMP14* promoter expression. B) Relative *MMP14* promoter activity after transfection with plasmids containing mutations in the *MMP14* promoter HREs. Mutations of HREs in the *MMP14* promoter significantly attenuated *MMP14* activity. C) Relative *MMP14* promoter activity after transfection with the *MMP14* gene promoter-firefly luciferase reporter gene and the *Renilla luciferase* gene in either hypoxia or normoxia, with simvastatin (2μM) or vehicle control. Simvastatin significantly attenuated *MMP14* activity in hypoxia, but had no effect when the HRE sites were mutated. Data shown are mean +SEM of relative *MMP14* promoter activity in three independent experiments * and ϯ= P<0.05 (Courtesy of Dr Conrad Hodgkinson)

4.1.4 Simvastatin Inhibits MMP14 in a HIF1α-dependent Manner

As it was shown that the *MMP14* promoter was regulated by HIF1α and its activity was decreased by simvastatin an investigation of the molecular mechanisms of this effect on MMP14 protein expression was conducted.

HUVECs were transfected, using nucleofection, with either a HIF1α specific siRNA (Santa Cruz, USA), a scramble control siRNA (Santa Cruz, USA) or a water control. Simvastatin (0.1μM) or a vehicle control was added to the cells in culture 24 hours prior to protein harvest. The protein was extracted and analysed using immunoblotting.

The knockdown of HIF1α was shown to be effective as HIF1α expression in the *HIF1α* siRNA targeted cells was reduced by approximately 50% as compared to the scramble control (Fig. 30A). MMP14 expression in hypoxia was reduced by 30% in the *HIF1α* knockdown cells compared to scramble control showing that MMP14 is under HIF1α control in hypoxic conditions (Fig. 30B). This was not seen however in normoxic conditions (Fig. 30C).

The addition of simvastatin significantly attenuated HIF1α and MMP14 activity in hypoxic conditions to a similar extent as HIF1α knockdown showed (Fig. 30A and B), however there was no effect seen in the normoxic MMP14 condition.

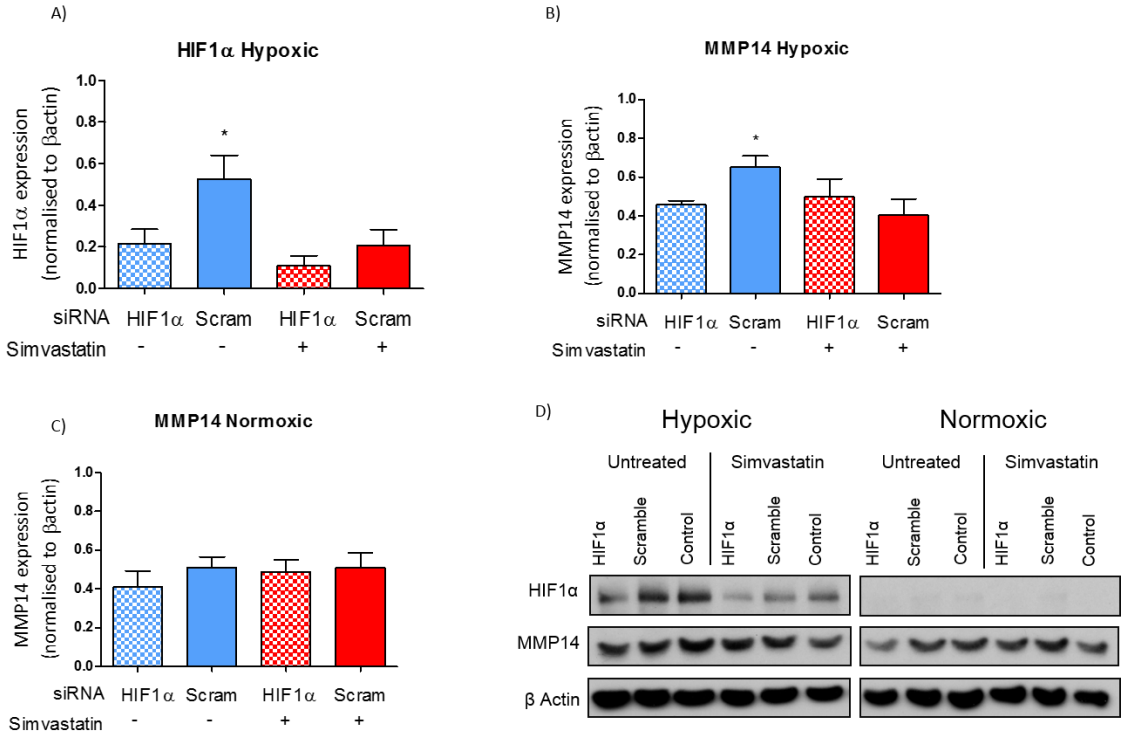

Fig. 30 – *HIF1α* knockdown and simvastatin decrease MMP14 expression in HUVECs in hypoxic conditions. Immunoblot analysis of HUVECs nucleofected with *HIF1α* siRNA, scramble siRNA, or water control, cultured in either hypoxic or normoxic conditions, with or without 0.1µM Simvastatin. A) Analysis of HIF1α expression in hypoxic conditions showing *HIF1α* knockdown was effective and simvastatin significantly reduced HIF1α expression. B) Analysis of MMP14 expression in hypoxic conditions showing MMP14 expression is significantly attenuated by *HIF1α* knockdown and simvastatin. C) Analysis of MMP14 expression in normoxic conditions showing there is no effect of *HIF1α* knockdown and simvastatin in normoxic conditions. D) A representative film image of immunoblots analysis. Bar charts represent the protein expression densitometry mean + SEM from 5 independent paired experiments. Statistical analysis was conducted using One Way ANOVA with Neuman-Keuls post testing. * = P<0.05

In order to further analyse the effect of *HIF1α* knockdown, hypoxia and simvastatin treatment on MMP14, flow cytometry assays were used. This enabled a more quantitative approach to the analysis of MMP14 expression.

For this experiment both HUVECs and MLECs were used in order to investigate any difference between the human cells and the murine cells. MLECs were isolated from the lungs of both the *Tie1 Cre+ HIF1α*$^{fl/fl}$ mice and wildtype littermates. HUVECs were transfected, using nucleofection, with either a HIF1α specific siRNA (Santa Cruz, USA), a scramble control siRNA (Santa Cruz, USA). Simvastatin (0.1μM) or a vehicle control was added to the cells in culture 24 hours prior to cell fixation. The cells were detached from the culture plates, fixed, permeabilised and stained for MMP14 activity before analysis with a Fortessa flow cytometer (BD Biosciences, UK).

The results showed that hypoxia increases MMP14 expression in the wildtype MLECs and the scramble control siRNA HUVECs by approximately 100%, but this is not the case for the *HIF1α* knockout and knockdown cells (Fig. 31A and B). Simvastatin significantly attenuated the hypoxic increase in MMP14 activity in the wildtype MLECs and control HUVECs, by approximately 40-60%, but had no effect on *HIF1α* knockout and knockdown cells or normoxic cells (Fig. 31). It could therefore be seen that simvastatin's inhibition of MMP14 was occurring in a HIF1α-dependent manner.

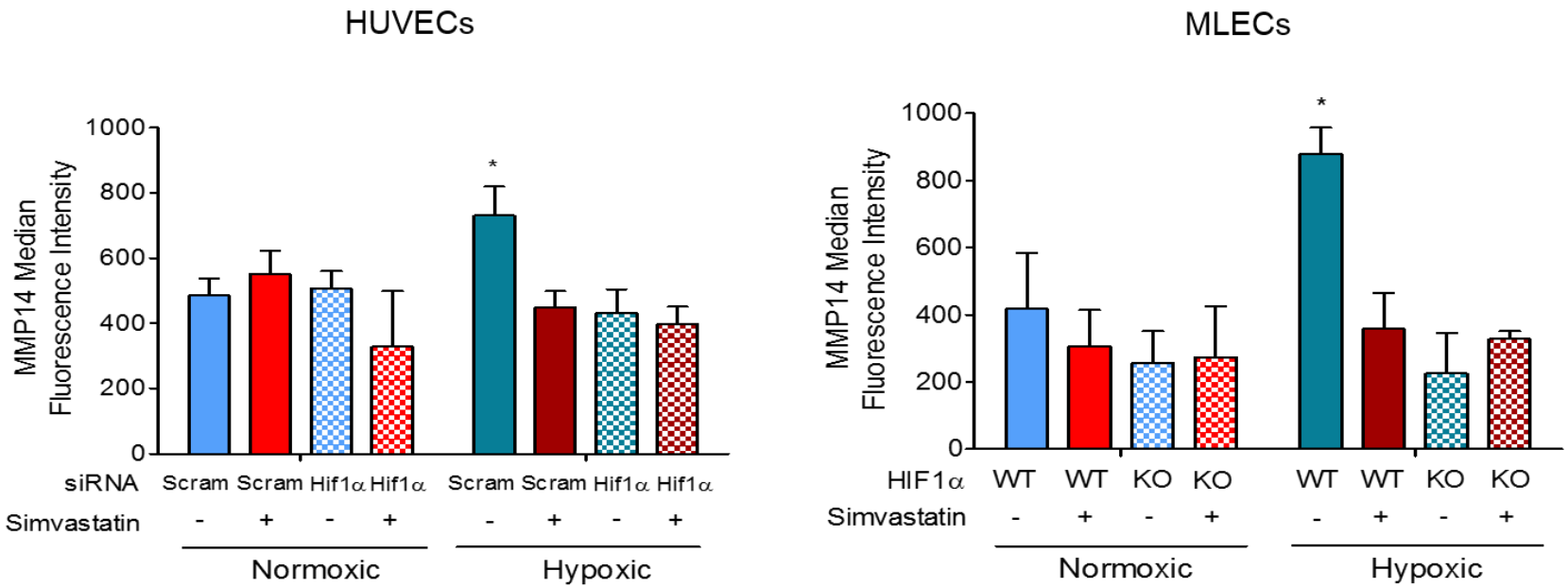

Fig. 31 – Simvastatin, *HIF1α* knockout and *HIF1α* knockdown inhibit hypoxic MMP14 expression. Flow cytometry analysis of MMP14 in HUVECs A) and MLECs B) cultured in hypoxia or normoxia, with or without 0.1µM simvastatin. A) HUVECs cultured in hypoxic conditions have significantly increased MMP14 levels than HUVECs grown in normoxia. Simvastatin significantly diminishes MMP14 levels in hypoxic conditions. B) *Tie1 Cre- HIF1α* WT and *Tie1 Cre+ HIF1α* KO MLECs were isolated and cultured in the specified conditions. Hypoxia significantly increased MMP14 levels compared to normoxia in *Tie1 Cre- HIF1α* WT MLECs. Simvastatin significantly reduces MMP14 levels in *Tie1 Cre- HIF1α* WT hypoxic MLECs. Hypoxic *Tie1 Cre- HIF1α* WT MLECs have a significantly increased MMP14 expression in comparison to *Tie1 Cre+ HIF1α* KO MLECs. Bar charts demonstrate the mean median fluorescence intensity of MMP14 levels + SEM from A) 6 and B) 5 independent experiments. Statistical analysis was conducted using One Way ANOVA with Neuman-Keuls post testing. * = $P<0.05$

4.1.5 Simvastatin Inhibits Hypoxic Endothelial Cell Migration and Proliferation

Given experimental evidence that both simvastatin and HIF1α had a role in regulating MMP14 expression, it was decided to investigate the effect of this on cellular function, specifically in roles related to angiogenesis. Therefore analysis of migration and proliferation of nucleofected HUVECs with simvastatin treatment was conducted.

HUVECs were nucleofected with either a *HIF1α* siRNA or scramble control siRNA (Santa Cruz, USA) and seeded onto 12 well culture plates for migration and 96 well culture plates for proliferation. The migration plates were allowed to reach full confluency before the addition of 0.1μM simvastatin, 24 hours prior to introducing a wound in the cell monolayer. The proliferation assay plates grew for 24 hours post-transfection before the addition of 0.1μM simvastatin.

The migration assays showed that both 0.1μM simvastatin and *HIF1α* knockdown significantly attenuate hypoxic migration of HUVECs by roughly 60% and 40%, respectively (Fig. 32A and B). The addition of 0.1μM simvastatin to *HIF1α* knockdown cells showed no significant difference compared to the vehicle control (Fig. 32B), thus showing the inhibition of migration was due to a HIF1α-dependent effect.

The proliferation assays showed a similar pattern with 0.1μM simvastatin and *HIF1α* knockdown significantly inhibiting the proliferation of HUVECs in hypoxia by around 50% and 40% respectively (Fig. 32C). In the *HIF1α* knockdown groups the addition of 0.1μM simvastatin also significantly decreased proliferation compared to the vehicle control (Fig. 32C).

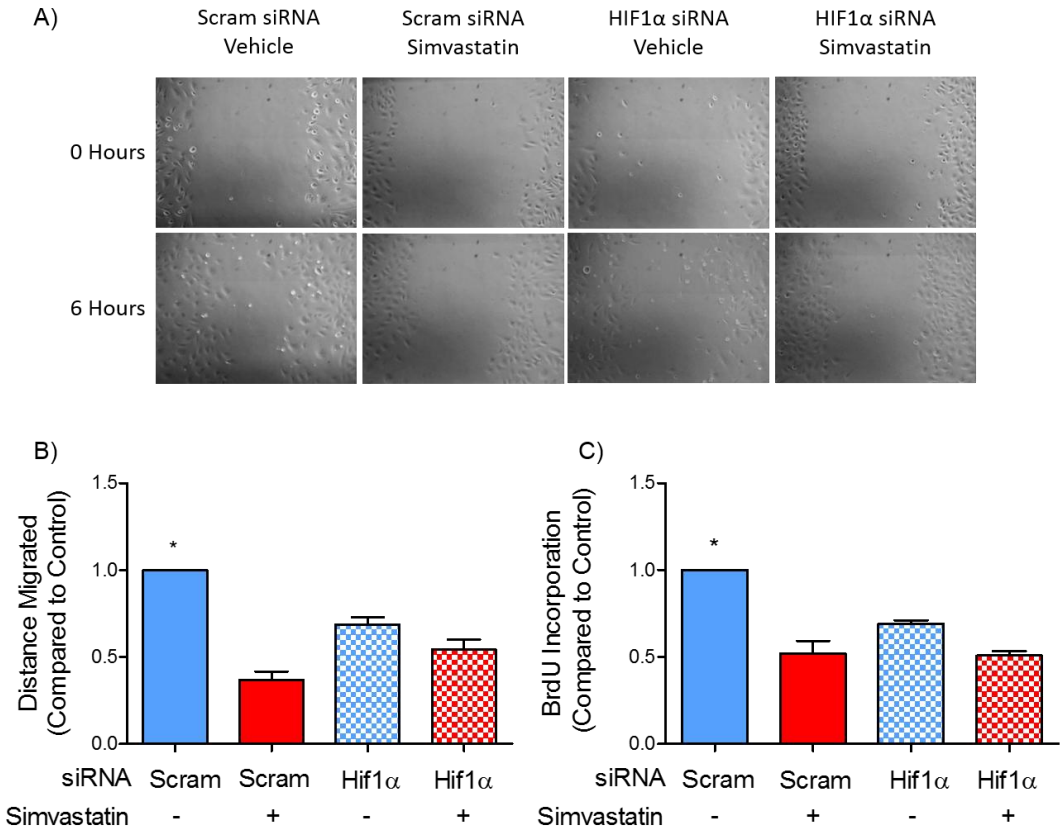

Fig. 32 – Simvastatin inhibits hypoxic endothelial cell migration and proliferation. HUVECs were nucleofected with either *HIF1α* siRNA or scramble siRNA were cultured in hypoxic condition with or without 0.1µM simvastatin. A) A representative image set for the scratch migration experiments from the start of the migration assay until completion after 6 hours. B) A bar chart representing the scratch assays performed and analysed over 6 hours. The resultant migration was compared to the control scramble siRNA without simvastatin. The data shows simvastatin significantly reduces hypoxic migration in control cells, but has no effect on *HIF1α* knockdown cells. C) A bar chart representing the BrdU incorporation proliferation assay performed with relevant proliferation compared to the control scramble siRNA without simvastatin. The data shows simvastatin significantly reduces hypoxic proliferation in both control and *HIF1α* knockout cells. The bar charts represent distance migrated and BrdU incorporation compared to controls + SEM (n=5 and n=6). Statistical analysis was conducted using One Way ANOVA with Neuman-Keuls post testing. * = P<0.05

4.1.6 MMP14 Inhibition Decreases Proliferation and Migration in Hypoxia

It had been shown that simvastatin decreased both hypoxic migration and proliferation of HUVECs but this could not be specifically related to MMP14. Therefore in order to test the effect of MMP14 inhibition on migration and proliferation of HUVECs in hypoxia an MMP14 inhibitory antibody (Merck Millipore, UK) or rabbit-IgG (Santa Cruz, USA) control antibody was added to the cultures.

The results showed that the addition of the MMP14 inhibitory antibody significantly decreased the migration of the HUVECs treated with scramble siRNA in hypoxia (Fig. 33A and B). The addition of simvastatin was again shown to significantly reduce migration of HUVECs in hypoxia but showed no extra inhibitory effect on both *HIF1α* knockdown and scramble control cells cultured with the MMP14 inhibitory antibody (Fig. 33A and B).

The proliferative potential of the HUVECs in hypoxia was also affected in a similar pattern to that of migration. The MMP14 inhibitor significantly inhibited proliferation of the HUVECs in hypoxia (Fig. 33C) and also showed that simvastatin had no added inhibitory effect on the *HIF1α* knockdown and scramble control cells cultured with the MMP14 inhibitory antibody (Fig. 33C).

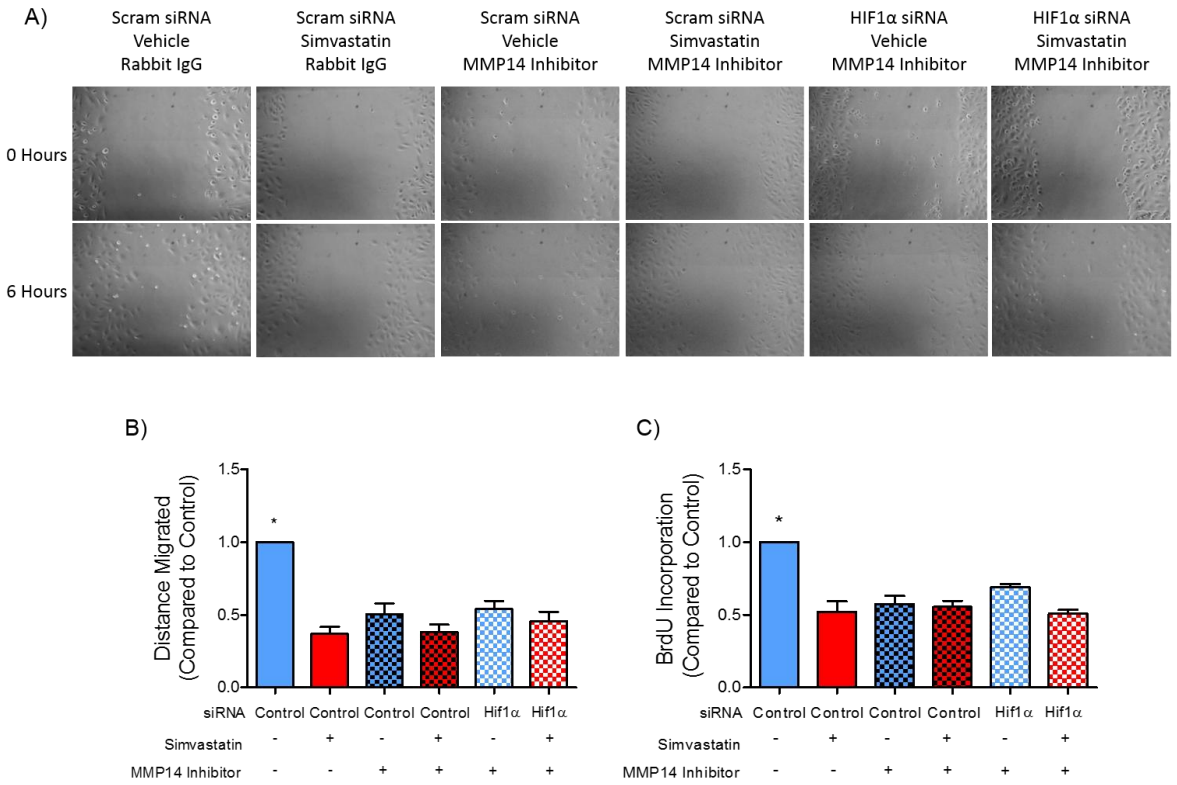

Fig. 33 – MMP14 inhibition decreases proliferation and migration of HUVECs in hypoxia. HUVECs nucleofected with either *HIF1α* siRNA or scramble siRNA were cultured in hypoxic condition with or without 0.1μM simvastatin and an MMP14 neutralising antibody or rabbit IgG control. A) A representative image set of the migration assay experiment. B) A scratch assay was performed and analysed over 6 hours. The resultant migration was compared to the control scramble siRNA without simvastatin with rabbit IgG. MMP14 inhibition decreases migration in control cells but not *HIF1α* knockdown cells or cells treated with 0.1μM simvastatin. C) BrdU incorporation assay with proliferation compared to the control scramble siRNA without simvastatin with rabbit IgG. MMP14 inhibition decreases scramble siRNA cells proliferation, but not the *HIF1α* knockdown cells. MMP14 inhibition does not affect proliferation in cells treated with 0.1μM simvastatin. The bar charts represent distance migrated and BrdU incorporation compared to controls + SEM (n=5 and n=6). Statistical analysis was conducted using One Way ANOVA with Neuman-Keuls post testing. * = $P<0.05$

4.2 HIF1α and Simvastatin Effect on MMP14 and Angiogenesis

4.2.1 Simvastatin Reduces Angiogenesis in a HIF1α-dependent Manner

HIF1α and simvastatin were shown to have a role in regulating MMP14 expression *in vitro* with a consequential functional effect on migration and proliferation. In order to see if this had a further effect on angiogenesis via HIF1α and MMP14 regulation aortic rings were used.

Aortic rings were cultured from *Tie1 Cre+ HIF1α*$^{fl/fl}$ mice and their wildtype littermates. They were cultured for six days in either normoxic or hypoxic (1% O_2) conditions with either 0.1μM simvastatin or a vehicle control. The results showed that hypoxia significantly increased new blood vessel sprouting in wildtype mice, but not the endothelial cell-specific *HIF1α* knockout mice (Fig. 34). Simvastatin decreased the hypoxia-induced blood vessel formation in the wildtype mice to levels that were similar to the normoxic results, with around a 25% decrease in sprouts formed (Fig. 34). However, simvastatin had no effect on the *Tie1 Cre+ HIF1α*$^{fl/fl}$ mice or in normoxic conditions (Fig. 34)

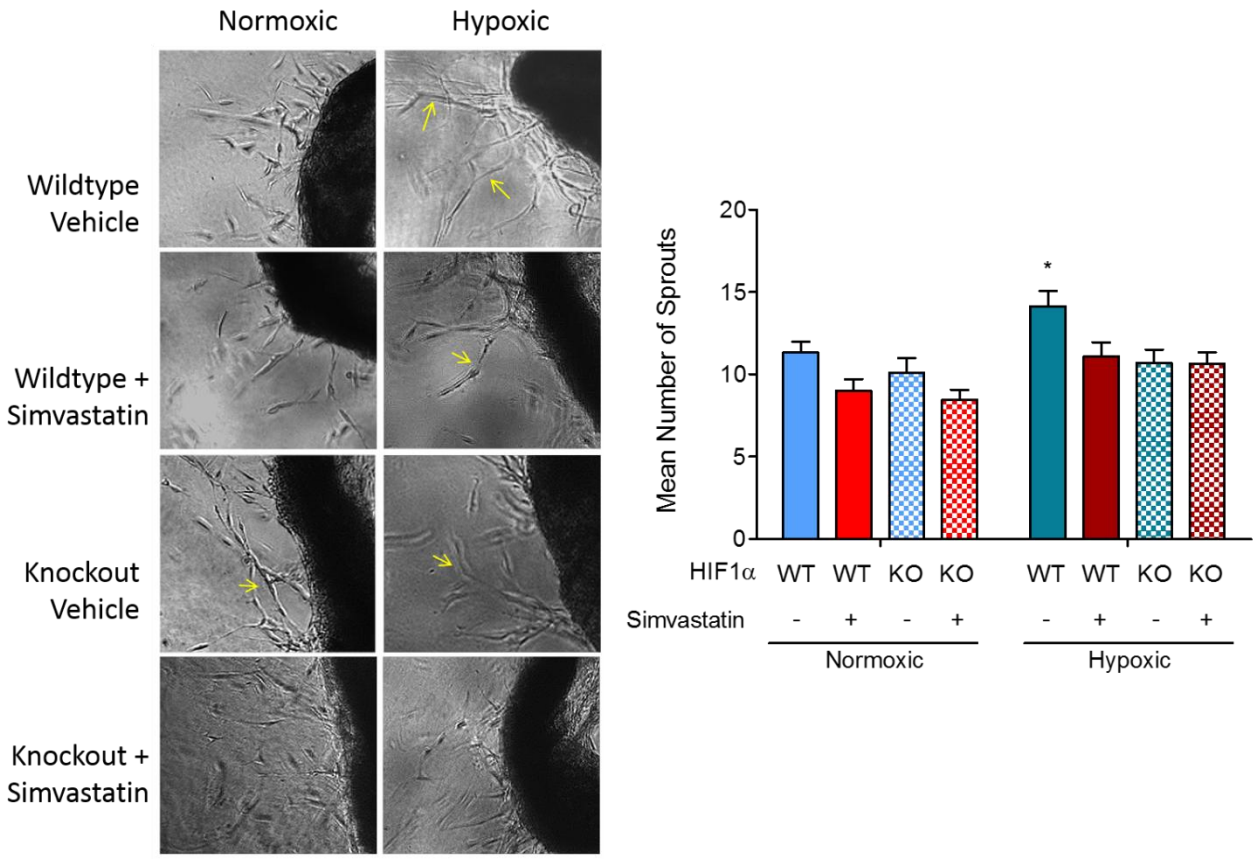

Fig. 34 – Simvastatin reduces angiogenesis in a HIF1α-dependent manner. The *ex vivo* aortic ring assay with aortas isolated from *Tie1 Cre+ HIF1α* KO mice and wildtype littermates, cultured in a three dimensional collagen matrix in hypoxia or normoxia, with or without 0.1µM simvastatin. Microvessel growth was analysed 6 days post-embedding. Wildtype mice show impaired microvessel sprouting with the addition of 0.1µM simvastatin in both normoxic and hypoxic conditions. Hypoxia significantly increased sprouting in wildtype mice compared to normoxia but this observation was not matched in the *HIF1α* knockout mice. Wildtype mice showed increased sprouting in hypoxic conditions in comparison to *Tie1 Cre+ HIF1α* KO mice. Yellow arrows indicate sprouts. The bar chart represents the mean number of microvessel sprouts per aortic ring mean + SEM (n=15). Statistical analysis was conducted using One Way ANOVA with Neuman-Keuls post testing. * = P<0.05

4.2.2 Simvastatin and *HIF1α* Knockout Reduce MMP14 Expression in Immature Endothelial Cells Perturbing Angiogenesis

It had been shown that both endothelial cell-specific *HIF1α* knockout mice and simvastatin significantly reduce angiogenesis in aortic ring cultures. As well as this a role of HIF1α and simvastatin in regulating MMP14, a promoter of angiogenesis, had been elucidated. Therefore in order to see if the perturbed angiogenesis was due to diminished MMP14 expression immunofluorescent staining of aortic ring microvessels was conducted.

Following the aortic ring culture the rings were fixed and stained for MMP14 using a FITC-conjugated MMP14 antibody (BIOSS antibodies, UK). Once the aortic rings had been stained and transferred to a microscope slide they were imaged for their fluorescence intensity.

The results showed higher expression of MMP14 in new blood vessels of wildtype hypoxic aortic ring cultures (Fig. 35). The addition of simvastatin significantly reduced the hypoxic upregulation of MMP14 in wildtype hypoxic aortic ring cultures (Fig. 35). *Tie1 Cre+ HIF1α*$^{fl/fl}$ showed less MMP14 expression than the wildtype littermates (Fig. 35).

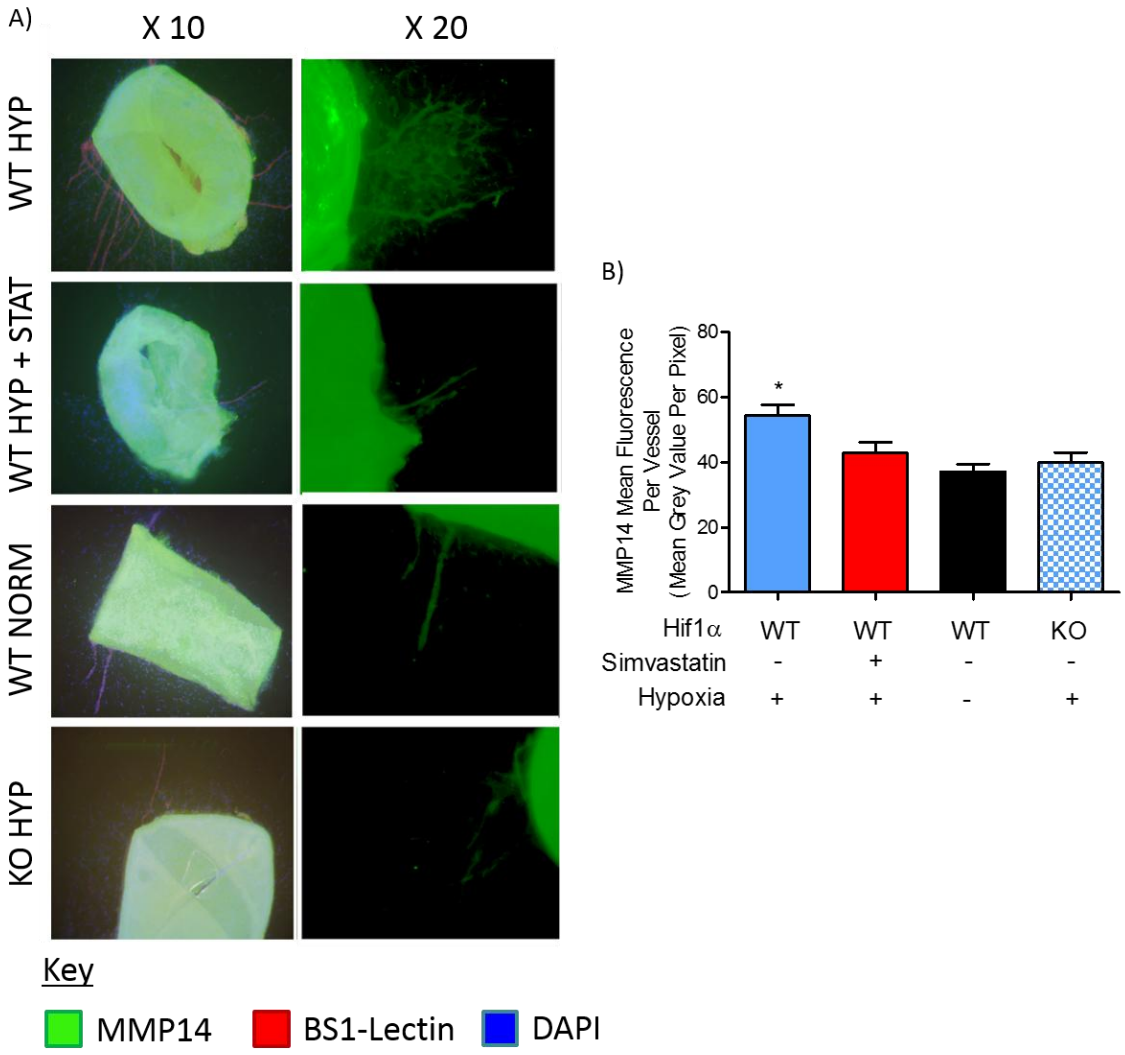

Fig. 35 – Hypoxia-stimulated MMP14 expression of new vasculature is significantly decreased in HIF1α KO and simvastatin-treated mice. The *ex vivo* aortic ring assay with aortas isolated from *Tie1 Cre- HIF1α* WT and *Tie1 Cre+ HIF1α* KO mice, cultured in a three dimensional collagen matrix in hypoxia or normoxia, with or without 0.1µM simvastatin. Following 6 days of culture the aortas were fixed and stained for MMP14 (Green), BS1-Lectin (Red) and DAPI (Blue). Fluorescence of MMP14 was analysed using FIJI software of individual microvessels in the green channel at X20 optical zoom, with the mean grey value per pixel per vessel taken for fluorescence intensity of each microvessel. MMP14 expression is significantly increased in hypoxia without simvastatin treatment in wildtype mice. The bar chart represents the mean MMP14 fluorescence of sprouts mean + SEM (n=10). Statistical analysis was conducted using One Way ANOVA with Neuman-Keuls post testing. * = $P<0.05$

4.2.3 VEGF-induced Angiogenesis is attenuated by MMP14 inhibition in a HIF1α-dependent Manner

To test the effect of MMP14 neutralisation on angiogenesis aortic rings of *Tie1 Cre+ HIF1α*$^{fl/fl}$ mice and their wildtype littermate controls were cultured with either an MMP14 inhibitory antibody (Merck Millipore, UK) or a rabbit isotype control, in the presence of either 0.1μM simvastatin or vehicle control in hypoxia (1% O_2). The results showed that after 6 days of culture there was a significant decrease in new blood sprouts from the aortic rings in MMP14 inhibited cultures (Fig. 36). The wildtype mice aorta showed a significantly reduced angiogenesis when cultured with the MMP14 antibody, as opposed to those cultured with the antibody control (Fig. 36). This effect was not replicated in the *Tie1 Cre*$^{+}$ *HIF1α*$^{fl/fl}$ mice thus showing the inhibition was HIF1α driven.

It was shown that simvastatin reduced the amount of new blood vessel formation from the aortic rings, similar to the previous observations (Fig. 36). However, it was shown that simvastatin had no effect on MMP14 inhibited aortic rings (Fig. 36).

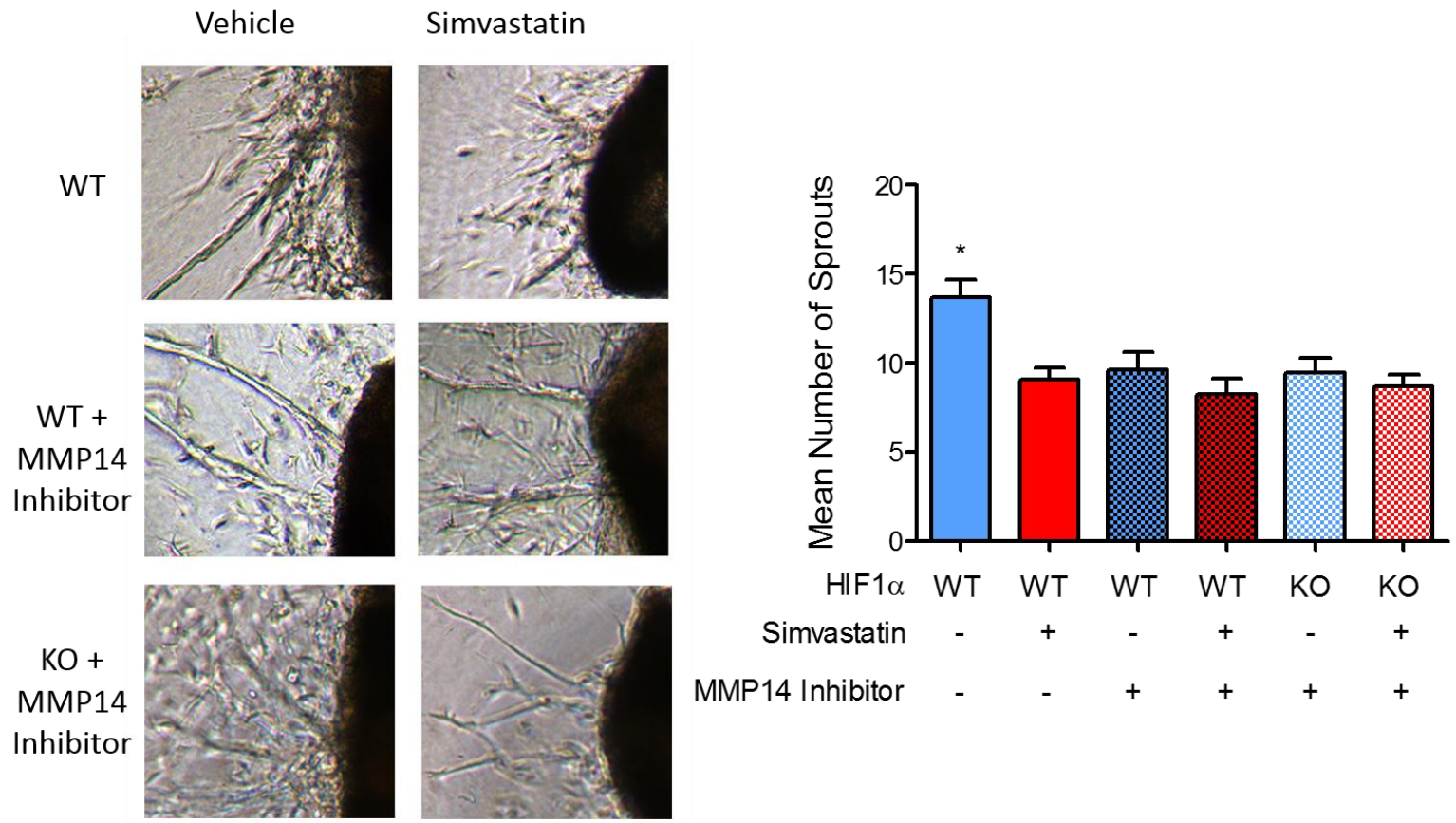

Fig. 36 – MMP14 inhibition decreases angiogenesis in a HIF1α-dependent manner. The *ex vivo* aortic ring assay with aortas isolated from *Tie1 Cre- HIF1α* WT and *Tie1 Cre+ HIF1α* KO mice, cultured in a three dimensional collagen matrix in 1% hypoxia, with or without 0.1µM simvastatin and MMP14 inhibitory antibody. Microvessel growth was analysed 6 days post embedding. The addition of an MMP14 antibody significantly reduced sprouting of *Tie1 Cre- HIF1α* WT mice. MMP14 inhibition has no effect on *Tie1 Cre+ HIF1α* KO mice. The bar chart represents the mean number of microvessel sprouts per aortic ring mean + SEM (n=8). Statistical analysis was conducted using One Way ANOVA with Neuman-Keuls post testing. * = $P<0.05$

4.3 HIF1α and Simvastatin Effect on *in vivo* Angiogenesis

4.3.1 Simvastatin Reduces *in* vivo VEGF-induced Angiogenesis via a HIF1α-dependent Mechanism

It had been shown that simvastatin and HIF1α reduced neovascularisation in *ex vivo* models. In order to see the effects of this *in vivo* the sponge angiogenesis assay was used. This incorporated the use of *Tie1 Cre+ HIF1α*$^{fl/fl}$ and their wildtype littermates which were injected subcutaneously with simvastatin or a PBS control for 4 weeks. On the 14th day a sponge was inserted into the flanks of the mice which were injected with VEGF or a PBS control on alternated days for the remaining 2 weeks. The sponges were harvested, fixed and sectioned before staining for the blood vessel marker endomucin.

It was shown that VEGF treatment significantly increased neovessel formation in wildtype mice, but not in their *Tie1 Cre+ HIF1α*$^{fl/fl}$ littermates (Fig. 37). The wildtype mice that were treated with simvastatin had significantly decreased neovascularisation compared to the PBS controls in the VEGF-treated groups (Fig. 37).

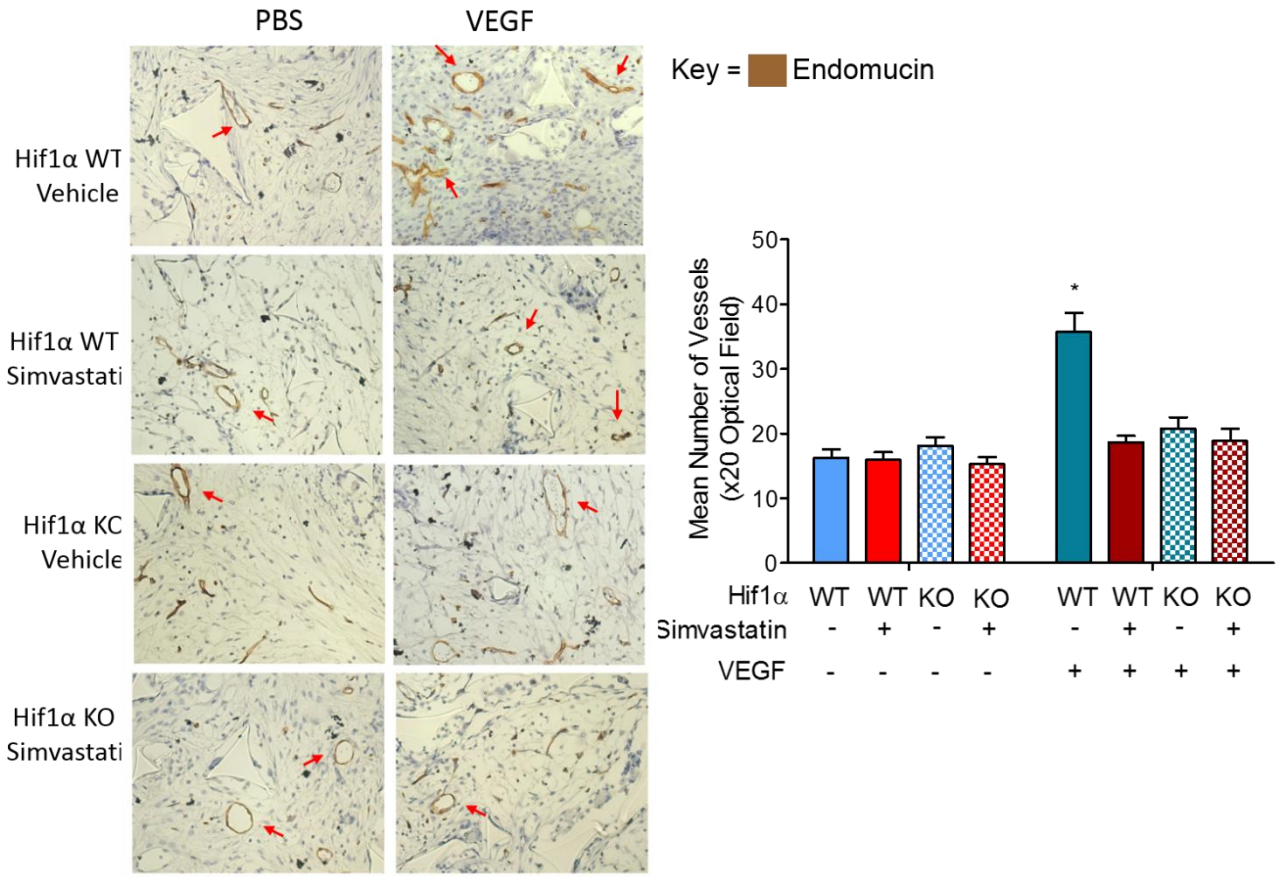

Fig. 37 – Simvastatin reduces VEGF-induced angiogenesis in a HIF1α-dependent manner. The *in vivo* sponge angiogenesis assay utilising *Tie1 Cre- HIF1α* WT and *Tie1 Cre+ HIF1α* KO mice, with sponges inserted in flanks and injections of either simvastatin or PBS subcutaneously for 4 weeks and VEGF or PBS into the sponges for 2 weeks on alternate days. Neovessel formation was assessed using IHC staining for endomucin and microscopic analysis at x20 magnification following harvesting and sectioning of sponges. Neovessel formation was significantly increased in wildtype mice with VEGF injections compared to *Tie1 Cre- HIF1α* KO mice. Simvastatin significantly attenuated neovessels formation in the VEGF-treated wildtypes. Red arrows indicate stained endothelial cells. The bar chart represents the mean number of neovessels per X20 image field mean + SEM (n=8). Statistical analysis was conducted using One Way ANOVA with Neuman-Keuls post testing. * = $P<0.05$

5. Discussion

The research presented here has shown that MMP14 is regulated by HIF1α which is, in turn, affected by simvastatin. This has implications in atherosclerosis treatment as atheromas express both HIF1α and MMP14 (Figs. 25 and 26). More specifically, the results have shown that HIF1α binds to the *MMP14* promoter through interaction with the two HREs (Figs. 27 and 28), HIF1α increases the gene activation and protein expression of MMP14 (Figs. 29, 30 and 31), simvastatin attenuates the upregulatory effect of HIF1α on MMP14 activity leading to functional effects including inhibition of angiogenesis. This indicates a role for simvastatin treatment in cardiovascular disease by inhibiting angiogenesis and therefore enhancing plaque stability.

5.1 HIF1α and MMP14 are Expressed in Endothelial Cells of Atheromas

Human atheroma sections and *APOE* KO mice atheroma sections immunostained for HIF1α and MMP14 showed strong staining in endothelial cells (Figs. 25 and 26).

Studies have shown that atheromas can contain hypoxic areas [40] as a result of both thickened intima and inflammation leading to increased oxygen demand [38]. This would lead to an expected upregulation of HIF1α within the atheroma. HIF1α expression upregulates angiogenesis and, therefore, its increased expression in the endothelial cells of the neovasculature is an important finding. Endothelial cell expression of HIF1α within the atheroma has been indicated before [39] but was not specifically stated. Here it has been confirmed that HIF1α is expressed in atheromas with specific localisation on endothelial cells and macrophages (Figs. 25A, 26A and 26C).

MMPs are known to be expressed in atheromas [90] where they are associated with the pathological development of atherosclerosis. MMP14 has been shown to be expressed in atheromas with commonly enhanced expression in the monocyte and macrophage populations [299]. As well as an increased expression in monocytes and macrophages, MMP14 has also shown to have increased expression in vascular smooth muscle cells and endothelial cells within the atheroma [236]. Here it has been confirmed that MMP14 is located in the atheroma with enhanced expression seen in endothelial cells (Figs. 25B and 26B).

With MMP14 and HIF1α showing expression in endothelial cells with apparent colocalisation it suggests that there may be a potential interaction between them. Coupled with the information that the *MMP14* promoter contains putative HREs [208] a regulatory mechanism was researched.

5.2 HIF1α Binding to the MMP14 Promoter in Hypoxia is Attenuated by Simvastatin Treatment

To analyse the regulation of MMP14 by HIF1α a bioinformatics search of *MMP14*s promoter region using TRANSFAC database for HREs was conducted. It was found that *MMP14* contains two putative HREs in the upstream gene promoter region at positions -125 to -129 [208] and from -3568 to -3572, respectively, relative to the start of transcription. As well as this, there is another HRE after the start of transcription at position +144 to +148 [208]. This suggests that MMP14 expression may be transcriptionally regulated by HIF1α.

The use of EMSA and ChIP assays has identified a binding of HIF1α to both the distal and proximal HREs at positions -3568 to 3571 and -125 to -129 in hypoxic conditions (Figs. 27 and 28). It has been shown that the *MMP14* promoter contains HREs and can interact with HIF2α [208], but this is the first time that an interaction of HIF1α with the *MMP14* promoter has been demonstrated.

It is also shown that low dose of simvastatin inhibits the interaction of HIF1α with the *MMP14* promoter, however the results show this may be due to reduced HIF1α availability (Fig. 30A). Simvastatin is known to affect binding of HIF1α to the promoter regions of other genes including those of platelet-derived growth factor B and endothelin-1 [140]. The hypoxia-induced attenuation detected in this study reinforces a role for simvastatin in affecting the functioning of the HIF response complex.

There is no interaction of HIF1α and the *MMP14* promoter region in normoxic conditions (Fig. 28). This could be due to HIF1α being rapidly degraded in normoxic conditions [48] and therefore a stable HIF response complex is not formed to target the *MMP14* gene.

5.3 Simvastatin Attenuates HIF1α-upregulated *MMP14* Promoter Activity

The results of EMSA and ChIP assays showed that HIF1α interacts with the *MMP14* promoter at the HREs (Figs. 27 and 28). Although this shows an interaction it provided no information on how this can affect the activity of the *MMP14* gene. Luciferase assays were used to establish if the interaction of HIF1α with the *MMP14* promoter had a regulatory affect.

Several other studies have shown that MMP14 expression is increased in hypoxic conditions, but have not shown a mechanism for this upregulation [237,300]. The research presented here shows a mechanism for the increase in MMP14 expression through an increase in *MMP14* gene activation. The results showed that in the presence of HIF1α and HIF1β *MMP14* gene activation is increased (Fig. 29A), but not with HIF1β alone. This showed that HIF1α was responsible for the upregulation of MMP14 expression with the formation of stable HIF1 complexes with HIF1β.

In order to confirm that the increase of *MMP14* activity was due to the interaction of the HIF response complex with the HREs, mutations were introduced into the HRE sequences of the reporter plasmid *MMP14* promoter sequence. The results showed that mutating the HREs at the proximal site, distal site, and both of the sites together significantly decreased the activity of *MMP14* in normoxic conditions (Fig. 29B). This shows that there may be some interaction and therefore upregulation of *MMP14* in normoxic conditions by the HIF response complex. However, this was not observed via the ChIP assay (Fig. 28). Interestingly, in hypoxic conditions it is shown that the proximal HRE is of great importance in the upregulation of *MMP14* promoter activity, as evidenced by the proximal HRE mutations which diminish *MMP14* promoter activity (Fig. 29B). This HRE site was also specified in another study to have an important role in the interaction of HIF2α in renal carcinoma cells, leading to an increase in tumourigenesis [208]. This shows that the proximal HRE is the dominant HRE in the activation of MMP14 by the HIF response complex. When the distal HRE is mutated there is not a reduction in *MMP14* promoter activity seen in hypoxic conditions. This indicates that the distal HRE is of less importance in the activation of the *MMP14* promoter by the HIF response complex.

Simvastatin had been shown to limit the interaction of HIF1α with the *MMP14* promoter in hypoxic conditions (Fig. 28). The luciferase assays have also shown that simvastatin significantly attenuates *MMP14* promoter activity in hypoxic conditions (Fig. 29C). Taking the EMSA and ChIP assays together, it is shown that the addition of simvastatin affects binding of HIF1α to the *MMP14* promoter which, in turn, affects the usual hypoxic upregulation on *MMP14* activity.

The inhibitory effect of simvastatin was not seen when the HREs were mutated, or in normoxic conditions, thus indicating the inhibition of *MMP14* promoter activity is HIF-dependent (Fig. 29C). A previous study has shown that the addition of 0.1μM simvastatin significantly inhibits the expression of MMP14 mRNA and protein in B16 melanoma cells [146]. This research was conducted in normoxic conditions but it is known that melanoma cells express an increased level of HIF1α [301], therefore HIF1α is likely to still have an effect here as very high levels of HIF1α may resist degradation. The research presented here shows that the inhibition of *MMP14* expression and activity is likely to occur at the gene regulatory level in the prevention of HIF1α interaction and activation of the *MMP14* promoter. The decrease in *MMP14* activity due to simvastatin may be linked to less HIF1α being available to interact with the *MMP14* promoter as we have shown that simvastatin reduces HIF1α expression.

Previous research has shown that *MMP14* transcription in endothelial cells is regulated by the transcription factors Egr-1 and Sp-1, through binding to GC-rich sequences at -288 to -275 relative to the start of transcription [209,210]. My research presents a new mechanism for the control of *MMP14* expression in endothelial cells with a further regulation by HIF1α through the interaction with HRE in the MMP14 promoter.

5.4 Simvastatin Inhibits MMP14 Protein Expression in a HIF1α-dependent Manner

HIF1α is known to be reduced by simvastatin, and hypoxia has been shown to upregulate several MMPs in a HIF1α-dependent manner [139,194,195]. However, the role of simvastatin in controlling MMP14 expression via a HIF1α-controlled mechanism has not been elucidated. Here the research has shown that MMP14 is inhibited by simvastatin in hypoxic conditions in a HIF1α-dependent mechanism.

The immunoblots show that under hypoxic conditions, both HIF1α and MMP14 expression are upregulated (Fig. 30A and B). However, the addition of simvastatin significantly reduces the hypoxia-driven increase in expression of both HIF1α and MMP14. It has been shown before that statins increase the degradation of HIF1α through increasing polyubiquitination, targeting it towards the proteosome [124]. It has also been shown that simvastatin is able to upregulate the expression of vHL which is an important cofactor for HIF1α degradation [302]. Here I have confirmed that the addition of simvastatin significantly reduces HIF1α protein levels, although whether this is due to decreased transcription, decreased translation or increased degradation cannot be elucidated (Fig. 30A).

MMP14 protein and mRNA levels being reduced as a consequence of simvastatin has previously been reported with the same concentration, 0.1μM [146]. Here we show however that the reduction of MMP14 expression is due to a HIF1α-dependent effect, as in normoxia there is no attenuation of MMP14 expression (Fig. 30C and 31). The use of siRNA targeting *HIF1α* in HUVECs and the use of *HIF1α* endothelial cell knockout mice showed that simvastatin only reduced MMP14 expression in hypoxic conditions when HIF1α was present (Fig. 30B and 31).

This shows that simvastatin inhibits MMP14 in a HIF1α-dependent manner in both human and mice endothelial cells.

MMP14 is not the first of the MMPs shown to be affected by statin treatment. There is evidence that statins inhibited the secretion of MMP1, MMP2, MMP3 and MMP9 from vascular smooth muscle cells and macrophages in rabbits that were fed a high cholesterol diet [142]. As well as an effect on MMPs, statins have also been shown to inhibit TIMPs, which would have a subsequent effect on MMP expression [303]. Statins are able to modulate expression of MMPs in a wide variety of cell types important in atheroma development including macrophages, vascular smooth muscle cells, fibroblasts and endothelial cells [142,303–305]. Here the research has confirmed a further inhibition of MMP14 with low-dose simvastatin treatment.

The trends of flow cytometry and immunoblotting on MMP14 expressions are similar with both low-dose simvastatin and HIF1α knockdown attenuating hypoxic MMP14 expression (Figs. 30 and 31). The flow cytometry results show a much more significant difference in MMP14 levels changing throughout the four conditions (Fig. 31) than immunoblotting is able to illustrate (Fig. 30). This is likely due to the more sensitive detection that flow cytometry allows whereby each single cell can be counted for MMP14 expression, rather than the whole cell lysates [306]. Flow cytometry is also a more quantitative method than immunoblotting as the fluorescence intensity can be measured and quantified between groups. Immunoblotting on the other hand is only semi quantitative and relies on the difference in saturation of a film to be analysed by densitometry software in order to compare groups.

5.5 Simvastatin Inhibits Hypoxic Endothelial Cell Migration and Proliferation

MMP14 is known to have an important role in cell migration as well as angiogenesis [235]. The immunostaining for both MMP14 and HIF1α showed that within atheromas their expression was particularly located in the neovasculature, which is indicative of a role in angiogenesis (Figs 25, 26A and 26B).

The investigations on the functional effects of MMP14 showed that hypoxic endothelial cell migration and proliferation are attenuated with HIF1α knockdown or simvastatin treatment. The results further showed that the attenuation of migration and proliferation by simvastatin is via a HIF1α-dependent effect (Fig. 32).

Simvastatin inhibition of HIF1α-induced MMP14 expression was shown to significantly attenuate hypoxic migration and proliferation of endothelial cells (Fig. 32). This both supports and conflicts with previous studies on the effect of simvastatin on migration and proliferation [302]. The use of 0.1μM simvastatin has previously been reported to significantly attenuate migration in melanoma cells [146], which is a similar finding to the research presented here. My research confirms that the inhibition of hypoxic migration occurs in a HIF1α-dependent manner (Fig. 32B).

Simvastatin has been shown to significantly attenuate atrial myofibroblast proliferation at concentrations ranging from 0.1-1μM [307]. This is in line with this study whereby I have shown an attenuation of proliferation by 0.1μM simvastatin (Fig. 32C). However, it has also been shown that simvastatin use on HUVECs at concentrations from 1μM has no effect on the proliferation

capacity [302]. This contradicts the current findings presented here. It is known that statins are pleiotropic and exert different effects at different concentrations, therefore the discrepancy in results may be due to the increased simvastatin dosage used. Also the use of the 3-(4,5-dimethylthiazol-2-yl)-2,5-diphenyltetrazolium bromide (MTT) assay to measure proliferation instead of the BrdU assay may have led to differences in observations as it is a different technique used which measures metabolic rate rather than DNA synthesis [308].

5.6 MMP14 Inhibition Decreases Proliferation and Migration in Hypoxia

It is well known that the matrix metalloproteinases have vital roles in migration and proliferation [309]. Our migration assays incorporating the MMP14 inhibitory antibody have shown that inhibiting MMP14 significantly reduces hypoxic cell migration and proliferation in our scramble-controlled cells (Fig. 33). This confirms that MMP14 has an important role in cell migration [216]. This effect is not seen in our HIF1α knockdown cells and therefore shows MMP14-driven hypoxic migration is governed by HIF1α.

MMP14 inhibition experiments have also shown that the inhibition of HIF1α-dependent migration by simvastatin is driven through MMP14. This is due to the cells grown with 0.1μM simvastatin and the MMP14 inhibitor having no effect in comparison to the cells grown in the presence of the MMP14 inhibitor alone (Fig. 33B).

Previous research has shown that MMP14 plays an important role in proliferation as when MMP14 is silenced there is a marked reduction in proliferation of glioma cells [310]. Here, I have

also shown that the inhibition of MMP14 can significantly attenuate proliferation in endothelial cells (Fig. 33C).

MMP14 is known to be heavily involved in cancer cell migration through the ECM during metastasis [216] . MMP14 is located on the leading edge of the invadopodia during cell migration. This allows for MMP14 to drive migration whilst also degrading the ECM to create a path for the cell to migrate through [311]. As well as cleaving the ECM, MMP14 is able to promote migration through the activation of cell surface molecules such as CD44, integrin alpha v integrins and tissue transglutaminase [312]. The effects of inhibiting MMP14 on migration has been shown before in endothelial cells where it was shown that siRNA targeted towards MMP14 disrupted migration and eventual tubulogenesis.

The use of the MMP14 inhibitory antibody, rather than an MMP inhibitor, was used to ensure a specific inhibition of MMP14 only. Many MMP inhibitors are broad MMP inhibitors which therefore would have off target effects what were unwanted for this research. There has been a specific inhibitor developed for MMP14, peptide G, which has shown promise in inhibiting cancer cell migration an invasion *in vitro* at high concentrations [313]. My research however, used an antibody as an inhibitor of MMP14 to specifically target the catalytic domain which had proved effective in previous publications [271].

5.7 Simvastatin Reduces Angiogenesis in a HIF1α-dependent Manner

The inhibition of migration and proliferation by simvastatin indicated that there may be a more important physiological role in the inhibition of angiogenesis. Here the *ex vivo* aortic ring assay has shown that the addition of 0.1μM simvastatin inhibits hypoxia-induced angiogenesis in a HIF1α dependent manner, decreasing sprout formation by around 25% (Fig. 34).

This finding is of importance, as atheromas contain hypoxic regions which lead to the upregulation of HIF1α and, in turn, angiogenesis. The new vasculature leads to plaque disruption and therefore increases the likelihood of plaque rupture. Statins have been known to stabilise atheromas and prevent neovascularisation [314]. My research has shown that this may be due to an inhibition of HIF1α and, therefore, angiogenesis.

Previous research has shown that *in vitro* assays with statins increase angiogenesis at concentrations ranging from 1-10μM. However in a similar finding to us when the statins are added to aortic ring cultures there is an inhibition of angiogenesis seen [315]. It is suggested that this may be due to a modification of the junction proteins that interact between endothelial cells, whereby they are upregulated in *ex vivo* assays preventing sprouting from intact cells but promote tube formation *in vitro* by encouraging cell-cell interaction [315]. The findings that are produced here complement the previous research showing that in *ex vivo* angiogenesis assays simvastatin inhibits sprouting of endothelial cells.

Interestingly, it has also been found that statins are able to promote angiogenesis *in vivo* [316], which has been suggested to be due to activation of the Rho and Akt pathways, as well as through increasing endothelial progenitor cell mobilisation [317]. There are disparate findings

with the use of statins and their role in angiogenesis. Statins have been shown to have biphasic effects on angiogenesis whereby at lower concentrations, less than 0.1µM, they promote angiogenesis and at concentrations greater than 0.1µM they inhibit angiogenesis [126]. This falls in line with data presented here where concentrations of 0.1µM have shown that simvastatin is able to inhibit angiogenesis (Fig. 34).

The disparate findings with the use of statins also seem to be related to the experimental conditions with either hypoxia, normoxia or other stimuli used and the type of assay that is performed [302,315]. The same concentrations of statins have been shown to promote tube formation *in vitro* whereas they inhibit angiogenesis *ex vivo* [315]. In this study the aortic ring *ex vivo* angiogenesis assay has been used and shown that 0.1µM simvastatin inhibits angiogenesis in hypoxia via a HIF1α dependent method.

5.8 Simvastatin and HIF1α Knockout Reduce MMP14 Expression in Immature Endothelial Cells Perturbing Angiogenesis

The effect of both 0.1µM simvastatin and HIF1α knockdown have shown to inhibit the expression of MMP14 on new microvessels (Fig. 35). As well as this, it has been shown that aortic ring cultures from HIF1α knockout mice, and wildtype controls, incubated with 0.1µM simvastatin have perturbed sprouting. On imaging the aortic ring sprouts which were stained for MMP14 it has become clear that hypoxia leads to an increase in MMP14 levels of sprouts in wildtype mice. However, this is attenuated in HIF1α knockout mice and wildtype aortas treated with 0.1µM simvastatin (Fig. 35). This result shows that the increased angiogenesis is due to increased MMP14 levels as compared with normoxia, simvastatin-treated and in KO mice.

Furthermore, this shows that the MMP14 increase is due to HIF1α upregulation which is perturbed by simvastatin.

MMP14 is known to promote angiogenesis and may have an important role in promoting neovascularisation into the atheromatous plaque [198,199,234,235]. MMPs have been studied in relation to angiogenesis using aortic ring cultures before. It has been found that MMP2 and MMP9 are important MMPs in mediating this process and, interestingly, it has been shown that MMP9 is specifically located in the microvessel sprouts [318]. As well as MMP2 and MMP9 other MMPs including MMP3, MMP10, MMP11, MMP13 and MMP14 have also been shown to be produced in aortic ring cultures [319]. However not all of these MMPs have a direct role on angiogenesis, such as MMP11 which has no effect on vessel sprouting [320].

MMP14 is known to be an inducer of angiogenesis via both ECM degradation and growth factor activation [234,235]. With defective angiogenesis seen in *MMP14* knockout mice, the importance of MMP14 in inducing angiogenesis is paramount [199]. The aortic rings presented here have shown that reduced MMP14 expression by simvastatin and HIF1α knockout reduces neovascularisation. This adds extra emphasis to the importance of MMP14 in inducing angiogenesis.

5.9 MMP14 Inhibition Attenuates VEGF-induced Angiogenesis in a HIF1α-dependent Manner

The inhibition of MMP14 expression in aortic ring cultures has confirmed that MMP14 is required for sprout formation in hypoxic conditions (Fig. 36). Interestingly the addition of simvastatin to aortic ring cultures grown with the MMP14 inhibitor did not affect sprout formation in comparison to those without the MMP14 inhibitor (Fig. 36). This shows that simvastatin decreases the formation of new blood vessels through inhibition of MMP14. With the antibody-based inhibition of MMP14, any upstream inhibition of simvastatin on MMP14 expression would not have an additive effect on inhibiting neovascularisation. If a decrease was seen however then it would suggest that simvastatin is acting in other mechanisms.

The defective vasculature seen in *MMP14* knockout mice, leading to premature death, confirms that MMP14 is vital in neovascularisation [199]. The use of broad spectrum MMP inhibitors such as batimastat and marimastat have been shown before to block the angiogenic potential of aortic rings in collagen gel cultures [318]. More specifically, the use of *MMP14*-null mice aortic rings have shown a complete attenuation of sprout formation[198]. In relation to this finding, other research has found that MMP14 is required for migration through the collagen matrix due to its location at the invadopodia of migrating cells providing a path clearing mechanism [321]. The inhibition of MMP14 though an inhibitory antibody, 0.1μM simvastatin, or HIF1α knockout leads to decreased sprout formation from aortic ring cultures, thus confirming the importance of MMP14 in hypoxic angiogenesis.

5.10 Simvastatin reduces *in vivo* VEGF-induced angiogenesis via a HIF1α-dependent Mechanism

The *ex vivo* angiogenesis models showed that simvastatin reduced neovascularisation in a HIF1α dependent mechanism through the inhibition of MMP14. In order to determine if these results were replicated *in vivo,* the sponge angiogenesis assay was performed. This showed that simvastatin significantly attenuated neovascularisation in a HIF1α-dependent manner (Fig. 37).

This is in line with previous research whereby the use of simvastatin inhibited angiogenesis when used at the same concentration, 10mg/kg per day [322]. The use of simvastatin at this concentration has also showed beneficial effects in reducing the neointimal thickening of atherosclerosis [323]. This is known as a relatively low dose of simvastatin and therefore falls in line with the rest of the research at the *in vitro* and *ex vivo* level.

Perturbed wound healing and neovascularisation has been shown in endothelial cell specific *HIF1α* knockout mice. These mice used a *Tie2* Cre^{+} system rather than *Tie1* Cre^{+} but the same $HIF1\alpha^{fl/fl}$ mice were used for the crossing as we have used here [324]. This research falls in line with our research whereby reduced angiogenesis was seen in endothelial cell specific $HIF1\alpha^{fl/fl}$ mice. This shows the importance of endothelial HIF1α in the promotion of angiogenesis.

5.11 Future Work

Although my study has shown that simvastatin has a beneficial effect on the prevention of angiogenesis there would need to be further work in order to relate this to clinical findings. A potential difficulty in the recommendation for the use of simvastatin to stabilise atheromas is that there is a great deal of variability in the responses of individuals to statins. This can be linked to pharmacogenetics whereby genome wide association studies have shown that SNPs in the *APOE* and *LPA* genes correlate with differing cholesterol-lowering response to statins [325].

Simvastatin is unlikely to exert its effects directly on HIF1α and is likely to affect upstream proteins and genes which subsequently effect HIF1α expression. A possible mechanism of action could involve eNOS, which is known to be upregulated by simvastatin [95], and subsequently an increase in nitric oxide production. The increase of nitric oxide upregulates PHD2 expression, by affecting random oxygen species production [326], which will in turn inhibit HIF1α. Thus, it could be this pathway that simvastatin is utilising to affect HIF1α regulation of MMP14 (Fig. 38).

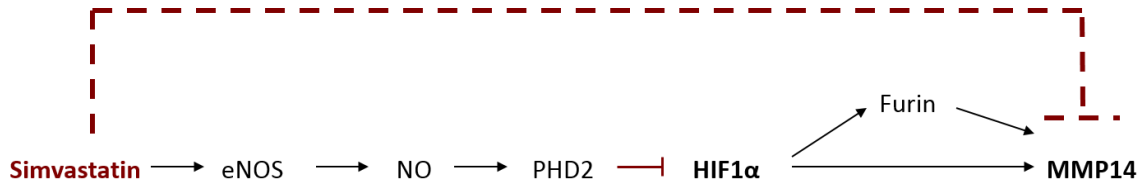

Fig. 38 – A possible mechanism for Simvastatin regulation of MMP14 via modulating HIF1α activity

It would be of interest to see if the proposed pathway of simvastatin's inhibition of MMP14 is correct (Fig. 38). Knockdown of eNOS would allow for the identification if simvastatin is working along the proposed pathway. If similar effects are seen as those with simvastatin treatment, then it would confirm that simvastatin is acting upon this pathway. If however different results are seen it would show that simvastatin is affecting MMP14 activity via modulating HIF1α in a different way.

In order to confirm the inhibition by simvastatin is due to the inhibition of HMG-CoA reductase, and therefore isoprenoid intermediates, mevalonate rescue studies could be used. These experiments bypass the actions of simvastatin and should return HIF1α and MMP14 expression back to base-line levels if simvastatin is working through the blockage of isoprenoid intermediates.

Other cell types, such as monocytes and smooth muscle cells, are known to express MMP14 within the atherosclerotic plaque [196,236] and may also play a role in the promotion of angiogenesis via a MMP14 mediated response. My research has focussed on endothelial cells but I have also shown that HIF1α is expressed in macrophages. Therefore simvastatin may also play a role in dampening MMP14 levels in a HIF1α dependent manner in other cell types, thus creating a more stable atheroma. However simvastatin is known to have tissue-specific [139] and microenvironment-specific responses [302] and therefore the expression pattern seen could either correlate or contradict my findings with HUVECs.

There are other potential transcription factors that are known to increase MMP14 activity, including Sp-1 and Egr-1 [209,210]. It would be interesting to know whether there is any interaction between HIF1α and the other transcription factors in upregulating hypoxic MMP14 expression. Ways of identifying any interactions could include co-immunoprecipitations and luciferase assays incorporating mutations in Sp-1 and Egr-1 sites of the *MMP14* promoter in conjunction with HIF1α expression plasmids.

In order to assess simvastatin's effects on angiogenesis *in vivo* another technique could be used which would also allow for detection of MMP14 levels, following immunostaining. The mouse injury angiogenesis model assesses wound repair of the aorta following a wire being passed through the blood vessels. Over a predetermined period, the vessel would be allowed to repair before analysis of the effects. The tissue could be sectioned and stained for their protein expression.

Another study could utilise the crossing of the HIF1α$^{fl/fl}$ Tie1 Cre^{+} mice with *APOE* KO mice, which is a recommended model for the study of atherosclerosis in mice due to the lesions having similarities with humans [264]. This would allow for the identification of neovascularisation *in vivo* within a developing atheroma and would also elucidate more clinically relevant information.

6. Conclusion

My research has shown that MMP14 protein expression is upregulated in hypoxic conditions through direct HIF1α interaction with the *MMP14* promoter. The addition of simvastatin significantly attenuates this upregulation, possibly through increased degradation of HIF1α. This has further physiological implications in relation to angiogenesis which is perturbed by simvastatin through the downregulation of MMP14 via a HIF1α-dependent mechanism.

This finding is of relevance to the use of statins in the treatment of atherosclerosis, which are known to stabilise atheromas [120]. The expression of MMPs varies between stable and vulnerable atheromas with the upregulation of some MMPs being characteristic of a vulnerable plaque [240]. MMPs such as MMP9, MMP12 and MMP14 have been shown to have a significantly increased expression in the vulnerable plaques in comparison to stable plaques [240]. As well as MMP levels, TIMPs have also been shown to have altered expression between stable and vulnerable atheromas with TIMP3 found to have a decreased expression in more vulnerable plaques [240]. This is important as TIMP3 is a MMP14 inhibitor, and *TIMP3* knockout is known to intensify the formation of atherosclerosis through the increase in the formation of invasive foam cells [197]. Other research has also shown that microRNAs have roles in the formation of vulnerable plaques with *mir-712* being shown to downregulate TIMP3 and therefore lead to an increase in MMP14 [327]. Taken with my research it would suggest that simvastatin downregulates MMP14 and could therefore be used to reduce the risk of progression to a vulnerable plaque.

With the increased expression of several MMPs being related to the formation of vulnerable plaques, the use of MMP inhibitors could be worthwhile. MMP inhibitors, however, have had

mixed outcomes when used in clinical trials with some studies being stopped prematurely due to their use leading to poorer survival outcomes [328]. New MMP inhibitors are being produced in order to counteract some of the issues seen with conventional MMP inhibitors, such as using different zinc binding domains to interact with the MMP catalytic site [329]. However, there is no guarantee that these new inhibitors will pass clinical trials. Statins are already widely prescribed in order to treat cardiovascular diseases and, although they have side effects, they are approved by FDA. Therefore, simvastatin could potentially have a more important role in the inhibition of MMP14 in disease.

In conclusion, I have shown a regulation of MMP14 by HIF1α with attenuation by simvastatin. The upregulation is mediated through direct binding of HIF1α to the *MMP14* promoter HIF binding sites. The attenuation of MMP14 by simvastatin is via a HIF1α-dependent mechanism and has further implications in limiting angiogenesis. In relation to atherosclerosis this could potentially be a mechanism for the stabilisation of atheromas by simvastatin. Future research could utilise murine models of atherosclerosis to further identify the effects of simvastatin and relate this to clinical situations.

7. Publications / Abstracts

Papers - 2013 - Fang, C., Wen, G., Zhang, L., Lin, L., **Moore, A.**, Wu, S., Ye, S., Xiao, Q. (2013) "An Important Role of Matrix Metalloproteinase-8 in Angiogenesis in Vitro and in Vivo" *Cardiovascular Research,* 44(0). doi:10.1093/cvr/cvt060

Presentations - 2014 - "Hypoxia-Inducible Factor-1 Regulates Matrix Metalloproteinase-14 Expression: Underlying Effects of Hypoxia and Statins" London Cardiovascular Society, April 2014

2013 - Junk the Jargon - Science Heat (Runner Up)
Junk the Jargon - Final

Posters - 2014 - **A.D. Moore**, C.P. Hodgkinson, A. Lapenna, F. Zhang, K. Witkowska, F. Liang Ng, S. E. Headland, L.E. Reynolds, D.M. Lees, T. Lechertier, A. Milsom, K. Hodivala-Dilke, S. Ye (2014) Hypoxia-Inducible Factor-1 Regulates Matrix Metalloproteinase-14 Expression: Underlying Effects of Hypoxia and Statins. *British Cardiovascular Society,* Manchester

2013 - **A.D. Moore**, C.P. Hodgkinson, A. Lapenna, L.E. Reynolds, D.M. Lees, T. Lechertier, R.S. Laxton, A. Milsom, K. Hodivala-Dilke, S. Ye (2013) Simvastatin Attenuates Hypoxic Effect on MMP14 Expression via Inhibiting HIF1α Interaction with the MMP14 Gene Promoter and Disrupts Angiogenesis. *British Heart Foundation Fellows Meeting 2013*

A.D. Moore, S. Ye. (2013) Simvastatin Attenuates Hypoxic Effect on MMP14 Expression via Inhibiting HIF1α Interaction with the MMP14 Gene Promoter *British Cardiovascular Society,* London

A.D. Moore, S. Ye. (2013) Hypoxia Increases MMP14 Expression Through HIF1α Interaction With The MMP14 Gene Promoter But Simvastatin Attenuates This Effect. *William Harvey Research Review*

A.D. Moore, C.P. Hodgkinson, A. Lapenna, R.S. Laxton, A. Milsom, S. Ye. (2013) HIF1α Binds to the MMP14 Promoter but With Less Affinity after Simvastatin Treatment. *British Microcirculation Society*

2012 - **A.D. Moore,** F. L. Ng (2012) Optimising Chromatin Immunoprecipitation Assays in HUVEC and HUVSMC cells in the study of protein-gene interactions in cardiovascular disease. *William Harvey Day*

Abstracts - 2014 - **A.D. Moore**, C.P. Hodgkinson, A. Lapenna, F. Zhang, K. Witkowska, F. Liang Ng, S. E. Headland, L.E. Reynolds, D.M. Lees, T. Lechertier, A. Milsom, K. Hodivala-Dilke, S. Ye (2014) Hypoxia-Inducible Factor-1 Regulates Matrix Metalloproteinase-14 Expression: Underlying Effects of Hypoxia and Statins. *Heart,* 203 (Suppl 3) A111-A112. 10.1136/heartjnl-2014-306118.203.

2013 – **Moore, A.,** and Ye, S. (2013) Simvastatin Attenuates Hypoxic Effect on MMP14 Expression via Inhibiting HIF1α Interaction with the *MMP14* Gene Promoter. *Heart*, 99 (Suppl 2), A110–A110. 10.1136/heartjnl-2013-304019.199

8. Bibliography

1. Swift MR, Weinstein BM. Arterial-venous specification during development. *Circ. Res.* 2009;104(5):576-88. doi:10.1161/CIRCRESAHA.108.188805.

2. Dela Paz NG, D'Amore P a. Arterial versus venous endothelial cells. *Cell Tissue Res.* 2009;335(1):5-16. doi:10.1007/s00441-008-0706-5.

3. Pugsley MK, Tabrizchi R. The vascular system. An overview of structure and function. *J. Pharmacol. Toxicol. Methods* 2001;44(2):333-40. Available at: http://www.ncbi.nlm.nih.gov/pubmed/11325577.

4. Servier. Servier Medical Art. *Powerpoint Image Bank* 2014. Available at: http://www.servier.com/Powerpoint-image-bank. Accessed July 21, 2014.

5. Aird WC. Phenotypic heterogeneity of the endothelium: I. Structure, function, and mechanisms. *Circ. Res.* 2007;100(2):158-73. doi:10.1161/01.RES.0000255691.76142.4a.

6. Ross R. Cell biology of atherosclerosis. *Annu. Rev. Physiol.* 1995;57:791-804. doi:10.1146/annurev.ph.57.030195.004043.

7. Mehta D, Malik AB. Signaling mechanisms regulating endothelial permeability. *Physiol. Rev.* 2006;86(1):279-367. doi:10.1152/physrev.00012.2005.

8. Page C, Rose M, Yacoub M, Pigott R. Antigenic heterogeneity of vascular endothelium. *Am. J. Pathol.* 1992;141(3):673-83. Available at: http://www.pubmedcentral.nih.gov/articlerender.fcgi?artid=1886681&tool=pmcentrez&rendertype=abstract.

9. Inagami T, Naruse M, Hoover R. Endothelium as an endocrine organ. *Annu. Rev. Physiol.* 1995;57:171-89. doi:10.1146/annurev.ph.57.030195.001131.

10. Hynes RO. The extracellular matrix: not just pretty fibrils. *Science* 2009;326(5957):1216-9. doi:10.1126/science.1176009.

11. Davis GE, Senger DR. Endothelial extracellular matrix: biosynthesis, remodeling, and functions during vascular morphogenesis and neovessel stabilization. *Circ. Res.* 2005;97(11):1093-107. doi:10.1161/01.RES.0000191547.64391.e3.

12. Labarthe D. *Epidemiology and Prevention of Cardiovascular Diseases: A Global Challenge*. Second Edi. Sudbury, Massachusetts: Jones & Bartlett Publishers; 2010.

13. Mendis S, Puska P, Norrving B. *Global Atlas on Cardiovascular Disease Prevention and Control*. Geneva: World Health Organisation; 2011.

14. Capewell S, Allender S, Critchley J, et al. *Modelling the UK Burden of Cardiovascular Disease to 2020 : A Research Report for the Cardio & Vascular Coalition and the British Heart Foundation*. London: British Heart Foundation; 2008.

15. WHO. Cardiovascular Disease. 2013. Available at: http://www.who.int/cardiovascular_diseases/en/. Accessed April 8, 2013.

16. Gaziano TA, Reddy KS, Paccaud F, Horton S. Cardiovascular Disease. In: Jamison DT, Breman JG, Measham AR, et al., eds. *Disease Control Priorities in Developing Countries*. 2nd Editio. Washington (DC): The International Bank for Reconstruction and Development/The World Bank Group; 2006:645-662.

17. Lusis AJ. Atherosclerosis. *Nature* 2000;407(6801):233-41. doi:10.1038/35025203.

18. Davies MJ. Stability and Instability: Two Faces of Coronary Atherosclerosis: The Paul Dudley White Lecture 1995 . *Circ.* 1996;94 (8):2013-2020. doi:10.1161/01.CIR.94.8.2013.

19. Agrogiannis G, Kavantzas N, Patsouris E. Effects of Green Tea Polyphenols under Hyperlipidemic Conditions through their Anti-Angiogenic Activity. In: *BT - Tea in Health and Disease Prevention*. Academic Press; 2013:859-870. doi:http://dx.doi.org/10.1016/B978-0-12-384937-3.00072-0.

20. Wang T, Palucci D, Law K, Yanagawa B, Yam J, Butany J. Atherosclerosis: pathogenesis and pathology. *Diagnostic Histopathol.* 2012;18(11):461-467. doi:10.1016/j.mpdhp.2012.09.004.

21. De Luca A, Warboys C, Amini N, et al. 170 Transcriptome Profiling in Porcine Arteries To Identify Novel Shear-Responsive Regulators of Endothelial Cell Fate. *Heart* 2013;99(Suppl 2):A98-A99. doi:10.1136/heartjnl-2013-304019.170.

22. Warboys CM, de Luca A, Amini N, et al. Disturbed flow promotes endothelial senescence via a p53-dependent pathway. *Arterioscler. Thromb. Vasc. Biol.* 2014;34(5):985-95. doi:10.1161/ATVBAHA.114.303415.

23. Grundtman C, Kreutmayer SB, Almanzar G, Wick MC, Wick G. Heat shock protein 60 and immune inflammatory responses in atherosclerosis. *Arterioscler. Thromb. Vasc. Biol.* 2011;31(5):960-8. doi:10.1161/ATVBAHA.110.217877.

24. Galdiero M, de l'Ero GC, Marcatili A. Cytokine and adhesion molecule expression in human monocytes and endothelial cells stimulated with bacterial heat shock proteins. *Infect. Immun.* 1997;65(2):699-707. Available at: http://www.pubmedcentral.nih.gov/articlerender.fcgi?artid=176116&tool=pmcentrez&rendertype=abstract. Accessed July 24, 2014.

25. Virmani R, Kolodgie FD, Burke AP, et al. Atherosclerotic plaque progression and vulnerability to rupture: angiogenesis as a source of intraplaque hemorrhage.

Arterioscler. Thromb. Vasc. Biol. 2005;25(10):2054-61. doi:10.1161/01.ATV.0000178991.71605.18.

26. Moore KJ, Tabas I. Macrophages in the pathogenesis of atherosclerosis. *Cell* 2011;145(3):341-55. doi:10.1016/j.cell.2011.04.005.

27. Brewer HB. The lipid-laden foam cell: an elusive target for therapeutic intervention. *J. Clin. Invest.* 2000;105(6):703-5. doi:10.1172/JCI9664.

28. Fantus D, Awan Z, Seidah NG, Genest J. Aortic calcification: Novel insights from familial hypercholesterolemia and potential role for the low-density lipoprotein receptor. *Atherosclerosis* 2012;226(1):9-15. doi:10.1016/j.atherosclerosis.2012.08.026.

29. Virmani R, Burke AP, Kolodgie FD, Farb A. Vulnerable plaque: the pathology of unstable coronary lesions. *J. Interv. Cardiol.* 2002;15(6):439-46. Available at: http://www.ncbi.nlm.nih.gov/pubmed/12476646. Accessed January 13, 2013.

30. Stary HC. Natural History and Histological Classification of Atherosclerotic Lesions : An Update. *Arterioscler. Thromb. Vasc. Biol.* 2000;20(5):1177-1178. doi:10.1161/01.ATV.20.5.1177.

31. Virmani R, Kolodgie FD, Burke a. P, Farb a., Schwartz SM. Lessons From Sudden Coronary Death : A Comprehensive Morphological Classification Scheme for Atherosclerotic Lesions. *Arterioscler. Thromb. Vasc. Biol.* 2000;20(5):1262-1275. doi:10.1161/01.ATV.20.5.1262.

32. Stary HC, Chandler a. B, Glagov S, et al. A definition of initial, fatty streak, and intermediate lesions of atherosclerosis. A report from the Committee on Vascular Lesions of the Council on Arteriosclerosis, American Heart Association. *Arterioscler. Thromb. Vasc. Biol.* 1994;14(5):840-856. doi:10.1161/01.ATV.14.5.840.

33. Stary HC. Evolution and progression of atherosclerotic lesions in coronary arteries of children and young adults. *Arteriosclerosis* 1989;9(1 Suppl):I19-32. Available at: http://www.ncbi.nlm.nih.gov/pubmed/2912430. Accessed April 21, 2013.

34. Stary HC, Chandler AB, Dinsmore RE, et al. A Definition of Advanced Types of Atherosclerotic Lesions and a Histological Classification of Atherosclerosis: A Report From the Committee on Vascular Lesions of the Council on Arteriosclerosis, American Heart Association. *Arterioscler. Thromb. Vasc. Biol.* 1995;15(9):1512-1531. doi:10.1161/01.ATV.15.9.1512.

35. Semenza GL. Hypoxia-inducible factors in physiology and medicine. *Cell* 2012;148(3):399-408. doi:10.1016/j.cell.2012.01.021.

36. Jiang Y-Z, Li Y, Wang K, et al. Distinct Roles of HIF1A in Endothelial Adaptations to Physiological and Ambient Oxygen. *Mol. Cell. Endocrinol.* 2014. doi:10.1016/j.mce.2014.04.008.

37. Hultén LM, Levin M. The role of hypoxia in atherosclerosis. *Curr. Opin. Lipidol.* 2009;20(5):409-14. doi:10.1097/MOL.0b013e3283307be8.

38. Torres Filho IP, Leunig M, Yuan F, Intaglietta M, Jain RK. Noninvasive measurement of microvascular and interstitial oxygen profiles in a human tumor in SCID mice. *Proc. Natl. Acad. Sci. U. S. A.* 1994;91(6):2081-5. Available at: http://www.pubmedcentral.nih.gov/articlerender.fcgi?artid=43313&tool=pmcentrez&rendertype=abstract.

39. Sluimer JC, Gasc J-M, van Wanroij JL, et al. Hypoxia, hypoxia-inducible transcription factor, and macrophages in human atherosclerotic plaques are correlated with intraplaque angiogenesis. *J. Am. Coll. Cardiol.* 2008;51(13):1258-65. doi:10.1016/j.jacc.2007.12.025.

40. Bjornheden T, Levin M, Evaldsson M, Wiklund O. Evidence of Hypoxic Areas Within the Arterial Wall In Vivo. *Arterioscler. Thromb. Vasc. Biol.* 1999;19(4):870-876. doi:10.1161/01.ATV.19.4.870.

41. Hulsmans M, Van Dooren E, Holvoet P. Mitochondrial reactive oxygen species and risk of atherosclerosis. *Curr. Atheroscler. Rep.* 2012;14(3):264-76. doi:10.1007/s11883-012-0237-0.

42. Semenza GL. Oxygen-dependent regulation of mitochondrial respiration by hypoxia-inducible factor 1. *Biochem. J.* 2007;405(1):1-9. doi:10.1042/BJ20070389.

43. Beck I, Ramirez S, Weinmann R, Caro J, Gene E. Enhancer element at the 3'-flanking region controls transcriptional response to hypoxia in the human erythropoietin gene. 1991:15563-15566.

44. Semenza GL, Nejfelt MK, Chi SM, Antonarakis SE. Hypoxia-inducible nuclear factors bind to an enhancer element located 3' to the human erythropoietin gene. *Proc. Natl. Acad. Sci. U. S. A.* 1991;88(13):5680-4. Available at: http://www.pubmedcentral.nih.gov/articlerender.fcgi?artid=51941&tool=pmcentrez&rendertype=abstract. Accessed November 9, 2014.

45. Wang GL, Semenza GL. Purification and Characterization of Hypoxia-inducible Factor 1. *J. Biol. Chem.* 1995;270(3):1230-1237.

46. Gao L, Chen Q, Zhou X, Fan L. The role of hypoxia-inducible factor 1 in atherosclerosis. *J. Clin. Pathol.* 2012;65(10):872-6. doi:10.1136/jclinpath-2012-200828.

47. Semenza GL. HIF-1 and mechanisms of hypoxia sensing. *Curr. Opin. Cell Biol.* 2001;1(2):167-171. Available at: http://www.ncbi.nlm.nih.gov/pubmed/11248550. Accessed January 21, 2013.

48. Huang LE, Arany Z, Livingston DM, Bunn HF. Activation of hypoxia-inducible transcription factor depends primarily upon redox-sensitive stabilization of its alpha subunit. *J. Biol.*

Chem. 1996;271(50):32253-9. Available at: http://www.ncbi.nlm.nih.gov/pubmed/8943284.

49. Millonig G, Hegedüsch S, Becker L, Seitz H-K, Schuppan D, Mueller S. Hypoxia-inducible factor 1 alpha under rapid enzymatic hypoxia: cells sense decrements of oxygen but not hypoxia per se. *Free Radic. Biol. Med.* 2009;46(2):182-91. doi:10.1016/j.freeradbiomed.2008.09.043.

50. Salceda S, Caro J. Hypoxia-inducible factor 1alpha (HIF-1alpha) protein is rapidly degraded by the ubiquitin-proteasome system under normoxic conditions. Its stabilization by hypoxia depends on redox-induced changes. *J. Biol. Chem.* 1997;272(36):22642-7. Available at: http://www.ncbi.nlm.nih.gov/pubmed/9278421. Accessed November 9, 2014.

51. Caprara C, Thiersch M, Lange C, Joly S, Samardzija M, Grimm C. HIF1A is essential for the development of the intermediate plexus of the retinal vasculature. *Invest. Ophthalmol. Vis. Sci.* 2011;52(5):2109-17. doi:10.1167/iovs.10-6222.

52. Forristal CE, Wright KL, Hanley N a, Oreffo ROC, Houghton FD. Hypoxia inducible factors regulate pluripotency and proliferation in human embryonic stem cells cultured at reduced oxygen tensions. *Reproduction* 2010;139(1):85-97. doi:10.1530/REP-09-0300.

53. Ema M, Taya S, Yokotani N, Sogawa K, Matsuda Y, Fujii-Kuriyama Y. A novel bHLH-PAS factor with close sequence similarity to hypoxia-inducible factor 1alpha regulates the VEGF expression and is potentially involved in lung and vascular development. *Proc. Natl. Acad. Sci. U. S. A.* 1997;94(9):4273-8. Available at: http://www.pubmedcentral.nih.gov/articlerender.fcgi?artid=20712&tool=pmcentrez&rendertype=abstract.

54. Qing G, Simon MC. Hypoxia inducible factor-2alpha: a critical mediator of aggressive tumor phenotypes. *Curr. Opin. Genet. Dev.* 2009;19(1):60-6. doi:10.1016/j.gde.2008.12.001.

55. Gu YZ, Moran SM, Hogenesch JB, Wartman L, Bradfield CA. Molecular characterization and chromosomal localization of a third alpha-class hypoxia inducible factor subunit, HIF3alpha. *Gene Expr.* 1998;7(3):205-13. Available at: http://www.ncbi.nlm.nih.gov/pubmed/9840812. Accessed May 9, 2014.

56. Lisy K, Peet DJ. Turn me on: regulating HIF transcriptional activity. *Cell Death Differ.* 2008;15(4):642-9. doi:10.1038/sj.cdd.4402315.

57. Richard DE, Berra E, Gothié E, Roux D, Pouysségur J. p42/p44 mitogen-activated protein kinases phosphorylate hypoxia-inducible factor 1alpha (HIF-1alpha) and enhance the transcriptional activity of HIF-1. *J. Biol. Chem.* 1999;274(46):32631-7. Available at: http://www.ncbi.nlm.nih.gov/pubmed/10551817. Accessed May 29, 2014.

58. Jiang BH, Jiang G, Zheng JZ, Lu Z, Hunter T, Vogt PK. Phosphatidylinositol 3-kinase signaling controls levels of hypoxia-inducible factor 1. *Cell Growth Differ.* 2001;12(7):363-9. Available at: http://www.ncbi.nlm.nih.gov/pubmed/11457733.

59. Appelhoff RJ, Tian Y-M, Raval RR, et al. Differential function of the prolyl hydroxylases PHD1, PHD2, and PHD3 in the regulation of hypoxia-inducible factor. *J. Biol. Chem.* 2004;279(37):38458-65. doi:10.1074/jbc.M406026200.

60. Foxler DE, Bridge KS, James V, et al. The LIMD1 protein bridges an association between the prolyl hydroxylases and VHL to repress HIF-1 activity. *Nat. Cell Biol.* 2012;14(2):201-8. doi:10.1038/ncb2424.

61. Wenger RH, Stiehl DP, Camenisch G. Integration of oxygen signaling at the consensus HRE. *Sci. STKE* 2005;2005(306):re12. doi:10.1126/stke.3062005re12.

62. Baba Y, Nosho K, Shima K, et al. HIF1A overexpression is associated with poor prognosis in a cohort of 731 colorectal cancers. *Am. J. Pathol.* 2010;176(5):2292-301. doi:10.2353/ajpath.2010.090972.

63. Semenza GL. Oxygen-regulated transcription factors and their role in pulmonary disease. *Respir. Res.* 2000;1(3):159-62. doi:10.1186/rr27.

64. Hirota K, Semenza GL. Regulation of angiogenesis by hypoxia-inducible factor 1. *Crit. Rev. Oncol. Hematol.* 2006;59(1):15-26. doi:10.1016/j.critrevonc.2005.12.003.

65. Fang H-Y, Hughes R, Murdoch C, et al. Hypoxia-inducible factors 1 and 2 are important transcriptional effectors in primary macrophages experiencing hypoxia. *Blood* 2009;114(4):844-59. doi:10.1182/blood-2008-12-195941.

66. Treins C, Giorgetti-Peraldi S, Murdaca J, Semenza GL, Van Obberghen E. Insulin stimulates hypoxia-inducible factor 1 through a phosphatidylinositol 3-kinase/target of rapamycin-dependent signaling pathway. *J. Biol. Chem.* 2002;277(31):27975-81. doi:10.1074/jbc.M204152200.

67. Zhou J, Hara K, Inoue M, et al. Regulation of hypoxia-inducible factor 1 by glucose availability under hypoxic conditions. *Kobe J. Med. Sci.* 2007;53(6):283-96. Available at: http://www.ncbi.nlm.nih.gov/pubmed/18762723.

68. Zhou J, Schmid T, Bru B. Tumor Necrosis Factor-α Causes Accumulation of a Ubiquitinated Form of Hypoxia Inducible Factor-1α through a Nuclear Factor-κB-Dependent Pathway. *Mol. Biol. Cell.* 2003;14(June):2216-2225. doi:10.1091/mbc.E02.

69. Hellwig-Bürgel T, Rutkowski K, Metzen E, Fandrey J, Jelkmann W. Interleukin-1beta and tumor necrosis factor-alpha stimulate DNA binding of hypoxia-inducible factor-1. *Blood* 1999;94(5):1561-7. Available at: http://www.ncbi.nlm.nih.gov/pubmed/10477681. Accessed May 29, 2014.

70. Frantz S, Vincent KA, Feron O, Kelly RA. Innate immunity and angiogenesis. *Circ. Res.* 2005;96(1):15-26. doi:10.1161/01.RES.0000153188.68898.ac.

71. Kumamoto M, Nakashima Y, Sueishi K. Intimal neovascularization in human coronary atherosclerosis: its origin and pathophysiological significance. *Hum. Pathol.* 1995;26(4):450-6. Available at: http://www.ncbi.nlm.nih.gov/pubmed/7535741.

72. Moulton KS. Angiogenesis in atherosclerosis: gathering evidence beyond speculation. *Curr. Opin. Lipidol.* 2006;17(5):548-55. doi:10.1097/01.mol.0000245261.71129.f0.

73. Zhang Y, Cliff WJ, Schoefl GI, Higgins G. Immunohistochemical study of intimal microvessels in coronary atherosclerosis. *Am. J. Pathol.* 1993;143(1):164-72. Available at: http://www.pubmedcentral.nih.gov/articlerender.fcgi?artid=1886935&tool=pmcentrez&rendertype=abstract.

74. O'Brien KD, McDonald TO, Chait A, Allen MD, Alpers CE. Neovascular Expression of E-Selectin, Intercellular Adhesion Molecule-1, and Vascular Cell Adhesion Molecule-1 in Human Atherosclerosis and Their Relation to Intimal Leukocyte Content. *Circ.* 1996;93 (4):672-682. doi:10.1161/01.CIR.93.4.672.

75. Ferrara N, Henzel WJ. Pituitary follicular cells secrete a novel heparin-binding growth factor specific for vascular endothelial cells. *Biochem. Biophys. Res. Commun.* 1989;161(2):851-858. doi:http://dx.doi.org/10.1016/0006-291X(89)92678-8.

76. Leung DW, Cachianes G, Kuang WJ, Goeddel D V, Ferrara N. Vascular endothelial growth factor is a secreted angiogenic mitogen. *Science* 1989;246(4935):1306-9. Available at: http://www.ncbi.nlm.nih.gov/pubmed/2479986.

77. Fett JW, Strydom DJ, Lobb RR, et al. Isolation and characterization of angiogenin, an angiogenic protein from human carcinoma cells. *Biochemistry* 1985;24(20):5480-5486. doi:10.1021/bi00341a030.

78. Leibovich SJ, Polverini PJ, Shepard HM, Wiseman DM, Shively V, Nuseir N. Macrophage-induced angiogenesis is mediated by tumour necrosis factor-[alpha]. *Nature* 1987;329(6140):630-632. Available at: http://dx.doi.org/10.1038/329630a0.

79. Schreiber AB, Winkler ME, Derynck R. Transforming growth factor-alpha: a more potent angiogenic mediator than epidermal growth factor. *Science* 1986;232(4755):1250-1253. Available at: http://europepmc.org/abstract/MED/2422759.

80. Pepper MS. Transforming growth factor-beta: vasculogenesis, angiogenesis, and vessel wall integrity. *Cytokine Growth Factor Rev.* 1997;8(1):21-43. Available at: http://www.ncbi.nlm.nih.gov/pubmed/9174661.

81. Sluimer JC, Kolodgie FD, Bijnens APJJ, et al. Thin-walled microvessels in human coronary atherosclerotic plaques show incomplete endothelial junctions relevance of

compromised structural integrity for intraplaque microvascular leakage. *J. Am. Coll. Cardiol.* 2009;53(17):1517-27. doi:10.1016/j.jacc.2008.12.056.

82. Moreno PR, Purushothaman KR, Fuster V, et al. Plaque neovascularization is increased in ruptured atherosclerotic lesions of human aorta: implications for plaque vulnerability. *Circulation* 2004;110(14):2032-8. doi:10.1161/01.CIR.0000143233.87854.23.

83. Jeziorska M, Woolley DE. Neovascularization in early atherosclerotic lesions of human carotid arteries: its potential contribution to plaque development. *Hum. Pathol.* 1999;30(8):919-25. Available at: http://www.ncbi.nlm.nih.gov/pubmed/10452504.

84. Farb A, Burke AP, Tang AL, et al. Coronary Plaque Erosion Without Rupture Into a Lipid Core: A Frequent Cause of Coronary Thrombosis in Sudden Coronary Death . *Circ.* 1996;93 (7):1354-1363. doi:10.1161/01.CIR.93.7.1354.

85. Rao DS, Goldin JG, Fishbein MC. Determinants of plaque instability in atherosclerotic vascular disease. *Cardiovasc. Pathol.* 2005;14(6):285-93. doi:10.1016/j.carpath.2005.07.003.

86. Shah PK. Molecular mechanisms of plaque instability. *Curr. Opin. Lipidol.* 2007;18(5):492-9. doi:10.1097/MOL.0b013e3282efa326.

87. Richardson PD, Davies MJ, Born G V. Influence of plaque configuration and stress distribution on fissuring of coronary atherosclerotic plaques. *Lancet* 1989;2(8669):941-4. Available at: http://www.ncbi.nlm.nih.gov/pubmed/2571862. Accessed April 25, 2013.

88. Loree HM, Tobias BJ, Gibson LJ, Kamm RD, Small DM, Lee RT. Mechanical properties of model atherosclerotic lesion lipid pools. *Arterioscler. Thromb. Vasc. Biol.* 1994;14(2):230-234. doi:10.1161/01.ATV.14.2.230.

89. Koenig W, Khuseyinova N. Biomarkers of atherosclerotic plaque instability and rupture. *Arterioscler. Thromb. Vasc. Biol.* 2007;27(1):15-26. doi:10.1161/01.ATV.0000251503.35795.4f.

90. Galis ZS, Sukhova GK, Lark MW, Libby P. Increased expression of matrix metalloproteinases and matrix degrading activity in vulnerable regions of human atherosclerotic plaques. *J. Clin. Invest.* 1994;94(6):2493-503. doi:10.1172/JCI117619.

91. Moulton KS, Heller E, Konerding M a., Flynn E, Palinski W, Folkman J. Angiogenesis Inhibitors Endostatin or TNP-470 Reduce Intimal Neovascularization and Plaque Growth in Apolipoprotein E Deficient Mice. *Circulation* 1999;99(13):1726-1732. doi:10.1161/01.CIR.99.13.1726.

92. Moulton KS, Vakili K, Zurakowski D, et al. Inhibition of plaque neovascularization reduces macrophage accumulation and progression of advanced atherosclerosis. *Proc. Natl. Acad. Sci. U. S. A.* 2003;100(8):4736-41. doi:10.1073/pnas.0730843100.

93. Wilson SH. Simvastatin Preserves the Structure of Coronary Adventitial Vasa Vasorum in Experimental Hypercholesterolemia Independent of Lipid Lowering. *Circulation* 2002;105(4):415-418. doi:10.1161/hc0402.104119.

94. Jasińska M, Owczarek J, Orszulak-Michalak D. Statins: a new insight into their mechanisms of action and consequent pleiotropic effects. *Pharmacol. Rep.* 2007;59(5):483-99. Available at: http://www.ncbi.nlm.nih.gov/pubmed/18048949.

95. Alegret M, Silvestre JS. Pleiotropic effects of statins and related pharmacological experimental approaches. *Methods Find. Exp. Clin. Pharmacol.* 2006;28(9):627-56. doi:10.1358/mf.2006.28.9.1003573.

96. Endo A, Kuroda M, Tanzawa K. Competitive inhibition of 3-hydroxy-3-methylglutaryl coenzyme A reductase by ML-236A and ML-236B fungal metabolites, having hypocholesterolemic activity. *FEBS Lett.* 1976;72(2):323-6. Available at: http://www.ncbi.nlm.nih.gov/pubmed/16386050. Accessed November 9, 2014.

97. Schachter M. Chemical, pharmacokinetic and pharmacodynamic properties of statins: an update. *Fundam. Clin. Pharmacol.* 2005;19(1):117-25. doi:10.1111/j.1472-8206.2004.00299.x.

98. Manzoni M, Rollini M. Biosynthesis and biotechnological production of statins by filamentous fungi and application of these cholesterol-lowering drugs. *Appl. Microbiol. Biotechnol.* 2002;58(5):555-64. doi:10.1007/s00253-002-0932-9.

99. Corsini A, Bellosta S, Baetta R, Fumagalli R, Paoletti R, Bernini F. New insights into the pharmacodynamic and pharmacokinetic properties of statins. *Pharmacol. Ther.* 1999;84(3):413-28. Available at: http://www.ncbi.nlm.nih.gov/pubmed/10665838.

100. Stancu C, Sima A. Statins: mechanism of action and effects. *J. Cell. Mol. Med.* 2001;5(4):378-87. Available at: http://www.ncbi.nlm.nih.gov/pubmed/12067471.

101. Shelness GS, Sellers JA. Very-low-density lipoprotein assembly and secretion. *Curr. Opin. Lipidol.* 2001;12(2):151-7. Available at: http://www.ncbi.nlm.nih.gov/pubmed/11264986.

102. Martin G, Duez H, Blanquart C, et al. Statin-induced inhibition of the Rho-signaling pathway activates PPAR α and induces HDL apoA-I. 2001;107(11):1423-1432.

103. Schaefer JR, Schweer H, Ikewaki K, et al. Metabolic basis of high density lipoproteins and apolipoprotein A-I increase by HMG-CoA reductase inhibition in healthy subjects and a patient with coronary artery disease. *Atherosclerosis* 1999;144(1):177-84. Available at: http://www.ncbi.nlm.nih.gov/pubmed/10381291.

104. Tall AR. An overview of reverse cholesterol transport. *Eur. Heart J.* 1998;19 Suppl A:A31-5. Available at: http://www.ncbi.nlm.nih.gov/pubmed/9519340. Accessed June 2, 2014.

105. Ohara Y, Peterson TE, Harrison DG. Hypercholesterolemia increases endothelial superoxide anion production. *J. Clin. Invest.* 1993;91(6):2546-51. doi:10.1172/JCI116491.

106. Treasure CB, Klein JL, Weintraub WS, et al. Beneficial effects of cholesterol-lowering therapy on the coronary endothelium in patients with coronary artery disease. *N. Engl. J. Med.* 1995;332(8):481-7. doi:10.1056/NEJM199502233320801.

107. Goldstein JL, Brown MS. Regulation of the mevalonate pathway. *Nature* 1990;343(6257):425-30. doi:10.1038/343425a0.

108. Kureishi Y, Luo Z, Shiojima I, et al. The HMG-CoA reductase inhibitor simvastatin activates the protein kinase Akt and promotes angiogenesis in normocholesterolemic animals. *Nat. Med.* 2000;6(9):1004-10. doi:10.1038/79510.

109. Wolfrum S, Dendorfer A, Schutt M, et al. Simvastatin acutely reduces myocardial reperfusion injury in vivo by activating the phosphatidylinositide 3-kinase/Akt pathway. *J. Cardiovasc. Pharmacol.* 2004;44(3):348-55. Available at: http://www.ncbi.nlm.nih.gov/pubmed/15475833.

110. Laufs U, La Fata V, Plutzky J, Liao JK. Upregulation of Endothelial Nitric Oxide Synthase by HMG CoA Reductase Inhibitors. *Circulation* 1998;97(12):1129-1135. doi:10.1161/01.CIR.97.12.1129.

111. Kosmidou I, Moore JP, Weber M, Searles CD. Statin treatment and 3' polyadenylation of eNOS mRNA. *Arterioscler. Thromb. Vasc. Biol.* 2007;27(12):2642-9. doi:10.1161/ATVBAHA.107.154492.

112. Margaritis M, Channon KM, Antoniades C. Statins as regulators of redox state in the vascular endothelium: beyond lipid lowering. *Antioxid. Redox Signal.* 2014;20(8):1198-215. doi:10.1089/ars.2013.5430.

113. Hillyard DZ, Nutt CD, Thomson J, et al. Statins inhibit NK cell cytotoxicity by membrane raft depletion rather than inhibition of isoprenylation. *Atherosclerosis* 2007;191(2):319-25. doi:10.1016/j.atherosclerosis.2006.05.037.

114. Chung HK, Lee IK, Kang H, et al. Statin inhibits interferon-gamma-induced expression of intercellular adhesion molecule-1 (ICAM-1) in vascular endothelial and smooth muscle cells. *Exp. Mol. Med.* 2002;34(6):451-61. Available at: http://www.ncbi.nlm.nih.gov/pubmed/12526087. Accessed March 24, 2013.

115. Rasmussen LM, Hansen PR, Nabipour MT, Olesen P, Kristiansen MT, Ledet T. Diverse effects of inhibition of 3-hydroxy-3-methylglutaryl-CoA reductase on the expression of VCAM-1 and E-selectin in endothelial cells. *Biochem. J.* 2001;360(Pt 2):363-70. Available at: http://www.pubmedcentral.nih.gov/articlerender.fcgi?artid=1222236&tool=pmcentrez&rendertype=abstract. Accessed November 9, 2014.

116. Romano M, Diomede L, Sironi M, et al. Inhibition of monocyte chemotactic protein-1 synthesis by statins. *Lab. Invest.* 2000;80(7):1095-100. Available at: http://www.ncbi.nlm.nih.gov/pubmed/10908155.

117. Laufs U, Marra D, Node K, Liao JK. 3-Hydroxy-3-methylglutaryl-CoA reductase inhibitors attenuate vascular smooth muscle proliferation by preventing rho GTPase-induced down-regulation of p27(Kip1). *J. Biol. Chem.* 1999;274(31):21926-31. Available at: http://www.ncbi.nlm.nih.gov/pubmed/10419514.

118. Aikawa M, Rabkin E, Sugiyama S, et al. An HMG-CoA Reductase Inhibitor, Cerivastatin, Suppresses Growth of Macrophages Expressing Matrix Metalloproteinases and Tissue Factor In Vivo and In Vitro. *Circulation* 2001;103(2):276-283. doi:10.1161/01.CIR.103.2.276.

119. Huhle G, Abletshauser C, Mayer N, Weidinger G, Harenberg J, Heene DL. Reduction of platelet activity markers in type II hypercholesterolemic patients by a HMG-CoA-reductase inhibitor. *Thromb. Res.* 1999;95(5):229-34. Available at: http://www.ncbi.nlm.nih.gov/pubmed/10515287. Accessed March 24, 2013.

120. Fukumoto Y, Libby P, Rabkin E, et al. Statins Alter Smooth Muscle Cell Accumulation and Collagen Content in Established Atheroma of Watanabe Heritable Hyperlipidemic Rabbits. *Circulation* 2001;103(7):993-999. doi:10.1161/01.CIR.103.7.993.

121. Davignon J, Jacob RF, Mason RP. The antioxidant effects of statins. *Coron. Artery Dis.* 2004;15(5):251-258. doi:10.1097/01.mca.0000131573.31966.34.

122. Takemoto M, Node K, Nakagami H, et al. Statins as antioxidant therapy for preventing cardiac myocyte hypertrophy. 2001;108(10):1429-1437. doi:10.1172/JCI200113350.Introduction.

123. Kwak B, Mulhaupt F, Myit S, Mach F. Statins as a newly recognized type of immunomodulator. *Nat. Med.* 2000;6(12):1399-402. doi:10.1038/82219.

124. Hisada T, Ayaori M, Ohrui N, et al. Statin inhibits hypoxia-induced endothelin-1 via accelerated degradation of HIF-1α in vascular smooth muscle cells. *Cardiovasc. Res.* 2012;95(2):251-9. doi:10.1093/cvr/cvs110.

125. Urbich C. Double-Edged Role of Statins in Angiogenesis Signaling. *Circ. Res.* 2002;90(6):737-744. doi:10.1161/01.RES.0000014081.30867.F8.

126. Weis M. Statins Have Biphasic Effects on Angiogenesis. *Circulation* 2002;105(6):739-745. doi:10.1161/hc0602.103393.

127. Scandinavian Simvastatin Survival Study Group. Randomised trial of cholesterol lowering in 4444 patients with coronary heart disease: the Scandinavian Simvastatin Survival Study (4S). *Lancet* 1994;344(8934):1383-9. Available at: http://www.ncbi.nlm.nih.gov/pubmed/7968073. Accessed March 24, 2013.

128. FDA. Drug Approval Package. *U.S. Dep. Heal. Hum. Serv.* 2001. Available at: http://www.accessdata.fda.gov/drugsatfda_docs/nda/98/119766-s28.cfm. Accessed March 26, 2013.

129. Kishore SP, Herbstman BJ. Adding a medicine to the WHO model list of essential medicines. *Clin. Pharmacol. Ther.* 2009;85(3):237-9. doi:10.1038/clpt.2008.258.

130. NICE. NICE implementation uptake report : statins for the prevention of cardiovascular events. 2008;(March).

131. Corsini A, Maggi FM, Catapano AL. Pharmacology of competitive inhibitors of HMG-CoA reductase. *Pharmacol. Res.* 1995;31(1):9-27. Available at: http://www.ncbi.nlm.nih.gov/pubmed/7784310. Accessed March 24, 2013.

132. Ohtawa M, Masuda N, Akasaka I, Nakashima a, Ochiai K, Moriyasu M. Cellular uptake of fluvastatin, an inhibitor of HMG-CoA reductase, by rat cultured hepatocytes and human aortic endothelial cells. *Br. J. Clin. Pharmacol.* 1999;47(4):383-9. Available at: http://www.pubmedcentral.nih.gov/articlerender.fcgi?artid=2014242&tool=pmcentrez&rendertype=abstract.

133. BNF. *British National Formulary*. May 2014. (Khanderia S, Jordan B, Martin J, Ryan RSM, Wagle SMS, eds.). London: BMJ Group ; Pharmaceutical Press; 2014.

134. Kyrklund C, Backman JT, Kivistö KT, Neuvonen M, Laitila J, Neuvonen PJ. Rifampin greatly reduces plasma simvastatin and simvastatin acid concentrations. *Clin. Pharmacol. Ther.* 2000;68(6):592-7. doi:10.1067/mcp.2000.111414.

135. Ghosh-Choudhury NN, Mandal CC, Ghosh Choudhury G. Simvastatin induces derepression of PTEN expression via NFkappaB to inhibit breast cancer cell growth. *Cell. Signal.* 2010;22(5):749-58. doi:10.1016/j.cellsig.2009.12.010.

136. Jin Z, Dicker DT, El-Deiry WS. Enhanced sensitivity of G1 arrested human cancer cells suggests a novel therapeutic strategy using a combination of simvastatin and TRAIL. *Cell Cycle* 2002;1(1):82-9. Available at: http://www.ncbi.nlm.nih.gov/pubmed/12429913.

137. Leung BP, Sattar N, Crilly A, et al. A novel anti-inflammatory role for simvastatin in inflammatory arthritis. *J. Immunol.* 2003;170(3):1524-30. Available at: http://www.ncbi.nlm.nih.gov/pubmed/12538717.

138. Kenis I, Tartakover-Matalon S, Cherepnin N, et al. Simvastatin has deleterious effects on human first trimester placental explants. *Hum. Reprod.* 2005;20(10):2866-72. doi:10.1093/humrep/dei120.

139. Shen W, Shi H-M, Fan W-H, Luo X-P, Jin B, Li Y. The effects of simvastatin on angiogenesis: studied by an original model of atherosclerosis and acute myocardial infarction in rabbit. *Mol. Biol. Rep.* 2011;38(6):3821-8. doi:10.1007/s11033-010-0497-0.

140. Dichtl W, Dulak J, Frick M, et al. HMG-CoA reductase inhibitors regulate inflammatory transcription factors in human endothelial and vascular smooth muscle cells. *Arterioscler. Thromb. Vasc. Biol.* 2003;23(1):58-63. doi:10.1161/01.ATV.0000043456.48735.20.

141. Zhang K, Meng X, Kong J, et al. Simvastatin increases Prolyl-4-Hydroxylase α1 expression in atherosclerotic plaque and ox-LDL-stimulated human aortic smooth muscle cells via p38 MAPK and ERK1/2 signaling. *J. Mol. Cell. Cardiol.* 2013;65:43-50. doi:10.1016/j.yjmcc.2013.09.010.

142. Luan Z, Chase AJ, Newby AC. Statins inhibit secretion of metalloproteinases-1, -2, -3, and -9 from vascular smooth muscle cells and macrophages. *Arterioscler. Thromb. Vasc. Biol.* 2003;23(5):769-75. doi:10.1161/01.ATV.0000068646.76823.AE.

143. Lazzerini PE, Capecchi PL, Nerucci F, et al. Simvastatin reduces MMP-3 level in interleukin 1beta stimulated human chondrocyte culture. *Ann. Rheum. Dis.* 2004;63(7):867-9. doi:10.1136/ard.2003.009746.

144. Wong B, Lumma W. Statins suppress THP-1 cell migration and secretion of matrix metalloproteinase 9 by inhibiting geranylgeranylation. *J. …* 2001;69(June):959-962. Available at: http://www.jleukbio.org/content/69/6/959.short. Accessed April 2, 2013.

145. Wang S, Lee S-R, Guo S-Z, et al. Reduction of tissue plasminogen activator-induced matrix metalloproteinase-9 by simvastatin in astrocytes. *Stroke.* 2006;37(7):1910-2. doi:10.1161/01.STR.0000226923.48905.39.

146. Kidera Y, Tsubaki M, Yamazoe Y, et al. Reduction of lung metastasis, cell invasion, and adhesion in mouse melanoma by statin-induced blockade of the Rho/Rho-associated coiled-coil-containing protein kinase pathway. *J. Exp. Clin. Cancer Res.* 2010;29:127. doi:10.1186/1756-9966-29-127.

147. Ye S. Influence of matrix metalloproteinase genotype on cardiovascular disease susceptibility and outcome. *Cardiovasc. Res.* 2006;69(3):636-45. doi:10.1016/j.cardiores.2005.07.015.

148. Brinckerhoff CE, Matrisian LM. Matrix metalloproteinases: a tail of a frog that became a prince. *Nat. Rev. Mol. Cell Biol.* 2002;3(3):207-14. doi:10.1038/nrm763.

149. Nagase H, Visse R, Murphy G. Structure and function of matrix metalloproteinases and TIMPs. *Cardiovasc. Res.* 2006;69(3):562-73. doi:10.1016/j.cardiores.2005.12.002.

150. Nagase H, Woessner JF. Matrix metalloproteinases. *J. Biol. Chem.* 1999;274(31):21491-4. Available at: http://www.ncbi.nlm.nih.gov/pubmed/10419448.

151. Visse R, Nagase H. Matrix metalloproteinases and tissue inhibitors of metalloproteinases: structure, function, and biochemistry. *Circ. Res.* 2003;92(8):827-39. doi:10.1161/01.RES.0000070112.80711.3D.

152. Qin L, Han Y-P. Epigenetic repression of matrix metalloproteinases in myofibroblastic hepatic stellate cells through histone deacetylases 4: implication in tissue fibrosis. *Am. J. Pathol.* 2010;177(4):1915-28. doi:10.2353/ajpath.2010.100011.

153. Chicoine E, Estève P-O, Robledo O, Van Themsche C, Potworowski EF, St-Pierre Y. Evidence for the role of promoter methylation in the regulation of MMP-9 gene expression. *Biochem. Biophys. Res. Commun.* 2002;297(4):765-72. Available at: http://www.ncbi.nlm.nih.gov/pubmed/12359218.

154. Yan C, Boyd DD. Regulation of matrix metalloproteinase gene expression. *J. Cell. Physiol.* 2007;211(1):19-26. doi:10.1002/jcp.20948.

155. Clark IM, Swingler TE, Sampieri CL, Edwards DR. The regulation of matrix metalloproteinases and their inhibitors. *Int. J. Biochem. Cell Biol.* 2008;40(6-7):1362-78. doi:10.1016/j.biocel.2007.12.006.

156. Couillard J, Demers M, Lavoie G, St-Pierre Y. The role of DNA hypomethylation in the control of stromelysin gene expression. *Biochem. Biophys. Res. Commun.* 2006;342(4):1233-9. doi:10.1016/j.bbrc.2006.02.068.

157. Xia H, Qi Y, Ng SS, et al. microRNA-146b inhibits glioma cell migration and invasion by targeting MMPs. *Brain Res.* 2009;1269:158-65. doi:10.1016/j.brainres.2009.02.037.

158. Galis Z, Khatri J. Matrix metalloproteinases in vascular remodeling and atherogenesis the good, the bad, and the ugly. *Circ. Res.* 2002:251-262. doi:10.1161/hh0302.105345.

159. Takahashi C, Sheng Z, Horan TP, et al. Regulation of matrix metalloproteinase-9 and inhibition of tumor invasion by the membrane-anchored glycoprotein RECK. *Proc. Natl. Acad. Sci. U. S. A.* 1998;95(22):13221-6. Available at: http://www.pubmedcentral.nih.gov/articlerender.fcgi?artid=23764&tool=pmcentrez&rendertype=abstract.

160. Bein K, Simons M. Thrombospondin type 1 repeats interact with matrix metalloproteinase 2. Regulation of metalloproteinase activity. *J. Biol. Chem.* 2000;275(41):32167-73. doi:10.1074/jbc.M003834200.

161. Griffin MO, Fricovsky E, Ceballos G, Villarreal F. Tetracyclines: a pleitropic family of compounds with promising therapeutic properties. Review of the literature. *Am. J. Physiol. Cell Physiol.* 2010;299(3):C539-48. doi:10.1152/ajpcell.00047.2010.

162. Brew K, Nagase H. The tissue inhibitors of metalloproteinases (TIMPs): an ancient family with structural and functional diversity. *Biochim. Biophys. Acta* 2010;1803(1):55-71. doi:10.1016/j.bbamcr.2010.01.003.

163. Hamze AB, Wei S, Bahudhanapati H, Kota S, Acharya KR, Brew K. Constraining specificity in the N-domain of tissue inhibitor of metalloproteinases-1; gelatinase-selective inhibitors. *Protein Sci.* 2007;16(9):1905-13. doi:10.1110/ps.072978507.

164. Moore L, Fan D, Basu R, Kandalam V, Kassiri Z. Tissue inhibitor of metalloproteinases (TIMPs) in heart failure. *Heart Fail. Rev.* 2012;17(4-5):693-706. doi:10.1007/s10741-011-9266-y.

165. Bertaux B, Hornebeck W, Eisen AZ, Dubertret L. Growth stimulation of human keratinocytes by tissue inhibitor of metalloproteinases. *J. Invest. Dermatol.* 1991;97(4):679-85. Available at: http://www.ncbi.nlm.nih.gov/pubmed/1940438. Accessed November 18, 2014.

166. Hayakawa T, Yamashita K, Tanzawa K, Uchijima E, Iwata K. Growth-promoting activity of tissue inhibitor of metalloproteinases-1 (TIMP-1) for a wide range of cells. A possible new growth factor in serum. *FEBS Lett.* 1992;298(1):29-32. Available at: http://www.ncbi.nlm.nih.gov/pubmed/1544418. Accessed November 18, 2014.

167. Wang T, Yamashita K, Iwata K, Hayakawa T. Both tissue inhibitors of metalloproteinases-1 (TIMP-1) and TIMP-2 activate Ras but through different pathways. *Biochem. Biophys. Res. Commun.* 2002;296(1):201-5. Available at: http://www.ncbi.nlm.nih.gov/pubmed/12147251. Accessed November 18, 2014.

168. Handsley MM, Edwards DR. Metalloproteinases and their inhibitors in tumor angiogenesis. *Int. J. Cancer* 2005;115(6):849-60. doi:10.1002/ijc.20945.

169. Silence J, Collen D, Lijnen HR. Reduced atherosclerotic plaque but enhanced aneurysm formation in mice with inactivation of the tissue inhibitor of metalloproteinase-1 (TIMP-1) gene. *Circ. Res.* 2002;90(8):897-903. Available at: http://www.ncbi.nlm.nih.gov/pubmed/11988491. Accessed November 18, 2014.

170. Fedak PWM, Smookler DS, Kassiri Z, et al. TIMP-3 deficiency leads to dilated cardiomyopathy. *Circulation* 2004;110(16):2401-9. doi:10.1161/01.CIR.0000134959.83967.2D.

171. Bode W, Gomis-Rüth FX, Stöckler W. Astacins, serralysins, snake venom and matrix metalloproteinases exhibit identical zinc-binding environments (HEXXHXXGXXH and Met-turn) and topologies and should be grouped into a common family, the “metzincins”. *FEBS Lett.* 1993;331(1-2):134-40. Available at: http://www.ncbi.nlm.nih.gov/pubmed/8405391.

172. Spinale FG. Matrix Metalloproteinases: Regulation and Dysregulation in the Failing Heart. *Circ. Res.* 2002;90(5):520-530. doi:10.1161/01.RES.0000013290.12884.A3.

173. Cha H, Kopetzki E, Huber R, Lanzendörfer M, Brandstetter H. Structural Basis of the Adaptive Molecular Recognition by MMP9. *J. Mol. Biol.* 2002;320(5):1065-1079. doi:10.1016/S0022-2836(02)00558-2.

174. Cauwe B, Van den Steen PE, Opdenakker G. The biochemical, biological, and pathological kaleidoscope of cell surface substrates processed by matrix metalloproteinases. *Crit. Rev. Biochem. Mol. Biol.* 2007;42(3):113-85. doi:10.1080/10409230701340019.

175. Mannello F, Medda V. Nuclear localization of matrix metalloproteinases. *Prog. Histochem. Cytochem.* 2012;47(1):27-58. doi:10.1016/j.proghi.2011.12.002.

176. Itoh T, Tanioka M, Matsuda H, et al. Experimental metastasis is suppressed in MMP-9-deficient mice. *Clin. Exp. Metastasis* 1999;17(2):177-81. Available at: http://www.ncbi.nlm.nih.gov/pubmed/10411111.

177. Noë V, Fingleton B, Jacobs K, et al. Release of an invasion promoter E-cadherin fragment by matrilysin and stromelysin-1. *J. Cell Sci.* 2001;114(Pt 1):111-118. Available at: http://www.ncbi.nlm.nih.gov/pubmed/11112695.

178. Rundhaug JE. Matrix metalloproteinases and angiogenesis. *J. Cell. Mol. Med.* 2005;9(2):267-85. Available at: http://www.ncbi.nlm.nih.gov/pubmed/15963249.

179. Gialeli C, Theocharis AD, Karamanos NK. Roles of matrix metalloproteinases in cancer progression and their pharmacological targeting. *FEBS J.* 2011;278(1):16-27. doi:10.1111/j.1742-4658.2010.07919.x.

180. Balbín M, Fueyo A, Tester AM, et al. Loss of collagenase-2 confers increased skin tumor susceptibility to male mice. *Nat. Genet.* 2003;35(3):252-7. doi:10.1038/ng1249.

181. Yong VW, Krekoski CA, Forsyth PA, Bell R, Edwards DR. Matrix metalloproteinases and diseases of the CNS. 1998:75-80.

182. Culpitt S V, Rogers DF, Traves SL, Barnes PJ, Donnelly LE. Sputum matrix metalloproteases: comparison between chronic obstructive pulmonary disease and asthma. *Respir. Med.* 2005;99(6):703-10. doi:10.1016/j.rmed.2004.10.022.

183. Ye S, Patodi N, Walker-Bone K, Reading I, Cooper C, Dennison E. Variation in the matrix metalloproteinase-3, -7, -12 and -13 genes is associated with functional status in rheumatoid arthritis. *Int. J. Immunogenet.* 2007;34(2):81-5. doi:10.1111/j.1744-313X.2007.00664.x.

184. Nikkari ST, O'Brien KD, Ferguson M, et al. Interstitial Collagenase (MMP-1) Expression in Human Carotid Atherosclerosis. *Circ.* 1995;92 (6):1393-1398. doi:10.1161/01.CIR.92.6.1393.

185. Sukhova GK, Schonbeck U, Rabkin E, et al. Evidence for Increased Collagenolysis by Interstitial Collagenases-1 and -3 in Vulnerable Human Atheromatous Plaques. *Circulation* 1999;99(19):2503-2509. doi:10.1161/01.CIR.99.19.2503.

186. Molloy KJ, Thompson MM, Jones JL, et al. Unstable carotid plaques exhibit raised matrix metalloproteinase-8 activity. *Circulation* 2004;110(3):337-43. doi:10.1161/01.CIR.0000135588.65188.14.

187. Laxton RC, Hu Y, Duchene J, et al. A role of matrix metalloproteinase-8 in atherosclerosis. *Circ. Res.* 2009;105(9):921-9. doi:10.1161/CIRCRESAHA.109.200279.

188. Fang C, Wen G, Zhang L, et al. An Important Role of Matrix Metalloproteinase-8 in Angiogenesis in Vitro and in Vivo. *Cardiovasc. Res.* 2013;44(0). doi:10.1093/cvr/cvt060.

189. Li Z, Li L, Zielke HR, et al. Increased expression of 72-kd type IV collagenase (MMP-2) in human aortic atherosclerotic lesions. *Am. J. Pathol.* 1996;148(1):121-8. Available at: http://www.pubmedcentral.nih.gov/articlerender.fcgi?artid=1861591&tool=pmcentrez&rendertype=abstract.

190. Henney a M, Wakeley PR, Davies MJ, et al. Localization of stromelysin gene expression in atherosclerotic plaques by in situ hybridization. *Proc. Natl. Acad. Sci. U. S. A.* 1991;88(18):8154-8. Available at: http://www.pubmedcentral.nih.gov/articlerender.fcgi?artid=52465&tool=pmcentrez&rendertype=abstract.

191. Halpert I, Sires UI, Roby JD, et al. Matrilysin is expressed by lipid-laden macrophages at sites of potential rupture in atherosclerotic lesions and localizes to areas of versican deposition, a proteoglycan substrate for the enzyme. *Proc. Natl. Acad. Sci. U. S. A.* 1996;93(18):9748-53. Available at: http://www.pubmedcentral.nih.gov/articlerender.fcgi?artid=38500&tool=pmcentrez&rendertype=abstract.

192. Williams H, Johnson JL, Jackson CL, White SJ, George SJ. MMP-7 mediates cleavage of N-cadherin and promotes smooth muscle cell apoptosis. *Cardiovasc. Res.* 2010;87(1):137-46. doi:10.1093/cvr/cvq042.

193. Morgan AR, Rerkasem K, Gallagher PJ, et al. Differences in matrix metalloproteinase-1 and matrix metalloproteinase-12 transcript levels among carotid atherosclerotic plaques with different histopathological characteristics. *Stroke.* 2004;35(6):1310-5. doi:10.1161/01.STR.0000126822.01756.99.

194. Noda K, Ishida S, Shinoda H, et al. Hypoxia induces the expression of membrane-type 1 matrix metalloproteinase in retinal glial cells. *Invest. Ophthalmol. Vis. Sci.* 2005;46(10):3817-24. doi:10.1167/iovs.04-1528.

195. Miyoshi A, Kitajima Y, Ide T, et al. Hypoxia accelerates cancer invasion of hepatoma cells by upregulating MMP expression in an HIF-1alpha-independent manner. *Int. J. Oncol.* 2006;29(6):1533-9. Available at: http://www.ncbi.nlm.nih.gov/pubmed/17088993. Accessed September 27, 2012.

196. Rajavashisth TB, Xu X-PX-O, Jovinge S, et al. Membrane Type 1 Matrix Metalloproteinase Expression in Human Atherosclerotic Plaques : Evidence for Activation by Proinflammatory Mediators. *Circulation* 1999;99(24):3103-3109. doi:10.1161/01.CIR.99.24.3103.

197. Johnson JL, Sala-Newby GB, Ismail Y, Aguilera CM, Newby AC. Low tissue inhibitor of metalloproteinases 3 and high matrix metalloproteinase 14 levels defines a

subpopulation of highly invasive foam-cell macrophages. *Arterioscler. Thromb. Vasc. Biol.* 2008;28(9):1647-53. doi:10.1161/ATVBAHA.108.170548.

198. Chun T-H, Sabeh F, Ota I, et al. MT1-MMP-dependent neovessel formation within the confines of the three-dimensional extracellular matrix. *J. Cell Biol.* 2004;167(4):757-67. doi:10.1083/jcb.200405001.

199. Zhou Z, Apte SS, Soininen R, et al. Impaired endochondral ossification and angiogenesis in mice deficient in membrane-type matrix metalloproteinase I. *Proc. Natl. Acad. Sci. U. S. A.* 2000;97(8):4052-7. doi:10.1073/pnas.060037197.

200. Sato H, Takino T, Okada Y, et al. A matrix metalloproteinase expressed on the surface of invasive tumour cells. *Nature* 1994;370(6484):61-5. doi:10.1038/370061a0.

201. Holopainen JM. Activation of Matrix Metalloproteinase-8 by Membrane Type 1-MMP and Their Expression in Human Tears after Photorefractive Keratectomy. *Invest. Ophthalmol. Vis. Sci.* 2003;44(6):2550-2556. doi:10.1167/iovs.02-1190.

202. Will H, Lo C, Smith B, et al. Cellular mechanisms for human procollagenase-3 (MMP-13) activation. Evidence that MT1-MMP (MMP-14) and gelatinase a (MMP-2) are able to generate active enzyme. *J. Biol. Chem.* 1996;271(29):17124-31. Available at: http://www.ncbi.nlm.nih.gov/pubmed/8663255. Accessed April 9, 2013.

203. Mignon C, Okada A, Mattei MG, Basset P. Assignment of the human membrane-type matrix metalloproteinase (MMP14) gene to 14q11-q12 by in situ hybridization. *Genomics* 1995;28(2):360-1. doi:10.1006/geno.1995.1159.

204. Sato H, Tanaka M, Takino T, Inoue M, Seiki M. Assignment of the human genes for membrane-type-1, -2, and -3 matrix metalloproteinases (MMP14, MMP15, and MMP16) to 14q12.2, 16q12.2-q21, and 8q21, respectively, by in situ hybridization. *Genomics* 1997;39(3):412-3. doi:10.1006/geno.1996.4496.

205. Mattei MG, Roeckel N, Olsen BR, Apte SS. Genes of the membrane-type matrix metalloproteinase (MT-MMP) gene family, MMP14, MMP15, and MMP16, localize to human chromosomes 14, 16, and 8, respectively. *Genomics* 1997;40(1):168-9. doi:10.1006/geno.1996.4559.

206. Apte SS, Fukai N, Beier DR, Olsen BR. The matrix metalloproteinase-14 (MMP-14) gene is structurally distinct from other MMP genes and is co-expressed with the TIMP-2 gene during mouse embryogenesis. *J. Biol. Chem.* 1997;272(41):25511-7. Available at: http://www.ncbi.nlm.nih.gov/pubmed/9325265.

207. Lu H, Hu L, Yu L, et al. KLF8 and FAK cooperatively enrich the active MMP14 on the cell surface required for the metastatic progression of breast cancer. *Oncogene* 2014;33(22):2909-17. doi:10.1038/onc.2013.247.

208. Petrella BL, Lohi J, Brinckerhoff CE. Identification of membrane type-1 matrix metalloproteinase as a target of hypoxia-inducible factor-2 alpha in von Hippel-Lindau renal cell carcinoma. *Oncogene* 2005;24(6):1043-52. doi:10.1038/sj.onc.1208305.

209. Haas TL, Stitelman D, Davis SJ, Apte SS, Madri J a. Egr-1 Mediates Extracellular Matrix-driven Transcription of Membrane Type 1 Matrix Metalloproteinase in Endothelium. *J. Biol. Chem.* 1999;274(32):22679-22685. doi:10.1074/jbc.274.32.22679.

210. Yun S, Dardik A, Haga M, et al. Transcription factor Sp1 phosphorylation induced by shear stress inhibits membrane type 1-matrix metalloproteinase expression in endothelium. *J. Biol. Chem.* 2002;277(38):34808-14. doi:10.1074/jbc.M205417200.

211. GeneCards®. matrix metallopeptidase 14 (membrane-inserted). 2013. Available at: http://www.genecards.org/cgi-bin/carddisp.pl?gene=MMP14. Accessed April 10, 2013.

212. Sato H, Kinoshita T, Takino T, Nakayama K, Seiki M. Activation of a recombinant membrane type 1-matrix metalloproteinase (MT1-MMP) by furin and its interaction with tissue inhibitor of metalloproteinases (TIMP)-2. *FEBS Lett.* 1996;393(1):101-4. Available at: http://www.ncbi.nlm.nih.gov/pubmed/8804434. Accessed April 10, 2013.

213. Mazzone M, Baldassarre M, Beznoussenko G, et al. Intracellular processing and activation of membrane type 1 matrix metalloprotease depends on its partitioning into lipid domains. *J. Cell Sci.* 2004;117(Pt 26):6275-87. doi:10.1242/jcs.01563.

214. Tyagi SC, Lewis K, Pikes D, et al. Stretch-induced membrane type matrix metalloproteinase and tissue plasminogen activator in cardiac fibroblast cells. *J. Cell. Physiol.* 1998;176(2):374-82. doi:10.1002/(SICI)1097-4652(199808)176:2<374::AID-JCP16>3.0.CO;2-3.

215. Itoh Y, Takamura a, Ito N, et al. Homophilic complex formation of MT1-MMP facilitates proMMP-2 activation on the cell surface and promotes tumor cell invasion. *EMBO J.* 2001;20(17):4782-93. doi:10.1093/emboj/20.17.4782.

216. Zarrabi K, Dufour A, Li J, et al. Inhibition of matrix metalloproteinase 14 (MMP-14)-mediated cancer cell migration. *J. Biol. Chem.* 2011;286(38):33167-77. doi:10.1074/jbc.M111.256644.

217. Brew K, Dinakarpandian D, Nagase H. Tissue inhibitors of metalloproteinases: evolution, structure and function. *Biochim. Biophys. Acta* 2000;1477(1-2):267-83. Available at: http://www.ncbi.nlm.nih.gov/pubmed/10708863.

218. Butler GS, Will H, Atkinson SJ, Murphy G. Membrane-type-2 matrix metalloproteinase can initiate the processing of progelatinase A and is regulated by the tissue inhibitors of metalloproteinases. *Eur. J. Biochem.* 1997;244(2):653-7. Available at: http://www.ncbi.nlm.nih.gov/pubmed/9119036.

219. Strongin AY, Collier I, Bannikov G, Marmer BL, Grant GA, Goldberg GI. Mechanism of cell surface activation of 72-kDa type IV collagenase. Isolation of the activated form of the membrane metalloprotease. *J. Biol. Chem.* 1995;270(10):5331-8. Available at: http://www.ncbi.nlm.nih.gov/pubmed/7890645. Accessed March 21, 2013.

220. DeClerck YA, Yean TD, Lee Y, Tomich JM, Langley KE. Characterization of the functional domain of tissue inhibitor of metalloproteinases-2 (TIMP-2). *Biochem. J.* 1993;289 (Pt 1:65-9. Available at: http://www.pubmedcentral.nih.gov/articlerender.fcgi?artid=1132131&tool=pmcentrez&rendertype=abstract. Accessed November 9, 2014.

221. Atkinson SJ, Crabbe T, Cowell S, et al. Intermolecular autolytic cleavage can contribute to the activation of progelatinase A by cell membranes. *J. Biol. Chem.* 1995;270(51):30479-85. Available at: http://www.ncbi.nlm.nih.gov/pubmed/8530478.

222. Kinoshita T, Sato H, Okada a, et al. TIMP-2 promotes activation of progelatinase A by membrane-type 1 matrix metalloproteinase immobilized on agarose beads. *J. Biol. Chem.* 1998;273(26):16098-103. Available at: http://www.ncbi.nlm.nih.gov/pubmed/9632662.

223. Ohuchi E, Imai K, Fujii Y, Sato H, Seiki M, Okada Y. Membrane type 1 matrix metalloproteinase digests interstitial collagens and other extracellular matrix macromolecules. *J. Biol. Chem.* 1997;272(4):2446-51. Available at: http://www.ncbi.nlm.nih.gov/pubmed/8999957.

224. Hiraoka N, Allen E, Apel IJ, Gyetko MR, Weiss SJ. Matrix metalloproteinases regulate neovascularization by acting as pericellular fibrinolysins. *Cell* 1998;95(3):365-77. Available at: http://www.ncbi.nlm.nih.gov/pubmed/9814707.

225. Holmbeck K, Bianco P, Caterina J, et al. MT1-MMP-deficient mice develop dwarfism, osteopenia, arthritis, and connective tissue disease due to inadequate collagen turnover. *Cell* 1999;99(1):81-92. Available at: http://www.ncbi.nlm.nih.gov/pubmed/10520996.

226. Sato T, del Carmen Ovejero M, Hou P, et al. Identification of the membrane-type matrix metalloproteinase MT1-MMP in osteoclasts. *J. Cell Sci.* 1997;110 (Pt 5:589-96. Available at: http://www.ncbi.nlm.nih.gov/pubmed/9092941.

227. Holmbeck K, Bianco P, Pidoux I, et al. The metalloproteinase MT1-MMP is required for normal development and maintenance of osteocyte processes in bone. *J. Cell Sci.* 2005;118(Pt 1):147-56. doi:10.1242/jcs.01581.

228. Schenk S, Hintermann E, Bilban M, et al. Binding to EGF receptor of a laminin-5 EGF-like fragment liberated during MMP-dependent mammary gland involution. *J. Cell Biol.* 2003;161(1):197-209. doi:10.1083/jcb.200208145.

229. Kajita M, Itoh Y, Chiba T, et al. Membrane-type 1 matrix metalloproteinase cleaves CD44 and promotes cell migration. *J. Cell Biol.* 2001;153(5):893-904. Available at:

http://www.pubmedcentral.nih.gov/articlerender.fcgi?artid=2174329&tool=pmcentrez&rendertype=abstract.

230. Kheradmand F, Rishi K, Werb Z. Signaling through the EGF receptor controls lung morphogenesis in part by regulating MT1-MMP-mediated activation of gelatinase A/MMP2. *J. Cell Sci.* 2002;115(Pt 4):839-48. Available at: http://www.pubmedcentral.nih.gov/articlerender.fcgi?artid=2788991&tool=pmcentrez&rendertype=abstract.

231. Maisi P, Prikk K, Sepper R, et al. Soluble membrane-type 1 matrix metalloproteinase (MT1-MMP) and gelatinase A (MMP-2) in induced sputum and bronchoalveolar lavage fluid of human bronchial asthma and bronchiectasis. *APMIS* 2002;110(11):771-82. Available at: http://www.ncbi.nlm.nih.gov/pubmed/12588417.

232. Chun T, Inoue M, Morisaki H, et al. Genetic link between obesity and MMP14-dependent adipogenic collagen turnover. *Diabetes* 2010;59(10):2484-94. doi:10.2337/db10-0073.

233. Konttinen YT, Ainola M, Valleala H, et al. Analysis of 16 different matrix metalloproteinases (MMP-1 to MMP-20) in the synovial membrane: different profiles in trauma and rheumatoid arthritis. *Ann. Rheum. Dis.* 1999;58(11):691-7. Available at: http://www.pubmedcentral.nih.gov/articlerender.fcgi?artid=1752794&tool=pmcentrez&rendertype=abstract.

234. Sounni NE, Devy L, Hajitou a, et al. MT1-MMP expression promotes tumor growth and angiogenesis through an up-regulation of vascular endothelial growth factor expression. *FASEB J.* 2002;16(6):555-64. Available at: http://www.ncbi.nlm.nih.gov/pubmed/11919158.

235. Basile JR, Holmbeck K, Bugge TH, Gutkind JS. MT1-MMP controls tumor-induced angiogenesis through the release of semaphorin 4D. *J. Biol. Chem.* 2007;282(9):6899-905. doi:10.1074/jbc.M609570200.

236. Ray BK, Shakya A, Turk JR, Apte SS, Ray A. Induction of the MMP-14 gene in macrophages of the atherosclerotic plaque: role of SAF-1 in the induction process. *Circ. Res.* 2004;95(11):1082-90. doi:10.1161/01.RES.0000150046.48115.80.

237. Ottino P, Finley J, Rojo E, et al. Hypoxia activates matrix metalloproteinase expression and the VEGF system in monkey choroid-retinal endothelial cells: Involvement of cytosolic phospholipase A2 activity. *Mol. Vis.* 2004;10(October 2003):341-50. Available at: http://www.ncbi.nlm.nih.gov/pubmed/15162095.

238. Hanna SC, Krishnan B, Bailey ST, et al. HIF1α and HIF2α independently activate SRC to promote melanoma metastases. 2013;123(5). doi:10.1172/JCI66715DS1.

239. Wan J, Chai H, Yu Z, et al. HIF-1α effects on angiogenic potential in human small cell lung carcinoma. *J. Exp. Clin. Cancer Res.* 2011;30(1):77. doi:10.1186/1756-9966-30-77.

240. Müller A, Krämer SD, Meletta R, et al. Gene expression levels of matrix metalloproteinases in human atherosclerotic plaques and evaluation of radiolabeled inhibitors as imaging agents for plaque vulnerability. *Nucl. Med. Biol.* 2014. doi:10.1016/j.nucmedbio.2014.04.085.

241. Zeng L, Zampetaki A, Margariti A, et al. Sustained activation of XBP1 splicing leads to endothelial apoptosis and atherosclerosis development in response to disturbed flow. *Proc. Natl. Acad. Sci. U. S. A.* 2009;106(20):8326-31. doi:10.1073/pnas.0903197106.

242. Roche Diagnostics. *Find a Quick Solution*. 4th Editio. (Eisel D, Hoffmann-Rohrer UW, Kruchen B, et al., eds.). Mannheim: Roche Diagnostics GmbH; 2011.

243. Wu J, Lu Z, Nie M, et al. Optimization of cryopreservation procedures for porcine endothelial progenitor cells. *J. Biosci. Bioeng.* 2012;113(1):117-23. doi:10.1016/j.jbiosc.2011.09.012.

244. Jin R, Zhu X, Liu L, Nanda A, Granger DN, Li G. Simvastatin Attenuates Stroke-induced Splenic Atrophy and Lung Susceptibility to Spontaneous Bacterial Infection in Mice. *Stroke.* 2013. doi:10.1161/STROKEAHA.111.000633.

245. Sadeghi MM, Collinge M, Pardi R, Bender JR. Simvastatin modulates cytokine-mediated endothelial cell adhesion molecule induction: involvement of an inhibitory G protein. *J. Immunol.* 2000;165(5):2712-8. Available at: http://www.ncbi.nlm.nih.gov/pubmed/10946302.

246. Wu D, Yotnda P. Induction and testing of hypoxia in cell culture. *J. Vis. Exp.* 2011;(54):4-7. doi:10.3791/2899.

247. Huang LE, Willmore WG, Gu J, Goldberg MA, Bunn HF. Inhibition of Hypoxia-inducible Factor 1 Activation by Carbon Monoxide and Nitric Oxide. 1999;274(13):9038-9044.

248. Li YM, Xu M, Lai MT, et al. Photoactivated gamma-secretase inhibitors directed to the active site covalently label presenilin 1. *Nature* 2000;405(6787):689-94. doi:10.1038/35015085.

249. Regnard C, Straub T, Mitterweger A, Dahlsveen IK, Fabian V, Becker PB. Global analysis of the relationship between JIL-1 kinase and transcription. *PLoS Genet.* 2011;7(3):e1001327. doi:10.1371/journal.pgen.1001327.

250. Huang LE, Gu J, Schau M, Bunn HF. Regulation of hypoxia-inducible factor 1alpha is mediated by an O2-dependent degradation domain via the ubiquitin-proteasome pathway. *Proc. Natl. Acad. Sci. U. S. A.* 1998;95(14):7987-92. Available at: http://www.pubmedcentral.nih.gov/articlerender.fcgi?artid=20916&tool=pmcentrez&rendertype=abstract.

251. Smith PK, Krohn RI, Hermanson GT, et al. Measurement of protein using bicinchoninic acid. *Anal. Biochem.* 1985;150(1):76-85. doi:http://dx.doi.org/10.1016/0003-2697(85)90442-7.

252. B. Antharavally , R. I. Krohn AKM and PAB. Development of a Detergent and Reducing Agent Compatible BCA Protein Assay. *FASEB J.* 2006. Available at: http://www.fasebj.org/cgi/content/meeting_abstract/20/5/A962.

253. Wang J, Lu Z, Wientjes MG, Au JL-S. Delivery of siRNA therapeutics: barriers and carriers. *AAPS J.* 2010;12(4):492-503. doi:10.1208/s12248-010-9210-4.

254. Hamm A, Krott N, Breibach I, Blindt R, Bosserhoff AK. Efficient transfection method for primary cells. *Tissue Eng.* 2002;8(2):235-45. doi:10.1089/107632702753725003.

255. Genois M-M, Mukherjee A, Ubeda J-M, et al. Interactions between BRCA2 and RAD51 for promoting homologous recombination in Leishmania infantum. *Nucleic Acids Res.* 2012;40(14):6570-84. doi:10.1093/nar/gks306.

256. Seewald S, Sachinidis A, Du R, et al. Lysophosphatidic acid and intracellular signalling in vascular smooth muscle cells. *Atherosclerosis* 1997;130(1-2):121-31. Available at: http://www.ncbi.nlm.nih.gov/pubmed/9126656.

257. Schindelin J, Arganda-carreras I, Frise E, et al. Fiji : an open-source platform for biological-image analysis. 2012;9(7). doi:10.1038/nmeth.2019.

258. Herzenberg L a, Parks D, Sahaf B, Perez O, Roederer M, Herzenberg L a. The history and future of the fluorescence activated cell sorter and flow cytometry: a view from Stanford. *Clin. Chem.* 2002;48(10):1819-27. Available at: http://www.ncbi.nlm.nih.gov/pubmed/12324512.

259. BD Biosciences. *Introduction to Flow Cytometry: A Learning Guide*.; 2000.

260. O'Donnell E a, Ernst DN, Hingorani R. Multiparameter flow cytometry: advances in high resolution analysis. *Immune Netw.* 2013;13(2):43-54. doi:10.4110/in.2013.13.2.43.

261. Linnoila I, Petrusz P. Immunohistochemical techniques and their applications in the histopathology of the respiratory system. *Environ. Health Perspect.* 1984;56(8):131-48. Available at: http://www.pubmedcentral.nih.gov/articlerender.fcgi?artid=1568194&tool=pmcentrez&rendertype=abstract.

262. Cote RJ, Peterson HF, Chaiwun B, et al. Role of immunohistochemical detection of lymph-node metastases in management of breast cancer. International Breast Cancer Study Group. *Lancet* 1999;354(9182):896-900. Available at: http://www.ncbi.nlm.nih.gov/pubmed/10489948. Accessed November 9, 2014.

263. Motterle A, Pu X, Wood H, et al. Functional analyses of coronary artery disease associated variation on chromosome 9p21 in vascular smooth muscle cells. *Hum. Mol. Genet.* 2012;21(18):4021-9. doi:10.1093/hmg/dds224.

264. Nakashima Y, Plump a. S, Raines EW, Breslow JL, Ross R. ApoE-deficient mice develop lesions of all phases of atherosclerosis throughout the arterial tree. *Arterioscler. Thromb. Vasc. Biol.* 1994;14(1):133-140. doi:10.1161/01.ATV.14.1.133.

265. Yan Y, Chen H, Costa M. Chromatin Immunoprecipitation Assays. *Epigenetics Protoc.* 2004.

266. Gilmour DS, Lis JT. Detecting protein-DNA interactions in vivo: distribution of RNA polymerase on specific bacterial genes. *Proc. Natl. Acad. Sci. U. S. A.* 1984;81(14):4275-9. Available at: http://www.pubmedcentral.nih.gov/articlerender.fcgi?artid=345570&tool=pmcentrez&rendertype=abstract.

267. Carey MF, Peterson CL, Smale ST. Chromatin immunoprecipitation (ChIP). *Cold Spring Harb. Protoc.* 2009;2009(9):pdb.prot5279. doi:10.1101/pdb.prot5279.

268. Loayza D, De Lange T. POT1 as a terminal transducer of TRF1 telomere length control. *Nature* 2003;423(6943):1013-8. doi:10.1038/nature01688.

269. Arnaoutova I, Kleinman HK. In vitro angiogenesis: endothelial cell tube formation on gelled basement membrane extract. *Nat. Protoc.* 2010;5(4):628-635.

270. Carpentier G. Angiogenesis Analyzer for ImageJ. *ImageJ User Dev. Conf. 2012* 2012:5. Available at: http://image.bio.methods.free.fr/ImageJ/?Angiogenesis-Analyzer-for-ImageJ.html. Accessed February 15, 2013.

271. Covington MD, Burghardt RC, Parrish AR. Ischemia-induced cleavage of cadherins in NRK cells requires MT1-MMP (MMP-14). *Am. J. Physiol. Renal Physiol.* 2006;290(1):F43-51. doi:10.1152/ajprenal.00179.2005.

272. Liang C-C, Park AY, Guan J-L. In vitro scratch assay: a convenient and inexpensive method for analysis of cell migration in vitro. *Nat. Protoc.* 2007;2(2):329-33. doi:10.1038/nprot.2007.30.

273. Yue PYK, Leung EPY, Mak NK, Wong RNS. A simplified method for quantifying cell migration/wound healing in 96-well plates. *J. Biomol. Screen.* 2010;15(4):427-33. doi:10.1177/1087057110361772.

274. Crane AM, Bhattacharya SK. The use of bromodeoxyuridine incorporation assays to assess corneal stem cell proliferation. *Methods Mol. Biol.* 2013;1014:65-70. doi:10.1007/978-1-62703-432-6_4.

275. Vermes I, Haanen C, Reutelingsperger C. Flow cytometry of apoptotic cell death. *J. Immunol. Methods* 2000;243(1-2):167-90. Available at: http://www.ncbi.nlm.nih.gov/pubmed/10986414.

276. Rieger AM, Nelson KL, Konowalchuk JD, Barreda DR. Modified annexin V/propidium iodide apoptosis assay for accurate assessment of cell death. *J. Vis. Exp.* 2011;(50):37-40. doi:10.3791/2597.

277. Han YH, Park WH. MG132 as a proteasome inhibitor induces cell growth inhibition and cell death in A549 lung cancer cells via influencing reactive oxygen species and GSH level. *Hum. Exp. Toxicol.* 2010;29(7):607-14. doi:10.1177/0960327109358733.

278. Eisinger J. Visible gel electrophoresis and the determination of association constants. *Biochem. Biophys. Res. Commun.* 1971;44(5):1135-42. Available at: http://www.ncbi.nlm.nih.gov/pubmed/4946185. Accessed June 12, 2014.

279. Garner MM, Revzin A. A gel electrophoresis method for quantifying the binding of proteins to specific DNA regions: application to components of the Escherichia coli lactose operon regulatory system. *Nucleic Acids Res.* 1981;9(13):3047-60. Available at: http://www.pubmedcentral.nih.gov/articlerender.fcgi?artid=327330&tool=pmcentrez&rendertype=abstract. Accessed June 12, 2014.

280. Hellman LM, Fried MG. Electrophoretic mobility shift assay (EMSA) for detecting protein-nucleic acid interactions. *Nat. Protoc.* 2007;2(8):1849-61. doi:10.1038/nprot.2007.249.

281. Allard STM, Kopish K. LUCIFERASE REPORTER ASSAYS : POWERFUL , ADAPTABLE TOOLS FOR CELL BIOLOGY RESEARCH. *Promega Corp.* 2008.

282. Sauer B. Inducible gene targeting in mice using the Cre/lox system. *Methods* 1998;14(4):381-92. doi:10.1006/meth.1998.0593.

283. Miller SA, Dykes DD, Polesky HF. A simple salting out procedure for extracting DNA from human nucleated cells. *Nucleic Acids Res.* 1988;16(3):1215. Available at: http://www.pubmedcentral.nih.gov/articlerender.fcgi?artid=334765&tool=pmcentrez&rendertype=abstract. Accessed April 24, 2014.

284. Iwai M, Tateishi Y, Hattori M, et al. Molecular cloning of mouse type 2 and type 3 inositol 1,4,5-trisphosphate receptors and identification of a novel type 2 receptor splice variant. *J. Biol. Chem.* 2005;280(11):10305-17. doi:10.1074/jbc.M413824200.

285. Soukup G a, Fritzsch B, Pierce ML, et al. Residual microRNA expression dictates the extent of inner ear development in conditional Dicer knockout mice. *Dev. Biol.* 2009;328(2):328-41. doi:10.1016/j.ydbio.2009.01.037.

286. Reynolds L, Hodivala-Dilke K. Primary mouse endothelial cell culture for assays of angiogenesis. *Methods Mol. Med.* 2006;120:503-509. Available at: http://www.ncbi.nlm.nih.gov/pubmed/16491622.

287. Nicosia RF, Ottinetti A. Growth of microvessels in serum-free matrix culture of rat aorta. A quantitative assay of angiogenesis in vitro. *Lab. Invest.* 1990;63(1):115-22. Available at: http://www.ncbi.nlm.nih.gov/pubmed/1695694. Accessed April 24, 2014.

288. Auerbach R, Lewis R, Shinners B, Kubai L, Akhtar N. Angiogenesis assays: a critical overview. *Clin. Chem.* 2003;49(1):32-40. Available at: http://www.ncbi.nlm.nih.gov/pubmed/12507958.

289. Baker M, Robinson SD, Lechertier T, et al. Use of the mouse aortic ring assay to study angiogenesis. *Nat. Protoc.* 2012;7(1):89-104. doi:10.1038/nprot.2011.435.

290. Andrade SP, Fan TP, Lewis GP. Quantitative in-vivo studies on angiogenesis in a rat sponge model. *Br. J. Exp. Pathol.* 1987;68(6):755-66. Available at: http://www.pubmedcentral.nih.gov/articlerender.fcgi?artid=2013085&tool=pmcentrez&rendertype=abstract. Accessed April 29, 2014.

291. Mahadevan V, Hart IR, Lewis GP. Factors influencing blood supply in wound granuloma quantitated by a new in vivo technique. *Cancer Res.* 1989;49(2):415-9. Available at: http://www.ncbi.nlm.nih.gov/pubmed/2463076. Accessed November 9, 2014.

292. Tavora B, Batista S, Hodivala-Dilke K. Measuring angiogenesis in mice. Wells CM, Parsons M, eds. *Methods Mol. Biol.* 2011;769:351-8. doi:10.1007/978-1-61779-207-6_23.

293. Akhtar N, Dickerson EB, Auerbach R. The sponge/Matrigel angiogenesis assay. *Angiogenesis* 2002;5(1-2):75-80. Available at: http://www.ncbi.nlm.nih.gov/pubmed/12549862. Accessed April 29, 2014.

294. Yamaji R, Fujita K, Takahashi S, et al. Hypoxia up-regulates glyceraldehyde-3-phosphate dehydrogenase in mouse brain capillary endothelial cells: involvement of Na+/Ca2+ exchanger. *Biochim. Biophys. Acta - Mol. Cell Res.* 2003;1593(2-3):269-276. doi:10.1016/S0167-4889(02)00397-X.

295. Haeberle H a, Dürrstein C, Rosenberger P, et al. Oxygen-independent stabilization of hypoxia inducible factor (HIF)-1 during RSV infection. *PLoS One* 2008;3(10):e3352. doi:10.1371/journal.pone.0003352.

296. Hunt M a, Currie MJ, Robinson B a, Dachs GU. Optimizing transfection of primary human umbilical vein endothelial cells using commercially available chemical transfection reagents. *J. Biomol. Tech.* 2010;21(2):66-72. Available at: http://www.pubmedcentral.nih.gov/articlerender.fcgi?artid=2884313&tool=pmcentrez&rendertype=abstract.

297. Jordan ET, Collins M, Terefe J, Ugozzoli L, Rubio T. Optimizing electroporation conditions in primary and other difficult-to-transfect cells. *J. Biomol. Tech.* 2008;19(5):328-34. Available at: http://www.pubmedcentral.nih.gov/articlerender.fcgi?artid=2628074&tool=pmcentrez&rendertype=abstract. Accessed November 4, 2014.

298. Lonza. Amaxa® HUVEC Nucleofector® Kit. 2008:4-7.

299. Newby AC. Metalloproteinase expression in monocytes and macrophages and its relationship to atherosclerotic plaque instability. *Arterioscler. Thromb. Vasc. Biol.* 2008;28(12):2108-14. doi:10.1161/ATVBAHA.108.173898.

300. Proulx-Bonneau S, Guezguez A, Annabi B. A concerted HIF-1α/MT1-MMP signalling axis regulates the expression of the 3BP2 adaptor protein in hypoxic mesenchymal stromal cells. *PLoS One* 2011;6(6):e21511. doi:10.1371/journal.pone.0021511.

301. Mills CN, Joshi SS, Niles RM. Expression and function of hypoxia inducible factor-1 alpha in human melanoma under non-hypoxic conditions. *Mol. Cancer* 2009;8:104. doi:10.1186/1476-4598-8-104.

302. Zhu X-Y, Daghini E, Chade AR, et al. Disparate effects of simvastatin on angiogenesis during hypoxia and inflammation. *Life Sci.* 2008;83(23-24):801-9. doi:10.1016/j.lfs.2008.09.029.

303. Izidoro-Toledo TC, Guimaraes D a, Belo V a, Gerlach RF, Tanus-Santos JE. Effects of statins on matrix metalloproteinases and their endogenous inhibitors in human endothelial cells. *Naunyn. Schmiedebergs. Arch. Pharmacol.* 2011;383(6):547-54. doi:10.1007/s00210-011-0623-0.

304. Ikeda U, Shimpo M, Ohki R, et al. Fluvastatin Inhibits Matrix Metalloproteinase-1 Expression in Human Vascular Endothelial Cells. *Hypertension* 2000;36(3):325-329. doi:10.1161/01.HYP.36.3.325.

305. Kamio K, Liu XD, Sugiura H, et al. Statins inhibit matrix metalloproteinase release from human lung fibroblasts. *Eur. Respir. J.* 2010;35(3):637-46. doi:10.1183/09031936.00134707.

306. Bachelet M, Mariéthoz E, Banzet N, et al. Flow cytometry is a rapid and reliable method for evaluating heat shock protein 70 expression in human monocytes. *Cell Stress Chaperones* 1998;3(3):168-76. Available at: http://www.pubmedcentral.nih.gov/articlerender.fcgi?artid=312961&tool=pmcentrez&rendertype=abstract. Accessed May 7, 2013.

307. Porter KE, Turner N a, O'Regan DJ, Balmforth AJ, Ball SG. Simvastatin reduces human atrial myofibroblast proliferation independently of cholesterol lowering via inhibition of RhoA. *Cardiovasc. Res.* 2004;61(4):745-55. doi:10.1016/j.cardiores.2003.11.032.

308. Kupcsik L. Estimation of cell number based on metabolic activity: the MTT reduction assay. Stoddart MJ, ed. *Methods Mol. Biol.* 2011;740:13-9. doi:10.1007/978-1-61779-108-6_3.

309. Newby AC. Matrix metalloproteinases regulate migration, proliferation, and death of vascular smooth muscle cells by degrading matrix and non-matrix substrates. *Cardiovasc. Res.* 2006;69(3):614-24. doi:10.1016/j.cardiores.2005.08.002.

310. Ulasov I, Thaci B, Sarvaiya P, et al. Inhibition of MMP14 potentiates the therapeutic effect of temozolomide and radiation in gliomas. *Cancer Med.* 2013;2(4):457-67. doi:10.1002/cam4.104.

311. Artym V V, Zhang Y, Seillier-Moiseiwitsch F, Yamada KM, Mueller SC. Dynamic interactions of cortactin and membrane type 1 matrix metalloproteinase at invadopodia: defining the stages of invadopodia formation and function. *Cancer Res.* 2006;66(6):3034-43. doi:10.1158/0008-5472.CAN-05-2177.

312. Seiki M. Membrane-type 1 matrix metalloproteinase: a key enzyme for tumor invasion. *Cancer Lett.* 2003;194(1):1-11. Available at: http://www.ncbi.nlm.nih.gov/pubmed/12706853.

313. Zucker S, Cao J. Selective matrix metalloproteinase (MMP) inhibitors in cancer therapy: ready for prime time? *Cancer Biol. Ther.* 2009;8(24):2371-3. Available at: http://www.pubmedcentral.nih.gov/articlerender.fcgi?artid=2829367&tool=pmcentrez&rendertype=abstract. Accessed July 30, 2014.

314. Karthikeyan VJ, Lip GYH. Statins and intra-plaque angiogenesis in carotid artery disease. *Atherosclerosis* 2007;192(2):455-6. doi:10.1016/j.atherosclerosis.2007.01.018.

315. Khaidakov M, Wang W, Khan J a, Kang B-Y, Hermonat PL, Mehta JL. Statins and angiogenesis: is it about connections? *Biochem. Biophys. Res. Commun.* 2009;387(3):543-7. doi:10.1016/j.bbrc.2009.07.057.

316. Chade AR, Zhu X, Mushin OP, Napoli C, Lerman A, Lerman LO. Simvastatin promotes angiogenesis and prevents microvascular remodeling in chronic renal ischemia. *FASEB J.* 2006;20(10):1706-8. doi:10.1096/fj.05-5680fje.

317. Skaletz-Rorowski A, Walsh K. Statin therapy and angiogenesis. *Curr. Opin. Lipidol.* 2003;14(6):599-603. doi:10.1097/01.mol.0000103614.38789.55.

318. Nicosia RF. The aortic ring model of angiogenesis: a quarter century of search and discovery. *J. Cell. Mol. Med.* 2009;13(10):4113-36. doi:10.1111/j.1582-4934.2009.00891.x.

319. Burbridge MF, Cogé F, Galizzi JP, Boutin JA, West DC, Tucker GC. The role of the matrix metalloproteinases during in vitro vessel formation. *Angiogenesis* 2002;5(3):215-26. Available at: http://www.ncbi.nlm.nih.gov/pubmed/12831062. Accessed June 27, 2014.

320. Masson V, Devy L, Grignet-debrus C, et al. Mouse Aortic Ring Assay : A New Approach of the Molecular Genetics of Angiogenesis. 2002;4(1):24-31.

321. Yana I, Sagara H, Takaki S, et al. Crosstalk between neovessels and mural cells directs the site-specific expression of MT1-MMP to endothelial tip cells. *J. Cell Sci.* 2007;120(Pt 9):1607-14. doi:10.1242/jcs.000679.

322. Zhang Y, Naggar JC, Welzig CM, et al. Simvastatin Inhibits Angiotensin II-Induced Abdominal Aortic Aneurysm Formation in Apolipoprotein E-Knockout Mice: Possible Role of ERK. *Arterioscler. Thromb. Vasc. Biol.* 2009;29(11):1764-1771. doi:10.1161/ATVBAHA.109.192609.

323. Chen Z. Simvastatin Reduces Neointimal Thickening in Low-Density Lipoprotein Receptor-Deficient Mice After Experimental Angioplasty Without Changing Plasma Lipids. *Circulation* 2002;106(1):20-23. doi:10.1161/01.CIR.0000022843.76104.01.

324. Sarkar K, Rey S, Zhang X, et al. Tie2-dependent knockout of HIF-1 impairs burn wound vascularization and homing of bone marrow-derived angiogenic cells. *Cardiovasc. Res.* 2012;93(1):162-9. doi:10.1093/cvr/cvr282.

325. Deshmukh H a, Colhoun HM, Johnson T, et al. Genome-wide association study of genetic determinants of LDL-c response to atorvastatin therapy: importance of Lp(a). *J. Lipid Res.* 2012;53(5):1000-11. doi:10.1194/jlr.P021113.

326. Callapina M, Zhou J, Schmid T, Köhl R, Brüne B. NO restores HIF-1alpha hydroxylation during hypoxia: role of reactive oxygen species. *Free Radic. Biol. Med.* 2005;39(7):925-36. doi:10.1016/j.freeradbiomed.2005.05.009.

327. Son DJ, Kumar S, Takabe W, et al. The atypical mechanosensitive microRNA-712 derived from pre-ribosomal RNA induces endothelial inflammation and atherosclerosis. *Nat. Commun.* 2013;4:3000. doi:10.1038/ncomms4000.

328. Coussens LM, Fingleton B, Matrisian LM. Matrix metalloproteinase inhibitors and cancer: trials and tribulations. *Science* 2002;295(5564):2387-92. doi:10.1126/science.1067100.

329. Marques SM, Abate CC, Chaves S, et al. New bifunctional metalloproteinase inhibitors: an integrated approach towards biological improvements and cancer therapy. *J. Inorg. Biochem.* 2013;127:188-202. doi:10.1016/j.jinorgbio.2013.03.003.

330. Ayaori M, Sawada S, Yonemura A, et al. Glucocorticoid receptor regulates ATP-binding cassette transporter-A1 expression and apolipoprotein-mediated cholesterol efflux from macrophages. *Arterioscler. Thromb. Vasc. Biol.* 2006;26(1):163-8. doi:10.1161/01.ATV.0000193513.29074.52.

331. Mimnaugh EG, Neckers LM. Measuring ubiquitin conjugation in cells. *Methods Mol. Biol.* 2005;301:223-41. doi:10.1385/1-59259-895-1:223.

Appendix I

Appendix I – A table of buffers used in the experiments showing their formulation and the application that they are used for. The buffers are presented in alphabetical order.

Name of Buffer		Formula	Application	Reference
ChIP Digestion Buffer		0.15M EDTA, 0.6M Tris-HCl pH 6.5 and 0.625mg/ml Proteinase K	ChIP Assay	Merck Millipore UK
ChIP Dilution Buffer		0.01% SDS, 16.7mM Tris-HCl pH 8.0, 1.2mM EDTA, 1.1% TritonX-100, 150mM NaCl	ChIP Assay	[268]
ChIP Elution Buffer		1%SDS, 0.1M NaHCO3	ChIP Assay	Merck Millipore UK
ChIP Lysis Buffer		1% SDS, 10mM EDTA, 50mM Tris-HCl pH8.0	ChIP Assay	[268]
DNA Lysis Buffer		1% SDS, 50mM Tris-HCl pH 8, 100mM EDTA, 100mM NaCl	DNA Extraction	[284]
EMSA binding buffer		2% v/v glycerol, 0.5mM $MgCl_2$, 0.25mM EDTA, 25mM NaCl, 5mM Tris, pH7.5	EMSA	
ECL Reagent	Solution 1	100mM Tris–HCl, pH 8.5, 2.5mM luminol, 400µM p-coumaric acid	Western Blot	[256]
	Solution 2	5.4mM H_2O_2, 100mMTris–HCl, pH 8.5		
High Salt Buffer		0.1% SDS, 1% Triton X-100, 2mM EDTA, 20mM Tris-HCl pH8.0, 500mM NaCl	ChIP Assay	[268]
HEPES Buffered Saline		20mM HEPES, 137mM NaCl, 5mM KCl, 6mM D-Glucose, 0.7mM Na_2HPO_4, pH 7.4	Nucleofection	[255]
Immunoprecipitation Buffer		0.9M Urea, 0.2% Triton-X100, 0.1% Dithiothreitol, 10% Lithium Dodecylsulphate	Immunoprecipitation	[330]

LiCl Buffer	0.25M LiCl, 1% NP-40, 1% SDC, 1mM EDTA, 10mM Tris-HCl pH 8.0	ChIP Assay	[268]
Low Salt Buffer	0.1% SDS, 1% Triton X-100, 2mM EDTA, 20mM Tris-HCl pH8.0, 150mM NaCl	ChIP Assay	[268]
MLEC Medium	200ml DMEM w Glutamax Low Glucose (Invitrogen, UK), 200ml Ham's F12 w Glutamax (Invitrogen, UK), 50mg Heparin, 250mg Penicillin and Streptomycin, 4mM L-Glutamine, 25mg Endothelial mitogen (AbD Serotech, UK), 100ml heat-inactivated FCS	Mouse Lung Endothelial Cell Preparation	[286]
PBLEC	PBS, 0.1µM $MnCl_2$, 1% Tween-20	Aortic Ring Assay Staining	[289]
PBS (pH 7.4)	10mM Na_2HPO_4, 136mM NaCl, 2.68mM KCl, 1.76mM KH_2PO_4	Cell culture, Protein Extraction, ChIP Assay, Immunohistochemistry	[242]
10X PCR Loading Buffer	50mM Tris-HCl pH 7.6, 0.025% Bromophenol Blue, 60% Glycerol	PCR	[242]
Permeabilisation Buffer	PBS + 0.25% Triton-X100	Aortic Ring Assay Staining	[289]
Protease Inhibitor Cocktail	1mM PMSF, 1 µg/ml Leupeptin , 1 µg/ml Aprotinin, 1 µg/ml Pepstatin	ChIP Assay, Protein Extraction, Protein Quantification	[249]
Radio Immunoprecipitation Assay (RIPA) Buffer	0.1% SDS, 50mM Tris-HCl pH7.4, 150mM NaCl, 0.5% sodium deoxycholate, 1% NP-40	Protein Extraction, Protein Quantification	[248]

TBST	50mM Tris-HCl pH 7.5, 150mM NaCl, 0.05% Tween	Western Blot	[242]
TE Buffer	20mM Tris-HCl pH 8.0, 1mM EDTA pH8.0	ChIP Assay	[268]
TNESV Buffer	50mM Tris-HCl pH 7.5, 1% v/v Nonidet P40, 2mM EDTA, 100mM NaCl, 10mM Sodium Orthovanadate, 1x Protease Inhibitors	HIF1α Ubiquitination Assay	[331]
Western Blot Running Buffer	0.1% SDS, 25mM Tris-HCl, 192mM Glycine	Western Blot	[242]
Western Blot Transfer Buffer	25mM Tris-HCl, 192mM Glycine, 20% Methanol	Western Blot	[242]
Western SDS Loading Buffer	1% SDS, 31.25mM Tris-HCl pH 6.8, 50% Glycerol, 5% β-Mercaptoethanol, 0.05% Bromophenol Blue	Western Blot	[242]
Western Stripping Buffer	2% SDS, 62.5mM Tris-HCl pH 6.8, 100mM β-Mercaptoethanol	Western Blot	[242]

Appendix II

Appendix II – A Table of Primers and Procedures they were used for

Primer Target	Procedure	Orientation	Nucleotide Sequence
MMP14 Promoter	ChIP Assay	Forward	CAGCCTGCACCACAAAAAG
		Reverse	CTTCTCCCACAGCCTCTCCT
Mouse HIF1α	HIF1α Genotyping	Forward	CGTGTGAGAAAACTTCTGGATG
		Reverse	AAAAGTATTGTGTTGGGGCAGT
Cre Recombinase	Cre Recombinase Genotyping	Forward	GCCTGCATTACCGGTCGATGCAACGA
		Reverse	GTGGCAGATGGCGCGGCAACACCATT